Game-Theoretic Approaches for Smart Prosumer Communities

By

MATTHIAS PILZ

Department of Computer Science and Mathematics
KINGSTON UNIVERSITY LONDON

A dissertation submitted in accordance with the requirements of the degree of DOCTOR OF PHILOSOPHY in the Faculty of Science, Engineering, and Computing.

OCTOBER, 2019

This almost blank page is intentional.

Abstract

Global warming is endangering the Earth's ecosystem. It is imperative for humanity to limit greenhouse gas emissions in order to combat rising global average temperatures. Demand-side management (DSM) schemes have widely been analysed in the context of the future smart grid. Often they are based on game-theoretic approaches to schedule the electricity consumption of its participants such that it results in small peak-to-average ratios (PAR) of the aggregated load.

In order to guarantee high comfort levels for the consumer, we investigate DSM schemes on the basis of individually owned energy storage systems. The scheduling of these batteries is incentivised by a specific pricing function offered to the users. Within this thesis we cover various aspects for these type of management schemes.

Firstly, we design a simple game-theoretic scheduling mechanism and analyse how the battery model, more specifically the round-trip efficiency, affects the outcome. From the simulations we find the importance of highly efficient energy storage systems for the engagement of participants.

Secondly, the simple scheduling mechanism is replaced with a more advanced dynamic game, that models fine-grained control over the battery. For this novel game, we derive an analytical solution for the best response of a user, considerably speeding up the solution algorithm for the game. Furthermore, a comparison between the two games also shows the improvements in reducing the PAR of the aggregated load. Based on the augmented game, we investigate the resilience of the equilibrium solution with respect to inevitable real-world forecasting errors. One of the main findings of this thesis is reflected in the results showing the robustness of the schedules for a large number of simulated scenarios and even in the worst-case.

Thirdly, we explicitly deal with the finite horizon effect that occurs due to the fixed time frame of the game mechanism. This eventually leads to a DSM system which results in a mean PAR of the aggregated load close to the optimum. Further studies show that these outcomes can be achieved due to the interaction of the households. Individual scheduling of batteries reduces the potential reduction of PAR and is especially detrimental for the robustness against forecasting errors.

Fourthly, the developed model is analysed with respect to cyber-physical attacks. We develop a novel type of data-injection attack on the forecasted data and show their impact. After suggesting suitable monitoring strategies to the utility company, a game-theoretic model is employed to understand their decision making process.

Finally, we investigate which battery size is optimal for such a DSM scheme. The respective experiments give insight into the different factors that determine the sizing of the battery. From the results we can infer that certain types of users only require a small scale battery system to achieve considerable gains.

Overall, this thesis provides an in-depth analysis of a demand-side management scheme that can be employed by prosumers all around the world in the nearest future. Furthermore, the experiments give insights to utility companies to focus on community approaches and how they can mitigate potential cyber attacks.

Dedication and acknowledgements

Firstly, I would like to express my sincere gratitude to my first supervisor Dr. Luluwah Al-Fagih for the continuous support. Throughout countless meetings she was guiding me on this PhD journey while also leaving space to develop my own ideas. Whenever she saw an interesting opportunity she encouraged me to join various extracurricular activities which greatly enhanced my experience as a PhD student.

My sincere thanks also goes to my second first supervisor Prof. Jean-Christophe Nebel. He always has a challenging question on hand that helps to put things into perspective and let me grow as a researcher. Even before he officially became my supervisor, I saw him as a mentor and learnt a lot from his wide range of experiences.

Besides my two first supervisors, I would like to thank the rest of my PhD committee: Prof. Gavin Gillmore, and Prof. Souheil Khaddaj for their insightful comments and encouragement.

Furthermore, I would like to thank Dr. Eckhard Pfluegel for proactively participating in my game theory reading group and pushing it forward to eventually becoming a full-scale research group (CYENS). These meetings were very important for my understanding of game theory as well as my personal development.

I thank colleagues and co-authors Dr. Nigel Atkins, Dr. Mastaneh Davis, Dr. Gordon Hunter, Dr. Peter Soan, Prof. James Orwell, Dr. Luluwah Al-Fagih, Prof. Jean-Christophe Nebel, and Dr. Eckhard Pfluegel, who were core to the positive atmosphere in the institute and making me feel welcome from the very beginning in summer 2016.

I would also like to thank Rosalind Percival for her support in all administrative concerns, her invaluable patience, and her dedication to work and assist even when she is in the hospital.

My gratitude also goes to the DTA team and especially Ben Diette, Jennie Eldridge, Dr. Vladimir Vukovic, and Prof. Amin Al-Habaibeh for making our cohort feel like a family. The prospects of joining the DTA was one of the key points when deciding for my PhD project and in hindsight this was a great decision.

Aside from my academic companions, I also would like to thank my friends and family. First of all, I would like to express my whole-hearted thanks to my girlfriend Johanna Mader for being there and standing up for me, especially in difficult times. Without her I would not even have dared to come to the UK. I am greatful we can share this experience together and grow.

Special thanks goes to Ron Watschke for his loyality and companionship on various trips and concerts throughout my time as a PhD student. I cannot thank him enough for reintroducing me to the joy of tasting and I am looking forward to the time we have ahead.

Who would have known that the very first person I ever met in the office (back in SB1031) would become one of my best friends. Thank you to Dr. Roshan Welikala for stimulating discussions, motivation, and making the office into what it became.

One of the most rewarding extracurricular activities I was involved in, was the organisation of the SEC Post Graduate Research Society. I would like to thank Cameron Robertson, Amtul Bhunnoo, and Jamila Rahim for their hard work and dedication to create a sense of community between researchers from various departments.

Außerdem möchte ich meinen Eltern und Großeltern danken für ihre immerwährende Unterstützung und Rückhalt in allen Phasen meiner Ausbildung. Schon als kleiner Junge war ihre Zuversicht und Ermutigung eine wichtige Motivationsquelle für mich. I widme diese Arbeit Oma Lotti und Oma Mille.

Last but not least, I would like to thank Alex Richardson, the perfect housemate. Since she moved in with us, I actually look forward to coming back home after a long day in the office.

Author's declaration

Hereby, I declare that the work in this dissertation was carried out in accordance with the requirements of the University's Regulations and Code of Practice for Research Degree Programmes and that it has not been submitted for any other academic award. Except where indicated by specific reference in the text, the work is the candidate's own work. Work done in collaboration with, or with the assistance of, others, is indicated as such. Any views expressed in the dissertation are those of the author.

1st April 2020

. . . .

Matthias Pilz Date

This almost blank page is intentional.

Contents

Page

List of Tables **xi**

List of Figures **xiii**

Notation and Abbreviations **xv**

List of Publications **xvii**

1 Introduction **1**

1.1 Methodology 5

1.2 Thesis Contributions 5

1.3 Structure of the Thesis 6

Part I Preliminaries **9**

2 Fundamental Game-Theoretic Concepts **11**

2.1 Brief History 12

2.2 Taxonomy 12

2.3 Definitions for Non-Cooperative Games 15

3 Systematic Literature Review **19**

3.1 Methodology 19

3.2 Classification of Papers 21

3.3 Discussions 28

3.3.1 Battery Storage 28

3.3.2 Uncertainties 30

3.3.3 Objectives of Demand-Side Management 31

4 System Model **35**

4.1 Neighbourhood and Demand-Side Management Programme 36

4.2 Individual Households 38
4.2.1 Battery Model 38
4.2.2 Renewable Energy Model 41
4.2.3 Demand, Net Demand, and Load 41
4.3 The Utility Company 42
4.4 Data Sets 43
4.4.1 Demand Data 43
4.4.2 Renewable Resource Data 45
4.4.3 Computing Errors for Forecasted Data 45
4.5 Evaluation Metrics 46

Part II Contributions **49**

5 Static Scheduling with an Advanced Battery Model **51**
5.1 The Battery Scheduling Game 52
5.1.1 Decision Variables 53
5.1.2 Definition 53
5.1.3 Solution Approach 54
5.2 Performance Evaluation 55
5.2.1 Parameters 55
5.2.2 Peak-to-Average Ratio 56
5.2.3 Consumer-Type Analysis 57
5.3 Discussions 58
5.3.1 Peak-to-Average Ratio 58
5.3.2 Involvement in the Game 59
5.3.3 Utility Function 59
5.4 Conclusions 60

6 A Dynamic Scheduling Game with Forecasting Errors **61**
6.1 The Dynamic Battery Scheduling Game 63
6.1.1 Definitions and Game Formulation 63
6.1.2 Analysis of the Game 65
6.1.3 The Algorithm and Execution of NE schedules 69
6.2 Performance Evaluation 70
6.2.1 Parameters 70
6.2.2 Convergence Behaviour of the Algorithm 71
6.2.3 Comparison Between a Static and a Dynamic DSM Scheme . 73
6.2.4 Influence of Participation Rate and Forecasting Errors 75
6.2.5 Consumer-Type Analysis 77

6.2.6 Robustness . . . 78
6.2.7 Influence of Pricing Parameters . . . 80
6.3 Discussions . . . 81
6.3.1 Convergence Behaviour of the Algorithm . . . 81
6.3.2 Comparison Between a Static and a Dynamic DSM Scheme . . . 82
6.3.3 Influence of Participation Rate and Forecasting Errors . . . 83
6.3.4 Consumer-Type Analysis . . . 85
6.3.5 Robustness . . . 86
6.4 Conclusions . . . 87

7 Finite-Horizon Effect and Added Value of the Game 89
7.1 Refined Scheduling Approach . . . 90
7.2 Results and Discussion . . . 92
7.2.1 Treatment of Horizon . . . 93
7.2.2 Added Value of the Proposed DSM Scheme . . . 95
7.3 Conclusions . . . 97

8 Cyber Attacks on Smart Grid Scheduling 99
8.1 False Data Injection On Forecasts . . . 103
8.1.1 Description of Attacks . . . 103
8.1.2 Attack Outcomes . . . 104
8.1.3 Attack Detection Strategies . . . 109
8.1.4 Attack Mitigation . . . 112
8.2 Game-Theoretic Defence Strategy . . . 113
8.2.1 Game Theory for Security . . . 113
8.2.2 Proposed Security Game . . . 114
8.2.3 Game Analysis . . . 117
8.2.4 Quantitative Examples . . . 119
8.2.5 Discussions . . . 120
8.3 Conclusions . . . 121

9 Optimal Battery Sizing in a DSM Scheme 123
9.1 Optimal Battery Sizing Results . . . 125
9.1.1 Self-Consumption . . . 127
9.1.2 PAR values . . . 128
9.1.3 Cost Reduction . . . 129
9.1.4 Centralised vs. Decentralised Storage Systems . . . 130
9.2 Discussion . . . 131
9.3 Conclusions . . . 135

Part III Conclusions & Future Work 137

10 Conclusions 139
10.1 Main Findings and Contributions to Knowledge . . . 139
10.2 Limitations of the Work . . . 140

11 Future Work 141
11.1 An Energy Sharing Concept . . . 141
11.1.1 Decision Variables . . . 142
11.1.2 The Utility Function . . . 145
11.1.3 The Non-Cooperative Game . . . 146
11.1.4 Conclusions . . . 147
11.2 Other Directions . . . 148

Part IV Appendix 151

A Battery Justification 153

B Literature Overview 155

C Curriculum Vitae 175

Bibliography 177

List of Tables

Table **Page**

3.1 Details about reviewed publications. 23

4.1 NREL demand data. 44

5.1 Battery parameters. 55
5.2 Peak-to-average ratios. 57
5.3 Comparison of involvement rates. 57
5.4 Activity occurrence. 57
5.5 Reduction of utility values. 59

6.1 Battery parameters. 70
6.2 Peak-to-average ratio comparison. 73
6.3 Parameter ranges. 78

8.1 Impact of undetected attacks despite average amount monitoring 111
8.2 Impact of undetected attacks despite deep aggregated monitoring. 111
8.3 IDS game of [Alpcan and Basar, 2010] in normal form. 115
8.4 Augmented security game in normal form. 116
8.5 Representative mixed strategy probabilities for Case 2 attacks. 119

9.1 Self-consumption improvements. 127

This almost blank page is intentional.

List of Figures

Figure **Page**

1.1 Potential load-shaping results. 3

2.1 Taxonomy of non-cooperative games. 13
2.2 Tree-structure illustration of the Rock-Paper-Scissors game. 14

3.1 Analysis of relevant publications 21
3.2 Storage usage in the literature. 29
3.3 PAR analysis. 32

4.1 Systematic sketch of the neighbourhood. 36
4.2 Schematic illustration of the charging and discharging behaviour of a lithium-ion battery. 39
4.3 Individual forecast created by adding random errors. 46

5.1 Aggregated load curves over four different one-week periods. 56
5.2 Illustration of equilibrium schedules. 58

6.1 Convergence analysis of Algorithm 4. 72
6.2 Iteration statistics. 72
6.3 Load comparison. 73
6.4 Nash equilibrium schedule comparison. 74
6.5 PAR reduction dependency on the participation rate. 75
6.6 Savings dependency on the participation rate. 76
6.7 PAR reduction for different neighbourhoods. 77
6.8 Savings for different neighbourhoods. 78
6.9 PAR value histograms. 79
6.10 Average savings. 80
6.11 Influence of forecasting error on the achieved PAR value. 84
6.12 Differences between neighbourhoods in PAR reduction. 85

7.1 Illustration of 'finite horizon effect'. 91

7.2 PAR reduction with respect to the participation rate. 93
7.3 Further analysis of results shown in Figure 7.2. 94
7.4 PAR reduction of the aggregated load over the participation rate. 96

8.1 Example of a shift attack. 104
8.2 Example of scale attacks. 105
8.3 Individual loads and unit price after scheduling. 106
8.4 Financial benefit for the attacker. 107
8.5 Aggregated load and battery schedule without and under a scale ($\tau = 2$) attack. 108
8.6 Peak-to-average ratio of the aggregated load for different attack scenarios. 109
8.7 Advanced security game flow diagram. 118

9.1 Optimal sizing considerations. 125
9.2 Optimal battery sizes. 126
9.3 Self-consumption analysis. 127
9.4 Peak-to-average ratio (PAR) of the aggregated load. 128
9.5 Cost reductions. 129
9.6 Comparison between centralised and decentralised approach. 130
9.7 Demand, generation, battery usage. 132
9.8 Demand, generation, battery usage. 133
9.9 Demand and generation for two seasons. 134

11.1 Electricity flows. 143
11.2 Generation and demand. 145
11.3 Outcome of the game. 148

A.1 Battery justification. 153

Notation and Abbreviations

This chapter gives an overview of the notation that is used consistently throughout this thesis. Vectors are labelled with bold font and denoted by square brackets, e.g. $\mathbf{a} = [a_1, \ldots, a_N]$. Vector elements may carry a superscript and/or a subscript. If so, the superscript refers to a temporal interval, while the subscript denotes the participating household. Sets are labelled with calligraphic font and denoted by curly brackets, e.g. $\mathcal{N} = \{1, \ldots, N\}$. What follows is a list of the commonly used notation:

$\mathcal{A}_n$	set of actions available to player n
$\mathbf{a}$	action profile
a_n^t	action of player n during interval t
B_n	electricity bill for household n
c_2, c_1, c_0	cost function coefficients
$\bar{d}_m^t$	demand of household m during interval t
d_n^t	net-demand of household n during interval t
g^t	quadratic const function
$\mathcal{H}^+$	set of possible charging decisions
$\mathcal{H}^-$	set of possible discharging decisions
l_m^t	load of household m during interval t
$\mathbf{l}_m$	schedule of loads for household m
L_{-n}^t	average aggregated load of all households other than n during interval t
L^t	aggregated load during interval t
$\mathcal{N}$	set of households that participate in the game
N	number of game participants
$\mathcal{M}$	set of all households
M	number of all households
N/M	participation rate
$\mathcal{S}_n$	set of mixed strategy profiles for player n
$\mathbf{s}$	mixed-strategy profile
$s_{\min}$	minimum state-of-charge

$s_{\max}$	maximum state-of-charge
$\mathcal{T}$	set of intervals for the scheduling period
T	number of intervals for the scheduling period
u_n	real-valued utility function for player n
w_n^t	renewable production of household n during interval t

ϵ_d	forecasting error for the demand
ϵ_w	forecasting error for the renewable generation
η^+	charging efficiency
η^-	discharging efficiency
η_{inv}	efficiency of hybrid inverter
λ	ratio of attacked players
Φ^+	charging limit
Φ^-	discharging limit
ρ^+	charging rate
ρ^-	discharging rate
$\bar{\rho}$	self-discharging rate

The following abbreviations are used:

CC	Constant Current
CV	Constant Voltage
DP	Dynamic Programming
DSM	Demand-Side Management
FDI	False-Data Injection
GTS	Game-Theoretic Scheduling
GTSWC	Game-Theoretic Scheduling With Constraint
IB	Ideal Battery
HAN	Home Area Network
LAN	Local Area Network
NE	Nash Equilibrium
PAR	Peak-to-Average Ratio
PV	Photovoltaic
RB	Realistic Battery
SOC	State-Of-Charge
UC	Utility Company
WAN	Wide Area Network

List of Publications

Journal Articles[1]

1.	**M.Pilz**, L.Al-Fagih; "Recent Advances in Local Energy Trading in the Smart Grid Based on Game–Theoretic Approaches"; *IEEE Transactions on Smart Grid*; 10, (2), 2019 [online] DOI: 10.1109/TSG.2017.2764275	published 10/2017
2.	**M.Pilz**, L.Al-Fagih, E.Pfluegel; "Energy Storage Scheduling with an Advanced Battery Model: A Game–Theoretic Approach"; *Inventions*; 2, (30), 2017 [online] DOI: 10.3390/inventions2040030	published 11/2017
3.	**M.Pilz**, L.Al-Fagih; "A Dynamic Game Approach for Demand-Side Management: Scheduling Energy Storage with Forecasting Errors"; *Dynamic Games and Applications*; 2019 [online] DOI: 10.1007/s13235-019-00309-z	published 04/2019
4.	**M.Pilz**, F.Baghaei, K.Grammont, C.Smagghe, M.Davis, J.-C.Nebel, L.Al-Fagih, E.Pfluegel; "Security Attacks on Smart Grid Scheduling and Their Defences: A Game–Theoretic Approach"; *International Journal of Information Security*; 2019 [online] DOI: 10.1007/s10207-019-00460-z	published 08/2019
5.	**M.Pilz**, O.Ellabban, L.Al-Fagih; "On Optimal Battery Sizing for Households Participating in Demand-Side Management Schemes"; *Energies*; 12, (18), 2019 [online] DOI: 10.3390/en12183419	published 09/2019

[1] In the thesis the publications are referred to as:
1. [Pilz and Al-Fagih, 2019b]
2. [Pilz et al., 2017b]
3. [Pilz and Al-Fagih, 2019a]
4. [Pilz et al., 2019a]
5. [Pilz et al., 2019b].

Conference Papers[2]

1. **M.Pilz**, J.-C.Nebel, L.Al-Fagih; “A Practical Approach to Energy Scheduling: A Game Worth Playing?”; *IEEE ISGT Europe 2018* — published 12/2018
   [online] DOI: 10.1109/ISGTEurope.2018.8571522

2. **M.Pilz**, L.Al-Fagih; “Selfish Energy Sharing in Prosumer Communities: A Demand-Side Management Concept”; *IEEE SmartGridComm 2019*
   [online] DOI: 10.1109/SmartGridComm.2019.8909791

[2] In the thesis the publications are referred to as:
1. [Pilz et al., 2018]
2. [Pilz and Al-Fagih, 2019c].

CHAPTER 1

INTRODUCTION

Global warming is posing a serious threat to the Earth's ecosystem. According to studies presented by NASA, eighteen of the nineteen warmest years have all occurred this century [NASA, 2019a]. The effects of this are felt all around the globe: more frequent wildfires, longer periods of drought, melting of polar ice caps and the resulting rise of seawater levels to name but a few [NASA, 2019b]. Since the keeping of reliable records in 1880, the seawater level has risen by approximately 20 cm and is expected to further rise by up to 120 cm until 2100.

Many countries have committed to the Paris Agreement of 2015 [European Commission, 2016] to limit global warming to below 2.0 degrees above pre-industrial levels. In order to achieve this, it is essential to restrict greenhouse gas emissions. Roughly a quarter of the total energy consumption in the EU stems from residential households; a majority of which comes from burning fossil fuels [Eurostat, 2019]. Instead, one should use carbon-friendly energy resources, such as renewable energy from wind or the sun. Unfortunately, their integration into the powergrid on a large scale is a challenging task due to the intermittent nature of these resources.

The requirement of advanced infrastructure to guarantee the stability of the power system led to the development of the smart grid concept. To put this idea into context let us briefly highlight how the current power grid developed. The first power grid was established in 1882 in a small neighbourhood of 85 households [Power2Switch, 2012]. It relied on direct current (DC). Soon afterwards it was understood that large scale centralised power plants will be able to operate more efficiently than the local dynamos. In combination with alternating currents (AC) to allow for long distance transmission with low losses, a power grid was implemented which essentially has not changed since then.

The smart grid can be seen as an extension to this. There is no universally accepted definition but the following will be used throughout this thesis [Jenkins et al., 2015]:

> "A Smart Grid is an electricity network that can intelligently integrate the actions of all users connected to it – generators, consumers and those that do both – in order to efficiently deliver sustainable, economic and secure electricity supplies."

That means, in addition to the legacy power grid infrastructure, the system also has a communication infrastructure that connects the different stakeholders in the network. Within the smart grid, the end users gain considerable importance. Whereas they were merely passive consumers beforehand, they now become proactive participants in the power network. A household that is equipped with a renewable energy resource is called a *prosumer*; a neologism based on the fact that they are *pro*ducer and con*sumer* at the same time.

A key element in the concept of a smart grid is the smart meter. It is a device that enables the monitoring of electricity usage at a substantially higher frequency than before. Instead of quarterly manual readings of the electricity meter, a smart meter remotely transmits consumption data that is collected at half-hour intervals over the course of a day. Furthermore, the smart meter is able to receive signals from the respective utility company. This is a major driver for the implementation of demand-side management (DSM) schemes. In contrast to the existing system in which production is always adjusted according to the demand of the users, here the users can be incentivised to change their consumption.

Figure 1.1 shows the six commonly sought after outcomes of how the users' load might be shaped. Depending on the type of signal and the reaction of the users one differs between three types of demand-side response[1]. The first one is referred to as automatic. It requires specialised hardware, i.e. smart appliances such as a smart washing machine, which can be remotely controlled. This signal comes directly from the utility company with the advantage of being very quick and less risky for them as they are in full control. A potential drawback for the utility company may be that in order to have a considerable impact on the aggregated load a large number of these appliances are necessary and it is unclear who is paying for those. For the

[1] Technically, demand-side response is not synonymous to demand-side management. Demand-side management aims to improve flexibility on the consumer side, whereas demand-response refers to approaches encouraging users to make short-term changes in their energy consumption [RESPOND, 2018].

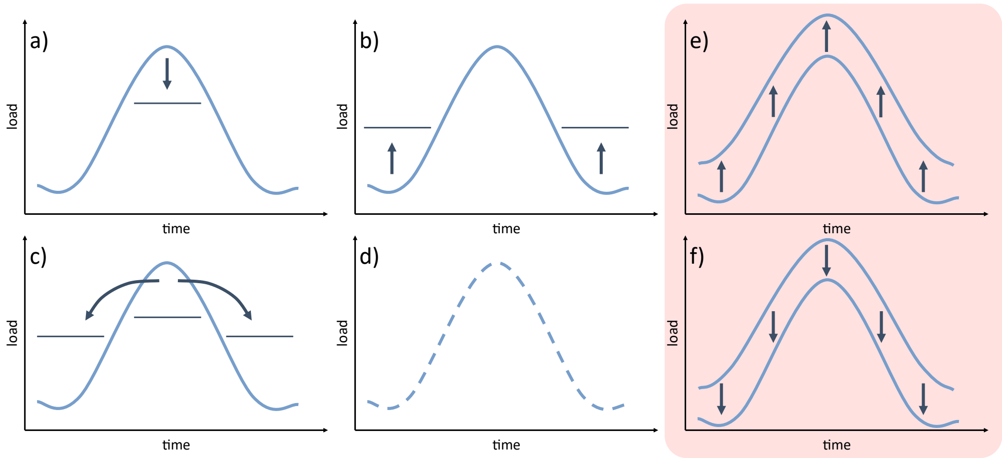

Figure 1.1. *Potential load-shaping results.*
The six panels show a schematic overview of the commonly sought after outcomes of load-shaping. While a) to d) (peak clipping, valley filling, load shifting, and flexible load shaping) fall under the category of demand-response activities, e) and f) are referred to as strategic load growth and energy efficiency, respectively. (Adapted from [Lampropoulos et al., 2013])

user the question is whether they are willing to completely give away their decision in return for a financial reward.

The second demand-side response type is known as manual DSR. In such a scheme, the utility company sends a signal for increasing or lowering the load and it is the consumer who decides how they want to react. As they stay in control of their appliances, the users are expected to be more accepting for such an approach. Nevertheless, it also gives less security to the utility company. Households might simply miss the signal or are not willing to react to it. Compared to the automatic approach, there is no special equipment needed other than the smart meter. There is a third type, called contractual DSR, but as this is first and foremost aimed at large scale consumers such as commercial or industrial customers, this is beyond the scope of this thesis.

Aside from DSR approaches, another way of changing the load is to implement the possibility for energy exchange between individual households. One has to distinguish between energy trading and energy sharing. The term energy trading is used whenever there is a direct financial reward for every transaction of electricity between two households. In contrast to this, during energy sharing, households share energy with one another for load shaping purposes, i.e. under the influence of an external incentivising signal. They receive an indirect financial reward according to how much the load shape follows the targeted one.

When discussing the methods that are used for smart energy management, there are two main approaches: optimisation and game theory. In their nature they are close to the automatic and manual types of DSR as discussed above, respectively. As the utility company has the control over the smart appliances in an automatic scheme, they aim to optimise their usage according to their internal criteria. The literature provides a plethora of examples including various approaches such as linear programming, non-linear programming and stochastic optimisation[2]. In approaches that make use of game theory, the players, i.e. the households, perform a sort of "distributed optimisation". That means in this case we model their decisions rather than the decision of the utility company. Often the game is directed through a specific pricing function, which can be understood as the signal we discussed in the manual DSR scheme. Under the assumption that all the households are rational and only care about their own good, the most common game form is a non-cooperative game. In case we also want to study the decision of the utility company, e.g. how they set the pricing, Stackelberg games would be the most suitable approach.

Within this thesis, I investigate a day-ahead demand-side management approach based on the usage of individually owned battery storage systems. It can be seen as a manual approach in which the utility company is only providing a specific pricing function as a signal and it is up to the consumers to react to it. As the households are using electricity storage to shape the load, none of their appliances are interfered with, giving them a high level of comfort. The resulting load shape that is aimed for is a flat profile.

Throughout the PhD, I explored various aspects of such a demand-side management scheme. This thesis aims at tying them all together to give a complete story that allows the reader to understand the journey I have taken over the past three years. To achieve the complete picture, several objectives were defined going both deeply into the game-theoretic approach as well as covering various aspects of applicability such as optimal sizing and cyber security. Firstly, I pursued to develop a game-theoretic model that captures the interaction of independent (and rational) households which also includes the uncertainty of necessarily forecasted data. The two main stages until the completion of this objective were eventually published in peer-reviewed journals and make up two chapters in Part II. A part of this objective was also to understand the robustness against inevitable forecasting errors. Secondly, it was the objective to understand the potential impact of cyber security attacks on the system and to be able to give sensible advice to utility companies who employ a demand-side management scheme of this type. The third major group of objectives was formulated around the applicability in realistic scenarios. This included the intention to understand the value of interaction between households

[2] For instance [Haider et al., 2016a,Bahrami and Amini, 2018,Liu et al., 2018a]. Further references are reviewed and discussed in Chapter 3

as well as an investigation into the optimal battery sizing.

1.1 Methodology

In order to study the aforementioned objectives, I considered a residential neighbourhood comprised of households that are equipped with lithium-ion batteries and/or a locally installed renewable energy resource, and those that do not have access to these devices. A demand-side management protocol was designed which clarifies the steps that are undertaken and who is involved in each of these. An essential part of the program is the specifically implemented pricing scheme that is known to every participant in advance. It relates the price per energy unit to the combined consumption of all households in the neighbourhood for each interval of the upcoming day. Thus it provides an indirect incentive for the users to 'collaborate' with each other. This collaboration is modeled by a game-theoretic approach.

Throughout the experiments, a detailed battery model is employed making the results more relateable to the real-world application. This is also done to evaluate the game-theoretic outcomes in challenging scenarios and providing evidence for the overall suitability of the approach.

Following this spirit, I also performed all of the simulation for extensive time periods. This allows for a more sophisticated analysis and gives the opportunity to gain deeper insight into the achievements and limitations. The data that was used as the input consists of both simulated and real-world data.

Considering the evaluation metrics, I specifically selected them to achieve the following: They should represent the outcomes for both sides, i.e. to answer the questions "How beneficial is the approach for the utility company?" and "How does the user benefit from taking part in the scheme?". Furthermore, the metrics are well established in the literature which allows for direct comparisons with other research groups. More details on the evaluation metrics are discussed in Section 4.5.

1.2 Thesis Contributions

The contributions of this PhD thesis are the following:

- The implementation of an advanced battery model for lithium-ion batteries and showed the importance of its characteristics in a game theoretic DSM scenario. In particular I studied the involvement of the households in the proposed battery scheduling game.
- The introduction of a novel discrete time dynamic game for energy storage scheduling and derived an analytic solution for the best-response problem of

each individual prosumer. The system is shown to be robust against forecasting errors of the demand and generation of the households even in the worst case scenario. Furthermore, I studied different compositions of neighbourhoods and how the participation rate of the game affect the potential outcome of the DSM scheme. Eventually I assessed the costs that are associated with the necessary interaction between the households and whether it is worth playing the game.

- The development of a class of false-data injection attacks on forecasting data to study the cyber-physical security of the system. In an international collaboration, we analysed the effects of these attacks and investigated the decision-making process of a utility company trying to defend against them.
- The performance of extensive simulations to provide an in-depth insight on how optimal sizing of batteries in DSM schemes depends not only on aggregated statistics but also on the specific temporal patterns that characterise individual households.

1.3 Structure of the Thesis

This section aims to give the reader an outline of the entire thesis. Each chapter starts with an overview of its content and how it fits into the overall thesis.

This thesis is split into three major parts: preliminaries, contributions, and conclusions & future work. Part I provides the required background to fully understand and relate to the contributions in the subsequent part. Part I starts with an introduction to fundamental concepts in game theory (cf. Chapter 2). Furthermore, it includes a focussed literature review in Chapter 3, that puts the contributions of the PhD thesis into perspective. Chapter 4 summarises the models for the neighbourhood, the individual households, the battery storage systems and the renewable energy resources. Additionally, it also describes the data sets that were used and the evaluation metrics that were applied throughout.

For a reader who is familiar with the topic, I would like to suggest skipping the first part (cf. Part I) entirely since the chapters in Part II are mostly self-contained and whenever necessary contain a reference to an earlier introduced concept. Moreover, each of the contribution chapters has been adapted from an original peer-reviewed publication in either a journal or a conference proceeding.

Chapter 5 introduces a static game approach for scheduling household batteries. Its content was initially presented at a conference [Pilz et al., 2017a] and awarded with the best paper prize. An extended version of the manuscript was subsequently published in a peer-reviewed journal [Pilz et al., 2017b]. The next chapter, published in [Pilz and Al-Fagih, 2019a], can be seen as the heart of this thesis. Within it the dynamic game approach is developed including its analytic solution for the best response problem. Furthermore, various aspects of the approach are studied such as the convergence behaviour of the solution algorithm, a detailed comparison to the scheme of the previous chapter, the influence of participation rate and forecasting errors, as well as the influence of the pricing parameters. Chapter 7 extends the dynamic game approach to deal with unwanted finite horizon effects. Additionally, it discusses the value of the game-theoretic approach compared to individual optimisation. The results were presented at a conference and published in the respective proceedings [Pilz et al., 2018]. Cyber security aspects are considered in Chapter 8, published in [Pilz et al., 2019a]. More precisely, a novel type of false data injection attack is introduced and analysed. Eventually, the decision-making process of an involved utility company is modelled from which we deduce some practical guidelines. This part concludes with a study on optimal battery sizing in such a demand-side management scheme (cf. Chapter 9). Our analysis of how the temporal patterns in demand and generation affect the optimal sizes was published in [Pilz et al., 2019b].

Part III includes the overall conclusions of the PhD project (cf. Chapter 10) as well as an outlook into future work (cf. Chapter 11). A particularly interesting concept is the one of energy sharing in a prosumer community. Preliminary work published in [Pilz and Al-Fagih, 2019c] is shown here together with other possible avenues for further studies.

This almost blank page is intentional.

Part I

Preliminaries

This almost blank page is intentional.

Chapter 2

Fundamental Game-Theoretic Concepts

This chapter provides background information to game-theoretic aspects that will play a role in Part II of this thesis. It aims to build a common basis for all readers, thus the advanced reader is encouraged to skip this chapter completely. Whenever suitable, later chapters will directly refer to the relevant sections.

Game theory has been applied in various areas. Its initial application was in economics to understand the behaviour of companies, markets, and consumers [Cournot, 1838]. Another well known example for game-theoretic applications in economics are auctions. Auctions such as the English auction, double auctions, or second-price auctions [Shoham and Leyton-Brown, 2009] are usually analysed with game theory.

In politics, game theory is used among other things to design and analyse voting schemes. This is especially important to guarantee a fair process. The Nobel laureate K. Arrow studied different notions of fairness and proved that there is no system that can satisfy all criteria at the same time [Shoham and Leyton-Brown, 2009].

Other areas of research in which game theory is playing an important role are: (i) Biology, most notably in form of evolutionary games [Hammerstein, 1998] and also signaling games [Shoham and Leyton-Brown, 2009] to study animal communication, (ii) Philosophy, when answering questions about common knowledge between different individuals and its consequences, and (iii) Computer science, for instance for the design of peer-to-peer systems and cyber security.

What all these examples have in common, is that they focus on the decisions of individuals who are rational and thus only interested in their own good. They want to understand/predict the behaviour of these rational individuals and how their interaction can lead to an equilibrium.

2.1 Brief History

In the 19th century several people, e.g. A. A. Cournot, F. Y. Edgeworth, and J. Bertrand, used what we would now call game-theoretic approaches. Yet, since they were all interested in analysing merely their specific problem, without the aim to develop a more general theory on strategic interaction, the notion of game theory was not established at this point.

J. von Neumann was the first to start formalising a more standardised approach in his seminal paper: "Zur Theorie der Gesellschaftsspiele" (1928) [von Neumann, 1928]. Eventually, together with O. Morgenstern, he published the book: "Theory of Games and Economic Behaviour" (1944) [von Neumann and Morgenstern, 1944] which summarises his work. Its main contributions are solutions for two-person zero-sum games. This was further generalised by J. F. Nash a few years later. In his PhD thesis he developed a solution approach for finite n-player, non-zero-sum games which is today known as the Nash equilibrium.

From then on, game theory developed quickly as a research topic and applications in various disciplines were explored. Between 1972 and 2012, five Nobel Prizes were awarded for major contributions to game theory. This includes for instance the 1994 Nobel Prize for Economics to J. F. Nash for his contributions to the equilibrium analysis of non-cooperative games. In 2007, L. Hurwicz, E. S. Maskin, and R. B. Myerson, received the Nobel Prize for the foundation of a completely new field of game theory: Mechanism design. Within this field, the usual question of "What equilibrium solution does this game have?" is reversed and the idea is to design a game which eventually leads to a desired equilibrium.

2.2 Taxonomy[1]

At the most abstract level, one can classify games into direct and indirect games. Direct game theory aims to find optimal strategies for players (cf. [von Neumann and Morgenstern, 1944]), while indirect game theory is concerned with designing games such that certain outcomes will be achieved by rational players (cf. [Shoham and Leyton-Brown, 2009]). Within this taxonomy, we focus our attention on direct

[1]This subsection was partly published in [Pilz and Al-Fagih, 2019b].

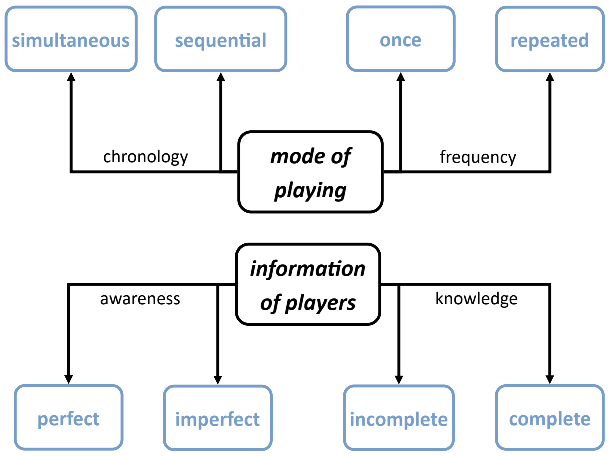

Figure 2.1. *Taxonomy of non-cooperative games.*
The 'mode of playing' and the 'information of players' are considered and split into the subcategories chronology and frequency, and awareness and knowledge, respectively. (©2019 IEEE)

games since these have played a major role in energy applications to this point in time.

Direct games are divided into two categories: Coalitional games and non-cooperative games. The difference between these branches of game theory are the level of modelling and the questions that can eventually be answered. In coalitional game theory, the basic modelling unit is a cooperative group. The focus is on what groups of individuals can achieve without explicitly modelling their individual actions. As a result it tries to answer questions like: "Which coalition will form?" and "How should the payoffs be divided among the members of this coalition?".

In contrast to this, non-cooperative games model the actions of individual rational players and their preferences. Here, the focus is on the individual and how they can achieve their own goals. Note that this does not necessarily mean that they want to harm others or solely focus on themselves. It rather means that each of them has their own view/description of what their preferences are and they strive to achieve those. As non-cooperative games are the game type that will be most important throughout this thesis, our taxonomy will focus on these.

To the best of our knowledge, a generally accepted characterisation of games cannot be found currently, as many properties overlap in their classification. In order to introduce a consistent framework, we propose to talk about the 'mode of playing' and the 'information' each player possesses (cf. Fig. 2.1). This leads to four key properties: frequency, chronology, awareness, and knowledge. There are other criteria, e.g. 'value' or symmetry [von Neumann and Morgenstern, 1944], but the ones discussed here are sufficient to cover the relevant aspects for this thesis.

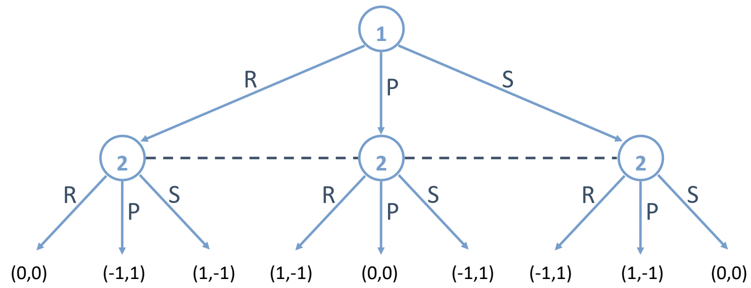

Figure 2.2. *Tree-structure illustration of the Rock-Paper-Scissors game.* Arrows represent possible moves: Rock (R), Paper (P), Scissors (S). Each leaf shows the utility function for both players, i.e. (outcome player 1, outcome player 2), with 1 denoting a win, 0 denoting a draw, and -1 denoting a loss. The dotted line shows that player 2 is not aware of which move was played by player 1.

Frequency of play Here, we differentiate between games that are played once and games that are played repeatedly. The repetition of a game with the same opponent usually results in different behaviours, as the players have to consider the impact of their actions on the opponent for the next round. The utility function, i.e. the outcome for each player, for such games is usually a (weighted) average over the payoffs of each round. The closely related topic of learning in games is discussed in [Shoham and Leyton-Brown, 2009].

Chronology of play This refers to either simultaneous or sequential games (cf. Figure 2.1). In a sequential game players move in turns and eventually reach the end of the game where the outcome is defined by a utility function. Moreover, in each turn players might have different actions available. In contrast, players of simultaneous games do not have the ability to react to their opponent. They choose their actions at the same time. This is why they are also called 'one-shot' or 'static' games.

Note that there is an important difference between a repeated static game and a sequential game. Whereas the utility function can be evaluated after each round of a repeated game, it can only be evaluated once at the end of a sequential game. An important class of sequential games are Stackelberg games [von Stackelberg, 2010]. They originated within an economic application where an established company and a startup compete for market share. The sequential nature is expressed by the burden (or chance) of the bigger company to move first, while the startup can react to the respective decision. More generally, the game exhibits a leader-follower structure. In the energy context we will see a dominant application of this structure, where the seller(s) takes the role of the leader, while the buyer(s) acts as a follower.

One way to represent sequential games is in the form of a tree structure (cf. Figure 2.2). Each node stands for a certain player and the links originating at the node show their current move set. The utility function is only defined for the leaves of the tree. This makes the analysis of such games more difficult, as no inbetween evaluation is available. The solution of such a game can be obtained by backward induction [Shoham and Leyton-Brown, 2009]. The backward induction algorithm defines values for the utility at each node of the tree. The equilibrium is then achieved by best response at every node. Unfortunately, the procedure might be intractable, for instance for chess or go, as the number of possible board configurations is extremely large [Goldberg, 1987]. J. von Neumann [von Neumann, 1928] pointed out that one could model a simultaneous game as a sequential game with players being unaware of the other player's move. His idea leads to the next classifier.

Awareness of players In the literature, one usually refers to perfect and imperfect information. The game of chess serves as a good example of a perfect information game. At every stage of the game, each player knows exactly about the history and in principle (though intractable [Goldberg, 1987]) about all future moves and their respective outcomes. In an imperfect information game the situation is different. If a player has imperfect information it means they are not aware of the move that has been played before, yet they still know about the general structure of the game, all the utility values, and all possible actions. In the tree representation this unawareness is shown by a dotted line (cf. Figure 2.2). Player 2 is not aware of which move was played by player 1 and has thus imperfect information of the game.

Knowledge of players The previous example showed a complete (but imperfect) information game. If the knowledge of a player is incomplete, they might not know about the payoffs, strategies, or structure of the game. In a series of papers from 1967-68 [Harsanyi, 1967, Harsanyi, 1968a, Harsanyi, 1968b], Harsanyi gave a first formal definition of such a game, for which he later obtained the Nobel prize. A key realisation for Harsanyi was that all uncertainties about the game can be captured by uncertainties about the payoffs. Nowadays, such a game is referred to as Bayesian game and mathematically consists of 5 ingredients: (1) a set of players, (2) a set of actions for each player, (3) a set of types for each player, (4) payoff functions for all combinations of types and actions for each player, and (5) a common prior probability function over the types of each player. The last one describes the beliefs of all players regarding another player's type.

2.3 Definitions for Non-Cooperative Games

We will follow the notation of the book: "Multiagent systems" by Y. Shoham and K. Leyton-Brown [Shoham and Leyton-Brown, 2009] for consistent definitions of non-cooperative games[2]. The most commonly used representation of a non-cooperative game is the *normal form*.

Definition 2.1. (Normal-form game) A (finite, n-person) normal-form game is a tuple $(\mathcal{N}, \mathcal{A}, \mathbf{u})$, where:

- $\mathcal{N}$ is a finite set of N players, indexed by n;
- $\mathcal{A} = \mathcal{A}_1 \times \cdots \times \mathcal{A}_N$, where $\mathcal{A}_n$ is a finite set of actions available to player n. Each vector $\mathbf{a} = [a_1, \ldots, a_N] \in \mathcal{A}$ is called an action profile;
- $\mathbf{u} = [u_1, \ldots, u_N]$, where $u_n : \mathcal{A} \mapsto \mathrm{I\!R}$ is a real-valued utility (or payoff) function for player n.

Each of the games discussed in Part II will consist of these three essential parts: players, their actions, and outcomes according to these actions. When analysing such a game from the perspective of an outside observer, we are interested to find strategies (choices of actions) that lead to an equilibrium solution. The most general definition of a strategy is given by a *mixed strategy*:

Definition 2.2. (Mixed strategy) Let $(\mathcal{N}, \mathcal{A}, \mathbf{u})$ be a normal-form game, and for any set $\mathcal{X}$ let $\Pi(\mathcal{X})$ be the set of all probability distributions over $\mathcal{X}$. Then the set of mixed strategies for player n is $\mathcal{S}_n = \Pi(\mathcal{A}_n)$.

Definition 2.3. (Mixed-strategy profile) The set of mixed-strategy profiles is the Cartesian product of the individual mixed-strategy sets, $\mathcal{S}_1 \times \cdots \times \mathcal{S}_N$.

The probability that an action a_n will be played under mixed strategy s_n is denoted by $s_n(a_n)$. A *pure strategy* is a particular case of a mixed strategy where one single action is played with a probability equal to one.

In Definition 2.1, the payoff function $\mathbf{u}$ is defined according to the choice of a pure-strategy profile. It can be generalised to cover mixed strategies with what is called the *expected utility*:

Definition 2.4. (Expected utility of a mixed strategy) Given a normal-form game $(\mathcal{N}, \mathcal{A}, \mathbf{u})$, the expected utility u_n for player n of the mixed-strategy profile $\mathbf{s} = [s_1, \ldots, s_N]$ is defined as

$$u_n(\mathbf{s}) = \sum_{\mathbf{a} \in \mathcal{A}} u_n(\mathbf{a}) \prod_{j=1}^{N} s_j\left(a_j\right) .$$

[2] At the beginning of my PhD, I was introduced to game theory by K. Leyton-Brown, Y. Shoham, and M. O. Jackson. Thus it feels natural to use their notation.

Based on these definitions for the game, strategies, and their respective outcome for the players, we can now look into the most important solution concept, the *Nash equilibrium*. To do so, we will analyse a game from the perspective of an individual player. Each player is interested in maximising their individual utility. That means, if they would know the choices of all the other participants, the problem would reduce to an optimisation problem of choosing the utility-maximising action. This can also be seen as the problem of determining the best response to the strategies $\mathbf{s}_{-n} = [s_1, \ldots, s_{n-1}, s_{n+1}, \ldots, s_N]$ of the other players. The full strategy profile can then be written as $\mathbf{s} = [s_n, \mathbf{s}_{-n}]$. Formally, the *best response* is defined as:

Definition 2.5. (Best response) Player n's best response to the strategy profile $\mathbf{s}_{-n}$ is a mixed strategy $\hat{s}_n \in \mathcal{S}_n$ such that $u_n(\hat{s}_n, \mathbf{s}_{-n}) \geq u_n(s_n, \mathbf{s}_{-n})$ for all strategies $s_n \in \mathcal{S}_n$.

The choice of the best response is not necessarily unique. Nevertheless, it is a useful concept to define the arguably most important solution idea for non-cooperative game theory, the *Nash equilibrium*.

Definition 2.6. (Nash equilibrium) A strategy profile $\mathbf{s} = [s_1, \ldots, s_N]$ is a Nash equilibrium if, for all agents n, s_n is a best response to $\mathbf{s}_{-n}$.

The Nash equilibrium is a stable strategy profile, since none of the players has an incentive to change his individual strategy. They are already reacting with their best response (cf. Definition 2.5). The definition of the Nash equilibrium based on the notion of the best response leads directly to a generic iterative approach for determining the solution of a (finite) non-cooperative game:

Algorithm 1: Best-response algorithm for finding a pure Nash equilibrium based on [Shoham and Leyton-Brown, 2009]

```
initialise random strategy profile s
while there exists a player n for whom s_n is not a best response to s_{-n} do
    for each n ∈ N do
        ŝ_n ← best response to s_{-n}
        s  ← [ŝ_n, s_{-n}]
    end
end
Output: ŝ = s
```

When this iteration procedure terminates, each player has determined a strategy s_n which is in equilibrium with all the other households. Any unilateral deviation can then only ever result in a worse (or identical) outcome. Algorithm 1 in different variations is used throughout the thesis to compute Nash equilibria.

Another solution concept that plays an important role in game theory is called Pareto Optimality. While a Nash equilibrium describes what is strategically feasible, the Pareto optimal solution expresses whether a given strategy is efficient. Since we put a strong emphasis on the individuality of the players in our games, the former notion is what we are interested in.

CHAPTER 3

SYSTEMATIC LITERATURE REVIEW

In light of the world's critical stage (cf. Chapter 1), it is understandable that topics such as smart grid technologies and demand-side management (DSM) approaches are very active fields of research. In this chapter, I conduct a structured literature review on these subject areas. The chapter is structured as follows. In Section 3.1, the methodology of the review process is explained. This includes the selection process of the reviewed publications while the introduction to the key focus areas that are investigated is topic of Section 3.2. Summaries of the reviewed scientific material can be found in the Appendix B[1]. Section 3.3 discusses the findings in the literature and highlights trends and common themes in the research area.

3.1 Methodology

I started my PhD by getting an overview of the subject area. To do so, I conducted a literature review based on the key terms specified in the original research proposal, i.e. "smart energy", "demand-side management", "game theory", all of it with a focus on residential applications. It quickly became clear that there are many different areas of research, each of which poses its own appealing questions. The one that was most interesting for me was the usage of home energy storage systems and the treatment of uncertainties. Furthermore, the exchange of electricity between

[1]Some of the papers have been reviewed by us in a literature review that was solely focused on energy trading approaches based on game-theoretic models [Pilz and Al-Fagih, 2019b].

households in a community had just started to gather traction, which is why I performed a more focused review on this specific topic (eventually published in [Pilz and Al-Fagih, 2019b]). This allowed me to identify the most important research groups and seminal publications. Based on this information, I set up alerts on both *Google Scholar* [Google, 2019] and *Web of Science* [Clarivate, 2019]. The former one was mainly used to follow specific authors, while the latter one offers suitable functionality to track citations related to specified publications as well as key words. To stay on top of large amount of new publications, I used Mendeley [Elsevier, 2019] as referencing software throughout my PhD journey. Within Mendeley I set up a group with my two first supervisors so that we can share and grow a library specifically focused on my project.

The alerts were evaluated once per month and relevant publications were added to Mendeley. Inside Mendeley, the papers were categorised by means of personalised tags based on their abstracts and conclusions. For instance, I created tags such as *#gameTheory*, *#PAR*, *#energyStorage*, and *#uncertainty* to name but a few.

For this thesis' literature review, I went through this library and selected those papers that are concerned with demand-side management approaches of all kinds in the future smart grid. The review covers the time from January 2010 to August 2019. As the aim is to present an overview of methods and techniques that can potentially be implemented in the future smart grid, only those publications were considered which were accepted by established journals and conferences. Following the approach presented in [Mengelkamp et al., 2019], this means I restricted the considered manuscripts to those from journals with an h-index of ≥ 50 and conferences with an h-index of ≥ 10 according to the rankings presented in the Scimago Journal & Country Rank database [Scimago Lab, 2019].

The initial selection of papers contained 117 journal and conference publications. Out of those 14 were identified to not meet the criteria detailed in the previous section[2]. The remaining papers were further narrowed down by reading their abstract, the introduction, and the conclusion. This eliminated another 15 papers for the following reasons: seven are pure survey papers[3], while the other eight are off-topic[4], e.g. they focus solely on the improvements of an optimisation algorithm, they prove specific mathematical properties of an auction mechanism, or they review data structures that can be used to implement a peer-to-peer energy trading market.

[2] [Goulden et al., 2014, Khan et al., 2015, Rahi et al., 2016b, Alam et al., 2017, Hunziker et al., 2017, Yaagoubi and Mouftah, 2017, Zhou et al., 2017, Brousmiche et al., 2018, Ghosh et al., 2018, Mengelkamp et al., 2018a, Myung and Lee, 2018, Thakur and Breslin, 2018, Tushar et al., 2018b, Liu et al., 2019]

[3] [Fadlullah et al., 2011, Saad et al., 2016, Jacquot et al., 2017, Zafar et al., 2017, Mengelkamp et al., 2018b, Shareef et al., 2018, Diestelmeier, 2019]

[4] [Pedrasa et al., 2010, Rahman et al., 2015, Zou et al., 2016, Reyhanian et al., 2017, Zou et al., 2017, Boomsma et al., 2018, Nguyen et al., 2018b, Morstyn et al., 2018]

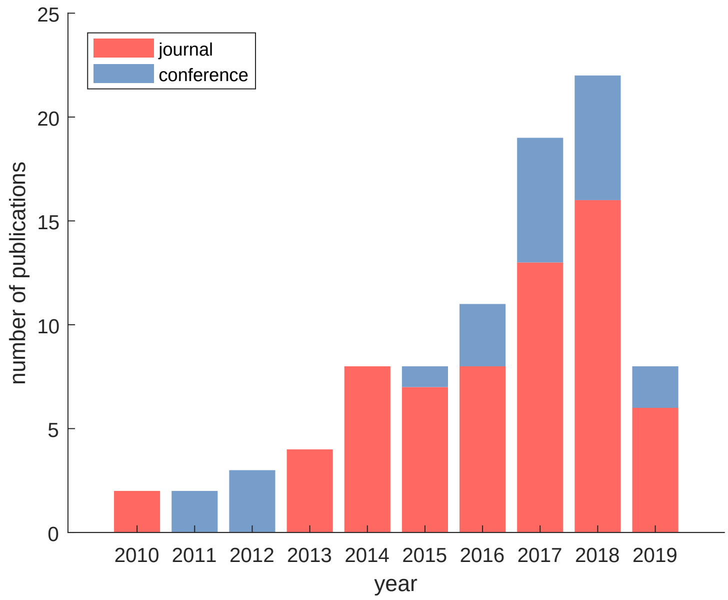

Figure 3.1. *Analysis of relevant publications.*
Similar to [Mengelkamp et al., 2019], only papers from high-quality journals and conference proceedings are considered, i.e. those with h-index of ≥ 50 and ≥ 10, respectively.

This means, I eventually ended up with 88 high quality research papers to be reviewed. Figure 3.1 gives an overview of the distribution of the manuscripts over time, as well as how many stem from journals and conferences. The trend indicates an exponential increase and thus shows the growing interest in this research topic. Note that the reduction of publications in 2019 is not representative because the review is not covering the entire year.

3.2 Classification of Papers

In this section, a detailed classification of all the papers is performed. For more details about the specific approaches of each publication, refer to Appendix B. The following categories are considered:

DSM aim: As we have seen in Chapter 1, demand-side management can have various different objectives. We differ between reducing the *peak-to-average ratio of the aggregated load* (PAR), *peak clipping* (PC) which is only concerned about reducing the highest consumption (cf. Figure 1.1(a)), *flexible load shaping* (FLS) which here usually refers to scenarios in which uncertain load and generation are matched, and *energy efficiency* (EE) (cf. Figure 1.1(f)).

System: Within this category, the parts that make up the system under investigation are listed. There can be a *utility company* (UC), *multiple utility companies* (mUC), a *household* (H), a *microgrid* (MG). If they are interacting with each other, this is denoted with a lower case i in front of the abbreviation, e.g. *interacting households* (iH), and *interacting microgrids* (iMG). There can also be an *aggregator/operator* (A). This is referred to a third party which performs the optimisation on behalf of the community or it could also be a third party which aggregates all sold electricity to then redistribute it to all buyers in the scheme. Furthermore, this category denotes whether there is individually owned *storage* (S), *community storage* (CS), *renewable energy resources* (R), *electric vehicles* (EV), *interacting electric vehicles* (iEV), and a specified energy market (EM).

Approach: This category tells the reader how the system is operated or how the participants specified in the previous category interact with each other. We differ between *scheduling of appliances* (SA), *scheduling of batteries* (SB), *scheduling of appliances and batteries* (SAB), *scheduling of resources* (SR), exchange of energy, i.e. *trading* (T), and more specifically when talking about *peer-to-peer trading* (P2P), and *pricing* (P) of energy. Here, we also mention whether the approach considers uncertainties (U), and whether a quadratic cost function (QCF) is employed[5].

Method: For better readability this category is subdivided into game theory and optimisation. For game theory we identify the following categories: *non-cooperative games* (NC), *Stackelberg games* (SG), *prospect theory* (PT), *double auctions* (DA), *Vickrey auctions* (VA), *coalitional games* (CG), *evolutionary games* (EG), *potential games* (PG), *stochastic differential game* (SDG), and *Bayesian games* (BG). For optimisation we differ between: *linear programming* (LP), *quadratic programming* (QP), *dynamic programming* (DP), *convex optimisation* (CO), *non-convex optimisation* (NCO), *multi-objective optimisation* (MOO), and *stochastic optimisation* (SO).

Time frame: This category does not only indicate the time frame of the respective method, but indirectly also whether any form of forecast is necessary for the computations. There are *one-off* (OO) decisions that can be determined based on the currently available data or decisions that are performed continuously in *real-time* (RT). In the other cases data is needed in advance that span at least the specified time frame: *day-ahead* (DA), *hour-ahead* (HA), and *sliding window* (SW).

A detailed overview of the papers is presented in Table 3.1. Note that whenever none of the introduced categories is applicable to the respective publication it is indicated by a dash.

[5] This is specifically mentioned because it is the cost function that is utilised throughout the thesis.

Table 3.1: *Details about reviewed publications.*
The papers are sorted by year of publication and within each year they are sorted alphabetically. All abbreviations are introduced in Section 3.2. Details for each publication can be found in the Appendix.

paper	DSM goal	System	Approach	Method		Time frame
				GT	O	
[Mohsenian-Rad et al., 2010]	PAR	UC, iH	SA, QCF	NC	-	DA
[Mohsenian-Rad and Leon-Garcia, 2010]	PAR	EM, H	P, SA	-	LP	DA
[Ramchurn et al., 2011]	PC	iH	SA	EG	-	DA
[Saad et al., 2011]	-	iEV, A	T	NC, DA		OO
[Ilic et al., 2012]	-	EM, iH	T	-	-	DA
[Nguyen et al., 2012]	PAR	UC, iH, S	SAB	NC	-	DA
[Zhu et al., 2012]	-	EM, iH	SA, U	SDG	CO	-
[Atzeni et al., 2013]	PAR	UC, iH, S	SB, SR	NC	NCO	DA
[Kim et al., 2013]	-	A, iH, EV	T, SAB, U	NC	-	DA
[Kim and Giannakis, 2013]	-	H, R, S	SAB, U	-	NCO	DA
[Maharjan et al., 2013]	-	mUC, iH	-	SG		OO
[Adika and Wang, 2014]	PC	A, iH, S	SAB	-	LP	DA
[Chai et al., 2014]	PAR	mUC, iH	-	SG	-	OO
[Fadlullah et al., 2014]	PAR	UC, iH	SA, P	-	-	DA
[Lee et al., 2014]	-	iH, R	T	CG	-	OO

paper	DSM goal	System	Approach	Method		Time frame
				GT	O	
[Liu et al., 2014]	PAR	iH	SA	-	MOO	DA
[Soliman and Leon-Garcia, 2014]	PAR	UC, iH, S	SAB	NC, SG	-	DA
[Tushar et al., 2014a]	-	iH, R	T	SG	-	OO
[Tushar et al., 2014b]	-	UC, iH, R	T	SG	-	OO
[Deng et al., 2015]	PAR	mUC, iH	SA, SR	-	CO	DA, RT
[Lee et al., 2015]	-	iMG, A	T	SG	-	OO
[Nguyen et al., 2015]	PAR	UC, iH, S	SAB	NC		DA
[Rahbar et al., 2015]	-	MG, R, S	SB, U	-	DP	SW
[Wang et al., 2015a]	EE	H, R	SR	CG	-	DA
[Wang et al., 2015b]	PC	UC, iH	SA	NC, PT	-	DA
[Yaagoubi and Mouftah, 2015b]	PAR	UC, iH	SA, QCF	NC	LP	DA
[Yaagoubi and Mouftah, 2015a]	EE	iH	P2P	NC	LP	OO
[Bahrami and Sheikhi, 2016]	PC	mUC, H	P, SR	PG	-	DA
[Haider et al., 2016a]	PC	H	SA, QCF	-	LP	DA
[Haider et al., 2016b]	PC	H	SA, QCF	-	-	OO
[He and Wei, 2016]	-	iMG, A	T	SG	-	OO
[Mediwaththe et al., 2016]	PAR	iH, R, CS	SB, (T)	NC	-	DA

[Mohsenian-Rad, 2016]	-	EM, S	SB, U	-	SO	DA, RT
[Park et al., 2016]	-	iMG, A	T	NC	-	OO
[Rahi et al., 2016a]	-	iH, R, S	T, U	NC, PT	-	OO
[Wang et al., 2016]	-	iMG, A	T	SG	-	OO
[Zhang et al., 2016]	PAR	iH	P2P	NC	-	OO
[Zhumabekuly Aitzhan and Svetinovic, 2016]	-	iH, A	P2P	-	-	OO
[Bae et al., 2017]	EE	R, EM	T,U	CG	-	DA, RT
[Bistarelli et al., 2017]	FLS	UC, iH	P	CG	-	DA
[Celik et al., 2017]	PC	iH, A, R, S	SAB, T, QCF	NC	-	DA
[Croce et al., 2017]	FLS	UC, H	SA	-	-	OO
[Hahn et al., 2017]	-	iH, R	P2P	VA	-	OO
[Kang et al., 2017]	-	iEV, A	P2P	DA	-	OO
[Liu et al., 2017a]	-	iH, R, A	T, SA, U	-	MOO	DA, HA
[Liu et al., 2017b]	EE	iH, R, A	T, U	SG	-	OO
[Liu et al., 2017c]	PAR	iEV	SB	NC	-	DA
[Long et al., 2017]	-	R	-	-	LP	DA
[Longe et al., 2017]	PAR	H, S	SAB	-	CO	DA
[Ma et al., 2017a]	-	UC, H	SA	-	NCO	OO
[Ma et al., 2017b]	-	iH, R, A	SR, SA, U	SG	-	OO

paper	DSM goal	System	Approach	Method		Time frame
				GT	O	
[Opadokin et al., 2017]	-	iH	T	SG	-	OO
[Park et al., 2017b]	-	H	SA	-	CO	DA
[Park et al., 2017a]	-	H	SA	-	LP	DA
[Park et al., 2017c]	-	iH, A	T	SG	-	OO
[Wang et al., 2017a]	-	iH	P2P	DA	-	OO
[Wang et al., 2017b]	-	MG, R, S	SAB, SR, U	-	MOO	DA
[Apostolopoulos et al., 2018]	PAR	mUC, iH, A	SA	NC	-	DA
[Bahrami and Amini, 2018]	PAR	A, R	T, U	-	QP	DA
[Celik et al., 2018]	PC	iH, A, R, S	SAB, QCF	-	QP	DA
[Cui et al., 2018]	-	iH, A,	T	SG	-	OO
[Gaba and Chanana, 2018]	PAR	UC, iH	SA, QCF	NC	CO	DA
[Horta et al., 2018]	EE	iH, A, R, EM	SA	DA	LP	DA
[Liu et al., 2018a]	-	iH, A, R, CS	SB, T, U	SG	SO	DA, RT
[Liu and Hsu, 2018]	PAR	UC, H, R, S	SAB	-	LP	DA
[Liu et al., 2018b]	EE	iMG, A, R, S	T	-	NCO	DA
[Liu et al., 2018d]	PC	R, S	SAB, QCF	NC	CO	DA
[Liu et al., 2018c]	PAR	iMG, EV	SAB, T, QCF	NC, BG	-	DA

[Long et al., 2018b]	EE	iH, A, R, S	T	-	LP	SW
[Long et al., 2018a]	EE	iH, A, R, CS	T	-	-	OO
[Lüth et al., 2018]	-	iH, R, CS	P2P	-	LP	DA
[Mediwaththe et al., 2018]	PAR	iH, R, CS, A	SB	SG	-	DA
[Nguyen et al., 2018a]	-	iH, R, S	T, SB	-	LP	DA
[Prudhviraj et al., 2018]	-	MG, R, S	SAB, QCF	-	LP	DA
[Rahbar et al., 2018]	-	iMG, R, S	T, SAB	-	LP	DA
[Sharma et al., 2018]	-	H, R, S	SB	-	LP	(DA-SW)
[Tushar et al., 2018a]	PAR	iH, A, R, S, EV	SB, U, QCF	NC	-	DA, RT
[Zhou et al., 2018a]	PAR	iH, iMG, S, EV, EM	SB, T	NC, SG	-	OO
[Zhou et al., 2018b]	PAR	iH, A, R	P2P	-	-	DA
[Alam et al., 2019]	-	iH, R, S	P2P	-	LP	DA
[Chouikhi et al., 2019]	PAR	mUC, iH	SA	NC, SG	-	DA
[Cui et al., 2019]	-	UC, iH, R, S	SAB, T, U	NC	CO	DA, RT
[Fanti et al., 2019]	-	iH	SA	-	LP	DA
[Hosseini et al., 2019]	-	H, R, S	SAB	-	LP	DA
[Mediwaththe et al., 2019]	PAR	UC, iH, R, CS	T, QCF	SG	-	DA
[Sivanantham and Gopalakrishnan, 2019]	PC	UC, iH	SA, QCF	-	CO	DA
[Zepter et al., 2019]	-	EM, iH, R, S	P2P, U	-	SO	DA

3.3 Discussions

The papers summarised in Table 3.1 and Appendix B show various similarities and differences. What becomes most apparent is that there does not exist a single scenario which needs to be improved by ever more sophisticated approaches and algorithms. There are rather different scenarios in almost all of the studies investigated by a range of methods. In order to extract the important insights from the classification in Section 3.2, this section discusses the connection between the publications and highlights developments over time. We focus on those aspects that are relevant for the contributions presented in Part II.

3.3.1 Battery Storage

First of all it has to be noted that all the papers in Table 3.1 that do use energy storage, employ batteries. In many cases the specific technology is not mentioned, but if it is, it is always lithium-ion batteries. According to [Gallo et al., 2016], other technologies that are applicable for demand-side management would be: pumped hydro storage, compressed air energy storage, liquid air energy storage, pumped thermal storage, power-to-gas, and power-to-liquid.

There are three types of battery storage devices found in the literature: (i) home energy storage, such as the Tesla Powerwall [Tesla, 2017]; (ii) community energy storage systems; and (iii) electric vehicles with the capability of vehicle-to-grid electricity transfer. Figure 3.2 gives an overview of the appearance of these systems in the literature and specifically highlights the temporal development.

Home energy storage: The first paper to consider storage for individual residential users in a game-theoretic setting is [Nguyen et al., 2012], which was later also published as a journal paper [Nguyen et al., 2015]. Here, the battery is used as a flexible load that lies between two boundaries. Negative values indicate discharging, while positive values refer to charging. There are no losses, neither from imperfect efficiencies nor self-discharging over time. The same model is used by [Kim and Giannakis, 2013, Soliman and Leon-Garcia, 2014]. While [Atzeni et al., 2013] introduced leakage into their model, realistic efficiencies for charging and discharging were first introduced by [Adika and Wang, 2014] and further employed by [Mohsenian-Rad, 2016, Celik et al., 2017, Wang et al., 2017b].

To the best of my knowledge, [Longe et al., 2017] is the first to include all of these parameters into their storage model. Unfortunately, since all of them investigate distinct problems, we are unable to compare the impact of the improved battery models among them. Nevertheless, it can be argued that more detailed models will result in scenarios that are more applicable, i.e. their outcomes are more

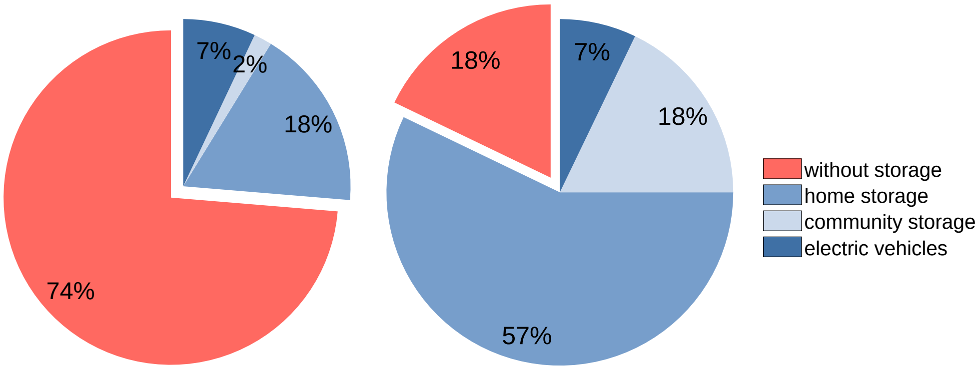

(a) 2010-2017 (b) 2018-2019

Figure 3.2. *Storage usage in the literature.*
The proportion of publications that include home storage, community storage, and electric vehicles as storage are shown for two different time periods.

expressive. Since 2017, energy storage systems have appeared in more than 80% of the publications with home storage making up almost 70% of it (cf. Figure 3.2(b)). Nevertheless, the models themselves did not become more sophisticated. Most of the models include linear charging and discharging at specific efficiencies.

As illustrated in Figure 3.2(a), the inclusion of home energy storage in publications before 2018 is the most prevalent when storage is considered but overall it is dwarfed by papers that do not model any type of storage. With my PhD starting in 2016, this gap in the literature was identified and consequently became one of the key approaches to be studied. What becomes apparent in Table 3.1 is also that even though these studies employ energy storage, they also rely on shifting appliances to reduce the peak-to-average ratio of the aggregated load (cf. [Adika and Wang, 2014, Soliman and Leon-Garcia, 2014, Nguyen et al., 2015]). We were motivated to achieve two things: (i) include an even more detailed battery model that also incorporates the specific charging curve of lithium-ion batteries, (ii) create a demand-side management system that achieves near-perfect PAR values and at the same time solely relying on the usage of energy storage. This has the advantage of not interrupting any habits of the users keeping their comfort at a maximum.

Community energy storage: The difference between home storage and community storage comes down to two points. Firstly, possible capacities, and charging and discharging rates are on a larger scale for community storage. Secondly, they can be accessed from all households at the same time. This also means that to some extent it is irrelevant who charges or discharges the battery. The advantages of community storage compared to household storage are lower (overall) costs, and easier management. C. P. Mediwaththe (cf. [Mediwaththe et al., 2016, Mediwaththe et al., 2018, Mediwaththe et al., 2019]) leads a very active research group on the applications of community energy storage. Their battery model is similar to the one introduced in [Adika and Wang, 2014], i.e. including realistic charging and discharging efficiencies.

Even though [Long et al., 2018a] refer to home energy storage within their model, they effectively consider community storage. Where, rather than modelling individual batteries, a central entity controlling all installations is considered. Most importantly they only consider aggregated values in their computations.

EV as storage: [Saad et al., 2011] seem to be the first to consider electric vehicles for demand-side management in a game-theoretic setting, i.e. energy trading is their application. At a closer look, the model does not indicate the usage of a vehicle. For [Kim et al., 2013, Kang et al., 2017, Zhou et al., 2018a] this is exactly the same. Similar to approaches like [Nguyen et al., 2015] they simply include the possibility of storing energy into their model. The scenarios are identical to home energy storage systems with larger capacities and higher potential charging and discharging rates. [Liu et al., 2017c] are the first to actually consider driving patterns, i.e. charging and discharging can only be done during certain intervals of the day (cf. [Liu et al., 2018c, Tushar et al., 2018a]).

3.3.2 Uncertainties

Only approximately one out of six papers consider uncertainties (cf. Table 3.1) connected to the generation of renewable energy, prices in the day-ahead market, or household consumption. There are three main streams in dealing with these.

The easiest is usually referred to as robust optimisation/scheduling [Kim and Giannakis, 2013, Kim et al., 2013, Wang et al., 2017b]. It does not require any changes within the model but rather adapts the input data to consider the worst-case. Nevertheless, it can deliver important insights. Together with a best-case scenario, it shows the span of all possible outcomes. Another way to treat uncertainties are two-stage approaches such as in [Mohsenian-Rad, 2016, Liu et al., 2017a, Tushar et al., 2018a, Cui et al., 2019, Zepter et al., 2019]. For instance [Tushar et al., 2018a] implement a game to optimise the day-ahead operations of their system. Then, during the actual day, the participants play a second game once per hour to minimise the differences with respect to the original plan. A slightly different approach is proposed in [Liu et al., 2017a]. Instead of minimising the differences in the second stage, they recompute the optimal solution for each following hour. The advantage of a two-stage approach is that the first stage does not need to be very sophisticated.

Lastly, there are models which directly incorporate stochastic variables and perform their optimisation based on given distributions for the various random variables, e.g. [Zhu et al., 2012, Bae et al., 2017]. [Zhu et al., 2012] use a stochastic differential game, while [Bahrami and Amini, 2018, Liu et al., 2018a] use approaches that are based on the notion of *conditional value at risk*. The authors of [Zepter et al., 2019] are the first to combine a stochastic treatment with a second stage that performs real-time updates. Similar to the effects of batteries, it is not possible to compare different approaches as every publication describes different scenarios and has different goals they aim to achieve.

Generally, more advanced methods allow for more fine grained scheduling. This is due to the fact that larger time intervals have a stronger averaging effects which makes it easier to perform highly accurate forecasts.

3.3.3 Objectives of Demand-Side Management

The objectives of demand-side management were discussed in Chapter 1. Our review of the relevant literature has found that there are three types that are most prevalent, that is the reduction of peak-to-average ratios of the aggregated load (cf. Figure 1.1(c)), clipping of peaks (cf. Figure 1.1(a)), and the overall improvement of energy efficiency (cf. Figure 1.1(f)).

Reduction of peak-to-average ratio: Approximately one in three papers is concerned with the reduction of PAR, which makes it the most sought after objective. We introduce the formal definition in Section 4.5. For the moment it is only important to know that in order to reduce costs and guarantee the stability of the power grid, one strives for PAR values that are as close as possible to 1.0. At that point, the parameter describes a perfectly flat load curve.

Figure 3.3 shows the achievements that were presented in studies between 2010 and 2019. Unfortunately, not all papers that include the PAR value in their investigations also report reference values. Thus these papers were excluded from the figure. The lowest value in this historic overview were achieved by [Soliman and Leon-Garcia, 2014] with their Stacklberg game approach coordinating pricing and scheduling of appliances and home energy storage systems. Note that they do not incorporate any kind of uncertainty in their research.

We also observe that the average of the best reported PAR results seem to be better when using game theory compared to using an optimisation scheme. This is misleading. In fact, most game-theoretic papers actually compare their results to a centralised optimisation to show that the equilibrium solution is not too far away from the optimum. e.g. [Nguyen et al., 2012, Atzeni et al., 2013, Fadlullah et al., 2014, Nguyen et al., 2015].

It can be noted that almost all studies that aim for the reduction of PAR values are based on scheduling of appliances, batteries or both. This also means they tend to

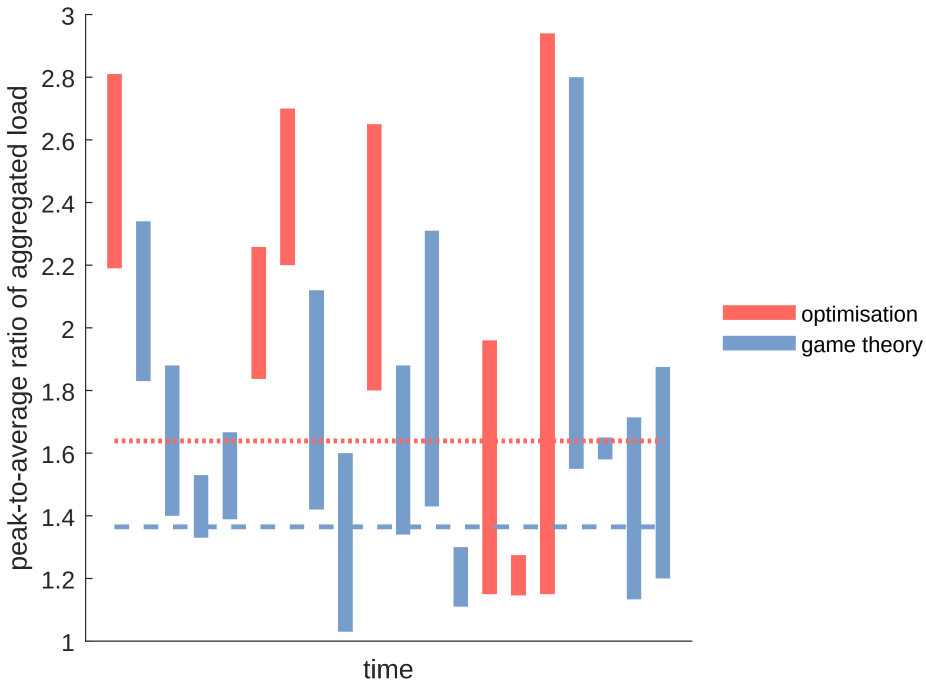

Figure 3.3. *PAR analysis.*
The achieved PAR reductions for papers investigated in Table 3.1 are presented. Each bar represents a publication and spans from the reference PAR value to the best reported result. Additionally, the average best result are shown with the dashed and dotted lines for game-theoretic and optimisation approaches, respectively. The publications are sorted by time (nonlinear).

consider the day ahead. Only two approaches do not use a day-ahead scheme [Zhang et al., 2016, Chai et al., 2014]. Both models formulate decision making processes for one instance in time and it is thus unclear how this can lead to a planned reduction of the PAR value.

Improvement in energy efficiency: While the reduction of the peak-to-average ratio of the aggregated load leads to improvements in energy efficiency on the side of the utility company, here we specifically highlight the improvements within the community. The interest in this objective for demand-side management started in 2015 with the papers by [Wang et al., 2015a, Yaagoubi and Mouftah, 2015a]. Wang *et al.* use a coalitional game to fairly distribute and eventually reduce losses in their system. Similarly, [Yaagoubi and Mouftah, 2015a, Liu et al., 2018b, Liu et al., 2017b] implement trading systems designed to reduce losses. In addition to the goal of reducing losses, [Liu et al., 2017b, Horta et al., 2018, Long et al., 2018a] aim to increase the utilisation of renewable energy resources. [Horta et al., 2018] does so by means of a blockchain-based platform which locally balances renewable production and flexible loads.

Peak clipping: This category of demand-side management objectives has conceptually a big overlap with the reduction of the peak-to-average ratio. Indeed, [Ramchurn et al., 2011] report their results of a 17% peak reduction, while also talking about flattening the load curve. Similar observations can be made for [Adika and Wang, 2014, Wang et al., 2015b, Sivanantham and Gopalakrishnan, 2019]. Within this category, the importance of data becomes clear with respect to two aspects: Variance, and granularity. For instance, [Bahrami and Sheikhi, 2016] reduce electricity peak loads by optimally using natural gas for heating and electricity. Their results show electricity-peak clipping of 27% and 46% for two consecutive days which indicates the sensitivity to the input data. This was a motivation for our research (cf. Part II) to present results for longer periods of time.

Granularity is especially important when considering peak loads. The averaging effect of longer time periods can hide realistic short term peaks. The mean length of intervals investigated in day-ahead scheduling approaches lies between 30-60 minutes. [Haider et al., 2016a] reports results for ten-minute intervals and five-minute intervals to achieve 20% and 35% peak clipping, respectively. Even shorter intervals are employed in [Celik et al., 2017, Celik et al., 2018] with a length of one minute. While [Celik et al., 2017] achieve a peak reduction of 27% over a one-day period, they later (cf. [Celik et al., 2018]) also analyse their results over the course of a full year and obtain reductions of 12% on average.

This almost blank page is intentional.

CHAPTER 4

System Model

Following the spirit of the other previous chapters in this preliminary part of the thesis, this chapter gives a general introduction to the overall system that is investigated throughout the main body (cf. Part II). Furthermore, the relevant mathematical notation for various models is introduced here. All of the subsequent chapters will consequently follow this notation to achieve a consistent story. The content of this chapter has partly been published in [Pilz and Al-Fagih, 2019a].

The chapter is structured as follows. In Section 4.1, the structure of a residential area of prosumers, i.e. households who consume and produce electricity, is introduced. Moreover, it is explained how the demand-side management (DSM) scheme is executed including the necessary exchange of data between the utility company (UC) and the respective households. In Section 4.2, the advanced battery model is established as well as the notation for renewable energy resources. Additionally, the terms demand, net-demand, and load are defined. The role of the UC as the initiator for the DSM scheme is explained in Section 4.3 together with the billing scheme that is used throughout most of this thesis. Section 4.4 deals with the data sets that are used as the input to our simulation runs. Over the course of this work we used two different data sets for household demand data as well as two for solar generation data. They differ in terms of resolution and source. Within this section, the mechanism to compute forecasting errors is explained. In order to allow for comparison with other studies in the literature, we define three evaluation metrics. These are introduced in Section 4.5 and used throughout this thesis.

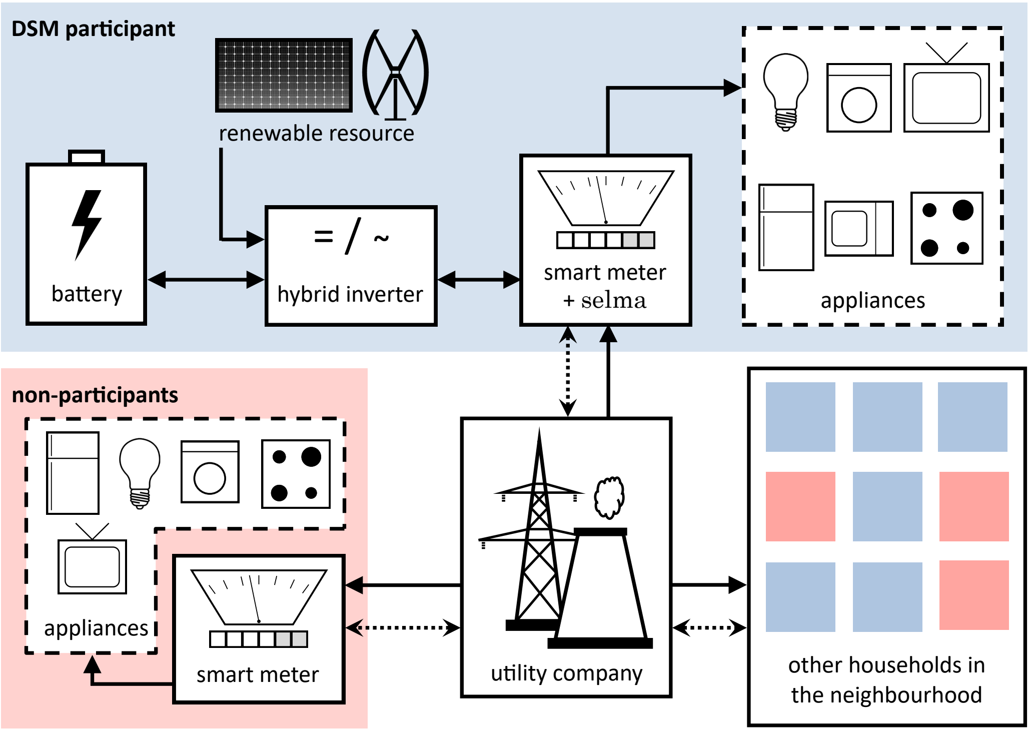

Figure 4.1. *Systematic sketch of the neighbourhood.*
Solid arrows stand for power flow, while dotted arrows stand for information flow. The top half of the figure represents a participating household of the DSM scheme. It is equipped with a lithium-ion battery and/or a renewable energy resource. The renewable energy can directly charge the battery, but to run any appliance its direct current needs to be converted to alternating current by the inverter. The smart meter collects data and executes the schedule obtained from the author's scheduling software `selma`, which is based on a game-theoretic approach. A non-participating household is depicted in the bottom left corner. It is also equipped with a smart meter, collecting data and communicating with the utility company. The complete neighbourhood consists of a number of households (cf. bottom right) that belong to either one of the shown categories. All of the households are served by the same utility company.

4.1 Neighbourhood and Demand-Side Management Programme

Consider a residential neighbourhood comprised of M houses. Each of these is equipped with a smart meter. Smart meters are capable of measuring electricity consumption accurately and at a higher frequency than the usual monthly or quarterly readings. Furthermore, these devices can communicate directly with the UC. This eventually allows for the implementation of the DSM program, and also eliminates the need for on-site readings. For our proposed model, we assume that we are able to obtain readings in regular intervals. Based on the reading-frequency, we split each day into T discrete intervals and denote the set of all intervals by $\mathcal{T}$.

We assume that the M houses are served by the same UC. In order to incentivise consumers to participate in the DSM scheme, the UC offers them a specific pricing scheme, which eventually reduces their electricity bills. Details can be found in Section 4.3. Let us denote the set of households who participate in the DSM program by $\mathcal{N} \subset \mathcal{M}$, where $\mathcal{M}$ is the set of all households in the neighbourhood. The total number of participants is $N = |\mathcal{N}|$. Besides the different pricing scheme, the participants of the DSM may possess their own battery storage system and have solar panels installed. An overview of the neighbourhood is given in Figure 4.1.

The DSM scheme can be seen as a protocol, which is gone through repeatedly. In our study the protocol is run once per day. Note that this is a completely automated process run by our scheduling software `selma` (short for: Scheduler for Electricity in Local MArkets), which needs to be installed on a consumer access device given to each participant of the scheme. Its aims is to find the best usage of the installed storage system for the upcoming day. The algorithm to obtain this battery schedules is based on a game-theoretic approach. During the journey of this PhD project, the specific game was refined step by step. Each contribution section in Part II will specifically define the employed game.

Before the start of each scheduling period, `selma` forecasts the demand[1] of the respective household for each interval $t \in \mathcal{T}$ of the upcoming day. This information is sent to the UC. The smart meters of non-participants are not able to forecast their own demand. Thus, the UC performs the forecasting step for these households, based on historically collected data. Eventually, forecasted demand curves are aggregated and the information is sent to each DSM participant. Note that no information about individual neighbours is shared, but only aggregated information. This provides privacy to all consumers.

Based on this input, the households play a game. The outcome of the game is a set of schedules, one for each household, which specify how they can make best use of their battery system. The households will follow these schedules throughout the day, even if their actual demand differs from the forecasted one. In Chapter 6, we investigate the influence of the forecasting error and show the robustness of the approach even in the worst-case scenario. At the end of the scheduling period, the electricity costs for each consumer is calculated based on the agreed pricing terms and the protocol starts over again.

[1]The actual forecasting algorithm is beyond the scope of this PhD thesis. It is rather assumed that the forecasts are given. Further information on demand forecasting can be found in [Bichpuriya et al., 2016, Dolara et al., 2015].

4.2 Individual Households

Households that participate in the DSM scheme are equipped with lithium-ion batteries and/or renewable energy resources. In this subsection, we introduce the battery model and clarify how the battery can be used. Moreover, details on the photovoltaic (PV) system are provided. Finally, we clarify the terminology of *demand*, *net-demand* and *load* of a household based on the usage of their battery and their renewable generation.

4.2.1 Battery Model

The battery model includes charging, discharging, and self-discharging characteristics of a lithium-ion battery. In fact, the same model may also be applied for lead–acid battery systems (but not nickel–based batteries due to their different charging behaviour). As all our simulations are based on a real-world lithium-ion battery system, in the remaining parts of this thesis we will only refer to them as such.

Charging: Lithium-ion batteries are charged in a two-stage process [Richtek, 2014]. In the first stage, the state-of-charge (SOC) increases linearly. This stage is called the 'constant current' (CC) stage, with a charging rate limited by $\rho^+ > 0$. In the second stage, i.e. the 'constant voltage' (CV) stage, the effective charging rate levels off exponentially towards the point where the SOC reaches the nominal maximum capacity $s_{\max}$ of the battery. The point of transition from the first stage to the second is indicated by a SOC s^* and an associated time t^*, which needs to be specified for the respective battery. During both stages, we additionally consider losses due to the specific charging efficiency η^+ with $0 < \eta^+ \leq 1$. Additionally, certain losses occur from the hybrid inverter (cf. Figure 4.1), modelled by η_{inv} with $0 < \eta_{\text{inv}} \leq 1$. The hybrid inverter transforms the direct current from either the battery or renewable resource into alternating current at usable voltage and frequency for the household appliances. It also works in the reverse direction to charge the battery.

To obtain an insight into how the households can make use of their battery system, let us look at a specific example (cf. Figure 4.2(a)). Given a certain value for the SOC, e.g. s', we can associate a time t', and thus specify a point on the charging curve.

Within the next interval of length Δt, the decision variable a^+ of how much to charge the battery will lie in $\mathcal{H}^+(s') = \{a^+ | \mathbf{h}^+(s', a^+) \leq 0\}$, with

$$\mathbf{h}^+(s', a^+) = \begin{bmatrix} -a^+ \\ a^+ - \phi^+(s') \end{bmatrix}. \tag{4.1}$$

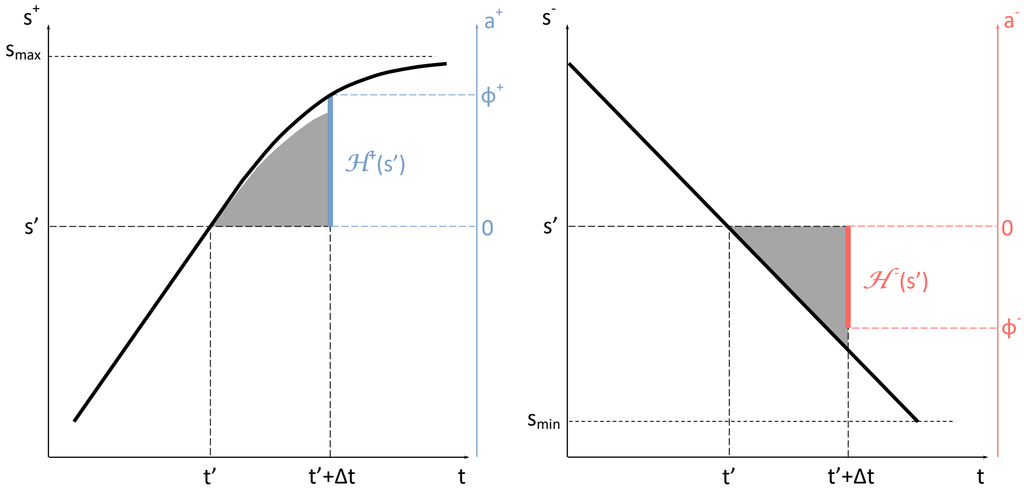

(a) charging (b) discharging

Figure 4.2. *Schematic illustration of the charging and discharging behaviour of a lithium-ion battery.*
The graph on the left (right) shows the characteristic charging (discharging) curve. Given a certain state of charge s', the grey area stands for the achievable state of charge within the following interval. The right axes represent the possible decisions when charging (discharging), where $\mathcal{H}^+(s')$ ($\mathcal{H}^-(s')$) summarise the decision intervals. The discrepancy between the achievable state of charge and the decision interval are due to losses, i.e. imperfect efficiencies while charging (discharging). (©2019 IEEE)

In other words, a^+ is limited by $0 < a^+ \leq \phi^+(s') < s_{\max} - s'$. We use the notation above to comply with the one shown in [Nie et al., 2006]. The upper limit $\phi^+(s')$ is described by the charging curve, as described above,

$$\phi^+(s') = \begin{cases} \rho^+ \Delta t & \text{if CC charged} \\ s_{\max}\gamma_1 \exp\left[-\frac{\Delta t}{\gamma_2}\right] & \text{if CV charged} \end{cases}, \tag{4.2}$$

where γ_1, γ_2 are defined such that the charging curve is smooth at the transition point (t^*, s^*). The discrepancy between the grey–shaded area and the charging curve in Figure 4.2(a) results from an imperfect charging efficiency. In fact, based on the decision variable a^+ the SOC of the battery changes according to the charging transition equation

$$s(t' + \Delta t) = s(t') + \eta_{\text{inv}}\,\eta^+ a^+ \,. \tag{4.3}$$

Discharging and Self-Discharging: We model the discharging behaviour of lithium-ion batteries by a linear decrease in the SOC. Here, the slope is given by the discharging rate $\rho^- < 0$. In order to account for the usual sharp drop off of the discharging rate at low capacities, discharging is prohibited below a minimum SOC

s_{min}. Again, we also consider losses due to the specific discharging efficiency η^- with $0 < \eta^- \leq 1$ and the hybrid inverter.

In Figure 4.2(b) a specific example is given, to clarify how the user can discharge its battery. Within the respective interval, the decision variable a^- of how much to discharge the battery will lie in $\mathcal{H}^-(s') = \{a^- | \mathbf{h}^-(s', a^-) \leq 0\}$, with

$$\mathbf{h}^-(s', a^-) = \begin{bmatrix} a^- \\ -a^- + \phi^-(s') \end{bmatrix} . \tag{4.4}$$

In other words, a^- is limited by $s' - s_{\text{min}} < \phi^-(s') \leq a^- < 0$ and

$$\phi^-(s') = \rho^- \Delta t \, \eta_{\text{inv}} \, \eta^- . \tag{4.5}$$

The dependency on s' in (4.5) is implicitly given by the fact that we cannot go lower than s_{min}. Note that ϕ^- also depends on the efficiency parameter, such that the actual amount taken from the battery in correspondence with the decision variable a^- (grey–shaded area in Figure 4.2(b)) is given by the discharging transition equation

$$s(t' + \Delta t) = s(t') + \frac{a^-}{\eta_{\text{inv}} \, \eta^-} . \tag{4.6}$$

In the following subsection, we will see that ϕ^- is additionally limited by the demand of the specific household, i.e. one can only discharge as much as is needed to run all appliances.

Whenever the battery is neither charging nor discharging, it will be subject to self-discharging. We model this type of behaviour with an exponential decline [Richtek, 2014]. This case corresponds to the decision variable $a = 0$. The respective self-discharging transition equation is given by

$$s(t' + \Delta t) = s(t') \cdot (1 + \bar{\rho})^{\Delta t} \tag{4.7}$$

where $\bar{\rho} < 0$ is the self-discharging rate.

For later usage (cf. Section 6.1), we summarise the transition equations for charging, discharging and self-discharging into a single transition equation f, i.e.

$$f(s(t), a) = s(t + \Delta t) = \begin{cases} s(t) + \eta_{\text{inv}} \, \eta^+ a & , a > 0 \\ s(t) + a/(\eta_{\text{inv}} \, \eta^-) & , a < 0 \\ s(t) \cdot (1 + \bar{\rho})^{\Delta t} & , a = 0 \end{cases} . \tag{4.8}$$

Furthermore, we combine the restrictions of the decision variable due to the battery restrictions for charging and discharging, i.e.

$$\mathbf{h}(s, a) = \begin{bmatrix} a - \phi^+(s) \\ -a + \phi^-(s) \end{bmatrix} . \tag{4.9}$$

4.2.2 Renewable Energy Model

We model the renewable energy resource as an additional source of electricity besides the grid connection. The output of the nth household's system during interval t is denoted by w_n^t. It can serve two purposes: (i) direct usage by household appliances, and (ii) charging the battery. Whereas direct usage is influenced by the efficiency of the hybrid inverter, charging the battery does not require any inversion and thus only depends on the charging efficiency of the battery.

Note that the actual source of locally produced renewable energy does not need to be specified to adhere to the household model described in Figure 4.1. The only requirement is that the output is delivered in direct current. This is naturally given for solar panels and can also be achieved for wind turbines. As our given data sets contain high quality solar data, we will concentrate on this type without loss of generality.

An important parameter of PV installations is the nominal kilowatt peak kWp of the system. It is a measure of the size of the system and denotes the maximum output that can be expected under standardised conditions. A PV system which operates at its maximum capacity, e.g. $kWp = 3\,\mathrm{kW}$, for one hour will produce $3\,\mathrm{kWh}$. Note that identifying the optimal size of the PV installation does not fall within the scope of this thesis. An approximated scale is obtained from [Zhang and Grijalva, 2016, Olaszi and Ladanyi, 2017].

4.2.3 Demand, Net Demand, and Load

We define the demand $\bar{d}_m^t \geq 0$ of a household $m \in \mathcal{M}$ as the amount of electricity that is needed to run all its appliances during the time interval $t \in \mathcal{T}$. Thus, the total daily demand-schedule can be written as $\bar{\mathbf{d}}_m = [\bar{d}_m^0, \ldots, \bar{d}_m^{T-1}]$. Throughout the thesis, we assume that the demand cannot be shifted. Thus our approach is fully non-intrusive and does not influence the behaviour of the user.

Combining the demand $\bar{d}_n^t$ of a household $n \in \mathcal{N}$ with the generated electricity w_n^t from the renewable resource, gives the net-demand

$$d_n^t = \bar{d}_n^t - \eta_{\text{inv}}\, w_n^t \,, \tag{4.10}$$

where η_{inv} is the efficiency of the inverter (cf. Figure 4.1). Theoretically, this value can be smaller than zero, i.e. when the effective generation is larger than the demand in the specific interval. Practically, we ensure $d_n^t \geq 0$ by storing all excess energy directly in the battery. For households $m \notin \mathcal{N}$, that do not participate in the DSM scheme, the net-demand is identical to the demand.

Let l_m^t denote the load, i.e. the amount of energy drawn from the grid by household $m \in \mathcal{M}$ during interval $t \in \mathcal{T}$. For households which do not participate in the DSM scheme, the load equals their demand. For the others, the load depends on the decision a_n^t taken at the specific interval. In other words, it combines the net-energy demand with the amount of energy that is charged or discharged by the battery

$$l_n^t = d_n^t + a_n^t \, , \tag{4.11}$$

where $\max\left(-d_n^t, \phi^-\right) \le a_n^t \le \phi^+$. The lower boundary expresses the fact that one cannot discharge more than is actually needed to fulfil the net-demand, while at the same time all battery restrictions remain valid. Due to this condition and (4.10), we ensure that $l_m^t \ge 0$ for all $m \in \mathcal{M}$ and all intervals $t \in \mathcal{T}$. We write $\mathbf{l}_m = [l_m^0, \ldots, l_m^{T-1}]$ for the schedule of loads of a specific household. Furthermore, we can calculate the total load on the grid for interval t by

$$L^t = \sum_{m \in \mathcal{M}} l_m^t \, . \tag{4.12}$$

Similarly, we define the average aggregated load of all households other than n during time interval t by

$$L_{-n}^t = \frac{1}{M-1} \sum_{m \in \mathcal{M} \setminus n} l_m^t \, . \tag{4.13}$$

4.3 The Utility Company

Throughout this thesis, we assume that a single UC serves all the consumers in the neighbourhood. The UC runs a DSM scheme in order to reshape the load profile. To be more precise, they want to achieve a flatter profile such that investments into fast ramping technology, which is needed to deliver peak demand, can be reduced. The incentive for the users to limit consumption during peak hours is given by a dynamic pricing tariff: The cost per energy unit is calculated separately for each interval and depends on the aggregated load of all users in the neighbourhood. Following [Mohsenian-Rad et al., 2010, Yaagoubi and Mouftah, 2015b, Nguyen et al., 2015], we employ a quadratic cost function g^t:

$$g^t(y) = c_2 \cdot y^2 + c_1 \cdot y + c_0 \, , \quad t \in \mathcal{T} \, , \tag{4.14}$$

where y is the aggregated load at time t given by L^t and the coefficients $c_2 > 0$, $c_1 \ge 0$ and $c_0 \ge 0$. We employ a proportional billing scheme in a similar manner to [Soliman and Leon-Garcia, 2014, Mohsenian-Rad et al., 2010], where each participant of the DMS scheme pays for their share of the consumption, i.e. the electricity bill B_n yields

$$B_n = -\Omega_n \sum_{t \in \mathcal{T}} g^t \quad \forall n \in \mathcal{N} \, , \quad \text{with} \quad \Omega_n = \frac{\sum_t l_n^t}{\sum_t \sum_k l_k^t} \, . \tag{4.15}$$

For households that do not participate in the DSM scheme, a standard fixed-price tariff is employed, i.e.

$$B_m = p \sum_t l_m^t \quad \forall m \in \mathcal{M} \setminus \mathcal{N} \,. \tag{4.16}$$

4.4 Data Sets

For all the simulations performed in Part II, certain data sets are required. The title of this thesis gives an indicator about the nature of these with the key words "... prosumer communities...". *Prosumer* is a constructed neologism from the two words 'consumer' and 'producer'. This means we need data about consumption and production (from renewable resources). The scale of these values is specified by the second key word. We are interested in communities, i.e. neighbourhoods of residential households.

Within our approach, households play a game to establish equilibrium schedules for their battery usage. This game is played before the actual scheduling period and is based on forecased data for the respective time frame. We take data from the given data sets and treat it as if it was forecasted data. In order to analyse the effect of realistically forecasted data, we add random errors to the data at the time of executing the equilibrium schedules. The explicit calculations of the errors are discussed in Section 4.4.3. Before that, the data sets themselves are introduced in more detail.

4.4.1 Demand Data

Throughout the journey of this PhD, two different data sets for household demand data were used: (i) The "NREL data set" [NREL, 2008], and (ii) The "Ausgrid data set"[2] [Ausgrid, 2019].

NREL data set: NREL stands for 'National Renewable Energy Laboratory'. It is a governmental research institute in the USA that focusses on energy efficiency, sustainable transportation, and renewable power technologies [NREL, 2008]. Their data set contains hourly load profiles of residential building. It is based on simulated data according to the "Building America House Simulation Protocols" [U.S. Dept. of Energy, 2010]. Within these simulations they account for various types of fuel used for heating, the size of the property, the type of wall construction, the roofing material, and several more aspects. Statistical references of building types and their locations are taken from the "Residential Energy Consumption Survey" [U.S. Energy Information Administration, 2019]. Eventually, household demand data is

[2] Note that these names are not official, but rather established themselves during everyday usage.

Table 4.1. *NREL demand data.*
An overview of the specific locations that were picked from the complete NREL data set [NREL, 2008] is presented. All cities are in the state of New Jersey, USA. The mean demand indicates the average consumption per day of the specific household.

Location	Category	Mean Demand
Atlantic City	LOW	18.33 kWh
Belmar-Monmouth	LOW	18.25 kWh
Cape May	LOW	18.42 kWh
McGuire	LOW	18.52 kWh
Millville	LOW	18.41 kWh
Newark	LOW	18.59 kWh
Teterboro	LOW	11.78 kWh
Atlantic City	BASE	33.55 kWh
Belmar-Monmouth	BASE	33.49 kWh
Cape May	BASE	33.70 kWh
McGuire	BASE	34.11 kWh
Millville	BASE	33.73 kWh
Newark	BASE	34.26 kWh
Teterboro	BASE	24.11 kWh
Caldwell-Essex	BASE	32.97 kWh
Trenton-Mercer	BASE	25.18 kWh
Atlantic City	HIGH	48.67 kWh
Belmar-Monmouth	HIGH	48.46 kWh
Cape May	HIGH	49.12 kWh
McGuire	HIGH	49.98 kWh
Millville	HIGH	49.09 kWh
Newark	HIGH	50.27 kWh
Teterboro	HIGH	36.65 kWh
Caldwell-Essex	HIGH	47.28 kWh
Trenton-Mercer	HIGH	39.96 kWh

generated for all 1020 TMY3 locations[3] in the USA. For each location, there are three categories of users: BASE, HIGH, and LOW. For our simulations we chose 9 locations that are physically close to each other. Furthermore, the chosen houses are from a mixed humid climate which is comparable to the UK's climate. Table 4.1 provides further information on selected houses.

Ausgrid data set: The Ausgrid data set contains half-hourly demand data from 300 randomly selected households in Australia. Overall, they come from approximately 100 different postcodes. The data set recorded shiftable and non-shiftable loads between 1^{st} July 2010 and 30^{th} June 2013. For our purpose, we are using the sum of these values as the overall consumption of this particular user. Ratnam *et*

[3]TMY3 stands for the third edition of the typical meteorological year. It contains long-term average weather data for various specified locations.

al. [Ratnam, 2016] performed an extensive analysis of the complete data set. As part of their work, they proposed a cleaned version of the data set which eliminates households with incomplete data and extreme outliers. Eventually, this leaves 54 households that have complete, uninterrupted data over the course of one year. The interested reader is referred to their publication (cf. [Ratnam, 2016]) for further information.

4.4.2 Renewable Resource Data

As was the case with the demand data discussed in Section 4.4.1, there were two sources for household renewable energy production data: (i) The "UK power networks data set" [UK Power Networks, 2015], and (ii) The "Ausgrid solar data set" [Ausgrid, 2019].

UK power network data set: In their project entitled "Validation of PV Connection Assessment Tool" [UK Power Networks, 2015], the UK power networks collected data from residential solar panels between January 2012 and November 2014. The trial had the aim to determine the impact of high levels of solar penetration on the network. At 20 different trial sites in the UK, PV installations were monitored with an hourly frequency. For our simulations, we used the information of one particular site called "Forest road" which has a size of 3.7 kWp. This relies on the assumption that all households are closely located to each other, thus they should have the same profile of solar irradiance. To accompany for differently sized PV systems, the values are scaled suitably.

Ausgrid solar data set: The Ausgrid data set [Ausgrid, 2019] discussed in Section 4.4.1 also contains production data from solar PV installations. It was captured along with the demand data for the same half-hourly intervals. In contrast to the first solar power data set, here every household has their own solar PV system, ranging between 1.5 kWp and 9.99 kWp. To be consistent, we used data from the same 54 households of the cleaned data set as discussed above.

4.4.3 Computing Errors for Forecasted Data[4]

Since forecasting electricity consumption is out of the scope of this study, forecasts were simulated instead of produced by a forecasting algorithm. However, in order to consider forecasts as realistic, they must show some deviation from the actual consumption. As it has been reported that the average error in individual forecasted data is around 3% [Bichpuriya et al., 2016], some random error is added to the actual consumption values to produce sufficiently inaccurate forecasts.

[4] This subsection was partly submitted for publication in [Pilz et al., 2019a]

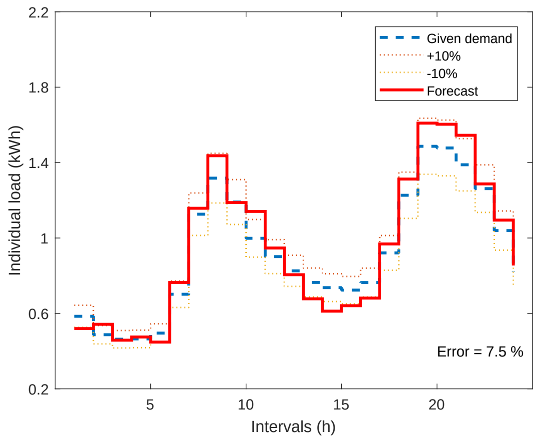

Figure 4.3. *Individual forecast created by adding random errors.*
While the dashed curve is the actual demand of an household, addition and subtraction of 10% are represented by the two dotted curves. The bold curve is one example of simulated forecast produced using the described method. Here, whereas the average error is 7.5%, there are some values outside the 10% error area.

Although errors could be added following a Gaussian law, the obtained forecasted profile would prove unrealistic since it would display random jumps. As a consequence, some smoothing effect is added by linking successive values. More specifically, for each value i, a random error is initially calculated e_i, then the actual error added to the value i is the average of the corresponding e_i and its neighbours, i.e.

$$E_i = \frac{1}{3}\left(e_{i-1} + e_i + e_{i+1}\right) . \tag{4.17}$$

As seen on Fig. 4.3, with this approach, simulated forecast is smoother and, as a consequence, more realistic.

4.5 Evaluation Metrics

Evaluation metrics are defined for two reasons: First, to quantify simulation results, and secondly to allow for comparison between our outcomes to those from other approaches in the literature. Due to the latter aspect it is natural to use metrics that have been used before. The three most important ones for this thesis are (i) The peak-to-average ratio (PAR) of the aggregated load, (ii) The self-consumption of a prosumer, and (iii) The savings off the energy bill.

The PAR value: In order to understand the PAR value, it is important to understand the term ‘load’. The load of a household is the amount of energy they request/draw from the utility company. Note that at a given point in time the load does not have to be equal to the actual consumption of the household, due to the usage of an energy storage system. Explicit mathematical connections between these quantities are given in Section 4.2.3. We are interested in the profile of the (aggregated) load of the households as this is relevant for the utility company. It requires specialised, fast-ramping technology to accommodate for peaks in household load which results in exponential cost increases [Bayram et al., 2014]. Furthermore, it would be beneficial to operate large-scale generation units at their point of highest efficiency and deliver a constant output. The PAR value is defined by

$$\mathrm{PAR} = \frac{\max_{t \in \mathcal{T}} L^t}{\frac{1}{T} \sum_{t \in \mathcal{T}} L^t}, \tag{4.18}$$

where $\mathcal{T}$ specifies the considered time period that is split into intervals indicated by t. Equation (4.18) shows that the PAR value is indeed defined as the ratio between the maximum value of the aggregated load L^t and its average over the time period $\mathcal{T}$. Following the discussion above, the optimal value is reached at 1.0. At this point the maximum is equal to the average value which describes a flat load profile. As a metric, we are both interested in the absolute value of the PAR as well as the relative change of it due to our solution.

Self-consumption: There are two sensible (but different) definitions for the term 'self-consumption'. In order not to confuse the reader, the one that was used in our paper [Pilz et al., 2019b], is adopted consistently throughout the thesis. It states: The renewable self-consumption rate of a household is the ratio between the renewable energy (from their own production) being used and its demand. This includes a direct part which is consumed immediately and an indirect part used to charge the battery when the generation exceeds the local demand. Higher self-consumption rates indicate a better utilisation of the available resources and are thus preferred.

Savings: Within our models, the possibility of saving money off the electricity bill is the key incentive proposed to the households. Under the assumption of full rationality, it is their desire to reduce their energy bill. When evaluating simulation runs, we compare the electricity bill for two scenarios: Firstly, a scenario which employs the respective billing scheme but does not utilise the proposed approach. Secondly, a scenario which utilises the approach. Both of these are run on exactly the same data. This then enables a direct relative comparison for each household. We are both interested in the savings of each individual as well as the difference between the households.

This almost blank page is intentional.

Part II

Contributions

This almost blank page is intentional.

Chapter 5

A Static Scheduling Game with Advanced Battery Model

Demand-side management (DSM) usually refers to the control of energy consumption by the utility company (UC) at the customer side. It relies on the two-way communication and energy transmission capabilities of the future smart grid [Ipakchi and Albuyeh, 2009]. In general, the main objective of such programs is to decrease the consumption during peak times and thus reduce the costs that are associated with peak loads [Bayram et al., 2014]. On the one hand, the practical implementation can be direct (i.e. through smart meters that shift high-power household appliances based on signals from the UC). On the other hand, the UC can indirectly incentivise the users to shift these loads themselves by time-of-use tariffs. Within these tariff schemes, the price per energy unit changes depending on the aggregated load of all users (cf. [Soliman and Leon-Garcia, 2014, Ma et al., 2017b, Celik et al., 2017]). Both ways can lead to a reduction of the peak-to-average ratio (PAR) of the aggregated load, which in turn increases the stability and power quality of the grid [Bayram et al., 2014].

Several such scenarios have been studied in the past and show great potential [Mohsenian-Rad et al., 2010, Wang et al., 2015b, Haider et al., 2016a, Soliman and Leon-Garcia, 2014]. However, there remains one issue: all of them interfere with the routines of users, who might not want to give away the freedom to run their appliances whenever they want. The tradeoff between comfort and energy costs has been addressed, for instance, in [Yaagoubi and Mouftah, 2015b]. In their study, they show that the amount of savings from the energy bill reduces by more than half of the optimum when acceptable comfort levels are preserved.

In this chapter[1], we investigate a scenario that does not interrupt the habits of the customers. Instead of shifting the loads directly, autonomously managed battery storage systems can be employed to achieve the same net effect. The idea is not new, but has been pushed forward, for instance, in [Nguyen et al., 2015, Mohsenian-Rad, 2016, Longe et al., 2017]. Within the idea of using the battery system as a load-shifting tool, it is essential to have a high-quality battery model. This is what was lacking in the literature at that point in time, but is now provided in our manuscript [Pilz et al., 2017b]. In this sense, the research in this chapter can be seen as an extension to [Nguyen et al., 2015], where a more realistic battery model replaces the one used in [Nguyen et al., 2015]. Only when all inherent characteristics of the whole system are incorporated can an insightful analysis be done. In fact, we will see that with an advanced battery model the outcome of the game changes drastically. Thus, the contributions covered in this chapter are the following:

(1) Analysis of the influence of the efficiency parameters of the battery on the PAR value and the resulting savings for each household, and

(2) Analysis of the participants' behaviour in the battery scheduling game.

The chapter is structured as follows. We introduce a static non-cooperative battery scheduling game in Section 5.1 including the battery model introduced in Section 4.2.1. Households decide between four discrete activities for each time slot when creating their day-ahead schedule. Furthermore, the solution approach and computational effort are highlighted. In Section 5.2, we analyse how an ideal battery, i.e. with 100% efficiency, differs from a system with realistic efficiency in terms of reducing the peak-to-average ratio of the load. Furthermore, the participation behaviour is analysed with a focus on how the battery efficiency, and consumer type influences it. To this end, we look at the activity occurrence within the equilibrium schedules, and the overall involvement rates. Section 5.3 includes discussions for the aforementioned results and Section 5.4 concludes this chapter.

5.1 The Battery Scheduling Game

In this section, the scheduling game is defined and the solution approach based on a best-response algorithm is discussed.

[1] An earlier version of the content of this chapter was presented at the IRCSEEME 2017 and awarded with the "Best Paper Prize" [Pilz et al., 2017a]. Subsequently, the sponsors of the conference invited us to revise and refine the manuscript to be submitted for peer review. The paper was eventually published after two rounds of revisions (cf. [Pilz et al., 2017b]). Please note that the chapter is not a copy of a paper, but rather an adjusted version of it to fit into the story of the thesis.

5.1.1 Decision Variables

Each household $n \in \mathcal{N}$ in the neighbourhood (cf. Figure 4.1) that owns an energy storage system will be a participant of the game. The decisions they take are day-ahead schedules $\mathbf{a}_n = [a_n^0, \dots, a_n^{T-1}]$. The battery activity a_n^t of household $n \in \mathcal{N}$ in interval $t \in \mathcal{T}$ can take on the following discrete values in reference to the battery model introduced in Section 4.2.1:

$$a_n^t = \begin{cases} 0 & \alpha_0 \mathrel{\hat{=}} \text{remain idle and subject to self-discharging} \\ \frac{1}{2}\phi^+ & \alpha_1 \mathrel{\hat{=}} \text{charge for half the interval} \\ \phi^+ & \alpha_2 \mathrel{\hat{=}} \text{charge for the full interval} \\ -d_n^t & \alpha_3 \mathrel{\hat{=}} \text{use the battery to fulfil demand} \end{cases} \tag{5.1}$$

Note that we introduced specific labels $\alpha_0 - \alpha_3$ to refer to the respective activities. Actions are deemed unplayable if they lead to invalid battery states, i.e. charge states that do not fulfil the requirements given in Section 4.1. The fact that there are two possibilities to charge the battery gives more flexibility for the user.

5.1.2 Definition

The objective for a rational player when playing a non-cooperative is always to maximise their individual utility value. In our model this is defined through the utility function $u_n(\mathbf{a}_n, \mathbf{a}_{-n})$. It reflects the bill player n has to pay for the upcoming day, given that they chose schedule $\mathbf{a}_n$, while their opponents chose the schedules $\mathbf{a}_{-n} = [\mathbf{a}_1, \dots, \mathbf{a}_{n-1}, \mathbf{a}_{n+1}, \dots, \mathbf{a}_N]$. We employ the proportional billing scheme introduced in Section 4.3 [Soliman and Leon-Garcia, 2014, Mohsenian-Rad et al., 2010], i.e.:

$$u_n(\mathbf{a}_n, \mathbf{a}_{-n}) = -\,\Omega_n \cdot \sum_{t \in \mathcal{T}} g^t \ , \quad \text{with} \quad \Omega_n = \frac{\sum_t l_n^t}{\sum_t \sum_k l_k^t} \ . \tag{5.2}$$

To sum up, we define the non-cooperative battery scheduling game $G = (\mathcal{N}, \mathcal{A}, \mathbf{u})$ in normal-form (cf. Definition 2.1), with

- the set of players $\mathcal{N}$,
- $\mathcal{A} = \mathcal{A}_1 \times \cdots \times \mathcal{A}_N$, where the set $\mathcal{A}_n$ consists of all valid schedules for player n, and
- $\mathbf{u} = [u_1, \dots, u_N]$, with the utility function $u_n : A \to \mathbb{R}$ for player n (cf. (5.2)) .

One can show that there exists a pure Nash equilibrium (NE) for this game. The proof can be done similarly to the one in [Nguyen et al., 2015] (Theorem 1), due to the similarity of the structure of the utility functions, the properties of the actions sets, and the fact that the demand d_n^t is bounded.

5.1.3 Solution Approach

The solution to the game (i.e. an NE) is computed by a best-response algorithm (cf. Algorithm 1). Through empirical studies, we found that there are usually many different NEs for each daily configuration. This is why the algorithm contains the additional *do*-loop in comparison to the "myopic best-response" algorithm [Shoham and Leyton-Brown, 2009] introduced in Section 2.3.

Algorithm 2: Best-response algorithm for finding a pure NE based on [Shoham and Leyton-Brown, 2009]

```
initialise counter
do
    initialise random action profile a = [a_n, a_{-n}]
    while there exists a player n for whom a_n is not a best response to a_{-n} do
        â_n ← some best response by n to a_{-n}
        a ← (â_n, a_{-n})
    end
    save equilibrium action profile a
    increase counter
while maximum counter not reached;
select 'best' equilibrium
```

Choosing the best NE is done by comparing the sum of the utility functions for every player. Please note that even when the existence of a pure NE is guaranteed, the algorithm might not converge to it. An additional counter variable prevents getting stuck in an infinite *while*-loop. Nevertheless, this exit condition was not triggered in any of our simulation runs.

In order to put the computational effort of this algorithm into perspective (especially in light of the upcoming chapter), let us look more specifically at what it means to determine the best response. We make use of a brute force approach. Due to the discretisation of the battery activities, i.e. four valid activities (cf. (5.1)), the number of possible schedules $\mathbf{a}_n$ is bounded. Depending on the number of intervals T, it can be computed to be 4^T. A day split into four-hour intervals, i.e. $T = 6$, results in 4,096 potential schedules. Halving this interval duration, i.e. $T = 12$, already allows for 16,777,216 schedules.

During the simulation each schedule is tested on whether it would lead to an invalid battery status and then the one that maximises the utility function is established. This process is performed for each household and repeated until convergence.

5.2 Performance Evaluation

In this section, our results are summarised. Firstly, we specify the specific simulation parameters. Secondly, the outcomes for the PAR reduction based on different battery types are presented. Lastly, the dependency of the results based on the consumer-type is investigated.

5.2.1 Parameters

The household consumption data for all simulations in this section stem from the NREL dataset [U.S. Dept. of Energy, 2013] (cf. Section 4.4). We picked $N = 25$ households (i.e. nine BASE, nine HIGH, and seven LOW) that are all within close vicinity to represent a small neighbourhood. In order to gain insight into seasonal effects, we chose four equally separated weeks from the data set, i.e. in particular weeks 12, 25, 38 and 51, and used it to represent the individual household demand. Nevertheless, the scheduling is done on a day-ahead basis as described in Section 5.1. To this end, we set $T = 12$, i.e. consider two-hour intervals, and initialise the battery at the beginning of the week with a small random capacity. From a NE, the battery states at the end of the day can be calculated and are used as initial data for the following day.

The parameters of the battery are inspired by the *Tesla Powerwall 2* [Tesla, 2017] data sheet, and can be found in Table 5.1. The efficiency variables η^+ and η^- are calculated under the assumption that charging and discharging contribute to equal amounts towards the given round-trip efficiency of $0.918 = \eta^+ \cdot \eta^-$. We denote this type of battery by the "realistic" battery (RB) model. For comparisons, we also run all the simulations with an "ideal" battery (IB) model, i.e. the same storage system but with $\eta^+ = \eta^- = 1$. We want to highlight that the IB still follows

Table 5.1. *Battery parameters.*
Parameters for a Tesla-inspired [Tesla, 2017] home battery storage system used throughout all simulations runs labelled with "realistic".

Variable	Value
η^+	0.958
ρ^+	3.3 kW/h
η^-	0.958
ρ^-	−3.3 kW/h
$\bar{\rho}$	−0.001
$s_{\max}$	14.0 kWh
$s_{\min}$	0.5 kWh
s^*	9.96 kWh

the proposed charging and discharging curves shown in Figure 4.2 and is also subject to self-discharging. Within the cost function (4.14), we use the coefficients $c_2 = 0.03125\,\$/\mathrm{MW}^2$, $c_1 = 1.0\,\$/\mathrm{MW}$, and $c_0 = 0$ [Rahbar et al., 2015].

5.2.2 Peak-to-Average Ratio

In Figure 5.1, the aggregated load curves resulting from playing the game with different battery models are shown – one of them with realistic parameters and the other with ideal 100% efficiency (see Section 5.2.1). The reference curve represents

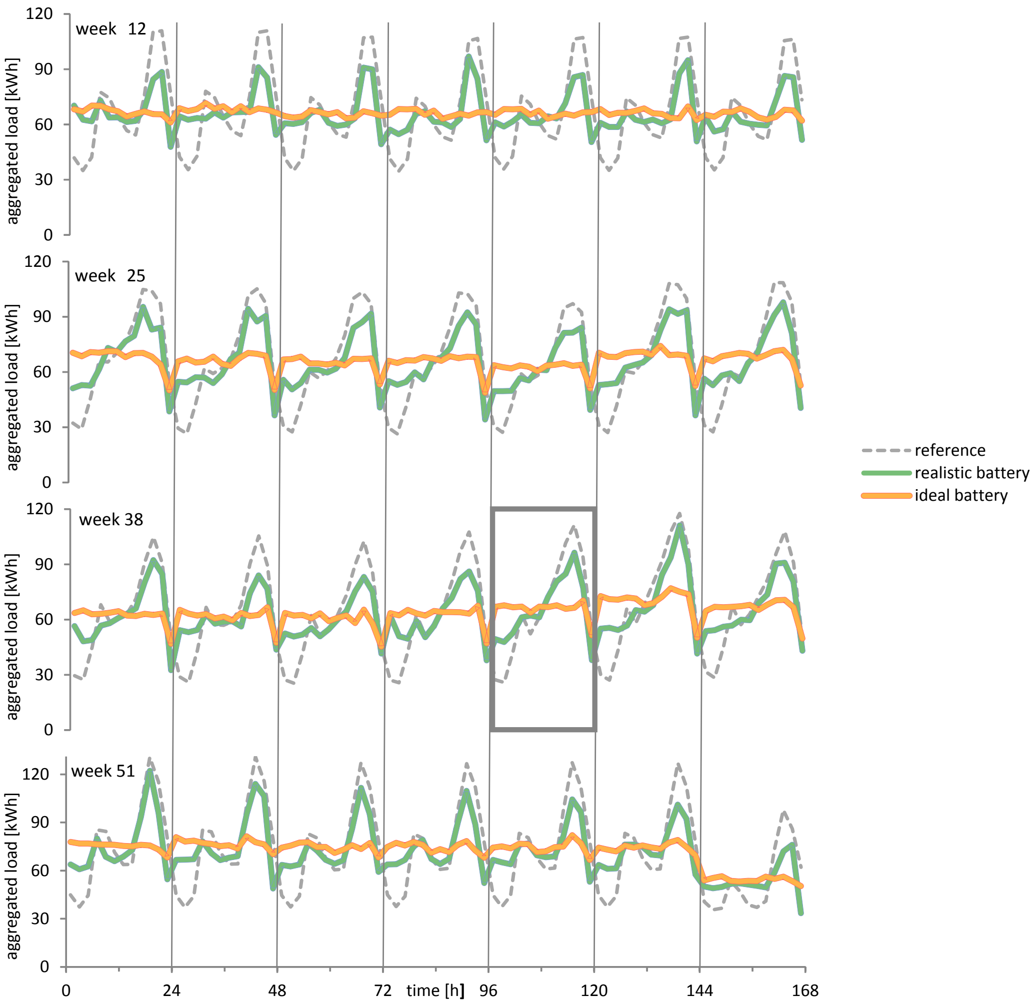

Figure 5.1. *Aggregated load curves over four different one-week periods.* The results for week 12, week 25, week 38, week 51 in the data set [U.S. Dept. of Energy, 2013] are presented. For each week, the results for not playing the game (reference) can be compared to the results obtained from playing the game with either a realistic battery or an ideal battery model. For week 38, day 5 is highlighted in reference to the results shown in Figure 5.2.

Table 5.2. *Peak-to-average ratios.*
Peak-to-average ratios of the aggregated load calculated as the average over the individual days of week 12, week 25, week 38, and week 51. The case without storage system and both battery models are shown. The average μ is given over the four week period. IB: "ideal" battery; RB: "realistic" battery.

	Reference	**RB Model**	**IB Model**
w12	1.623	1.374	1.044
w25	1.574	1.410	1.059
w38	1.685	1.439	1.077
w51	1.718	1.468	1.056
μ	1.650	1.423	1.059

the aggregated load of the system without the battery scheduling game. The average PAR values (cf. Section 4.5) over the seven days of the respective weeks are shown in Table 5.2. On average, a 14% and a 36% decrease of the PAR value was achieved by employing a game with an RB and IB model, respectively.

5.2.3 Consumer-Type Analysis

When considering the participation behaviour of the households, we look at two things: (i) the rate at which players choose to play any action other than the *zero*-schedule $\mathbf{a}_n = [\alpha_0, \alpha_0, \dots, \alpha_0]$ in the Nash equilibrium (cf. (5.1)); and (ii) the distribution of activities chosen for each individual interval. A visualisation of the

Table 5.3. *Comparison of involvement rates.*
A comparison of involvement rates depending on the battery model and consumption category is shown. Results are obtained by averaging over all weeks.

	RB Model	**IB Model**
LOW	68%	36%
BASE	98%	82%
HIGH	87%	64%

Table 5.4. *Activity occurrence*
Occurrence of different activities within the equilibrium schedules for different player categories and both battery models. Results are obtained by averaging over all weeks.

	RB Model				**IB Model**			
	α_0	α_1	α_2	α_3	α_0	α_1	α_2	α_3
LOW	81%	6%	0%	13%	75%	6%	2%	18%
BASE	72%	11%	1%	16%	39%	17%	9%	34%
HIGH	76%	9%	3%	12%	56%	14%	8%	23%

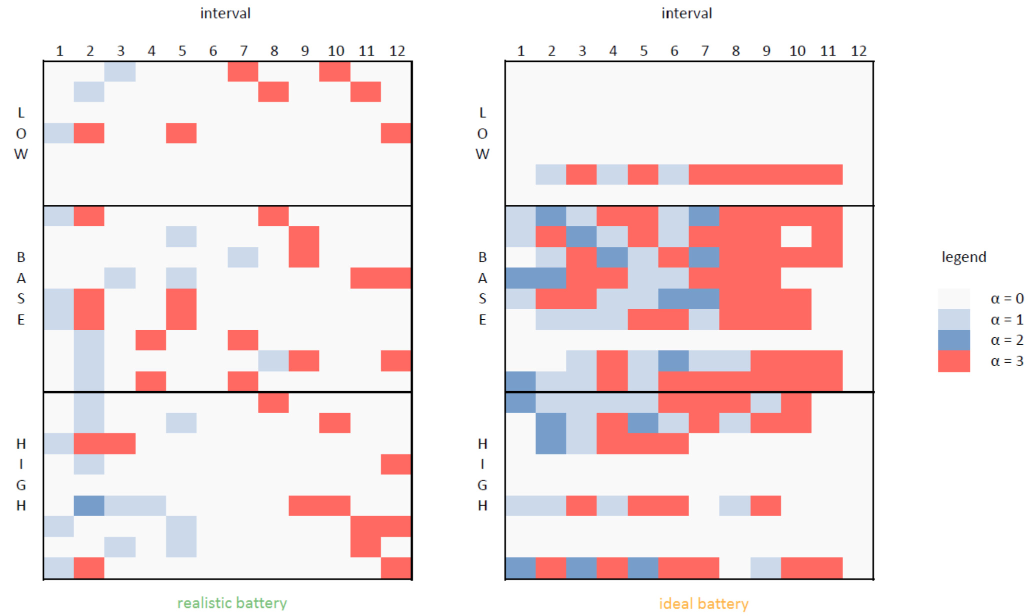

Figure 5.2. *Illustration of equilibrium schedules.*
Illustration of Nash equilibrium for the scheduling game at day 5 in week 38. Each row represents a schedule (i.e. a set of options – one for each interval; cf. (5.1)), chosen by the respective player. On the left, the results under consideration of a realistic battery model are shown, whereas on the right an ideal battery model is applied.

schedules of a randomly chosen day (week 38, day 5) is shown in Figure 5.2 for both battery models. It can be seen as a representative example of the schedules for all other days. A summary for the different user classes of the involvement rate and the activity distribution can be found in Tables 5.3 and 5.4, respectively.

Table 5.5 shows by how much the utility function of the consumers, i.e. the energy costs for each of them, was reduced. The results for each of the four different weeks are averaged over the consumer categories for both battery models.

5.3 Discussions

In this section, we discuss the results presented in the previous section and explain the most interesting outcomes of this study.

5.3.1 Peak-to-Average Ratio

By playing the game the usual evening peaks of each individual day were decreased. This effect was stronger for simulation runs that apply an IB model, where an almost flat load profile was produced. Troughs are visible at the end of several

Table 5.5. *Reduction of utility values.*
Amount of reduction of the utility function (i.e. energy costs). Results averaged over the different consumption categories are shown for each week together with an overall average μ.

	RB Model			**IB Model**		
	LOW	BASE	HIGH	LOW	BASE	HIGH
week 12	6.4%	6.5%	6.3%	7.1%	7.1%	7.1%
week 25	6.0%	6.2%	6.1%	8.8%	8.8%	8.8%
week 38	6.8%	6.8%	6.8%	8.9%	8.9%	8.9%
week 51	6.7%	6.6%	6.4%	8.1%	8.0%	8.1%
μ	6.5%	6.5%	6.4%	8.2%	8.2%	8.2%

days (e.g., in weeks 25 and 38) due to a finite-horizon effect that occurs when the aggregated demand during the final interval is lower than the average load in the previous intervals. This results in the players choosing to play α_0 in the respective interval, see Figure 5.2. As the load can only be increased by charging the battery, this would have caused an increase in costs (for this day) and thus would not have been beneficial for the players.

From our results we see the importance of the battery efficiency for reducing the PAR value. With state-of-the-art technology such as the *Tesla Powerwall 2* [Tesla, 2017], the PAR value was reduced by 14% to ≈ 1.4. Under the assumption of an IB, PAR values close to the optimum were achieved (i.e. a reduction of 36%). It is worth highlighting that these results do not seem to depend on seasonal effects, as fluctuations of PAR values between the four simulated weeks were less than 0.05.

5.3.2 Involvement in the Game

We observe that the involvement rate was higher overall for the RB model. Nevertheless, the players who did participate in the IB scheduling game were more active, i.e. chose more activities $a \neq \alpha_0$. It becomes apparent that the lack of efficiency causes a disincentive to charge the battery for many users. While charging for shorter time periods (i.e. α_1) was still occasionally done during low-demand intervals, charging throughout the whole interval (i.e. α_2) was almost non-present in the NE schedules. None of the LOW households with an RB made use of this activity within any of the 28 simulated days (cf. Figure 5.2).

5.3.3 Utility Function

In direct relation to the smaller PAR value reduction of the game with RB model is the smaller reduction in energy costs (see Table 5.5). Similar to results regarding the PAR value, we observe that there seems to be no seasonal dependency. Furthermore, within each separate week, the differences between the three consumer classes is negligible. This was anticipated and intentionally pushed forward by the introduction of the proportionality factor Ω_n in the utility function (5.2). It should be noted that the pricing scheme benefits all users whether they participate in the DSM scheme or not. A tariff that gives a higher share of savings towards the contributors might be a fairer approach.

5.4 Conclusions

In this chapter, we investigated an advanced battery model for a DSM program: residential customers play a battery scheduling game to decrease their own costs which eventually reduce the PAR value of the aggregated neighbourhood load. The advantage of this approach is that every household can make its own decision, thereby addressing concerns of individual freedom.

It turns out that the round-trip efficiency of the storage system has a negative impact on the participants' behaviour. In fact, it lowers the PAR reduction by more than half of what can be achieved by a system with perfect efficiency. This is accompanied by a lower reduction in energy bills for all participants. Thus, our studies underline the importance of further advancements in battery technology. An important question arises: How can we positively impact the participation behaviour given a realistic battery system? The answer will lie in a more advanced game-theoretic approach and is the topic of the following chapter.

CHAPTER 6

A Dynamic Scheduling Game with Forecasting Errors

Day-ahead scheduling that does not interfere with the users can solely be realised through energy storage systems. [Nguyen et al., 2015, Pilz et al., 2017b] followed this approach and showed that considerable gains are achievable without interrupting the habits of the consumers. Nguyen *et al.* [Nguyen et al., 2015] put their focus on developing a distributed algorithm, while we [Pilz et al., 2017b] implemented an advanced battery model, providing insight into how specific battery characteristics influence the participation behaviour and thus the outcome of the game.

In this chapter[1], we build on these previous results and extend the approach of Chapter 5 in two directions. Firstly, we introduce a more sophisticated underlying game structure for the demand-side management (DSM) scheme, namely a discrete time dynamic game. Within this formulation the action space is continuous instead of the discrete options available in Chapter 5 [Pilz et al., 2017b]. As a consequence, the players can make more fine-grained decisions which improves their outcome. Another advantage is that this allows for the derivation of a best response strategy and thus does not require a computationally expensive search for the best response. Secondly, we analyse the influence of the forecasting error for demand and energy generation on the scheduling outcome. In order to assure the stability of the grid,

[1]The content provided here has been peer-reviewed and published in [Pilz and Al-Fagih, 2019a]. Furthermore, it was partly rewritten to fit the flow of the thesis.

a real-world application requires the mechanism to be resilient against eventual errors in the predictions, as they will undoubtedly occur.

The contributions of this chapter can be summarised as follows:

(1) We introduce a novel discrete time dynamic game for energy storage scheduling among prosumers in the smart grid. The closed form solution to the best-response problem is derived by means of a dynamic-programming approach. The ensuing iterative algorithm converges quickly towards the Nash-equilibrium. Direct comparison to similar approaches, i.e. [Nguyen et al., 2015, Pilz et al., 2017b, Yaagoubi and Mouftah, 2015b], reveals the superiority both in terms of achieved peak-to-average ratio (PAR) reduction and computational costs.

(2) A complete day-ahead DSM scheme, consisting of prosumers with realistically modelled batteries, local renewable energy resources, and forecasting errors for demand and generation is simulated. In contrast to previous works (e.g. [Nguyen et al., 2015, Soliman and Leon-Garcia, 2014, Mohsenian-Rad et al., 2010] which merely simulate individual days, our scheduling period covers a full year. The length of the simulation allows for an in-depth analysis of the influence of the forecasting errors as well as the impact of the number of participants in the DSM scheme.

(3) We show that the proposed dynamic game approach is robust with respect to the forecasting errors, even in the worst-case scenario. The respective results exhibit only small deviations in the PAR reduction outcomes compared to runs with accurate predictions, and hardly any influence on the financial benefits for the DSM participants. This is furthermore supported by an extensive analysis of scenarios with randomly generated battery and generation parameters, indicating the overall robustness of our game-theoretic approach.

(4) We present a comparison of how different compositions of neighbourhoods perform in the DSM scheme. We find that a community consisting of a mix of consumer types can achieve best results.

The chapter is structured as follows. In Section 6.1, an advanced discrete time dynamic non-cooperative game is introduced. Its advantage is that the action space is continuous in contrast to the discrete actions of the previously analysed game (cf. Section 5.1). Based on the formulation of subgames and a dynamic programming (DP) approach, we derive an analytic expression for the best-response of an individual player. Through this, a speedup of several orders of magnitude is achieved when compared to the simulation runs in Chapter 5. Section 6.2 shows our simulation results. Firstly, we provide insight into the convergence behaviour of the scheduling algorithm. Secondly, a detailed comparison to the results of the static non-cooperative game is presented, revealing considerable improvements. We follow up with simulations to investigate the influence of participation rate and forecasting error on the gains in terms of PAR reduction. Furthermore, we study different distributions of consumer types within a community and provide evidence for the robustness of the game-theoretic approach by simulating many randomly generated scenarios. Finally, the influence of the pricing parameters is investigated. Eventually, in Section 6.3, the results of the preceding section are discussed and whenever suitable compared to the relevant literature.

6.1 The Dynamic Battery Scheduling Game

In this section, we formulate the non-cooperative dynamic game between the households that possess individual energy storage and photovoltaic (PV) installations. To do so, we introduce the relevant notation and relate it to their respective 'real-world' meaning according to our system (cf. Section 4.1). Furthermore, the notion of a Nash equilibrium (NE) is defined and an important result concerning the link between the NE for the whole game and the NE for a subgame is provided. Subsequently a DP algorithm is presented from which we derive a closed form expression of the best response, i.e. the best decision a player can make in response to fixed decisions of other players. Eventually we use this result to construct an iterative algorithm that computes an NE of the game.

6.1.1 Definitions and Game Formulation

Formally, the game belongs to the category of discrete time dynamic games (cf. [Nie et al., 2006]), where players make their decisions sequentially in stages. These stages directly correspond to the daily intervals introduced in Section 4.1. For each stage we define a state of the game, i.e. the current state-of-charge (SOC) of all batteries, representing the configuration of the overall system. Furthermore, we define a transition equation that models the evolution of this state based on the decisions of the players. In other words, the players will choose actions that are directly related to their battery usage, which in turn depends on the state of the game. We consider a game with open-loop information structure, which means that the initial state of the game is known by all players. In this game, players want to minimise their energy bill, i.e. their utility function, which depends not only on their own but also on the decisions of all other players. In a nutshell, we have:

Definition 6.1. Our discrete time dynamic game with open-loop information structure consists of the following components:

(1) A set of *players*, i.e. participating households (cf. Section 4.2), $\mathcal{N} = \{1, 2, \ldots, n, \ldots, N\}$, where N denotes the number of players.

(2) A set of *stages*, i.e. intervals (cf. Section 4.1), $\mathcal{T} = \{0, 1, \ldots, t, \ldots, T-1\}$, where T denotes the number of stages and thus the number of decisions a player can make in the game.

(3) Scalar *state variables* $s_n^t \in \mathcal{S}_n \subset \mathrm{I\!R}$ denoting the SOC of the nth player's battery at stage $t \in \mathcal{T} \cup \{T\}$. Collectively, we denote the state variables of all players at stage t by $\mathbf{s}^t := \left[s_1^t, s_2^t, \ldots, s_N^t\right] \in \mathcal{S} := \mathcal{S}_1 \times \mathcal{S}_2 \times \cdots \times \mathcal{S}_N \subset \mathrm{I\!R}^N$. In the open-loop information structure it is assumed that the *initial state* s^0 is known[2] to all players $n \in \mathcal{N}$.

(4) Scalar *decision variables* $a_n^t \in \mathcal{H}_n^t\left(s_n^t\right) \subset \mathcal{A}_n \subset \mathrm{I\!R}$ (for definition of $\mathcal{H}_n^t$ see item (5) and Section 4.2.1) denoting the usage of the battery of the nth player at time $t \in \mathcal{T}$. Collectively, we denote the decision variables of all players at stage t by $\mathbf{a}^t := \left[a_1^t, a_2^t, \ldots, a_N^t\right] \in \mathcal{A} := \mathcal{A}_1 \times \mathcal{A}_2 \times \cdots \times \mathcal{A}_N \subset \mathrm{I\!R}^N$. Furthermore we define the *schedule of battery usage* of an individual player $n \in \mathcal{N}$ as a collection of all its decisions in the stages of the game by $\mathbf{a}_n := \left[a_n^0, a_n^1, \ldots, a_n^{T-1}\right]$. A *strategy profile* is denoted by $\mathbf{a} := [\mathbf{a}_1, \mathbf{a}_2, \ldots, \mathbf{a}_N]$.

(5) A set of *admissible decisions* $\mathcal{H}_n\left(s_n^0\right) := \left\{\mathbf{a}_n \mid h_n^t\left(s_n^t, a_n^t\right) \leq 0,\ t \in \mathcal{T}\right\} \subset \mathrm{I\!R}^T$ for the nth player. The function $h_n^t\left(s_n^t, a_n^t\right)$ has been defined in (4.9) Section 4.2.1, capturing the restrictions posed on the battery. We denote $\mathcal{H}_n^t\left(s_n^t\right) := \left\{a_n^t \mid h_n^t\left(s_n^t, a_n^t\right) \leq 0\right\} \subset \mathrm{I\!R}$

(6) A *state transition equation*

$$s_n^{t+1} = f_n^t\left(s_n^t, a_n^t\right), \quad t \in \mathcal{T},\ n \in \mathcal{N}, \tag{6.1}$$

governing the state variables $\left\{\mathbf{s}^t\right\}_{t=0}^T$. The function $f_n^t\left(s_n^t, a_n^t\right)$ is the discretised version of the transition equation (4.8) defined in Section 4.2.1, showing how a decision of the player influences the state of its battery for the upcoming stage.

[2] Later we will see that the solutions/schedules require the players to deplete their battery towards the end of the scheduling period (cf. finite horizon effect) to achieve maximum utility. This means as long as none of the players deviates from their respective schedule this knowledge is implicitly shared.

(7) A *stage additive utility function*

$$u_n\left(s_n^0,[\mathbf{a}_n,\mathbf{a}_{-n}]\right) = -g_n^T\left(s_n^T\right) - \sum_{t=0}^{T-1} g_n^t\left(s_n^t,\left[a_n^t,\mathbf{a}_{-n}^t\right]\right) \tag{6.2}$$

for the nth player, where $\mathbf{a}_{-n} := [\mathbf{a}_1,\mathbf{a}_2,\ldots,\mathbf{a}_{n-1},\mathbf{a}_{n+1},\ldots,\mathbf{a}_N]$ denotes the decisions of all other players. The function $g_n^t\left(s_n^t,\left[a_n^t,\mathbf{a}_{-n}^t\right]\right)$ has been defined in (4.14) Section 4.3 capturing the costs to the nth player at the tth stage. Note that the utility function depends only on the initial state variable s_n^0, since the subsequent is presented states s_n^t are determined by (6.1). The function

$$g_n^T\left(s_n^T\right) = s_n^T \tag{6.3}$$

can be interpreted as a penalty for the nth player that is incurred by ending up in state s_n^T, i.e. its SOC, at the end of the scheduling period.

Each participant of the game is thought to be rational, i.e. they are only interested in improving their individual utility value (6.2). We represent the decision problem of the nth player as the following optimisation problem:

$$\boxed{\begin{array}{lll} G_n(\mathbf{a}_{-n}) & \text{given} & \mathbf{s}^0 \in \mathcal{S} \\ & \underset{a_n}{\text{maximise}} & u_n\left(s_n^0,[\mathbf{a}_n,\mathbf{a}_{-n}]\right) \\ & \text{subject to} & a_n^t \in \mathcal{H}_n^t\left(s_n^t\right) \\ & & s_n^{t+1} = f_n^t\left(s_n^t,a_n^t\right)\ \forall t \in \mathcal{T}\cup\{T\} \end{array}} \tag{6.4}$$

Moreover, the game is referred to as $\{G_1,G_2,\ldots,G_N\}$.

Definition 6.2. A strategy profile $\hat{\mathbf{a}} = [\hat{\mathbf{a}}_1,\ldots,\hat{\mathbf{a}}_N]$ is a *Nash equilibrium* for the game $\{G_1,\ldots,G_N\}$ if and only if for all players $n \in \mathcal{N}$ we have

$$u_n\left(s_n^0,[\hat{\mathbf{a}}_n,\hat{\mathbf{a}}_{-n}]\right) \geq u_n\left(s_n^0,[\mathbf{a}_n,\hat{\mathbf{a}}_{-n}]\right),\ \ \forall \mathbf{a}_n \in \mathcal{H}_n\left(s_n^0\right)\ . \tag{6.5}$$

6.1.2 Analysis of the Game

In order to analyse the game $\{G_1,\ldots,G_N\}$, we follow the DP idea by Nie *et al.* [Nie et al., 2006]. To do so, we introduce notation for subproblems of (6.4). Furthermore, we show an important result about Nash equilibria for these subproblems, which constitutes the basis for the DP-algorithm. Applying the general algorithm eventually leads us to an analytic formulation of the nth player's best response $\hat{\mathbf{a}}_n$, given the strategies $\mathbf{a}_{-n}$ of other players.

6.1.2.1 Subgame Formulation

For subproblems that are only interested in decisions taken from stage t' onwards, we write:

$$\mathbf{s}_n^{t',T-1} := \left[s_n^{t'},\ldots,s_n^{T-1}\right], \ \mathbf{s}^{t',T-1} := \left[\mathbf{s}^{t'},\ldots,\mathbf{s}^{T-1}\right]$$
$$\mathbf{a}_n^{t',T-1} := \left[a_n^{t'},\ldots,a_n^{T-1}\right], \ \mathbf{a}^{t',T-1} := \left[\mathbf{a}^{t'},\ldots,\mathbf{a}^{T-1}\right]$$
$$u_n^{T-t'}\left(s_n^{t'},\left[\mathbf{a}_n^{t',T-1},\mathbf{a}_{-n}^{t',T-1}\right]\right) = -g_n^T\left(s_n^T\right) - \sum_{\tau=t'}^{T-1} g_n^\tau\left(s_n^\tau,\left[a_n^\tau,\mathbf{a}_{-n}^\tau\right]\right)$$
$$\mathcal{H}_n^{t',T-1}\left(s_n^{t'}\right) := \left\{\mathbf{a}_n^{t',T-1} \mid h_n^\tau\left(s_n^\tau,a_n^\tau\right) \le 0, \ \tau = t',t'+1,\ldots,T-1\right\} .$$

For $t' \in \mathcal{T}$ we define a subproblem of the nth player as the following optimisation problem:

$$\begin{array}{lll} G_n^{T-t'}\left(\mathbf{a}_{-n}^{t',T-1}\right) & \text{given} & \mathbf{s}^{t'} \in \mathcal{S} \\ & \underset{\mathbf{a}_n}{\text{maximise}} & u_n^{T-t'}\left(s_n^{t'},\left[\mathbf{a}_n^{t',T-1},\mathbf{a}_{-n}^{t',T-1}\right]\right) \\ & \text{subject to} & \mathbf{a}_n^{t',T-1} \in \mathcal{H}_n^{t',T-1}\left(s_n^{t'}\right) \\ & & s_n^{t+1} = f_n^t\left(s_n^t,a_n^t\right) \ \forall t \in \{t',t'+1\ldots,T-1\} \end{array} \tag{6.6}$$

Therefore, the subgame is referred to as $\left\{G_1^{T-t'},G_2^{T-t'},\ldots,G_N^{T-t'}\right\}$.

Theorem 6.3. Let $\hat{\mathbf{a}} = \left[\hat{\mathbf{a}}^0,\ldots,\hat{\mathbf{a}}^{T-1}\right]$ constitute a Nash equilibrium for the game $\{G_1,\ldots,G_N\}$ with the corresponding trajectories of states $\hat{\mathbf{s}} = \left[\hat{s}^0,\ldots,\hat{s}^T\right]$. Consider the subgame $\{G_1^{T-t},\ldots,G_N^{T-t}\}$ for each $t \in \mathcal{T}$. Then, the truncated strategy $\hat{\mathbf{a}}^{t,T-1} = \left[\hat{\mathbf{a}}^t,\hat{\mathbf{a}}^{t+1},\ldots,\hat{\mathbf{a}}^{T-1}\right]$ comprises a Nash equilibrium for the subgame $\{G_1^{T-t},\ldots,G_N^{T-t}\}$.

Proof. We prove the theorem by contradiction. Suppose $\hat{\mathbf{a}}^{t,T-1}$ is not a Nash equilibrium to the subgame $\{G_1^{T-t},\ldots,G_N^{T-t}\}$. Then, for some $n \in \mathcal{N}$, there must exist another strategy $\bar{\mathbf{a}}_n^{t,T-1}$ with the corresponding sequence of states $\{\bar{\mathbf{s}}_n^\tau\}_{\tau=t}^T$ such that

$$u_n^{T-t}\left(\left(\bar{s}_n^t,\hat{\mathbf{s}}_{-n}^t\right),\left(\bar{\mathbf{a}}_n^{t,T-1},\hat{\mathbf{a}}_{-n}^{t,T-1}\right)\right) > u_n^{T-t}\left(\hat{\mathbf{s}}^t,\hat{\mathbf{a}}^{t,T-1}\right)$$

Therefore, we obtain

$$\begin{aligned} u_n\left(s_n^0,\left(\hat{\mathbf{a}}^{0,t-1},\left(\bar{\mathbf{a}}_n^{t,T-1},\hat{\mathbf{a}}_{-n}^{t,T-1}\right)\right)\right) &= u_n^{T-t}\left(\left(\bar{s}_n^t,\hat{\mathbf{s}}_{-n}^t\right),\left(\bar{\mathbf{a}}_n^{t,T-1},\hat{\mathbf{a}}_{-n}^{t,T-1}\right)\right) \\ &\quad - \sum_{\tau=0}^{t-1} g_n^\tau\left(\hat{s}_n^\tau,\left(\hat{a}_n^\tau,\hat{\mathbf{a}}_{-n}^\tau\right)\right) \\ &> u_n^{T-t}\left(\hat{\mathbf{s}}^t,\hat{\mathbf{a}}^{t,T-1}\right) - \sum_{\tau=0}^{t-1} g_n^\tau\left(\hat{s}_n^\tau,\left(\hat{a}_n^\tau,\hat{\mathbf{a}}_{-n}^\tau\right)\right) \\ &= u_n\left(\hat{\mathbf{s}}^0,\hat{\mathbf{a}}^{0,T-1}\right) = u_n\left(\hat{\mathbf{s}}^0,\hat{\mathbf{a}}\right) \end{aligned}$$

That is in contradiction to our assumption that $\hat{\mathbf{a}}$ is a Nash equilibrium for the game $\{G_1,\ldots,G_N\}$. Consequently, our assumption about $\hat{\mathbf{a}}^{t,T-1}$ is proved to be false. Thus $\hat{\mathbf{a}}^{t,T-1}$ indeed comprises a Nash equilibrium of the subgame $\{G_1^{T-t},\ldots,G_N^{T-t}\}$. $\square$

6.1.2.2 The DP-Algorithm and Derivation of the Best Response Solution

Based on the results of the previous subsection, we can formulate the following DP-algorithm to find the solution to the decision problem $G_n(\mathbf{a}_{-n})$ (6.4), i.e. the optimal decision for the nth player given the decisions $\mathbf{a}_{-n}$ of the other players.

Algorithm 3: DP algorithm for player $n \in \mathcal{N}$ to find the solution to (6.4).

Input: T, $\mathbf{a}_{-n}$, $\mathbf{s}^0$

$t \leftarrow T$

1 **for each** $\mathbf{s}^T \in \mathcal{S}$ **do**

    $V_n^0(s_n^T) \leftarrow g_n^T\left(s_n^T\right)$

2   **while** $t > 0$ **do**

        $t \leftarrow t-1$

3   **for each** $\mathbf{s}^t \in \mathcal{S}$ **do**

$$\hat{a}_n^t \leftarrow \underset{a_n^t \in \mathcal{H}_n^t(s_n^t)}{\operatorname{argmax}} -g_n^t\left(s_n^t,[a_n^t,\mathbf{a}_{-n}^t]\right) - V_n^{T-t-1}\left(f_t\left(s_n^t,a_n^t\right)\right)$$

$$V_n^{T-t}(s_n^t) \leftarrow \max_{a_n^t \in \mathcal{H}_n^t(s_n^t)} -g_n^t\left(s_n^t,[a_n^t,\mathbf{a}_{-n}^t]\right) - V_n^{T-t-1}\left(f_t\left(s_n^t,a_n^t\right)\right)$$

        end

    end

end

Output: $\hat{a}_n$

Let us apply Algorithm 3 to obtain the result to the decision problem $G_n(\mathbf{a}_{-n})$ (6.4) in closed form. Note that both for-loops (line 1 and line 3) are treated implicitly by keeping s^T and s^t unspecified throughout the computations.

Given the total scheduling length T, the aggregated decisions $\mathbf{a}_{-n}$ of all other players, and the initial SOC s^0 of the batteries, at the first step ($t = T$) we set $V_n^0(s_n^T) = s_n^T$ according to (6.3). With this we enter the while-loop (line 2) which overwrites t to now represent $t = T-1$. We solve for the best decision $\hat{a}_n^{T-1}$ by solving the following problem

$$\hat{a}_n^{T-1} = \underset{a_n^{T-1}}{\operatorname{argmax}} \overbrace{-c_2\left(d_n^{T-1}+a_n^{T-1}+L_{-n}^{T-1}\right)^2 - c_1\left(d_n^{T-1}+a_n^{T-1}+L_{-n}^{T-1}\right) - c_0}^{g_n^{T-1}}$$
$$\underbrace{-s_n^{T-1} - a_n^{T-1}}_{V_n^0}$$

where we made use of the transition equation (6.1) to rewrite V_n^0. The solution is computed as

$$\hat{a}_n^{T-1} = -s_n^{T-1} \,,$$

and subsequently we have

$$V_n^1 = -c_2\left(d_n^{T-1} - s_n^{T-1} + L_{-n}^{T-1}\right)^2 - c_1\left(d_n^{T-1} - s_n^{T-1} + L_{-n}^{T-1}\right) - c_0 \,.$$

With this, the first step is done and we again overwrite t to now represent $t = T-2$. In this stage we solve the following problem

$$\begin{aligned}\hat{a}_n^{T-2} = \underset{a_n^{T-2}}{\operatorname{argmax}}\ & -g_n^{T-2}\left(s_n^{T-2}, \left[a_n^{T-2}, \mathbf{a}_{-n}^{T-2}\right]\right) \\ & + c_2\left(d_n^{T-1} - s_n^{T-2} - a_n^{T-2} + L_{-n}^{T-1}\right)^2 \\ & + c_1\left(d_n^{T-1} - s_n^{T-2} - a_n^{T-2} + L_{-n}^{T-1}\right) + c_0 \,.\end{aligned}$$

The solution is computed as

$$\hat{a}_n^{T-2} = \frac{1}{2}\left(d_n^{T-1} - d_n^{T-2} - s_n^{T-2} + L_{-n}^{T-1} - L_{-n}^{T-2}\right) \,,$$

from which we obtain

$$\begin{aligned}V_n^2 = & -\frac{c_2}{2}\left(d_n^{T-1} - d_n^{T-2} - s_n^{T-2} + L_{-n}^{T-1} - L_{-n}^{T-2}\right)^2 \\ & - c_1\left(d_n^{T-1} - d_n^{T-2} - s_n^{T-2} + L_{-n}^{T-1} - L_{-n}^{T-2}\right) - 2c_0 \,,\end{aligned}$$

finalising the second step. This procedure can be done for all subsequent steps. As the equations increase quickly in size, they become infeasible to quote here. Fortunately though, our calculations provided insight into apparent recurring patterns, which all the solutions follow. Eventually, the solution for an arbitrary stage t of the T-stage dynamic game can be written as

$$\boxed{\hat{a}_n^t = \frac{1}{T-t}\left[\sum_{\tau=t+1}^{T-1}\left(d_n^\tau + L_{-n}^\tau\right) - s_n^t - (T-t-1)\left(d_n^t + L_{-n}^t\right)\right]} \tag{6.7}$$

Note that during the derivation the non-linear battery constraints are not strictly considered. Similar to the forecasting errors (cf. Section 4.4.3), these are considered in our simulation when the equilibrium schedules are actually executed. Furthermore, we want to highlight that the optimal decision (6.7) for nth player at time t only depends on the current and future forecasted net-demand data, the current SOC of the battery, and the average load (4.13) on the grid caused by all the other households. This is vaguely reminiscent of an alternative and elegant mean-field type approach [Huang et al., 2006, Lasry and Lions, 2007] in which each player reacts directly to an aggregated signal from the group.

6.1.3 The Algorithm and Execution of NE schedules

As in [Pilz et al., 2017b], we make use of a best-response algorithm (cf. Algorithm 1) to find the solution to the game. Whereas in [Pilz et al., 2017b] an extensive search

Algorithm 4: Best-response algorithm for finding a pure NE based on [Shoham and Leyton-Brown, 2009]

Input: T, s^0

initialise random strategy profile $\mathbf{a} = [\mathbf{a}_n, \mathbf{a}_{-n}]$

1 **while** *there exists a player* n *for whom* $\mathbf{a}_n$ *is not a best response to* $\mathbf{a}_{-n}$ **do**

2   **for each** $n \in \mathcal{N}$ **do**

3   **for each** $t \in \mathcal{T}$ **do**

            $\hat{a}_n^t \leftarrow$ best response to $\mathbf{a}_{-n}^t$ based on (6.7)

        end

        $\mathbf{a}_n \leftarrow [\hat{a}_n^0, \ldots, \hat{a}_n^{T-1}]$

    end

end

Output: $\hat{\mathbf{a}}$

for optimal schedules $\hat{\mathbf{a}}_n$ was performed, here we can compute the best response for each stage (line 3) analytically by means of (6.7) and concatenate the results to obtain the optimal schedule $\hat{\mathbf{a}}_n$ in response to $\mathbf{a}_{-n}$. Performing this computation for each player $n \in \mathcal{N}$ (line 2) results in a new strategy profile $\mathbf{a}$. We iterate this (line 1) as long as "there exists a player n for whom $\mathbf{a}_n$ is not a best response to $\mathbf{a}_{-n}$". In the actual implementation, this check is done by comparing the current strategy profile with the one obtained from the previous iteration. If it did not change, up to machine precision, an equilibrium is reached and $\hat{\mathbf{a}} = [\hat{\mathbf{a}}_n, \hat{\mathbf{a}}_{-n}]$ constitutes the Nash equilibrium. This iterative approach is a type of cobweb method [Bahn et al., 2009] which theoretically does not converge for every given scenario. An analysis of the convergence behaviour is performed in Section 6.2.2.

Based on the definition of a NE, no household can benefit from unilaterally deviating from its respective schedule. Nonetheless, we have to keep in mind that it is based on forecasted demand and renewable generation. Whenever either the demand or the generation does not match the forecasted value, it might not be possible anymore to strictly follow this NE schedule. In the analysis in the subsequent sections, we assume that every individual always seeks to be as close as possible to their determined NE schedule. To illustrate the idea: Imagine a NE schedule of household n requires them to discharge an amount x in a certain interval. Due to a forecasting error for the renewable generation, this has not been charged fully and can thus not be delivered. In this case, the schedule will discharge as much as possible during this interval. The deviation from the NE will decrease the benefit in terms of PAR reductions and achieved savings for the consumer. Anticipating the results, we want to highlight that in the following section we show that the solution is robust with respect to these deviations and gives considerable improvements in comparison to other approaches in the literature.

6.2 Performance Evaluation

The results with respect to convergence, demand-side management behaviour, influence of participation rate and forecasting errors, influence of consumer-type distribution, robustness, and influence of pricing parameters are collectively reported within this section.

6.2.1 Parameters

In this section, we consider the worst-case scenario with respect to the forecasting accuracy. Bichpuriya *et al.* [Bichpuriya et al., 2016] give a comprehensive overview of current techniques for short term demand forecasting. They specifically investigate how combining forecasts obtained from an integrated auto-regressive moving average, an artificial neural network, and a similar day approach can improve the short term load forecast. From [Bichpuriya et al., 2016], we obtain an upper limit for the forecasting error ϵ_d, expressed as a percentage of the actual demand. Similarly, [Dolara et al., 2015] gives an insight into 24 hour PV power output prediction. The forecasting error ϵ_w is also given as a percentage of the actual generation.

The worst-case scenario is constituted when these two errors carry opposing signs and are correlated between all the participants. This becomes clear from the definition of the net-demand (4.10), since both contributions enter with different signs. Intuitively, it makes sense that in the worst-case the forecasted net-demand is smaller than the actual demand. This is because a too small forecasted net-demand does disguise the incentive to make use of the battery system. With the same argument, the worst-case solar forecast is higher than the actual one. It might imply a sufficient SOC of the battery, when in reality more charging would have been necessary.

Table 6.1. *Battery parameters.*
Parameters for a Tesla-inspired [Tesla, 2017] home battery storage system.

Efficiencies	Charging rates	Capacities
$\eta^+ = 0.958$	$\rho^+ = 5.0$ kW/h	$s_{\text{max}} = 13.5$ kWh
$\eta^- = 0.958$	$\rho^- = -7.0$ kW/h	$s_{\text{min}} = 0.0$ kWh
$\eta_{\text{inv}} = 0.960$	$\bar{\rho} = -0.001$	$s^* = 9.46$ kWh

In the real-world application, the smart meter of individual households collects data about electricity demand and generation from the available PV installation. As specified in Section 4.1, the DSM protocol requires participants to send forecasts of the demand and generation to the utility company. These forecasts are based on historically collected data. In order to run our simulations, we omit this forecasting step and rather make use of the publicly available data sets introduced in Section 4.4.

Demand data: The demand data stem from the NREL dataset [U.S. Dept. of Energy, 2013]. For all simulation runs, we picked the same $M = 25$ households, in close vicinity to each other, to represent our neighbourhood (cf. Table 4.1). With respect to their consumption categories, we have seven LOW, nine BASE and nine HIGH users.

PV data: Data for the PV generation are based on real-world measurements [Power Networks, 2014] in the UK. An estimate for the kWp value is obtained from looking at the highest hourly output in the course of a whole year. Its value is $w_{\max} = 3.7\,\text{kWh}$, which is why we assume $kWp \approx 4\,\text{kW}$. We account for different sizes of PV installations by scaling the data set with a household specific factor p_n. About 6% of the collected data was corrupted. We set all these values to $w = 0.0\,\text{kWh}$. This does not pose any problem for our simulation results, but can be seen as realistic failures of the installation.

Battery and pricing parameters: The parameters of the battery are based on the Tesla Powerwall 2 [Tesla, 2017] data sheet. The choice to employ this battery system is motivated by two reasons: (i) The same battery was used in the previous chapter (i.e. [Pilz et al., 2017b]), allowing for a direct comparison of the results. (ii) A non-extensive analysis of different battery systems showed that the Tesla Powerwall 2 qualifies as a representative of state-of-the-art technology. Please see the Appendix A for more details. A summary of the battery parameters can be found in Table 6.1. The data sheet only specifies the round-trip efficiency $\eta = \eta^+ \cdot \eta^-$ of the battery. Without loss of generality, we assume that charging and discharging contribute equally, yielding $\eta^+ = \eta^- = \sqrt{0.918}$.

For the parameters in the cost function (4.14) we use $c_2 = 0.03125$ \$/MW^2, $c_1 = 1.0$ \$/MW, and $c_0 = 0$, following other studies [Pilz et al., 2017b, Rahbar et al., 2015]. This allows to directly compare our results.

6.2.2 Convergence Behaviour of the Algorithm

Let us provide an insight into the convergence behaviour of Algorithm 4. The condition that needs to be fulfilled to declare equilibrium is stated as "there exists no player n for whom his current action $\mathbf{a}_n$ is not a best response to the actions $\mathbf{a}_{-n}$

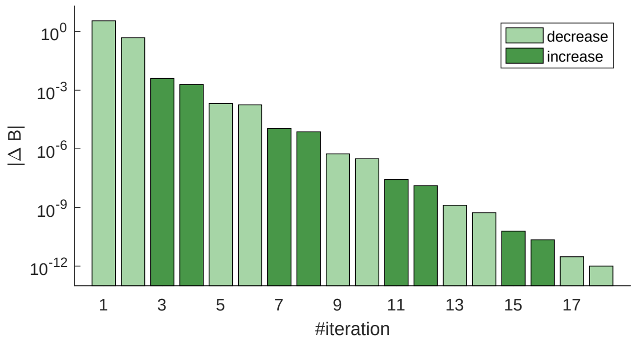

Figure 6.1. *Convergence analysis of Algorithm 4.*
The change of the average bill of the DSM participants between consecutive iterations is plotted over the iteration number. The ordinate is scaled logarithmically. Bars are coloured according to the algebraic sign of the change. The specific data points stem from a simulation in Section 6.2.4 with 64% participation rate and without forecasting errors.

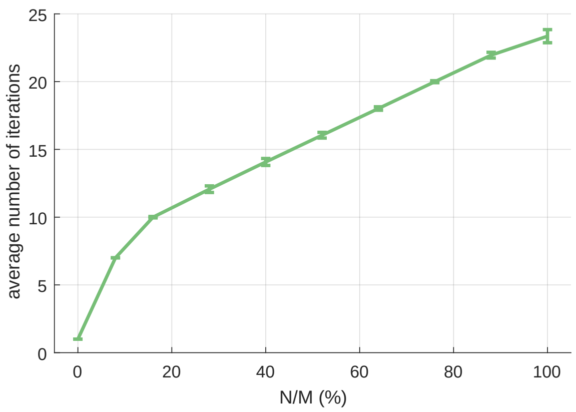

Figure 6.2. *Iteration statistics.*
The mean number of iterations per day is plotted over the participation rate in per cent. The values stem from the simulations undertaken in Section 6.2.4. In addition to the average over 365 days, the standard deviation is shown for each data point.

of the other players” (cf. Algorithm 4, line 1). Within our specific implementation of `selma`, the stopping criteria is based on the average L2 difference between the action profiles of two consecutive iterations i and $i+1$, i.e.

$$\left| {}^{i+1}\mathbf{a} - {}^{i}\mathbf{a} \right|_{L2} := \frac{1}{N\,T} \sqrt{\sum_{n=1}^{N} \sum_{t=0}^{T-1} \left| {}^{i+1}a_n^t - {}^{i}a_n^t \right|^2} \,. \tag{6.8}$$

When this difference is smaller or equal to 10^{-15} the algorithm breaks out of the loop. Associated with the current action profile during each iteration are also the energy bills for each participant.

Results: In Figure 6.1, the absolute change of the average bill $B = {}^{1}\!/\!{}_{N} \sum_n B_n$ (cf. (4.15)) is shown for a randomly selected day of the simulation shown in Section 6.2.4. To cover the large scale of different changes, a logarithmic representation is chosen. The respective sign of the change is then expressed in the colour of the bar. Figure 6.2 shows how the number of average iterations per day depends on the number of participants in the DSM scheme. The values are again taken from the simulations in Section 6.2.4.

6.2.3 Comparison Between a Static and a Dynamic DSM Scheme

In Chapter 5 (cf. [Pilz et al., 2017b]), a similar DSM scheme to the one described in this chapter was examined. Both are based on a battery scheduling game for

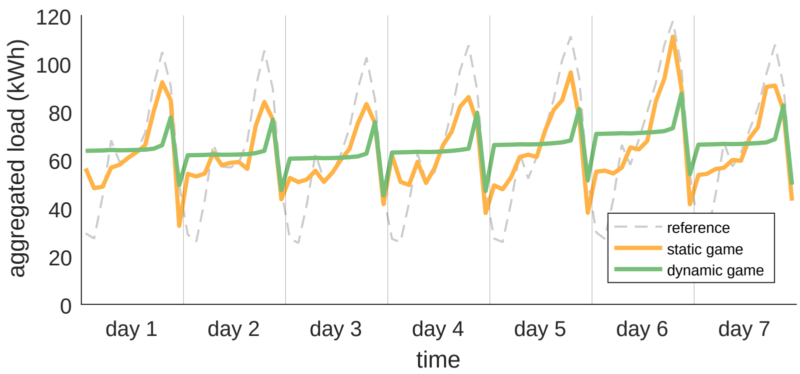

Figure 6.3. *Load comparison.*
The aggregated load of all households in the neighbourhood is plotted over time. The simulation domains cover seven days, that were each scheduled consecutively. The aggregated demand is given as a reference. The orange curve results from a DSM scheme employing a static scheduling game (cf. Chapter 5), while the green one stems from a DSM scheme employing a dynamic game. Other than the underlying game structure, all parameters are identical.

Table 6.2. *Peak-to-avergage ratio (PAR) comparison.*
PAR values calculated as the average over the individual days of week 12, 25, 38, and 51 for the case without storage system (Reference) and both underlying games of the DSM scheme. Static: game employed in Chapter 5; Dynamic: game described in Section 6.1. The values in parentheses represent the standard deviation.

		Reference	**Static**	**Dynamic**
Period	week 12	1.623 (0.005)	1.374 (0.070)	1.013 (<0.001)
	week 25	1.574 (0.033)	1.410 (0.035)	1.198 (0.016)
	week 38	1.685 (0.031)	1.439 (0.080)	1.231 (0.015)
	week 51	1.718 (0.037)	1.468 (0.082)	1.015 (0.001)
	average	1.650 (0.064)	1.423 (0.040)	1.114 (0.117)

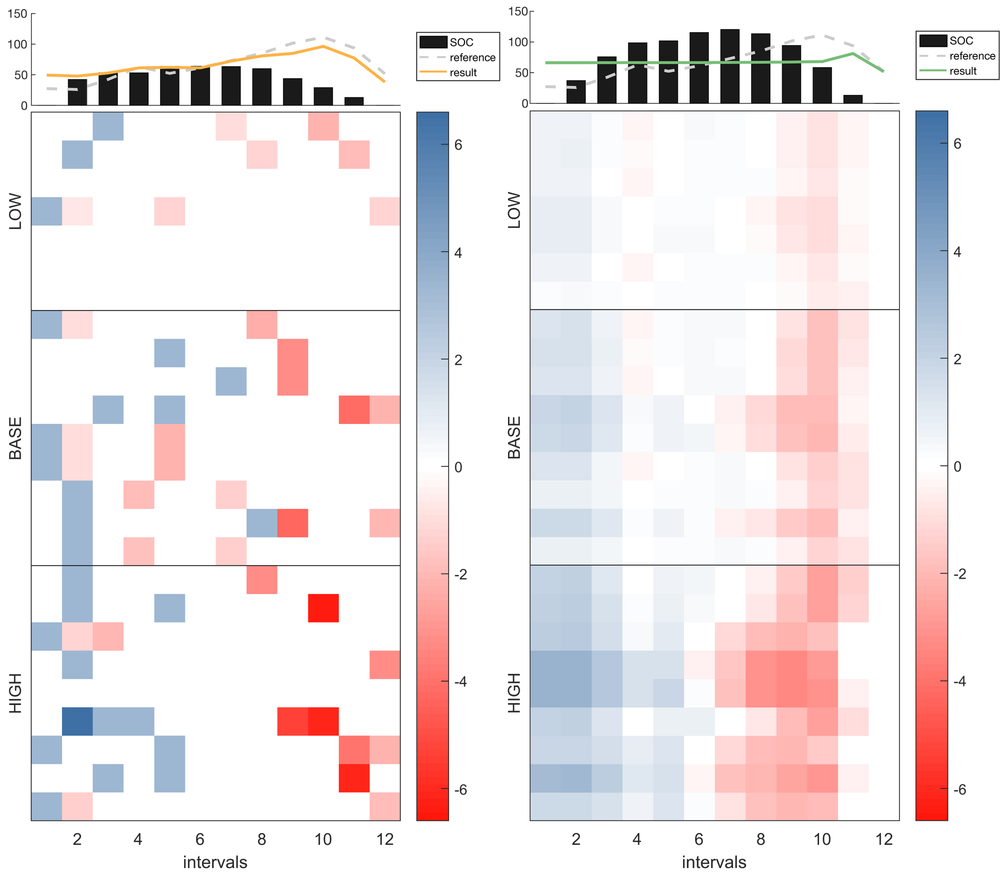

(a) static scheduling game (b) dynamic scheduling game

Figure 6.4. *Nash equilibrium schedule comparison.*
The schedules for all participating households of the demand-side management scheme for a single scheduling period (week 38, day 5, cf. Chapter 5) are shown together with their respective aggregated load and aggregated state-of-charge (SOC). (a) The underlying game structure is a static non-cooperative game from the previous chapter. Within each interval, players can choose between four discrete decisions. (b) Here, the game structure is the dynamic game introduced in Section 6.1. Note that the schedules employ the same scaling.

households of a neighbourhood served by the same utility company (UC). Their main difference is the underlying game that determines the schedules for the upcoming day. Whereas here we employ a discrete time dynamic game, in the previous chapter we made use of a simpler non-cooperative static game in which players were only able to choose between four discrete options for each interval. For the sake of comparison, none of the households is equipped with PV cells.

In this subsection, we compare the two approaches with respect to their success in reducing the PAR of the aggregated load. To this end, the same parameters for each household and also the same demand data are used. Households do not have the capability of on-site generation, but are equipped with the same batteries (cf. Table 5.1). The upcoming day is divided into $T = 12$ intervals and we assume $N = M = 25$, i.e. every household takes part in the DSM scheme. As in the previous chapter, we simulate full weeks by using the SOC values of the batteries at the end of the scheduling period as the initial configuration for the following one.

Results: Figure 6.3 shows the aggregated load curves achieved by the DSM schemes for forecasts given by week 38 of the demand data set [U.S. Dept. of Energy, 2013]. For completion, we also simulated week 12, week 25, and week 51 as done in Chapter 5. A summary of the achieved results can be seen in Table 6.2.

On average, a 14% and a 32% decrease of the PAR value was achieved by the static and the dynamic games, respectively. To understand the differences of the outcomes, we explicitly look at the schedules that are obtained in the NE of the respective games. Figure 6.4 shows these schedules exemplarily for day 5 of week 38 (Figure 6.3, cf. Figure 3 in [Pilz et al., 2017b]) together with the aggregated load and aggregated SOC above it. Each row illustrates the equilibrium schedule of one household.

6.2.4 Influence of Participation Rate and Forecasting Errors

The question of how many participants are needed to obtain considerable gains in terms of PAR reduction and savings is important. Moreover, within this sub-

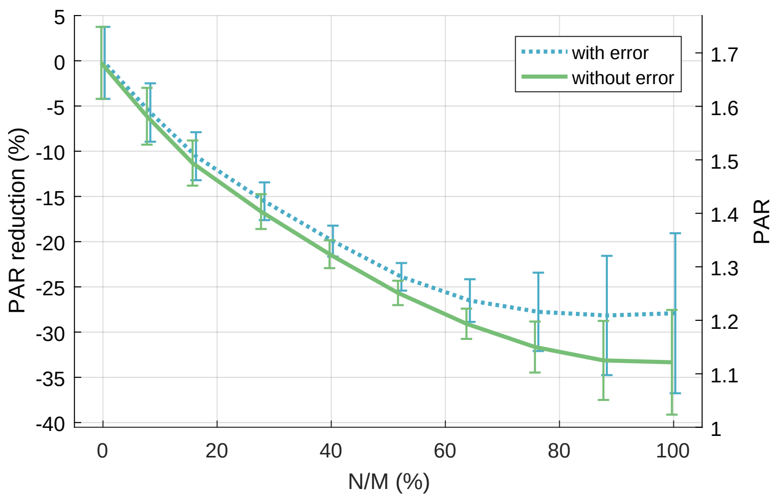

Figure 6.5. *Peak-to-average ratio (PAR) reduction over participation rate.* The mean PAR reduction in per cent is plotted over the participation rate in per cent. The right-hand axis shows the absolute values of the PAR. In addition to the average over 365 days, the standard deviation is shown for each data point. The simulations were run for a scenario with forecasting errors and one without forecasting errors. Note that the data points are slightly shifted along the abscissa to increase readability.

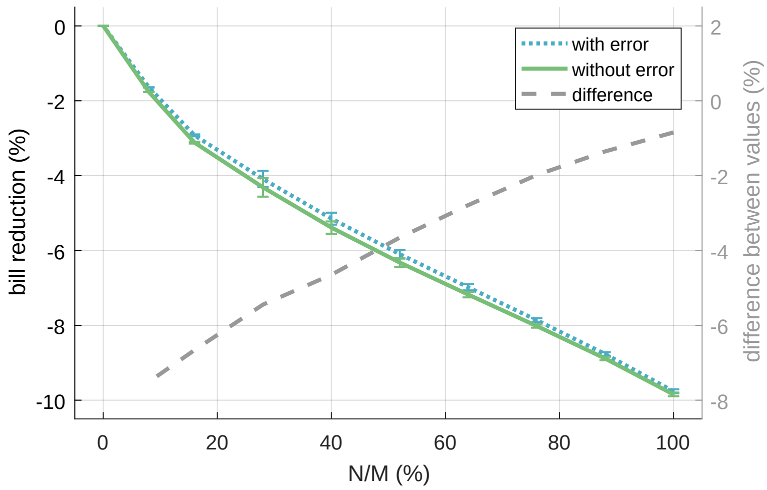

Figure 6.6. *Savings dependency on the participation rate.*
The mean bill reduction in per cent for participants of the demand-side management scheme are plotted over the participation rate in per cent. In addition to the average over 365 days and participants, the standard deviation between different participants is shown for each data point. The simulations were run for a scenario with forecasting errors and one without forecasting errors. The difference between the two curves is plotted against the right-hand axis.

section the robustness with respect to the forecasting errors (cf. Section 4.4.3) is shown. To do so, we assume the forecasting error for the demand to be $\epsilon_d = 8\%$ for every household [Bichpuriya et al., 2016], which could be obtained from a forecast performed by an artificial neural network, and is approximately 2.5 times higher than the best forecast obtained by them. This is independent of whether the household participates in the DSM scheme or not. The forecasting error for the solar generation is set to $\epsilon_w = 10\%$ in accordance with [Dolara et al., 2015, Rana et al., 2016]. Rana *et al.* [Rana et al., 2016] make use of a neural network and clustering of weather data to forecast half hourly solar power output for the upcoming day. Note that only participants of the DSM scheme are equipped with PV cells and thus subject to the forecasting error. The values are taken to represent a worst-case scenario. Thus, any real-world scheduling result should fall in the interval between the worst-case outcome and the respective outcome without any forecasting error.

We simulate a full year and average over the obtained PAR values for the individual days. All participants are equipped with a lithium-ion battery (cf. Table 6.1) and solar panels. The size of the PV installation depends on the user's category. For LOW, BASE, and HIGH consumers, we use $p_n = 0.3$, $p_n = 0.5$, and $p_n = 0.7$, respectively. Starting with all 25 households taking part in the DSM scheme, we eliminated three users, i.e. one randomly selected from each consumer category, in each subsequent run. Non-participant still exhibit the specified forecasting error for their demand.

Results: Figure 6.5 shows the reduction of the PAR value over the rate of participating consumers for the scenarios with and without forecasting errors. It includes not only the mean values, but also the standard deviation. Note that we slightly shifted the results for both runs along the abscissa to increase readability. An additional axis on the left indicates the absolute PAR values. Whereas the PAR reduction is the interest of the UC, the financial rewards, i.e. savings off the energy bill, are the interests of the participants of the DSM scheme. Figure 6.6 shows the average saving per day for all participants both with and without forecasting error. For further insight, it also illustrates the difference between the two curves.

6.2.5 Consumer-Type Analysis

The results in Section 6.2.3 and Section 6.2.4 are all based on a neighbourhood consisting of a mix of the three different consumer types (LOW, BASE, HIGH). Figure 6.7 shows the possible PAR reductions for mono-type neighbourhoods. To allow for comparison $M = 25$ is kept constant. Furthermore, we use the same forecasting errors of $\epsilon_d = 8\%$ and $\epsilon_w = 10\%$ for the demand and renewable energy generation, respectively (cf. Section 6.2.4). All the simulations consider a scheduling period of a full year.

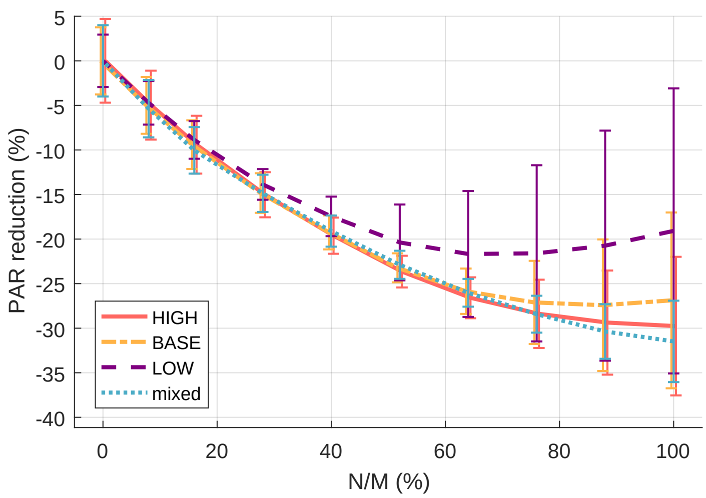

Figure 6.7. *PAR reduction for different neighbourhoods.*
The mean PAR reduction in per cent is plotted over the participation rate in per cent for different mono-type consumer neighbourhoods. In addition to the average over 365 days, the standard deviation is shown for each data point. For comparison, the results of a mixed neighbourhood (cf. Figure 6.5) are also presented. Note that the data points are slightly shifted along the abscissa to increase readability.

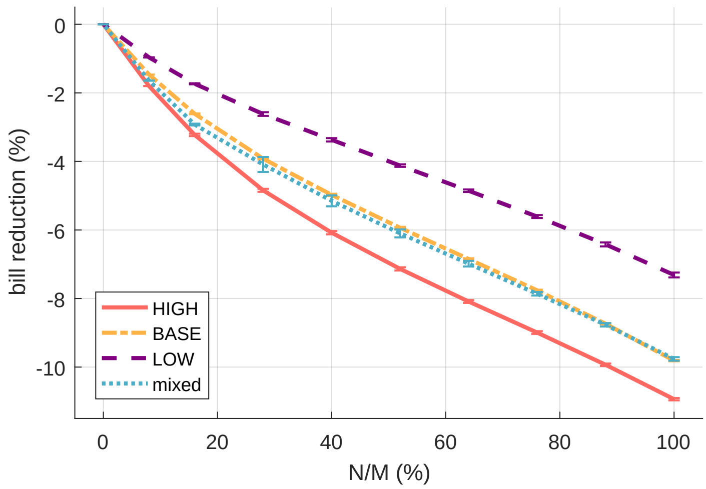

Figure 6.8. *Savings for different neighbourhoods.*
The mean bill reduction in per cent for participants of the demand-side management scheme are plotted over the participation rate in per cent for different mono-type consumer neighbourhoods. In addition to the average over 365 days and participants, the standard deviation between different participants is shown for each data point. For comparison, the results of a mixed neighbourhood (cf. Figure 6.6) are also presented.

We also calculated the average savings that are achieved by the participants of the DSM scheme. These results are presented in Figure 6.8 together with the reference of a mixed neighbourhood (cf. Figure 6.6) with forecasting errors.

6.2.6 Robustness

In order to evaluate the robustness of the game-theoretic approach, we simulate a large set of scenarios with randomly generated parameters. The parameters under consideration are the size of the PV array of the individual households, the maximum capacity of the lithium-ion battery, and the charging and discharging

Table 6.3. *Parameter ranges.*
Instead of using the same battery and (scaled) PV installation for each participant of the DSM scheme, the parameters are drawn uniformly from the given ranges in the simulation runs to analyse the robustness of the scheduling performance.

	Robustness Study	**Other Studies**
	Uniformly drawn from	Fixed at
$w_{\max}$ (kWh)	$[0.0, 8.0]$	4.0
$s_{\max}$ (kWh)	$[2.8, 13.5]$	13.5
η^+	$[0.900, 0.958]$	0.958
η^-	$[0.900, 0.958]$	0.958

efficiencies. The change of capacity and efficiency can either be interpreted as an ageing effect of the Tesla Powerwall 2, or as using batteries from different manufacturers for different participating households. An overview of the range of

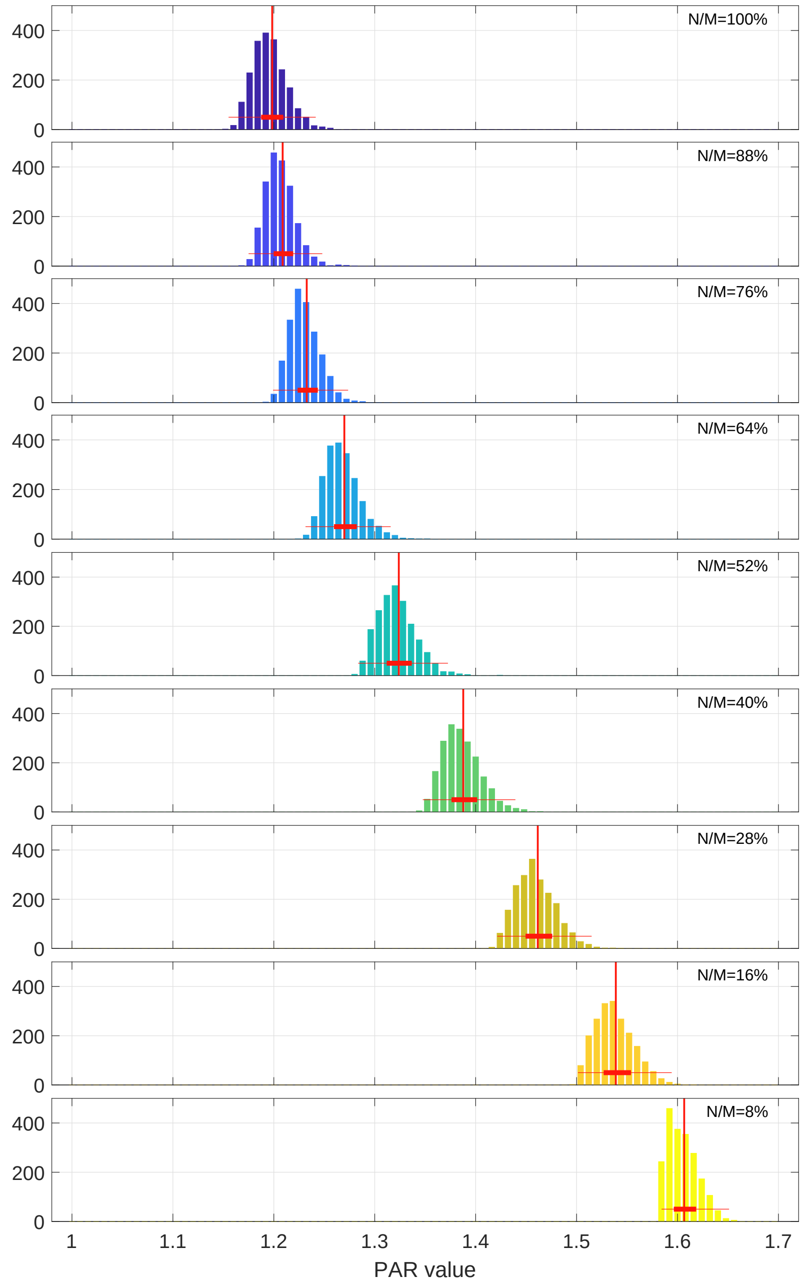

Figure 6.9. *PAR value histograms.*
The yearly median PAR values for scenarios with randomly generated parameters are shown for various participation rates N/M. The possible ranges for the solar and battery parameters are indicated in Table 6.3. The bin size for the histogram is 0.008. Additionally, box-and-whisker plots are overlaid for each histogram.

these parameters is shown in Table 6.3. All other parameters are kept constant at the values used throughout the other experiments, i.e. $M = 25$, $T = 24$, $\epsilon_d = 8\%$, $\epsilon_w = 10\%$, and all other battery parameters as in Table 6.1, to allow for a fair comparison. For each set of random parameters we consider a simulation period of one year. Figure 6.9 shows the results for various participation rates for 2048 years each.

6.2.7 Influence of Pricing Parameters

Throughout the thesis, a quadratic cost function (4.14) with constant coefficients is used based on previous studies, e.g. [Pilz et al., 2017b, Rahbar et al., 2015]. In this section the specific choice of these coefficients is justified and the influence of them on the obtainable savings for the consumers is analysed. In order to get a thorough overview, a wide range of coefficients was considered, i.e. $c_2 \in [10^{-4}, 10^6]$, and $c_1 \in [10^{-3}, 10^5]$. Note that for simplicity the constant term is kept at $c_0 = 0$. The average savings over a simulation period of one year for $N/M = 100\%$, including forecasting errors as discussed in Section 4.1 is shown in Figure 6.10. We can observe three regions in this representation: (i) A plateau, where the relative savings are equal to $\approx 17\%$, (ii) A transitional region where the savings are diminishing, and (iii) A second plateau of negative savings ($\approx -1.5\%$), i.e. the consumers actually have to pay more given these pricing coefficients. The previously used pricing coefficients,

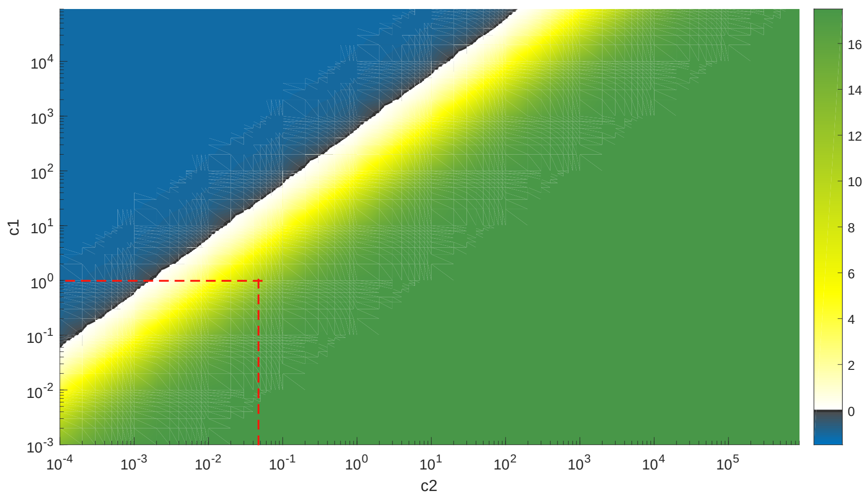

Figure 6.10. *Average savings.*
The average savings in per cent over one year for various pricing coefficients c_2 and c_1 in (4.14) is shown. Furthermore, the values $c_2 = 0.03125$ and $c_1 = 1.0$, that are used throughout the manuscript, are highlighted.

that lead to an average saving of 10% per year, are located in the second region. This means that by changing the pricing coefficients an even higher cost reduction could be achieved. It can be observed that as long as the quadratic term in the cost function is dominant the consumers can expect a financial gain from playing the game. Only when $c_2 \ll c_1$ the advantage is lost.

While these results are all based on simulations in the presence of forecasting errors, we can report that without forecasting errors the resulting savings differ by $< 1\%$ for each of the considered sets of coefficients in the represented range, following the results shown in Figure 6.6. This can be explained when looking at the effect the forecasting error has on the actual load curve of the households. In Section 6.2.4, we saw that the PAR of the aggregated load changes by only a few per cent when introducing inaccurate forecasted demand and generation data. A rough estimate shows that changing the load x percent could also be interpreted as a change of the coefficients c_1, c_2 by the same amount and twice the amount, respectively.

$$\begin{aligned}
c_2' \cdot l^2 \quad &\stackrel{!}{=} c_2 \cdot \left(l + l \cdot \frac{x}{100}\right)^2 \\
&= c_2 \cdot l^2 + c_2 \cdot l^2 \cdot \frac{2x}{100} + c_2 \cdot l^2 \cdot \cancelto{\approx 0}{\frac{x^2}{10000}} \\
&\Rightarrow \frac{c_2'}{c_2} \approx 1 + \frac{2x}{100}
\end{aligned}$$

In such a narrow margin the function plotted in Figure 6.10 is indeed almost flat.

6.3 Discussions

Within this section, the results studied in the previous one are discussed and whenever suitable compared to the literature.

6.3.1 Convergence Behaviour of the Algorithm

The results give evidence of a correctly working iteration algorithm (cf. Algorithm 4). From Figure 6.1 we see that between any two consecutive iterations, the absolute change of the average electricity bill is monotonically decreasing. Furthermore, we observe that the rate of this decrease is almost linear in the semi-logarithmic plot, hinting towards an exponential relationship.

Due to the exponential convergence towards a Nash equilibrium, only few iterations are needed to obtain the equilibrium schedules. The specific number of iterations depends on the number of participants taking part in the DSM scheme. This is comparable to the ones shown in [Nguyen et al., 2015]. Figure 6.2 shows that the average number of iterations increases monotonically with the number of participants. Moreover, the variation across the number of iterations for individual scheduling periods is small, as shown by the standard deviation. This is a strong result, as it shows that the convergence properties are insensitive to different demand data of the individual participants. During experimentations with the code, more than one million games were solved which all converged to a Nash equilibrium.

The small number of iterations directly translates to small computational times and thus does not hinder a real-world application. Typical 365-day simulation runs take about 30 s on a single core of an `i7-3770S` CPU and require less than 1 GB of memory. Note that in the real-life scenario, the scheduling process is initiated once before the scheduling period and only needs to calculate the equilibrium schedules for the upcoming day. In summary, we expect no difficulties in implementing a DSM scheme based on our scheduling software `selma`.

6.3.2 Comparison Between a Static and a Dynamic DSM Scheme

Comparing the aggregated load curves (cf. Figure 6.3) shows that a DSM scheme based on a dynamic game can achieve an almost flat profile. Nevertheless, depending on the given data, the outcome of the scheduling is subject to a finite-horizon effect. Empirically, we observe peaks and troughs at the end of the scheduling period if the demand for the final interval is lower than the average demand of the whole day. This indicates that the starting time of the DSM scheme has an influence on the achievable outcome. Nonetheless, this parameter is fixed through the DSM scheme protocol, thus asking for alternative solutions to the finite-horizon effect. In the following chapter, we will introduce a refined calculation of the best-response that is able to improve on this effect.

In Table 6.2, we observe that on average the dynamic game reduces the PAR value more than twice as much as the static game. However, with respect to the individual weeks the static game shows a smaller standard deviation of 0.04 and thus seems to be more consistent. Its achieved reductions are all between 10.4% – 15.3%, while the range of reductions by the DMS scheme with the dynamic game is 23.9% – 40.9%. The differences with respect to the standard deviations is again owed to the finite-horizon effect. It is also present in the case with the static game, but due to generally worse outcome, does not alter it as much as the results of the dynamic scheduling game.

We can further understand the differences between the static and dynamic game from Figure 6.4. The restriction to four discrete options for each interval in the static case, i.e. (i) remain idle, (ii) charge half interval, (iii) charge full interval, and (iv) use battery, results in a majority of intervals where the battery remains idle.

This is because of a lack of incentive to charge the battery by the two given amounts. In the dynamic game, players can choose to charge their battery from a continuous spectrum of decisions in a given interval. This difference becomes most apparent when looking at the aggregated SOC of all participants. Whereas the maximal SOC in the static case is approximately 64 kWh, almost twice as much (120 kWh) is charged in the dynamic case. In summary, it shows that the increased flexibility of the dynamic game is better suited to minimise the PAR of the aggregated load.

Note that all these comparisons allow for strong conclusions as they are based on the identical data set [U.S. Dept. of Energy, 2013] and also all the other parameters, such as number of players N, number of time intervals T, etc. are chosen to be the same. Nevertheless, comparisons to other results in the literature are possible: Compared to the work by Nguyen *et al.* [Nguyen et al., 2015], a better PAR reduction is achieved while also the number of iterations to obtain the equilibrium solution is lower by two orders of magnitude. Similarly, the PAR reduction of Yaagoubi *et al.* [Yaagoubi and Mouftah, 2015b] is worse than the approach shown in this chapter. As they schedule not only the battery but also shift other household appliances, a comparison of the computational costs is not appropriate.

6.3.3 Influence of Participation Rate and Forecasting Errors

Although a worst-case scenario is simulated, the outcome with respect to PAR reduction (cf. Figure 6.5) and electricity bill (cf. Figure 6.6) reduction show considerable gains for the UC and the participants of the DSM scheme.

Without forecasting error the PAR reduction monotonically improves with the proportion of the participants. This stands in contrast to the results shown in [Soliman and Leon-Garcia, 2014], where a minimum is reached at medium range participation rate. In comparison to other studies, such as [Nguyen et al., 2015,Longe et al., 2017], we conclude that our dynamic game performs as good as their respective scheduling approach. At 100% participation rate, a reduction of −33.3% (5.8%) is achieved, in agreement with the results shown in Section 6.2.3. It should be noted that a perfectly flat load profile corresponds to an approximately −40% reduction of the PAR. Thus the outcome is close to the theoretical optimum. When looking at the standard deviation, we observe that it is lowest for the simulation run with 52% participation rate and increases towards both ends of the spectrum. On the lower end of participation rate the fluctuations of the PAR value for different days is just an artefact of the data set in use. Small numbers of participants have not enough influence on the overall neighbourhood to change this. When regarding large participation rates, the PAR value is considerably reduced. The increase of the standard variation for these runs stem directly from the finite-horizon effect already discussed in Section 6.2.3.

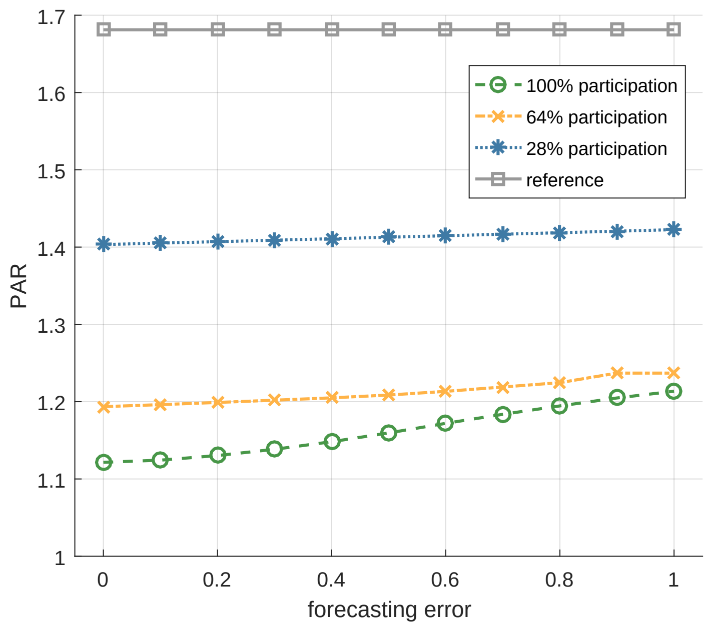

Figure 6.11. *Influence of forecasting error on the achieved PAR value.* The PAR values for three different participation rates are plotted over the forecasting error. Here the abscissa refers to the worst-case scenario as described in Section 6.2.4, e.g. at 0.6 a forecasting error with the magnitude of 60% of the worst-case is assumed. In the reference case no game is played, so the forecasting error does not influence the PAR value.

The results for runs with forecasting errors follow the results without errors closely. Figure 6.11 shows how the forecasting error affects the achieved PAR values for three selected participation rates when transitioning from the perfect forecast to the worst-case scenario as depicted in Figure 6.5. For low participation rates the difference is negligible but starts to increase when more households participate in the DSM scheme. Nevertheless, even in the worst-case scenario, a reduction of −27.8% (8.9%) is achieved at 100% participation rate (cf. Figure 6.5). With respect to the standard deviation, we again recognise similarities to the runs without forecasting errors. Smallest variations in the PAR reduction are obtained for participation rates around 50%, while we again see increasing variations at high participation rates. Here, the increase is distinctly larger than in the other runs. The reason behind this difference is directly explained by the forecasting error. As more participants join the DSM scheme, the absolute amount of deviation from the actual demand and production is increasing.

It is worth noting that the result for a participation rate of 76%, i.e. a reduction of −27.7% (4.4%) (cf. Figure 6.5), are very promising from a practical point of view. The

UC might not be able to convince everybody to participate in the DSM scheme, but can still gain reductions of the PAR value close to what is achievable at maximum participation.

The savings that participants of the DSM scheme can gain increase monotonically with the share of participants. Furthermore, we observe that the variations between different participants are negligible. This is due to the particular proportional billing scheme employed in the scheme (cf. Section 4.3). It ensures fairness in the sense that LOW and HIGH consumers can gain equally by signing up for the DSM scheme. The difference between runs with and without forecasting errors reveals that the forecasting error does not influence the bill reduction to a great extent. Since the two curves are almost non-separable to the unaided eye, the difference is shown in the same plot (cf. Figure 6.6). It becomes clear that the difference is actually decreasing for larger numbers of participants.

This highlights that the dynamic scheduling game ensures robust and beneficial results for the participants of the DSM scheme, even in the worst-case scenario.

6.3.4 Consumer-Type Analysis

When comparing different compositions of neighbourhoods, we can gain further insight into the conditions for which the DSM scheme works most efficiently. At first glance, Figure 6.7 reveals that given a low rate of participants in the scheme, the actual type of consumer is not crucial. Figure 6.12 shows the difference between the respective results for mono-type neighbourhoods and a mixed neighbourhood. A closer look shows that mono-LOW communities are always worse in reducing the PAR value of the aggregated load than any of the other ones. The results in terms of

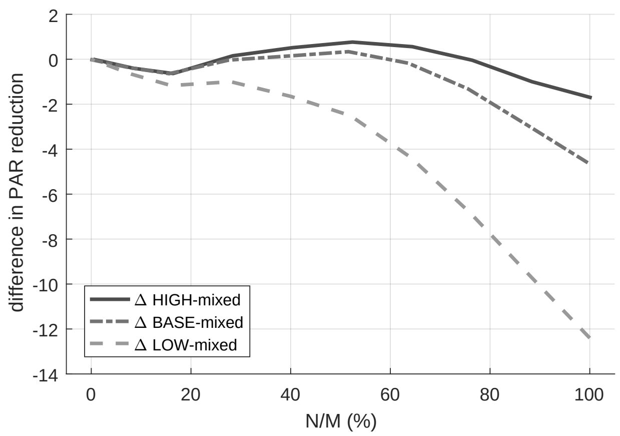

Figure 6.12. *Differences between neighbourhoods in PAR reduction.*
The values shown are based on the results represented in Figure 6.7.

both the mean PAR reduction and the standard deviation get even worse with more than two thirds of households participating in the scheme. Similar observations for mono-type neighbourhoods are found in [Soliman and Leon-Garcia, 2014].

For both mono-BASE and mono-HIGH neighbourhoods it can be observed that they perform better ($< 1\%$) in an interval of medium participation rate than the mixed neighbourhood. Nevertheless, at $N = M$ the obtained PAR reduction is smaller by 1.8% and 4.5%, respectively. Considering the variation of these mean PAR reduction values, it becomes clear that it is most beneficial to have a mixed-consumer neighbourhood.

Figure 6.8 shows the average bill reduction for the participants of the DSM scheme for different participation rates. Generally, they show the same behaviour already observed in Figure 6.6. The influence of the proportionality factor in the billing scheme (4.15) is clearly visible. Although the mixed-consumer neighbourhood achieves better PAR reduction, the average savings are almost identical to a mono-BASE neighbourhood. A neighbourhood that purely consists of HIGH consumers can save about 11% off the energy bill and is consistently most rewarding for the participants independent of the participation rate.

6.3.5 Robustness

The median PAR value over all the simulated years is monotonically decreasing with an increase in the participation rate. At 100% participation rate a median PAR value of 1.198 is achieved, which equals a reduction of -28% when compared to the scenario without the DSM scheme.

When comparing the median PAR values over 2048 years and random parameters with the ones obtained over one year and fixed parameters (cf. Figure 6.5) it becomes clear that the former ones perform slightly worse, differing by $< 2.5\%$. This was expected due to the following reason: Since all of the randomly generated scenarios have the previously analysed scenario as an upper limit in terms of the available storage capacity, a decreased performance can be explained by the loss of effective flexibility.

Note that the same iteration statistics as shown in Figure 6.2 are observed independently of the chosen parameters. With a total of > 6.7 million simulated days, this provides further confidence in the correctly working iteration algorithm and its convergence behaviour.

All in all, we see that with the more realistic assumption of differing battery and solar installations the DSM scheme performs well and shows inherent robustness.

6.4 Conclusions

In this chapter, we propose a DSM scheme based on a discrete time dynamic game. Its purpose is to reduce the peak-to-average ratio of the aggregated electricity load by scheduling the usage of individually owned (lithium-ion) energy storage systems. The utility company running the scheme, incentivises users to take part by offering fair financial benefits. To ensure realistic outcomes, an advanced battery model is employed. Furthermore, the integration of local energy generation in form of photovoltaic cells is taken into account.

The DSM scheme is suitable for real-world implementation for several reasons: Firstly, it is based on a complete model of the neighbourhood including storage systems, local energy generation, and crucially forecasting errors of both demand and generation. Secondly, computational costs to obtain schedules for the upcoming period are small and require only little amounts of memory. This was achieved by deriving a closed form solution for the best-response problem of an individual player. The ensuing iterative algorithm shows exponential convergence towards a Nash-equilibrium and thus obtains the strategy profiles for one scheduling period in a fraction of a second. Thirdly, the resulting schedules are robust with respect to the worst-case forecasting errors. Whereas the error weakens the effect of the PAR reduction by $\leq 5.5\%$, the corresponding savings off the energy bill for the participants of the scheme are hardly changed. Fourthly, we provide evidence that a neighbourhood that consists of various types of consumers performs best in such a DSM scheme. Since a mixed community is more probable than a mono-type community, this is a promising result. Finally, simulations with randomly generated parameters for battery and photovoltaic installation have provided insight into the expected outcomes of the DSM scheme for batteries of different age and performance. The effective loss of flexibility lead to a PAR reduction of $< 2.5\%$, showing the robustness of the DSM scheme.

A direct and in-depth comparison to a DSM scheme with an underlying static game, revealed the advantages of the dynamic game approach. Players are overall more active and thus able to achieve distinctly better results. Further comparisons with the literature in terms of PAR reduction and computational costs show the superiority of our approach.

This almost blank page is intentional.

CHAPTER 7

Finite-Horizon Effect and Added Value of the Game

This chapter[1] directly extends the study presented in Chapter 6 with regards to two aspects. Firstly, the solution to the undesirable finite-horizon effect. Secondly, the practical relevance of the scheduling game. Thus the contributions covered in this chapter are the following:

(1) We implement two refinements to the dynamic game which governs the demand-side management (DSM) scheme. They are specifically targeted to treat boundary effects that can occur due to the finite length of the scheduling period. Statistical analysis of long term simulations show improvements in both mean peak-to-average ratio (PAR) reduction and standard deviation, i.e. robustness, compared to previous studies.

(2) We analyse the benefits of the dynamic game and compare it to a scenario without interaction between the households. Furthermore, we assess the costs that are associated with the different approaches. Based on these discussions we find that the DSM scheme is beneficial for both the utility company (UC) and the consumers.

The chapter is structured as follows. Section 7.1 describes the two mitigation strategies to combat the undesirable finite-horizon effect that occurred in Sec-

[1]The content of this chapter has been presented at the 2018 IEEE PES Innovative Smart Grid Technology Conference Europe in Sarajevo, Bosnia and Herzegovina. It was subsequently published in [Pilz et al., 2018].

tion 6.2.3. The outcome in terms of the reduction of the PAR value is studied separately and when the two strategies are combined, providing evidence for their success. The question whether it is worth playing the game is answered in Section 7.2, where we compare the results of game-theoretic scheduling with those obtained when there is no interaction between the households. It becomes clear, that especially at realistic participation rates ($\approx 60\%$ [Schumacher et al., 2019]) the exchange of data is indeed valuable.

7.1 Refined Scheduling Approach

Formally, the game belongs to the category of discrete time dynamic games (cf. [Nie et al., 2006]), where players make their decisions sequentially in stages. These stages directly correspond to the daily intervals introduced in Section 4.1. For each stage we define a state of the game, i.e. the current state-of-charge (SOC) of all batteries. The players will choose actions that are directly related to their battery usage, which in turn depends on the state of the game.

In this game, players want to minimise their energy bill, which depends not only on their own decision but also on the decisions of all the other players[2].

Definition 7.1. Our discrete time dynamic game with open-loop information structure consists of the following components:

(1) A set of *players*, i.e. participating households, $\mathcal{N} = \{1, 2, \ldots, n, \ldots, N\}$.

(2) A set of *stages*, i.e. intervals (cf. Section 4.1), $\mathcal{T} = \{0, 1, \ldots, t, \ldots, T-1\}$.

(3) Scalar *state variables* $s_n^t \in \mathcal{S}_n \subset \mathbb{R}$ denoting the SOC of the nth player's battery at stage $t \in \mathcal{T} \cup \{T\}$.

(4) Scalar *decision variables* $a_n^t \in \mathcal{H}_n^t\left(s_n^t\right) \subset \mathbb{R}$ denoting the usage of the battery of the nth player at time $t \in \mathcal{T}$. Furthermore we define the *schedule of battery usage* of an individual player $n \in \mathcal{N}$ as a collection of all its decisions in the stages of the game by $\mathbf{a}_n := \left(a_n^0, a_n^1, \ldots, a_n^{T-1}\right)$. A *strategy profile* is denoted by $\mathbf{a} := (\mathbf{a}_1, \mathbf{a}_2, \ldots, \mathbf{a}_N)$.

(5) A set of *admissible decisions* $\mathcal{H}_n\left(s_n^0\right) := \left\{\mathbf{a}_n \mid h_n^t\left(s_n^t, a_n^t\right) \le 0,\ t \in \mathcal{T}\right\} \subset \mathbb{R}^T$ for the nth player. Note that $\mathcal{H}_n^t\left(s_n^t\right) := \left\{a_n^t \mid h_n^t\left(s_n^t, a_n^t\right) \le 0, \right\} \subset \mathbb{R}$

(6) State transition equations f_n^t governing the state variables $\left\{s^t\right\}_{t=0}^T$:

$$s_n^{t+1} = f_n^t\left(s_n^t, a_n^t\right), \quad t \in \mathcal{T},\ n \in \mathcal{N},$$

[2]Note that the game is identical to the one introduced in the previous Chapter (cf. 6) and is shown here for completeness.

(7) *Stage additive utility functions*

$$u_n\left(s_n^0,[\mathbf{a}_n,\mathbf{a}_{-n}]\right)=g_n^T\left(s_n^T\right)+\sum_{t=0}^{T-1} g_n^t\left(s_n^t,[a_n^t,\mathbf{a}_{-n}^t]\right),$$

where $\mathbf{a}_{-n} := (\mathbf{a}_1,\mathbf{a}_2,\ldots,\mathbf{a}_{n-1},\mathbf{a}_{n+1},\ldots,\mathbf{a}_N)$ denotes the decisions of all other players.

The best response of player n for an arbitrary stage t of the T-stage dynamic game can be written as (cf. [Pilz and Al-Fagih, 2019a])

$$\hat{a}_n^t = \frac{1}{T-t}\left[\sum_{\tau=t}^{T-1}\left(d_n^\tau + L_{-n}^\tau\right) - s_n^t\right] - \left(d_n^t + L_{-n}^t\right). \tag{7.1}$$

The results in the previous chapter (cf. Section 6.1 and [Pilz and Al-Fagih, 2019a]) have shown good scheduling performance, especially in the presence of forecasting errors. The outcomes are based on the best-response formula (7.1) that only considers the current day and is thus subject to a 'finite horizon effect'. We can demonstrate this from the formula directly by calculating the best response for the final interval, i.e. $t = T-1$. Independent of the demand of either household, it will always result in $a_n^{T-1} = -s_n^{T-1}$ for all $n \in \mathcal{N}$, draining the battery towards the end of the day. This might not be beneficial for future days and eventually leads to an aggregated load curve as shown in Figure 7.1, which is undesirable from the UC's point of view. In the following we propose two refinements, i.e. the reward term and the artificial interval, to the original approach set out in Section 6.1 and [Pilz and Al-Fagih, 2019a].

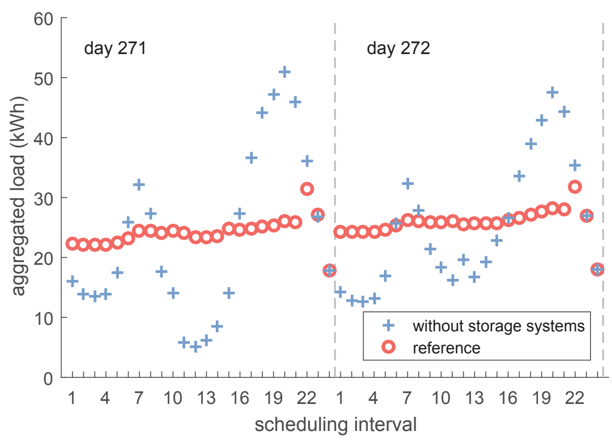

Figure 7.1. *Illustration of 'finite horizon effect'.*
The aggregated load of the neighbourhood is plotted against the scheduling interval for two randomly chosen days. Blue crosses show the values if no batteries are present, while red circles are the results of the dynamic scheduling game proposed in [Pilz and Al-Fagih, 2019a]. Before the horizons (vertical dashed lines) the reference curve displays spikes. (©2018 IEEE)

The reward term: The additional term changes the influence of the current SOC s_n^t on the decision taken in dependence of the interval. Its idea is to let participants keep some of their stored energy towards the end of the scheduling period. Thus, this is directly concerned with the best-response formula (7.1), which is replaced by:

$$\hat{a}_n^t = \frac{1}{T-t}\left[\sum_{\tau=t}^{T-1}\left(d_n^\tau + L_{-n}^\tau\right) - s_n^t\left\{1-\left(\frac{t}{T}\right)^\alpha\right\}\right] - \left(d_n^t + L_{-n}^t\right) \;, \tag{7.2}$$

where the 'reward term' is highlighted in grey and the value of $\alpha > 0$ specifies how long that condition should influence the decisions.

The artificial interval: This is concerned with the structure of the game. Instead of solving the game for T intervals, an additional interval is appended at the end of the scheduling period, thus solving the game for $T+1$ intervals. The demand data for this interval is not taken from any forecast, but is computed to be the average of the forecasted demand from the previous T intervals. Once the solution $\mathbf{\hat{a}}$, i.e. a Nash equilibrium, for this game is determined, it is truncated to the original scheduling period (cf. Section 6.1 and [Pilz and Al-Fagih, 2019a]). From the truncated schedule, one obtains the final SOC for each battery, which is then used as initial data for next day's game.

7.2 Results and Discussion

In this section, two sets of simulations are performed and analysed. The first one is concerned with the validation of the novel scheduling approach. The second one answers the question: "Is the game worth playing?", i.e. does playing the game always provide benefits to both the UC and the households in comparison to a scenario in which households would individually schedule their batteries?

All simulations are performed for a neighbourhood of M=25 households over a period of 365 consecutive days to allow for statistical analysis of the outcomes. Scheduling is performed on a day-ahead basis, where each day is split into T=24 intervals. The respective demand data are taken from [U.S. Dept. of Energy, 2013] and the respective data for renewable energy generation are taken from [Power Networks, 2014]. The accompanying forecasting errors are set to the worst-case scenario (cf. Section 4.4.3) of $\epsilon_d = 8\%$ and $\epsilon_w = 10\%$, based on estimates from [Bichpuriya et al., 2016] and [Dolara et al., 2015], respectively. Every participant of the DSM scheme is equipped with the same type of battery, i.e. the *Tesla Powerwall 2* (cf. [Tesla, 2017]). Values for the battery's efficiency, capacity, charging and discharging rates, and degeneration behaviour are read off its data sheet. In order to allow for a direct comparison, all these data as well as the parameters of the cost function (4.14) are the same as those used in Chapter 6, i.e. Table 6.1.

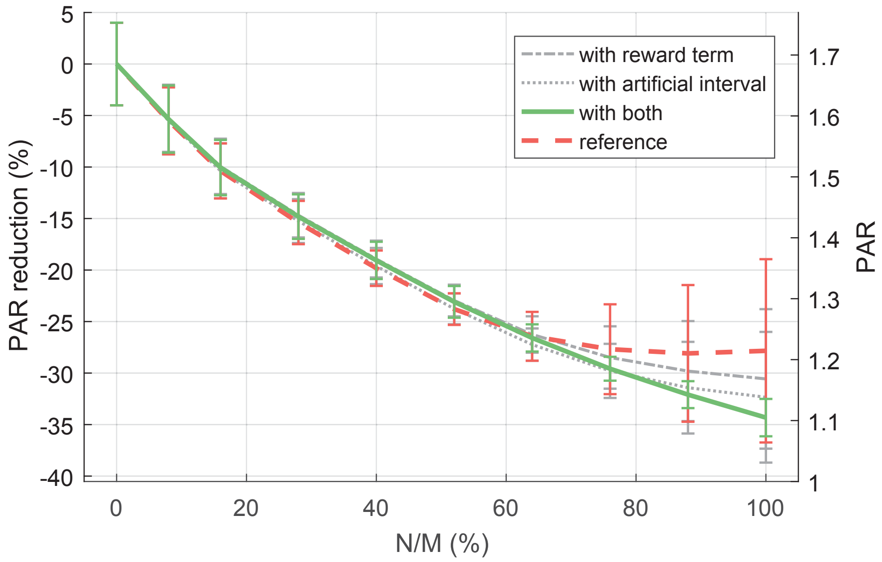

Figure 7.2. *PAR reduction with respect to the participation rate.*
The mean PAR reduction in per cent is plotted over the participation rate in per cent. The right-hand axis shows the absolute values. In addition to the average over 365 days, the standard deviation is shown for each data point. The simulations were run for scenarios which include the proposed amendments individually, i.e. 'with reward term' and 'with artificial interval', and both at the same time, i.e. 'with both'. (©2018 IEEE)

The aim of the UC running the DSM scheme, and thus the main measure for success, is to reduce the PAR of the aggregated load of the neighbourhood as defined in Section 4.5.

7.2.1 Treatment of Horizon

We examine the influence of the two changes regarding the scheduling approach (cf. Section 7.1) individually as well as their combined effect. We chose $\alpha = 10$ in (7.2). This choice means, that the reward term affects mainly (weight > 10%) the last four intervals of the scheduling period, which coincides with the number of intervals that would be necessary to fully charge the battery. The results for the PAR reduction over the rate of participation N/M are presented in Figure 7.2. We observe a monotonic improvement of the PAR value for all cases. At 100% participation rate, the scheduling approach that uses both proposed amendments achieves a mean PAR of 1.10, which equates to a reduction of -34.3%. From Figure 7.3(a) we see that this is an improvement by $\approx 6.5\%$ compared to the results obtained earlier (cf. Section 6.2.4). It also becomes clear that the novel scheduling approach is only beneficial (compared to the reference) for a neighbourhood in which more than 60%

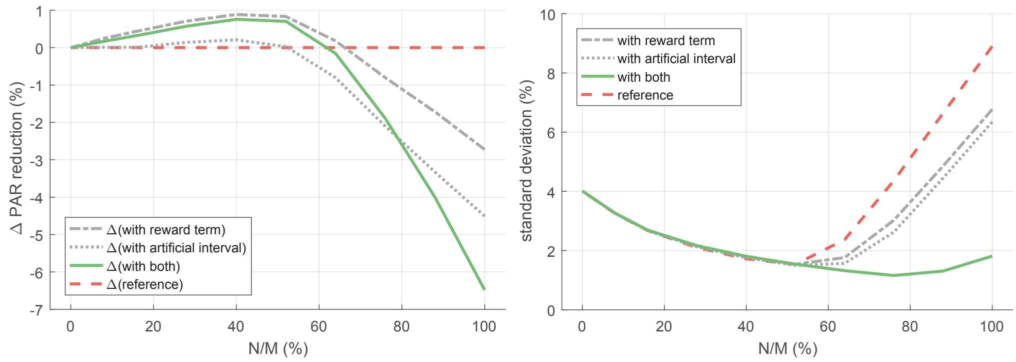

(a) Changes in PAR reduction with respect to [Pilz and Al-Fagih, 2019a].

(b) Standard deviations for all four setups.

Figure 7.3. *Further analysis of the reduction of the PAR value.*
The results plotted in Figure 7.2 are analysed in more detail. The augmented best response with the reward term is based on (7.2). We make use of a single artificial interval, thus extending the scheduling period to $T = 25$ intervals. (©2018 IEEE)

of the households participate. Since the rate of participation roughly corresponds to the rate of the load to be scheduled, below a critical point any changes to the scheduling approach are drowned in the noise of unscheduled load. Furthermore, Figure 7.3(a) shows how the individual adjustments to the best-response formula (7.1) influence the PAR reduction compared to the reference results of Section 6.2.4. They both show similar behaviour. After reaching a critical participation rate both improve the scheduling outcome, though the approach with an artificial interval always outperforms the one with the reward term.

It is important to not only examine the mean PAR reductions, but also the fluctuations of individual days as expressed by the standard deviation. It gives an indicator of the robustness of the game's solution with respect to its inputs, i.e. the daily changing demands of the households. The respective results are shown in Figure 7.3(b). We observe that there is no difference between the approaches up to a participation rate of $\approx 50\%$, emphasising the claim that this range is dominated by noise from unscheduled households. Above 50% the standard deviation of the PAR from the reference approach (cf. Section 6.2.4 and [Pilz and Al-Fagih, 2019a]) is monotonically increasing up to a value of $\approx 9\%$. The same trend can be observed for the scheduling approaches which incorporate individual changes, with the difference that they perform better than the reference. At full participation their standard deviation is 6.3% and 6.8%. For the combined approach the standard deviation is smaller than the reference (above 50% participation rate). If every household participates in the DSM scheme, the standard deviation is reduced by a factor of 5 to a value of 1.8%. The combined effect of the individual refinements leads to a distinct improvement of the standard deviation compared to the reference results. This means the fluctuations of the individual changes statistically cause opposing effects which cancel each other.

Note that all results presented in this paper stem from simulations which include forecasting errors in a worst-case scenario (cf. [Pilz and Al-Fagih, 2019a, Section 3]). Without forecasting error, the achieved mean PAR is even closer to the optimal value of 1.0 over the whole range of participation rates. Nevertheless, the standard deviation is almost identical to the case with both amendments. An analysis of the bills for the individual households revealed that the novel scheduling approach does not alter the outcomes on the mean savings when compared to the results presented in the previous chapter.

In summary, the proposed scheduling approach performs distinctly better than what was previously achieved. Especially at high participation rates the improvements in both PAR reduction and standard deviation result in a more beneficial and stable system.

7.2.2 Added Value of the Proposed DSM Scheme

Motivated by the results of the previous subsection, all simulations here are based on the new scheduling approach. We compare three scenarios: Firstly, we consider a DSM scheme based on the dynamic game introduced in Section 6.1. Note that this is exactly the simulation undertaken in Section 7.2.1 which incorporates both amendments (cf. green curve in Figure 7.2 and 7.3(b) denoted by 'with both'). Secondly, we look at a scenario in which households are equipped with batteries and photovoltaic cells but do not take part in the dynamic scheduling game. Instead they perform the scheduling of their battery solely on the forecasting of their individual demand. This also means, that there is no need for the UC to collect demand data and redistribute the aggregated data at the beginning of the DSM protocol. Lastly, the third scenario differs from the second one in the fact that no forecasting is performed. Instead the scheduling of the battery for the day ahead is based on the demand recorded of the current day.

The results for the mean PAR values against the number of households equipped with batteries and the corresponding standard deviations are shown in Figure 7.4. We observe that the scenario in which the households play the game is always most effective in terms of PAR reduction independently of the number of participants. The largest difference to the simulations without the game are realised at $\approx 50\%$ participation rate, where PAR reductions of -16.2% and -23.1% are achieved. For higher participation rates the difference between the two approaches monotonically decreases. The third scenario achieves comparable results to the one without the

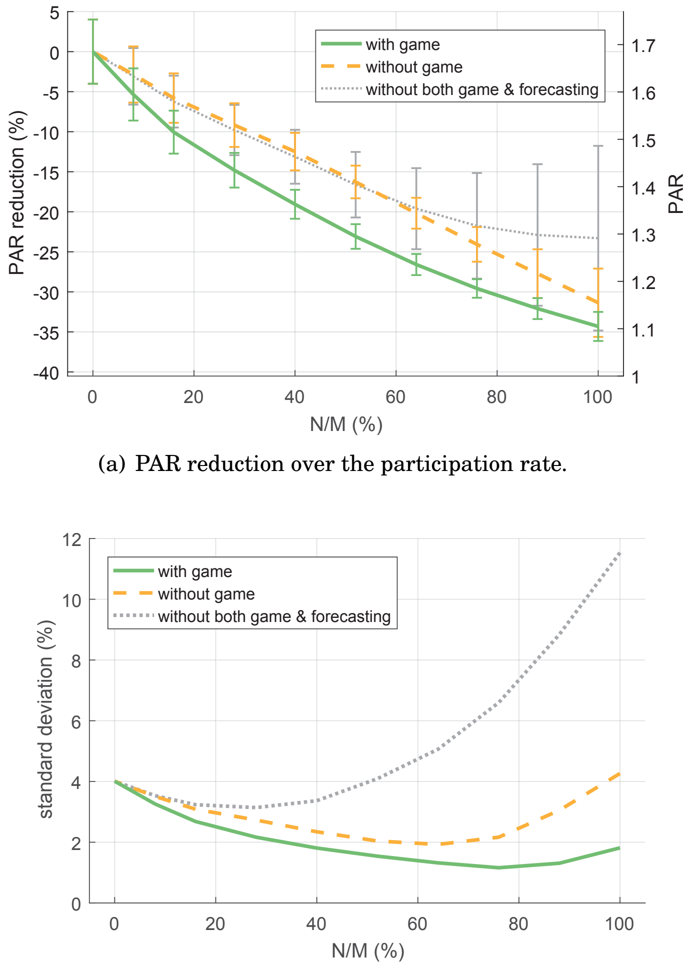

(a) PAR reduction over the participation rate.

(b) Standard deviations for the three setups over the participation rate.

Figure 7.4. *PAR reduction of the aggregated load over the participation rate.*
(a) The mean PAR reduction over 365 days in per cent is plotted over the participation rate in per cent. The right-hand axis shows the absolute values of the PAR. The simulations were run for scenarios with and without the game as explained in Section 7.2.2. Furthermore, results for a scenario without both the game and forecasting are presented. (b) For clarity, the standard deviations are shown separately. (©2018 IEEE)

game for low participation rates, but provides distinctly worse outcomes for high participation rates. At full participation we obtain PAR reductions of −34.3%, −31.4%, and −23.3% for the scenarios with game, without game, and without both game and forecasting, respectively. An analysis of the standard deviations (cf. Figure 7.4(b)) reveals that the results from the game scenario also perform better in this aspect. This highlights the importance of forecasting (even if it contains errors). Both scenarios that use forecasted demands as input for their scheduling outperform the third one. In short, we see that the third approach is oversimplified and thus not suitable. Furthermore, the approach utilising the dynamic game between the households is better in both the mean PAR reduction and standard deviation than the approach without the game.

Let us discuss the 'costs' associated with the game for both the UC and the households. The costs for the UC of guaranteeing secure transmission of the aggregated demand data to the individual households would have already been incorporated when setting up the required infrastructure and can thus be neglected. For the households, the dependence on external information for their battery scheduling creates an additional risk. The UC must therefore provide a guarantee to the participants of the DSM scheme that they would never be penalised financially for participating in the game.

7.3 Conclusions

In this chapter, we provided strategies addressing undesired 'finite horizon effects' that can occur in game-theoretic DSM schemes. Experiments conducted for 25 households based on an advanced battery model, and realistic demands over a period of one year revealed that the combination of those strategies ensures reductions in terms of load PAR and robustness, without affecting individual households' savings. Secondly, an evaluation of the respective impacts of battery usage, demand forecasting and implementation of the enhanced DSM scheme was performed. Although energy storage leads to significant PAR and bill reduction even without the game and forecasting, improved performance is achieved using both. However, since gains by participating in the DSM are relatively modest for households and the game relies on receiving external data, security concerns may lead them not to wish to participate in the scheme. The UC is advised to incentivise participants by guaranteeing (financial) security in case of data corruption in addition to the already considered tariff incentive. The topic of cyber security is investigated in the next chapter.

This almost blank page is intentional.

CHAPTER 8

CYBER ATTACKS ON SMART GRID SCHEDULING

To this point, we were only interested in advancing the management of batteries in future prosumer communities. This chapter[1] approaches the topic from a different angle, i.e. the cyber security side. Can a malicious user topple the demand-side management (DSM) system? How should the utility company react, if at all? These questions are addressed in this chapter.

Taking advantage of smart meters, energy storage and trading strategies, a variety of energy consumption scheduling techniques aiming at optimally distributing daily power consumption has been put forward to reduce a smart grid's peak-to-average ratio (PAR) of the aggregated load. In particular, dynamic game-theoretic frameworks have been proposed to optimise energy cost using their Nash Equilibrium (NE) [Mohsenian-Rad et al., 2010, Mohsenian-Rad and Leon-Garcia, 2010]. We considered advanced battery models (cf. Chapter 5) and integrate forecasting errors (cf. Chapter 6). Alternatively, usage of a Stackelberg game minimising both the PAR and the system total cost has also proved promising [Soliman and Leon-Garcia, 2014]. More generally, comprehensive reviews reveal the significant contribution that game-theoretic solutions offer in terms of reducing consumer costs and PAR values [Pilz and Al-Fagih, 2019b, Gupta and Yadav, 2017, Saad et al., 2012, Fadlullah et al., 2011].

[1]This chapter was accepted and published after one round of peer review in [Pilz et al., 2019a]. My contributions were focussed on the first part of the paper with minor contributions in the second part. Nevertheless, the whole story is presented here for completeness.

Although those solutions are becoming more sophisticated, the smart grid can only be realised once appropriate security measures are in place. None of these papers [Mohsenian-Rad et al., 2010, Mohsenian-Rad and Leon-Garcia, 2010, Pilz et al., 2017b, Pilz and Al-Fagih, 2019a, Soliman and Leon-Garcia, 2014] are concerned with the security of the respective systems. Since smart grids rely on a communication network and smart meters, they may be vulnerable to cyber attacks [Mo et al., 2012]. As a result, appropriate defence strategies need to be put in place [Liu et al., 2009, Yan et al., 2012, Wang and Lu, 2013, Rawat and Bajracharya, 2015, He and Yan, 2016, Tan et al., 2017]. The main issue is the robustness and security of the communication channel between the smart meter and the utility company. Typically, the smart meter connects to the home Local Area Network (LAN) and from there to the Wide Area Network (WAN). Recently, there has been a move towards the systematic adoption of so-called Home Area Networks (HANs) for communication within the end-user's home.

HANs are based on wireless communication using Internet of Things (IoT) technologies and protocols, and over time this will involve a more and more diverse and large number of devices, appliances, vendors and protocols, lacking of compatibility and standards – in particular, in the area of security. As mentioned in [Batalla et al., 2017], there are two particularly worrying trends in HANs: The increased usage of external cloud providers in order to cope with the growing number of data, and the lack of security awareness and commitment on behalf of end-users who opt for convenience rather than precaution. We argue that all these phenomena lead to a rapidly growing attack surface of the smart meter system, making interception and modification of HAN traffic including forecasting data more realistic, easier and probable. Thus the most pressing security attacks on a smart home environment are typical examples of novel IoT security challenges that require specific and novel security mitigation techniques. In this paper, we propose the use of game theory in order to address these attacks.

False Data Injection (FDI) is one of the most common approaches to attack cyber-physical systems [Lun et al., 2016]. In general, FDI attacks target data integrity breaches to make profit or disturb a system. Since, in power grids, state estimators are the main data sources used for monitoring and controlling purposes, they are the target of data injection [Liang et al., 2017]. Such FDI attacks and possible defence strategies have been investigated in several scenarios: (i) the 'ideal' undetectable attack where the attack vector is built from complete knowledge of the state estimators' parameters [Liu et al., 2009]; (ii) a more realistic attack relying on a probability distribution function where only incomplete information about the system's parameters is available [Rahman and Mohsenian-Rad, 2012]; (iii) a stealth data injection in which an attacker has complete information about the system's topology [Huang et al., 2013]. Detection of cyber attacks and associated defence strategies are essential for a reliable grid. For instance, a fast detection algorithm has been proposed to deal with FDI and jamming attacks in smart grids [Kurt et al., 2018].

Since game theory has been successful to design cyber security solutions [Wu and Wang, 2018], it has been applied in several scenarios dealing with grid security. When attackers target either a single or multiple state estimators, both Markovian and static strategies have been investigated to defend against load redistribution attacks by allocating optimal budgets to energy suppliers [Xiang and Wang, 2017]. If attackers manipulate price information from the utility companies, the resulting impact can be mitigated exploiting a Stackelberg formulation [Maharjan et al., 2013]. Furthermore, it has been proposed to defend against coalitional attacks by multiple attackers using an iterated game-theoretic model [Yang et al., 2016], where a probability of attack detection is considered in each iteration: correlation between payoffs and penalty factors demonstrated the effectiveness of the defence system. A defence system against switching attacks based on a zero-determinant iterative game between controller and attacker showed that transient stabilisation could be achieved over time [Farraj et al., 2016].

A different security game in [Law et al., 2015] is proposed, which considers a variety of risk assessment measures integrated to a stochastic game to choose the best defence strategies. The simulated results illustrate that a conditional value-at-risk measure enables the defender to prioritise the most significant attacks. Moreover, a scenario with multiple adversaries and a single defender in smart grids is studied [Sanjab and Saad, 2016]. This framework considers two Stackelberg games to analyse the interaction between attackers and the defender. To solve the hybrid Nash equilibrium game, a search based algorithm is introduced showing that the defender can achieve the minimal loss by protecting a limited number of parameters. Also, the results indicate that multiple attackers can be destructive to each other leaving the smart grid unaffected. Another hybrid model in [Zhu and Başar, 2011] proposes a hybrid zero-sum differential game and a stochastic zero-sum game for the physical layer and cyber layer respectively. On the other hand, a multi-adversarial FDI attack is considered in [Boudko and Abie, 2018] where the data is manipulated in the network transmission layer. In this scenario, the model is formulated by evolutionary game theory to maximise the adversaries' payoff in the grid. Although grid cyber security has been an active field of research, no defence scheme has yet been proposed to protect forecasting data in smart grids.

The contributions covered in this chapter are the following[2]:

(1) We design a novel class of false data injection attacks, preserving average daily load in a smart energy scheduling system. The forecasted demand data is corrupted by a single attacker, targeting one or several households. Using extensive simulations, two families of attacks are investigated. The impact on both the PAR of the aggregated load and consumer bills as well as the resulting benefit for the attacker are analysed.

(2) We design and analyse an augmented security game for monitoring average-preserving false data injection attacks, based on a detailed model with strategies and payoff functions informed by the simulation findings. The conditions under which a pure NE exists are derived. This extends previous work by providing additional strategies and a more detailed payoff design, informed by the various cost and benefit functions of the utility company and the attacker.

(3) We give practical guidelines to the utility company on how to protect itself against such attacks. The recommendations are based on combining a range of mitigation strategies and the results of the equilibrium analysis of the game, to aid the utility company with the decision–making process of investing in the security defence. The given advice is motivated by the simulation scenario, but can also be adapted to other situations. This is demonstrated using a concrete example.

The chapter is structured as follows. It is split into two major sections. Section 8.1 deals with potential attacks on the game-theoretic scheduling mechanism established in the previous chapters, and Section 8.2 deals with defence strategies for the utility company. More specifically the following aspects are included. In Section 8.1 we firstly define a novel class of false data injection attack based on the tampering of forecasting data and introduce two types of attacks. Secondly, the outcome for the attacker, the utility company, as well as the other participants of the DSM are investigated in great detail. Based on these results, we identify detection strategies based on different levels of system monitoring. Lastly, the impact of the aforementioned attacks is discussed with respect to the applied monitoring. In Section 8.2, a non-cooperative game to analyse the decision-making process for the utility company is introduced. It can be seen as an extension to previous investigations in the literature. The augmented security game is analysed and three cases are highlighted. Eventually, we connect the results of the first part with the insights of the second one and give direct advice to the utility company.

[2]My personal contributions are concentrated in the first bullet point. Throughout the chapter, there will be further highlights of my involvements whenever suitable.

Important notice: With respect to this thesis, I want to highlight that the outcomes of Section 8.1 are directly based on my contributions. In Section 8.2, I was only involved in the analysis of the quantitative example (cf. Section 8.2.4). Other parts of this section are the work of the co-authors of the respective paper [Pilz et al., 2019a] and are shown here only for completeness.

8.1 False Data Injection On Forecasts

The security of a smart energy system is of extreme importance and there is a lack of research on possible attacks on forecasted data. This section describes different types of potential attacks that may take advantage of the game-theoretic smart grid management model presented previously (cf. Chapter 6,7). Furthermore, outcomes of those attacks are analysed from the point of view of the attacker, the utility company (UC) and the other players. Various defence strategies to detect those attacks are proposed and analysed. Finally, attack mitigation is discussed.

8.1.1 Description of Attacks

All attack scenarios investigated in this section rely on the following assumptions. First, the attacker (who is one of the players) exploits the vulnerability of the smart grid communication network: They have the ability not only to intercept forecasting data from all the other players, but also to replace them. Second, after the game has been played based on the tampered data, the attacker adapts their storage schedule and takes advantage of the erroneous schedules that the other players follow. Finally, in order to limit the risk of having their attack detected, the attacker makes sure that the average daily aggregated load is not affected by their actions. Although there are many strategies which can be applied to change forecasts while maintaining a constant aggregated value of the load, this study investigates two simple families of attacks: Forecast shifting and scaling.

Shift attack: The shift attack replaces a given forecast with the original forecast after having undergone a circular shift of σ time intervals, where σ is an integer. Since experimental results have shown that a shift attack of 4 hours, see Fig. 8.1, produces the most dramatic impact for the dataset of interest (cf. Section 4.4), that value is used for the rest of the study.

Scale attack: The scale attack substitutes a given forecast with a scaled version centred around its average value for the day. To ensure that the day average is not affected, the scaling parameter τ should be chosen such that no load becomes negative after scaling. Note that for the dataset of interest (cf. Section. 4.4), a value

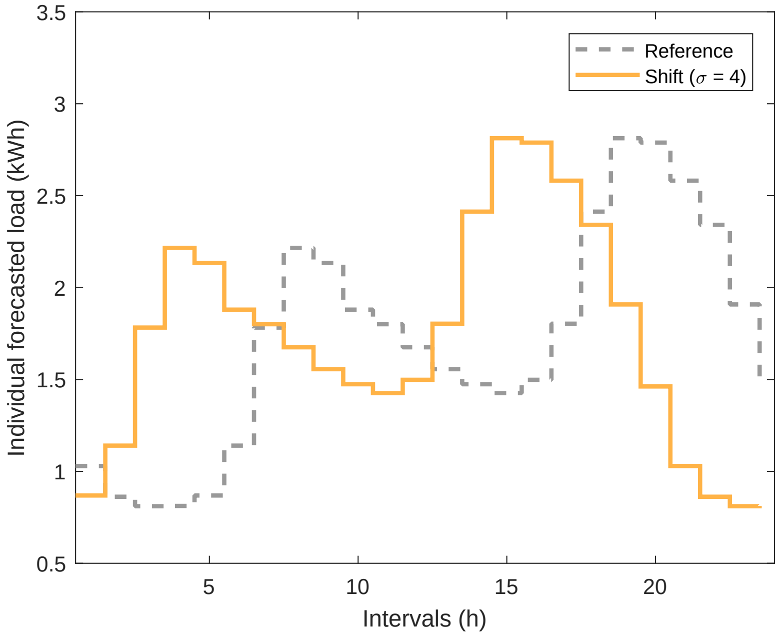

Figure 8.1. *Example of a shift attack.*
The reference curve shows the forecasted load of an individual household for the upcoming day. When the attacker applies the shift attack, they perform a circular shift of the interval data. The result of a shift with $\sigma = 4$ is shown as an example.

of $\tau = 2$ remains acceptable: Although a couple of values do become negative, they are set to 0; the daily average is slightly increased, but it remains within a realistic forecast uncertainty (cf. Section 4.4.3). Fig. 8.2 illustrates the effect of various scale attacks, i.e. $\tau = -1$, $\tau = 0$ and $\tau = 2$. While $\tau = 1$ returns the initial forecast, $\tau = 0$ and $\tau = -1$ produces a flat, and mirrored forecast, respectively. In the rest of the chapter, these two different attacks are called flat attack and mirror attack.

The outcome of an attack does not only depend on the type of attack and its associated parameter, but also on the number of forecasts which are replaced among all the players of a game: the higher the percentage λ of attacked households, the more room for manoeuvre the attacker has to profit from their attack.

8.1.2 Attack Outcomes

What effect do the different false data injection attacks have?

Outcome for the attacker: Fig. 8.3 illustrates the resulting load curves of attacker and victim in the case of a shift attack ($\sigma = 4$). The attacker benefits by having a high load during the periods when the victims have a low one and vice versa, so that the attacker's higher consumption takes place when the aggregated load, and thus unit price, is low. This is exactly what the attacker tried to achieve by manipulating the forecasting data and thus the input to the scheduling game.

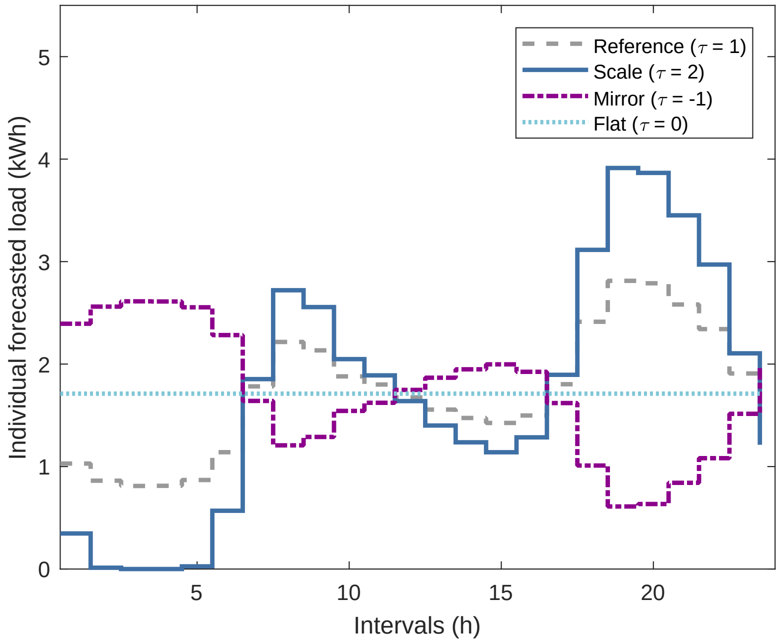

Figure 8.2. *Example of scale attacks.*
The reference curve shows the forecasted load of an individual household for the upcoming day. It is identical to the reference shown in Fig. 8.1. When the attacker applies the scale attack, they scale the interval data with respect to the daily average of the forecasted load. Scaling with a factor $\tau = 2$ leads to more severe troughs and peaks, while using $\tau = -1$ results in a mirrored forecast. $\tau = 0$ gives a perfectly flat load profile.

Note that the same cost function as in Section 4.3 and [Rahbar et al., 2015, Pilz et al., 2017b] was used. In this attack example, there is a high inverse correlation, i.e. ≈ -0.96, between the attacker's load and the unit price.

An attacker's financial benefit depends not only on the type of attack, but also the number of households using a battery, i.e. the participation rate N/M, as well as the proportion of targeted households λ whose forecasts have been changed. In order to investigate this, attack simulations were conducted on a smart grid comprising $M = 25$ households for a duration of one year. Compared to the non-attack scenario, Fig. 8.4 displays the percentage change on the attacker's bill (yearly median of the daily changes) according to those parameters in the cases of shift ($\sigma = 4$), mirror ($\tau = -1$) and scale ($\tau = 2$) attacks. Simulations have revealed that a flat attack ($\tau = 0$) results in benefits similar to those of the shift attack ($\sigma = 4$) and is thus not shown.

Fig. 8.4 reveals that for shift ($\sigma = 4$) and mirror ($\tau = -1$) attacks the attacker is never penalised by their action and their gains increase with both participation rate and percentage of targeted players. Bill reductions for the attacker reach up to 25.5% and 35.7%, respectively. However, in the case of the scale attack ($\tau = 2$), the graph displays a different picture: Up to a relatively high participation rate

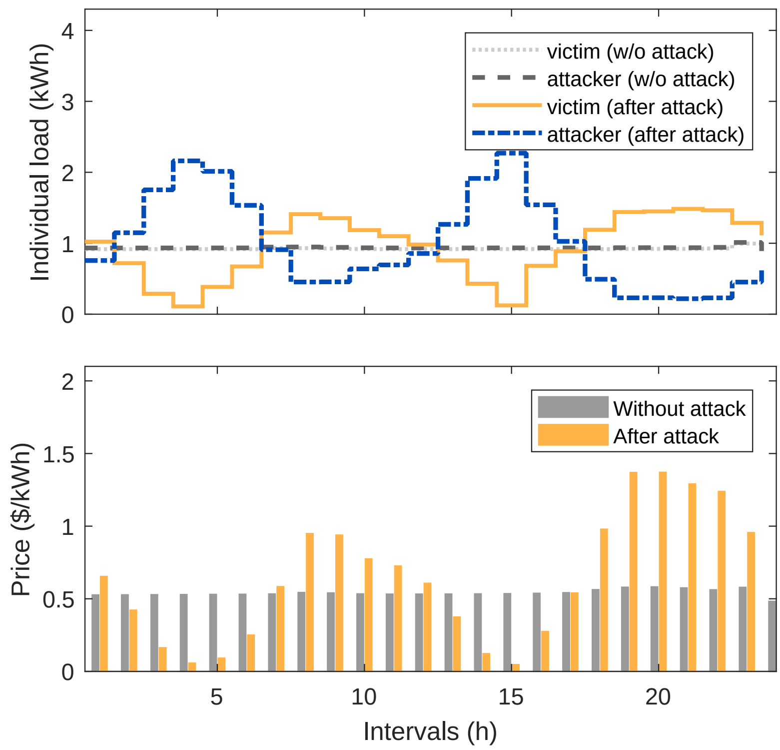

Figure 8.3. *Individual loads and unit price after scheduling.*
The top graph displays load profiles for one day of a randomly picked victim and the attacker for two different scenarios: with and without attack. While both references show an almost flat profile, the load curves after the attack differ considerably. This is a direct result of the attacker taking advantage of the falsely injected data. The bottom graph displays the change of price per unit during those two scenarios. As expected, the attacker's load has a high inverse correlation with the unit price (≈ -0.96).

($N/M > 55\%$), the attacker is financially penalised by their attack. Indeed, while the other attacks lead players to charge their battery at a wrong time, this scale attack tends to make players charge their battery more than they need at a time when the attacker would also need to charge their battery. As Fig. 8.5 reveals, when the participation rate is high, the aggregated load profile is inverted due to a large number of players charging their battery excessively at a time that was initially of low load and discharging their battery when a peak was expected. As a consequence, the aggregated load profile is now almost ideal for the attacker who can benefit from low prices at their time of high needs. Thus, they hardly need to use their battery and can gain up to 9.5% of bill reduction.

Outcome for the utility company and the other players: As mentioned in Section 4.5, for the utility company, the efficiency of a microgrid is assessed by its PAR value. Since attacks change the aggregated load, it is directly affected. The effect of the previously introduced attacks on PAR values is presented in Fig. 8.6.

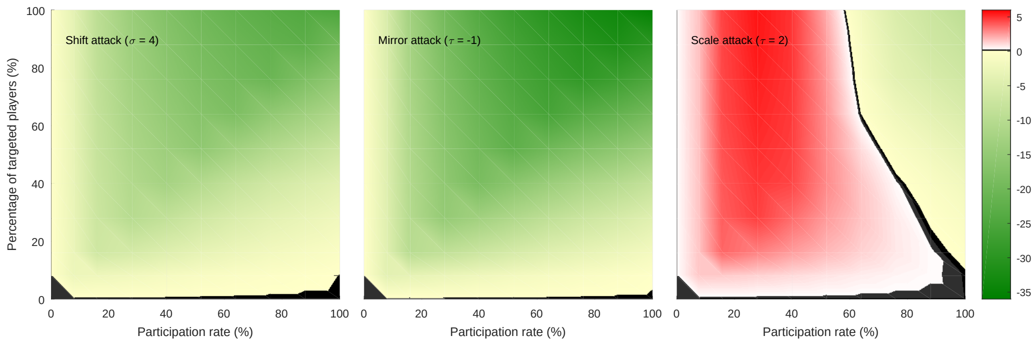

Figure 8.4. *Financial benefit for the attacker.*
The median change (compared to the non–attack scenario) over 365 days of the energy bill for the attacker is shown in per cent. The outcomes for three different attacks, i.e. shift attack with $\sigma = 4$, mirror attack, and scale attack with $\tau = 2$, are presented. The simulations were performed for $M = 25$ using various participation rates and percentages of targeted players. While the first two attacks display similar benefits, the third one indicates that for specific scenarios the attacker also has an increased electricity bill.

The different attack types are associated to a different graph, which presents several curves, each for a different percentage λ of targeted players, showing the relationship between participation rates N/M and PAR values. For the shift ($\sigma = 4$) and mirror ($\tau = -1$) attacks, an increase of λ leads to a worsening of PAR values. Moreover, as in the non–attack scenario, PAR values tend to improve with an increase of participation rate. Note for the case of the mirror attack: If a high percentage of players are targeted, an increase of the participation rate contributes to the degradation of PAR values.

As analysed in the previous section, the outcomes of the scale attack ($\tau = 2$) are different from the others when the participation rate is below $N/M = 55\%$. In fact, Fig. 8.6 shows an improvement of the PAR values compared to the non–attack scenario when the percentage λ of targeted players increases. Fig. 8.5 clearly shows that at low participation rates the aggregated load is flatter than without an attack. The explanation is that this positive scaling incentivises participating households to work harder to flatten the load curve: As seen in Fig. 8.5, charging takes place at the same time but with a higher intensity. As a consequence, a 52% participation rate is sufficient to achieve a PAR that is similar to the one resulting from a 100% participation rate without any attack, i.e. PAR = 1.11 and PAR = 1.07, respectively. Participants work twice harder, which has the same effect as if everybody was working as they should. This extra work leads to higher bills for those households. An improved PAR value may suggest that the UC benefits from such attacks. In practice, this is not the case because in those scenarios the electricity bills of all

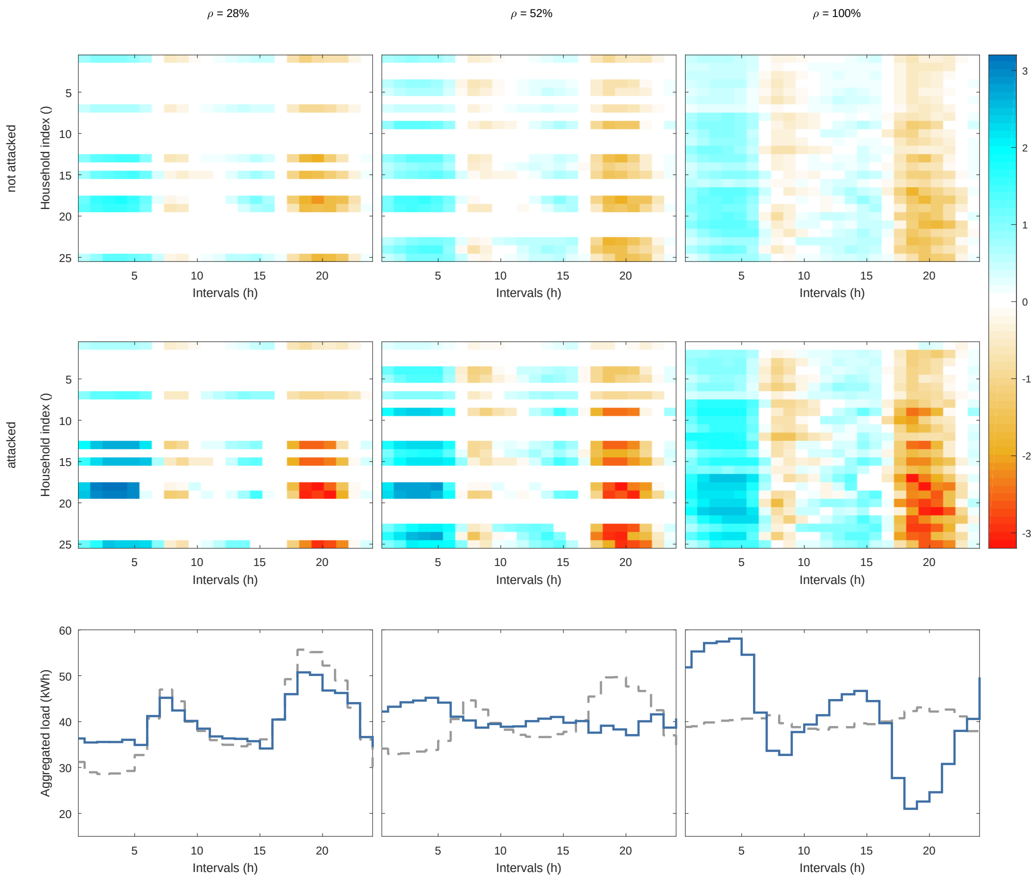

Figure 8.5. *Aggregated load and battery schedule without and under a scale ($\tau = 2$) attack targeting all players for different household participation rates (N/M).* Each column corresponds to a different participation rate, i.e. from left to right $N/M = 28\%$, $N/M = 52\%$ and $N/M = 100\%$. The first row shows battery schedules of each individual household; the second row shows battery schedules of each individual household under attack - note that the first household is the attacker; the third row compares aggregated loads without - dashed curves - and with - bold curves - attacks. Without attack, participation of all households, i.e. $N/M = 100\%$, is required to flatten the aggregated load (PAR = 1.07). However, excessive battery usage by attacked households (the second row shows stronger charges and discharges) leads to a relatively flat (PAR = 1.11) aggregated load at $N/M = 52\%$. However, at $N/M = 100\%$ the aggregated load profile is almost inverted; in this case the attacker hardly needs to use their battery.

players, including the attacker, increase substantially (data not shown), which will eventually lead to a loss of reputation and customers for the UC.

All attacks leading to the reduction of a single player's (the attacker) bill result in an increase of all the other players' bills by usually a comparable amount (details are discussed in the following section, cf. Table 8.1 and 8.2). As a consequence, the aggregated bill for the whole neighbourhood is significantly increased. For example,

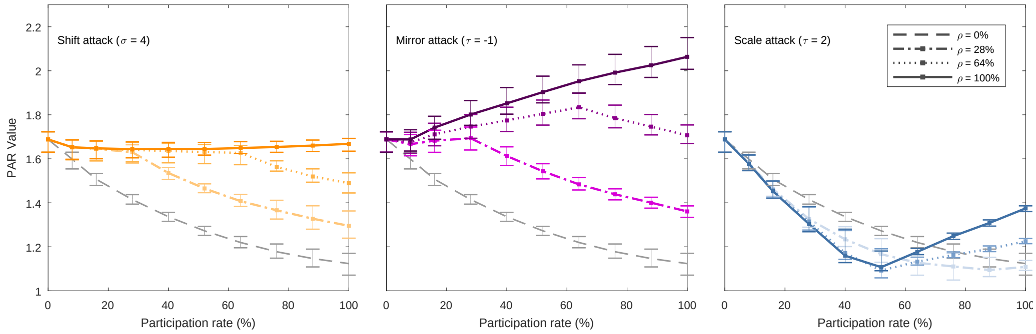

Figure 8.6. *Peak-to-average ratio (PAR) of the aggregated load for different attack scenarios.*
The median PAR value for a 365 day simulation is plotted together with the range between the first and third quartile over the participation rate. The outcomes for three different attacks, i.e. shift attack with $\sigma = 4$, mirror attack, and scale attack with $\tau = 2$, are presented. For each attack, the individual graphs differ in their number of attacked players. This also includes the reference outcome of the scheduling game in which no player is attacked.

a mirror ($\tau = -1$) attack targeting all players ($\lambda = 100\%$) rewards the attacker with a 35.7% bill cut, while the other players must endure a 54.0% rise on average. Similarly, the attacker benefits from a scale attack ($\tau = -2$, $\lambda = 28\%$) with a bill reduction of 1%, penalising the other households by a 2.3% increase.

8.1.3 Attack Detection Strategies

All investigated attacks affect the utility company negatively: When the participation rate is high, PAR values are systematically degraded compared to the non–attack scenario; otherwise, either PAR values worsen, or their improvement is at the cost of higher electricity bills for the average household. This is detrimental to the UC's credibility and competitiveness. Consequently, the UC needs to design defence strategies to prevent attacks that affect the storage scheduling process. In this section, the focus is on the detection of false data injection by monitoring the forecasting data that are transmitted every day on the smart grid communication system.

Attack detection through system monitoring: Forecast monitoring is considered at three different levels:

- Aggregated consumption forecast average, i.e. average amount monitoring
- Aggregated consumption forecast profile, i.e. deep aggregated monitoring
- Household consumption forecast profiles, i.e. deep individual monitoring

In each case, the UC would compare the received forecast data with its own estimate. While monitoring the aggregated consumption forecast total only requires the UC to forecast the daily total electricity consumption of the smart grid community as a whole, deep monitoring relies on producing hourly consumption estimates for either the entire community or each individual household. The more precise the monitoring, the more resources are needed to implement it.

Since an individual average hourly forecast error for a 24-hour period is expected to be lower than 8% [Bichpuriya et al., 2016], the expectation is that the difference between two forecasts, i.e. the forecast provided by the received forecast data and the forecast estimated by the UC, to be lower than twice the 8% error of a single forecast. As a consequence, it is reasonable to assume that the UC could use a threshold of 20% to identify an attack when using deep individual monitoring. In the case of deep aggregated monitoring, the combination of forecasts tends to lead to error reduction. As a consequence, here a discrepancy of at least 10% is used to detect an attack. Finally, since in the proposed attack scenarios, the attacker always makes sure that their attack does not change the average daily aggregated forecast, a UC relying only on average amount monitoring would not be able to detect any attack. Eventually, the detection of a given attack depends not only on the chosen monitoring strategy, but also the type of attack, the participation rate N/M, and the percentage λ of targeted players.

Attack impact analysis: Based on the three proposed monitoring strategies, the consequences of undetected attacks are studied. These are evaluated by estimating an attack's impact in terms of average bill change for the attacker and the other players, bill revenue change for the UC and PAR values. Assuming a participation rate of $N/M = 100\%$, this set of experiments considers, for each attack type of interest, i.e. shift ($\sigma = 4$), flat ($\tau = 0$), mirror ($\tau = -1$) and scale ($\tau = 2$ and $\tau = 1.29$), the most severe attack, in terms of the highest percentage λ of targeted players, that has remained undetected according to the monitoring strategy.

As Tables 8.1 and 8.2 show, all of those attacks prove beneficial to the attacker in terms of reducing their bill, while other players suffer a bill increase. Regarding the UC, it benefits financially from the general bill rise, but sees its PAR value degraded. Note that the impact of a scale ($\tau = 1.29$) attack is evaluated because it is the most powerful scale attack which can target all players ($\lambda = 100\%$) without being detected by any of the proposed monitoring strategies.

Table 8.1 reports the impact of undetected attacks despite average amount monitoring. As such monitoring is ineffective against the considered attacks, the attacker is able to carry out their attack with maximum strength, i.e. ($\lambda = 100\%$), without being detected. The mirror ($\tau = -1$) attack is particularly efficient: The

Table 8.1. *Impact of undetected attacks despite average amount monitoring.*
Results show median values over 365-day simulations together with their respective interquartile range. The participation rate is $N/M = 100\%$.

Attack type	λ (%)	Attacker	Other players	Utility company	
		Bill change (%)	Bill change (%)	Revenues change (%)	PAR value
Shift ($\sigma = 4$)	100	−25.5 (5.8)	28.3 (13.1)	26.3 (12.3)	1.67 (0.06)
Flat ($\tau = 0$)	100	−21.0 (6.6)	16.7 (4.3)	15.1 (4.0)	1.66 (0.09)
Mirror ($\tau = -1$)	100	−35.7 (12.5)	54.0 (11.1)	50.3 (10.5)	2.06 (0.14)
Scale ($\tau = 2$)	100	−9.5 (2.8)	21.4 (4.4)	20.1 (4.2)	1.37 (0.03)
Scale ($\tau = 1.29$)	100	−1.5 (0.8)	3.1 (0.8)	2.9 (0.7)	1.13 (0.03)

Table 8.2. *Impact of undetected attacks despite deep aggregated monitoring.*
Results show median values over 365-day simulations together with their respective interquartile range. The participation rate is $N/M = 100\%$.

Attack type	λ (%)	Attacker	Other players	Utility company	
		Bill change (%)	Bill change (%)	Revenues change (%)	PAR value
Shift ($\sigma = 4$)	16	−0.8 (0.7)	1.1 (0.5)	1.0 (0.5)	1.22 (0.11)
Flat ($\tau = 0$)	28	−1.9 (1.1)	0.3 (0.5)	0.2 (0.5)	1.23 (0.05)
Mirror ($\tau = -1$)	16	−1.7 (1.1)	0.9 (0.7)	0.8 (0.7)	1.25 (0.06)
Scale ($\tau = 2$)	28	−1.0 (0.7)	2.3 (0.7)	2.2 (0.7)	1.11 (0.04)
*Scale ($\tau = 1.29$)	100	−1.5 (0.8)	3.1 (0.8)	2.9 (0.7)	1.13 (0.03)

* denotes attack that remains undetected even when applying deep individual monitoring

attacker's bill is reduced by 35.7% at the cost of the other players' bills, i.e. 54.0%, and a large increase of the PAR value to 2.06 from a non–attack value of 1.12.

Once deep aggregated monitoring is in place, the strength of the attacks that remain undetectable is reduced significantly. As Table 8.2 shows, the attacker's bill is lowered by 1.9% at most. However, although, in this case, the other players are hardly affected - their bills only increase by 0.3%, the UC suffers from a significant degradation of the PAR to 1.23. One should note that although the scale ($\tau = 2$) attack with ($\lambda = 28\%$) produces a slightly better PAR value, i.e. 1.11 instead of 1.12 from the non–attack scenario, this is achieved by increasing the average electricity costs by 2.2% (cf. discussions in Section 8.1.2 Figure 8.5).

Finally, although the most stringent monitoring strategy, i.e. deep individual monitoring, would detect most attacks whatever λ, i.e. shift ($\sigma = 4$), flat ($\tau = 0$), mirror ($\tau = -1$) and scale ($\tau = 2$), some limited scale attacks such as ($\tau = 1.29$, $\lambda = 100\%$) still cannot be discovered (cf. last line of Table 8.2). Although none of the proposed monitoring strategies can detect all attacks, they are able to recognise the most severe ones. Moreover, they can detect false data injection for a wide range of attacks.

8.1.4 Attack Mitigation

Once an attack has been detected, some response needs to be provided. For the most serious attacks, households may be instructed not to follow the calculated battery schedule, but use an alternative one. Several options are possible such as keeping the same schedule as the previous day or recalculating their schedule only taking into account their own data. In the latter case, scheduling is executed without using the game-theoretic framework, but by performing a simple optimisation of battery usage for their own consumption forecast.

These options were evaluated in the previous chapter (cf. Figure 7.4). It showed that, although both approaches lead to a PAR reduction, local scheduling should be the defence of choice since it systematically outperforms previous day scheduling. Still, this mitigating strategy has its own cost: At medium participation rates N/M, the PAR reduction can be up to $\approx 25\%$ lower than when the game is played. As Tables 8.1 and 8.2 show, only the most powerful attacks have an impact on the PAR which is higher than reverting to the local scheduling strategy. This suggests that the best reaction to a low impact attack would be to let it happen. In terms of monitoring, only deep aggregated monitoring would prove useful, since it is able to detect all attacks for which the proposed mitigation strategy is beneficial. Therefore, a two-level detection system may be the most suitable strategy for the UC: It should conduct either no monitoring at all, or deep aggregated monitoring.

Before deciding on a complete defence strategy, which includes detection and mitigation, all costs and benefits must be taken into account by the UC, i.e. cost of monitoring, cost of mitigating action, cost of reputation loss and benefit of increased consumption. The main challenge for the utility company is to control the spending on their security measures, as organisations typically have a restricted budget. For example, if the expected probability of an attack is low, a low investment in security could be justified. On the other hand, if an attacker is aware of such a strategy, they would be more likely to attack as they would expect less resistance. Finding a solution to this decision–making problem cannot be achieved by optimisation alone, but instead non-cooperative game theory helps in devising suitable models and advising on the expected likelihood of attacks.

8.2 Game-Theoretic Defence Strategy

> *This section, i.e. the remainder of this chapter, is included in this thesis for completeness. The main contributors were Eckhard Pfluegel, Coline Smagghe, and Mastaneh Davis, while the other authors of [Pilz et al., 2019a] (including myself) delivered minor contributions.*

When planning to defend against the false data injection attacks described in the previous section, the need for the utility company to allocate resources for the defence in the most efficient way has been highlighted. This section proposes to use game theory in order to support this decision–making process. The game is motivated and introduced based on detailing the payoff functions of the two players describing the game normal form. This is followed by solving the game using various assumptions. Finally, the solution is discussed with respect to their implications for the simulated scenario and potential alternatives.

8.2.1 Game Theory for Security

Game theory is increasingly being employed for modelling attacker-defender scenarios in cyber security, for a broad range of scenarios such as intrusion detection in network security [Alpcan and Basar, 2010], managing the security of information in an organisation [Panaousis et al., 2014] and predicting the likelihood of cyber attacks [Bao et al., 2017].

Non-cooperative game theory is based on the assumption that players are rational, i.e. they choose between actions such that they maximise their payoffs. The associated *optimal strategies* can be identified using the fundamental concept of the NE (cf. Section 2.3). Although not all games have a NE, Nash's theorem states that nonzero-sum games always admit a mixed strategy equilibrium. However, for practical applications it may not be easy to interpret [Aumann, 1985].

In this paper, $\mathbf{x}$ and $\mathbf{y}$ denote a pure or mixed strategy of the first and second player in a two-player game, and $\hat{\mathbf{x}}$ and $\hat{\mathbf{y}}$ are used for optimal strategies of these players. A *strategy profile* $\mathbf{s} = [\mathbf{x}, \mathbf{y}]$ groups strategies of each player together. If the grouped strategies are optimal, the optimal strategy profile is written as $\hat{\mathbf{s}}$. A two-player nonzero-sum game can be represented in normal form, based on the players' payoff matrices A and B [Shoham and Leyton-Brown, 2009].

An *optimal Nash Equilibrium strategy profile* is a strategy profile $\hat{\mathbf{s}} = [\hat{\mathbf{x}}, \hat{\mathbf{y}}]$ satisfying

$$\hat{\mathbf{x}} A \hat{\mathbf{y}} \geq \mathbf{x} A \hat{\mathbf{y}} \ \forall \mathbf{x}, \quad \hat{\mathbf{x}} B \hat{\mathbf{y}} \geq \hat{\mathbf{x}} B \mathbf{y} \ \forall \mathbf{y} \ . \tag{8.1}$$

Here, the strategies may be pure or mixed, and the corresponding NE is referred to as pure or mixed. Furthermore, if all of the inequalities in the above definition are strict, one has a *strict* NE. Otherwise, the NE is *non-strict*.

8.2.2 Proposed Security Game

The proposed security game is a two-player nonzero-sum *complete information* game [Shoham and Leyton-Brown, 2009] between the utility company $\mathcal{U}$ and the attacker $\mathcal{A}$. The game is inspired by the nonzero-sum Intrusion Detection System (IDS) game of [Alpcan and Basar, 2010] which has been thoroughly analysed in the literature and is well understood. Table 8.3 illustrates the game where the two strategies available to the defender are to monitor or not, denoted by the strategy space $S_{\mathcal{D}} = \{s^{\mathcal{D}}_{mon}, s^{\mathcal{D}}_{-mon}\}$, and the attacker chooses between attacking or not attacking: $S_{\mathcal{A}} = \{s^{\mathcal{A}}_{att}, s^{\mathcal{A}}_{-att}\}$. The positive parameters $\alpha_c, \alpha_f, \alpha_m, \beta_c$ and β_s are used to denote the payoffs corresponding to the various strategies. The main characteristic of this game is the design of the payoff functions in such a way that the monitoring defender only has an incentive to defend in the presence of an attack. The attacker is discouraged from attacking if there is defence in place. This design leads to a circular path when considering payoff-incrementing unilateral changes of strategy, hence prohibiting the existence of a pure NE.

Description of the game: Here, an augmented security game is introduced, extending the IDS game described previously by an additional action. The rationale behind this extended game model is twofold: Section 8.1.3 demonstrated the existence of low-impact attacks which cannot be detected by standard monitoring techniques, and it would be desirable to capture these in a more sophisticated game model. Second, an extended game might better match real-world scenarios and might lead to simpler solutions, in this case pure equilibria rather than mixed ones.

Table 8.3. *IDS game of [Alpcan and Basar, 2010] in normal form.*
In this two player game between the attacker $\mathcal{A}$ and the defender $\mathcal{D}$ both have two possible actions, i.e. for the attacker to attack ($s^{\mathcal{A}}_{att}$) or to not attack ($s^{\mathcal{A}}_{-att}$), and for the defender to monitor ($s^{\mathcal{D}}_{mon}$) or to not monitor ($s^{\mathcal{D}}_{-mon}$). The resulting utility values are represented in matrix notation with α_c, α_f, α_m, β_c, $\beta_s > 0$.

$\mathcal{D}\downarrow$ $\mathcal{A}\rightarrow$	$s^{\mathcal{A}}_{att}$	$s^{\mathcal{A}}_{-att}$
$s^{\mathcal{D}}_{mon}$	$\alpha_c,\quad -\beta_c$	$-\alpha_f,\quad 0$
$s^{\mathcal{D}}_{-mon}$	$-\alpha_m,\quad \beta_s$	$0,\quad 0$

Game strategies: Section 8.1.3 presented three possible monitoring strategies for $\mathcal{U}$: to monitor the daily average of forecasting data, to inspect the daily profile of the aggregated forecast, and to inspect the individual forecast data with the same level of detail. In this work, the assumption is made that the first and second monitoring strategies are most useful in a realistic setting, as they have an observable impact on the strength and outcome of successful attacks while the third monitoring strategy merely eliminates attacks that are possible for weaker monitoring levels. Furthermore, as the data of aggregated forecasts is readily available to the UC, the first monitoring strategy is not very costly and is identified with the strategy $s^{\mathcal{U}}_{-mon}$. The second monitoring strategy is denoted as $s^{\mathcal{U}}_{mon}$ so that the strategy space for the defender $\mathcal{U}$ is as in the previous game $S_{\mathcal{U}} = \{s^{\mathcal{U}}_{mon}, s^{\mathcal{U}}_{-mon}\}$. The attacker $\mathcal{A}$ has three different strategies: to attack strongly with high impact, to perform a weaker attack with low impact, or not to attack at all. This is denoted by the strategy space $S_{\mathcal{A}} = \{s^{\mathcal{A}}_{att^\circ}, s^{\mathcal{A}}_{att}, s^{\mathcal{A}}_{-att}\}$.

The additional weak attack strategy $s^{\mathcal{A}}_{att^\circ}$ offers an alternative incentive of not monitoring to the UC, preferring to save monitoring cost when facing a weak attack. No assumption is made on the relationship between the attacker's overall payoff when choosing the two different attack types, and a discussion of conditions clarifying this relationship is the main subject of the game analysis in the next section.

Game payoff functions: The following notations for the payoffs for $\mathcal{U}$ are introduced: $c^{\mathcal{U}}_{mon}$ is the cost for monitoring the daily profile of the aggregated forecast (second monitoring strategy) and $c^{\mathcal{U}}_{def}$ is an additional cost for investing in defence mechanisms such as actions discussed in Section 8.1.4. Losses from weak and strong attacks are denoted by $l^{\mathcal{U}}_{att^\circ}$ and $l^{\mathcal{U}}_{att}$ respectively. The payoff functions corresponding to $\mathcal{A}$ are the benefits and costs associated with weak and strong attacks, denoted by $b^{\mathcal{A}}_{att^\circ}$, $c^{\mathcal{A}}_{att^\circ}$, and $b^{\mathcal{A}}_{att}$ and $c^{\mathcal{A}}_{att}$, respectively. The monitoring activity always leads to monitoring costs for $\mathcal{U}$. If there is no monitoring, $\mathcal{U}$ incurs losses $l^{\mathcal{U}}_{att^\circ}$ and $l^{\mathcal{U}}_{att}$ due to weak and strong attacks, respectively. Otherwise, despite monitoring, weak attacks

Table 8.4. *Augmented security game in normal form.*
In this two player game between the attacker $\mathcal{A}$ and the utility company $\mathcal{U}$ the former has three possible actions while the latter has two. The options for the attacker are to attack ($s^{\mathcal{A}}_{att}$), to not attack ($s^{\mathcal{A}}_{-att}$), or to attack weakly ($s^{\mathcal{A}}_{att^{\circ}}$), and for the utility company to monitor ($s^{\mathcal{U}}_{mon}$) or to not monitor ($s^{\mathcal{U}}_{-mon}$). The resulting utility values are represented in matrix notation with all parameters being positive.

$\mathcal{U}\downarrow\ \mathcal{A}\rightarrow$	$s^{\mathcal{A}}_{att^{\circ}}$		$s^{\mathcal{A}}_{att}$		$s^{\mathcal{A}}_{-att}$	
$s^{\mathcal{U}}_{mon}$	$-c^{\mathcal{U}}_{mon}-l^{\mathcal{U}}_{att^{\circ}}$,	$l^{\mathcal{U}}_{att^{\circ}}-c^{\mathcal{A}}_{att^{\circ}}$	$-c^{\mathcal{U}}_{mon}-c^{\mathcal{U}}_{def}$,	$-c^{\mathcal{A}}_{att}$	$-c^{\mathcal{U}}_{mon}$,	0
$s^{\mathcal{U}}_{-mon}$	$-l^{\mathcal{U}}_{att^{\circ}}$,	$l^{\mathcal{U}}_{att^{\circ}}-c^{\mathcal{A}}_{att^{\circ}}$	$-l^{\mathcal{U}}_{att}$,	$l^{\mathcal{U}}_{att}-c^{\mathcal{A}}_{att}$	0,	0

cannot be detected, hence there is a resulting loss $l^{\mathcal{U}}_{att^{\circ}}$. Strong attacks however are detected and mitigated against through some countermeasures, preventing any losses but leading to a defence cost $c^{\mathcal{U}}_{def}$. Finally, if there is no attack, then the only arising nonzero payoff function involved is the monitoring cost for $\mathcal{U}$. The attacker $\mathcal{A}$ obtains a benefit $b^{\mathcal{A}}_{att^{\circ}}$ from a weak attack, but has to invest in attack costs $c^{\mathcal{A}}_{att^{\circ}}$. Similarly, the cost $c^{\mathcal{A}}_{att}$ arises from a strong attack, however the model assumes the lack of a benefit for $\mathcal{A}$ due to the UC's defence mechanism. Using these notations, the proposed security game $\mathcal{G}$ can be represented in normal form as shown in Table 8.4.

Assumptions from the IDS game: The cost for missing an attack $\alpha_m = l^{\mathcal{U}}_{att} > 0$ is interpreted as losses from an attack that is not mitigated against, the false alarm cost $\alpha_f = c^{\mathcal{U}}_{mon} > 0$ as an ongoing monitoring cost and the detection penalty $\beta_c = c^{\mathcal{A}}_{att} > 0$ as the cost for the attacker to conduct a strong attack. The gain from detection $\alpha_c = -c^{\mathcal{U}}_{mon} - c^{\mathcal{U}}_{def} > 0$ is reformulated as necessary cost to monitor and to defend in order to prevent damage. In order to preserve the mixed equilibrium property of the security game given by $-\alpha_m < \alpha_c$ it is then assumed that this attack prevention cost is less than the actual incurring attack damage, i.e. $c^{\mathcal{U}}_{mon}+c^{\mathcal{U}}_{def} < l^{\mathcal{U}}_{att}$. This assumption is natural: In a typical security game, the defender does not spend more on attack prevention than what they potentially loose from an attack. Finally, $\beta_s = l^{\mathcal{U}}_{att}-c^{\mathcal{A}}_{att} > 0$ is the difference between the benefit from an undetected attack and the attack effort. This expresses a similar principle as above, but this time applied to the attacker $\mathcal{A}$ who does not spend more on an attack than the expected gain from it. These assumptions can be referred to as the Security Game Assumptions.

Augmented security game: The assumptions required for the augmented security game are in parts inspired by those of the IDS game, and also motivated by the experimental results presented in Section 8.1.3 which suggest that strong attacks require targeting more victims, i.e. a bigger effort.

For a weak attack, the attacker receives a greater payoff than the cost of the attack, implying

$$c^{\mathcal{A}}_{att^{\circ}} < l^{\mathcal{U}}_{att^{\circ}} \; . \tag{8.2}$$

It can also be assumed that the cost for launching a strong attack is higher than that for a weak attack since a higher number of households has to be attacked

$$c^{\mathcal{A}}_{att} > c^{\mathcal{A}}_{att^{\circ}} \; . \tag{8.3}$$

Finally, a strong attack leads to higher losses for the utility (cf. Section 8.1.2)

$$l^{\mathcal{U}}_{att} > l^{\mathcal{U}}_{att^{\circ}} \; . \tag{8.4}$$

Note that in order to aid the game analysis, an assumption made in this game is that the benefit of the attacker is equal to the loss of the defender, $b^{\mathcal{A}}_{att} = l^{\mathcal{U}}_{att}$ and $b^{\mathcal{A}}_{att^{\circ}} = l^{\mathcal{U}}_{att^{\circ}}$.

8.2.3 Game Analysis

In this section, analysis of the security game $\mathcal{G}$ reveals existence of several NE strategies. Following the study of practical examples, the relevance of these strategies are discussed so that they can be used to inform UC's security investments.

To solve the augmented security game, three distinct cases are considered. This is based on discussing the second order difference

$$\Delta = q_{att^{\circ}} - q_{att} \; , \tag{8.5}$$

where $q_{att^{\circ}} = l^{\mathcal{U}}_{att^{\circ}} - c^{\mathcal{A}}_{att^{\circ}}$ and $q_{att} = l^{\mathcal{U}}_{att} - c^{\mathcal{A}}_{att}$ describe the net-benefit for the attacker in case of a weak and strong attack, respectively.

Case 1 ($\Delta > 0$)**:** In this case, the existence of a unique pure NE for the game $\mathcal{G}$ can be asserted. The corresponding NE strategy is for the UC to not monitor, and for the attacker to carry out a weak attack. Due to the uniqueness property these solutions are globally optimal.

Proposition 8.1. If $l^{\mathcal{U}}_{att^{\circ}} - c^{\mathcal{A}}_{att^{\circ}} > l^{\mathcal{U}}_{att} - c^{\mathcal{A}}_{att}$, the game $\mathcal{G}$ admits a unique pure NE strategy profile of the form $s^* = (s^{\mathcal{U}}_{-mon}, s^{\mathcal{A}}_{att^{\circ}})$ and the corresponding payoffs $s^*_{\mathcal{U}} = -l^{\mathcal{U}}_{att^{\circ}}$ and $s^*_{\mathcal{A}} = l^{\mathcal{U}}_{att^{\circ}} - c^{\mathcal{A}}_{att^{\circ}}$ are globally optimal.

Proof. First, it needs to be verified that when choosing the pure strategy profile $(s^{\mathcal{U}}_{-mon}, s^{\mathcal{A}}_{att^{\circ}})$, none of the two players benefits from a unilateral change of pure strategy.

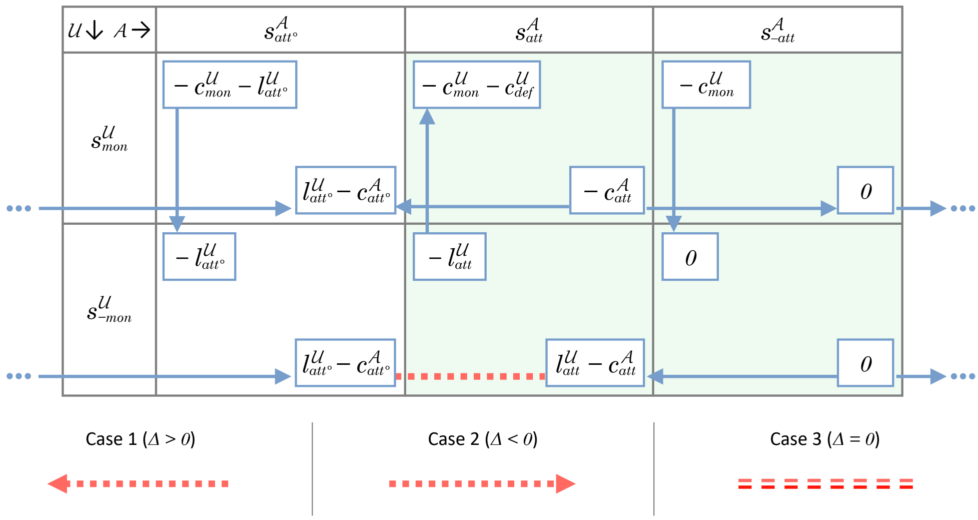

Figure 8.7. *Advanced security game flow diagram.*
This figure is a more extensive representation of the game shown in Table 8.4, including the relations between the respective quantities. The arrows indicate which strategy would be more preferable in terms of the individual players' utility function. As discussed in Section 8.2.3 the connection between the IDS game (in green) and the proposed augmented security game is defined by the second order difference Δ (8.5) which is highlighted here by the red dotted lines. Depending on the sign of Δ (8.5), the direction of the arrows varies as illustrated in the three cases. Note that the double line represents equality.

Focusing on the UC, the change of strategy $s^{\mathcal{U}}_{-mon} \rightarrow s^{\mathcal{U}}_{mon}$ diminishes its payoff since $-l^{\mathcal{U}}_{att^\circ} > -c^{\mathcal{U}}_{mon} - l^{\mathcal{U}}_{att^\circ}$ due to the assumption of a positive monitoring cost. Considering the attacker, the change $s^{\mathcal{A}}_{att^\circ} \rightarrow s^{\mathcal{A}}_{att}$ is not beneficial because of the main assumption $\Delta > 0$ of this case. Finally, the change of strategy $s^{\mathcal{A}}_{att^\circ} \rightarrow s^{\mathcal{A}}_{-att}$ reduces the payoff due to Assumption (8.2). Second, a careful inspection of the payoff functions of the remaining strategies of the game, together with the fact that the assumption of Case 1 implies $l^{\mathcal{U}}_{att^\circ} - c^{\mathcal{A}}_{att^\circ} > -c^{\mathcal{A}}_{att}$, shows that there is no other pure NE. □

Case 2 ($\Delta < 0$)**:** Similarly to the IDS game, the augmented security game has the same property of circular paths when performing unilateral changes strategy with increasing payoffs, hence prohibiting the existence of any pure NE.

Proposition 8.2. If $l^{\mathcal{U}}_{att^\circ} - c^{\mathcal{A}}_{att^\circ} < l^{\mathcal{U}}_{att} - c^{\mathcal{A}}_{att}$, the game $\mathcal{G}$ admits no pure NE.

Proof. The proof of this proposition is done very similarly to that of Proposition 1 by comparing the changes in payoff, following a unilateral change of strategy. It is clear that there is no pure NE in the game restricted to the attacker strategies $s^{\mathcal{A}}_{att}$

Table 8.5. *Representative mixed strategy probabilities for Case 2 attacks.*
The results are based on simulations presented in Section 8.1.3. In this particular example the mirror attack was employed by the attacker. A thorough overview of the specific parameters can be found in Section 8.2.4.

	$p_{att^\circ} = 36.3\%$	$p_{att} = 63.7\%$	$p_{-att} = 0\%$
$p_{mon} = 71.7\%$	26.0%	45.7%	0%
$p_{-mon} = 28.3\%$	10.3%	18.0%	0%

and $s^{\mathcal{A}}_{-att}$, as the resulting subgame is identical to the IDS game. When augmented by the weak attack strategy $s^{\mathcal{A}}_{att^\circ}$, two cases may arise, depending on which of the strategy changes $s^{\mathcal{A}}_{att} \to s^{\mathcal{A}}_{att^\circ}$ or $s^{\mathcal{A}}_{att^\circ} \to s^{\mathcal{A}}_{att}$, starting from the initial strategy profile $(s^{\mathcal{U}}_{mon}, s^{\mathcal{A}}_{att})$, lead to an increased payoff for the attacker.

In the first case, one observes the additional sequence of strategy changes $s^{\mathcal{U}}_{mon} \to s^{\mathcal{U}}_{-mon}$, $s^{\mathcal{A}}_{att^\circ} \to s^{\mathcal{A}}_{att}$ and $s^{\mathcal{U}}_{-mon} \to s^{\mathcal{U}}_{mon}$ leading back to the original strategy profile. These changes entail increased payoffs due to the assumption of positive monitoring cost, the condition $\Delta < 0$ and the Security Game Assumptions. In the second case, the unilateral payoff change joins the circular path of the IDS game, from which the proof follows as shown earlier. □

Case 3 ($\Delta = 0$)**:** In this last case, one derives the inequality $l^{\mathcal{U}}_{att^\circ} - c^{\mathcal{A}}_{att^\circ} = l^{\mathcal{U}}_{att} - c^{\mathcal{A}}_{att} > -c^{\mathcal{A}}_{att}$ as in Case 1 and obtains a similar but weaker result, as the pure NE is not strict. A formal proof of the following proposition is omitted as it can be done similarly as that of Proposition 1 since the same payoff deviations are involved.

Proposition 8.3. If $l^{\mathcal{U}}_{att^\circ} - c^{\mathcal{A}}_{att^\circ} = l^{\mathcal{U}}_{att} - c^{\mathcal{A}}_{att}$, the game $\mathcal{G}$ admits a unique pure non-strict NE strategy profile of the form $s^* = (s^{\mathcal{U}}_{-mon}, s^{\mathcal{A}}_{att^\circ})$ and the corresponding optimal payoffs are $s^*_{\mathcal{U}} = -l^{\mathcal{U}}_{att^\circ}$ and $s^*_{\mathcal{A}} = l^{\mathcal{U}}_{att^\circ} - c^{\mathcal{A}}_{att^\circ}$.

8.2.4 Quantitative Examples

Attacks discussed in Section 8.1 are further analysed using the proposed augmented security game. In order to establish which case they correspond to, estimations of the sign of Δ (8.5) are performed using previous simulation calculations. More specifically, $b^{\mathcal{A}}_{att}$ and $b^{\mathcal{A}}_{att^\circ}$ are represented by the values of the Àttacker bill change' (γ and $\gamma_\circ$), reported in Tables 8.1 and 8.2 respectively, multiplied by the actual amount of the bill μ, e.g. $b^{\mathcal{A}}_{att} = l^{\mathcal{U}}_{att} = \gamma \cdot \mu$. Moreover, assuming a linear relationship between the number of attacked players and the cost of an attack, $c^{\mathcal{A}}_{att}$ and $c^{\mathcal{A}}_{att^\circ}$ can be expressed using the values of percentage of targeted players (λ and $\lambda_\circ$) shown in Tables 8.1 and 8.2 respectively, e.g. $c^{\mathcal{A}}_{att} = \lambda \cdot \kappa$. As a consequence, an attack type corresponds to Case 2, i.e. ($\Delta < 0$), if and only if the following inequality is satisfied:

$$\frac{\gamma_\circ - \gamma}{\lambda_\circ - \lambda} > \frac{\kappa}{\mu} \; . \tag{8.6}$$

with Assumption (8.2) stating $\gamma_\circ/\lambda_\circ > \kappa/\mu$.

Evaluations of attacks reported in Tables 8.1 and 8.2 show that Case 2 applies to the shift ($\sigma = 4$), flat ($\tau = 0$), mirror ($\tau = -1$) and scale ($\tau = 2$) attacks. Hence, for none of those attacks a pure NE exits and only mixed strategies can be offered. Using the mirror attack as an example, Equation (8.6) requires $0.41 > \kappa/\mu$ and Assumption (8.2) imposes $0.11 > \kappa/\mu$.

Since the scale ($\tau = 1.29$) attack was especially designed to be undetectable by the proposed monitoring solution, it cannot be analysed by the game which assumes that a successful monitoring strategy is available. On the other hand, the best strategy for such an attack is self-evident: Since all attack results in gains for the attacker, they should attack, while the UC should not waste any resources in ineffective defence.

In order to investigate the mixed strategies associated to those attacks, numeral values were selected so that mixed strategies could be computed using an NE solver [Avis et al., 2009]: $\mu = 100$, $\kappa = 10$, $c^{\mathcal{U}}_{mon} = 10$ and $c^{\mathcal{U}}_{def} = 20$. Table 8.5 shows representative mixed strategy probabilities associated with the investigated Case 2 attacks, here the mirror attack. The attacker either performs a strong (63.7% probability) or weak (36.3% probability) attack, while the UC chooses to use monitoring with a 71.7% probability. Note that the choice of numerical values is not critical. As long as all the game assumptions are fulfilled, the probability for the monitoring action of the UC is at least 70%.

8.2.5 Discussions

Theoretical analysis of the proposed extended game model has shown that according to the sign of Δ (8.5), three different cases should be considered. While, both Case 1 ($\Delta > 0$) and Case 3 ($\Delta = 0$) are associated to a pure NE, only Case 1's is strict. However, in both cases, the optimal NE strategy for the UC is the same: not to monitor. On the other hand, Case 2 ($\Delta < 0$) only leads to mixed strategies. Practical analysis, investigating the attack examples described in Section 8.1 based on a 100% participation rate, revealed that only Case 2 was practically relevant. This is in line with expectations that the net benefits, i.e. benefits minus costs, of strong attacks are supposed to be higher than those of weak attacks. Note that for the scale ($\tau = 2$) attack, different cases could arise at lower participation rates due to its specific behaviour as shown in Fig. 8.4 and Fig. 8.5.

Regarding Case 2, for a UC, the practical application of optimal strategies, as illustrated in Table 8.5, is not straightforward. Actually many suggestions have been made regarding possible interpretations of mixed strategies [Aumann, 1985, Aumann and Brandenburger, 1995, Chen et al., 2017]. In the specific context of this work, that proposed by [Chen et al., 2017] is of particular interest: Indeed, assuming that the UC supplies a set of microgrids, where security strategy is decided at the microgrid level, they, seen as a population, would choose defence strategies following the mixed probabilities. Alternatively, as suggested in [Maghrabi et al., 2017, Shoham and Leyton-Brown, 2009], the probability associated to defence could be interpreted as an index of security criticality which would inform the UC's decisions regarding its defence investments. Interestingly, experiments (not shown) indicates that when the cost of attacking a single player, i.e. κ, decreases, the mixed strategy probability for monitoring grows, increasing defence needs.

Finally, the undetectable scale ($\tau = 1.29$) attack is a reminder that no practical monitoring strategy is perfect and the best defence strategy may be not to defend if the losses associated to an attack can be considered as acceptable.

8.3 Conclusions

Protecting smart grids from cyber attacks is essential for them to deliver their promises. Investigating different classes of false data injection attacks against the forecasts required for smart energy scheduling, extensive simulations showed the extent of damages that a single attacker can cause to both the utility company (growth of PAR value by up to 84%) and its consumers (bill increase by up to 54%). The need for mitigation having been established, monitoring and defence strategies were proposed. In order to assess their value and advise utility companies on their optimal attack prevention strategy, a novel and generic security game that considers low and high-impact attacks was designed. Its analysis highlighted, in particular, conditions under which a NE exists. Interestingly, in those cases, the best strategy is for the utility company not to invest in any monitoring and the attacker to conduct low-impact attacks. Numerical evaluations considering the previously studied classes of attacks revealed that there is a type of attack where, indeed, no monitoring is the best strategy. However, in all the other cases, only mixed strategies can be offered. Their practical interpretation by UCs was discussed. As a conclusion, the proposed security game offers utility companies the ability to investigate the most appropriate monitoring and defence strategies so that false data injection attacks have only very limited, if any, impact on smart energy scheduling.

This almost blank page is intentional.

CHAPTER 9

Optimal Battery Sizing in a Demand-Side Management Scheme

In this chapter, the functionality to exchange data between individual households is being used to schedule energy storage installations such that the grid stability is guaranteed even though a considerable amount of demand is served from solar power generation facilities. A key element to achieve a high self-consumption rate of solar energy, i.e. the ratio between the consumed solar energy to the actual demand, is the utilisation of energy storage. Various research studies are concerned with energy storage management [Soliman and Leon-Garcia, 2014, Nguyen et al., 2015, Li and Dong, 2018, Luthander et al., 2015, Li and Danzer, 2014, Pilz and Al-Fagih, 2019a].

Luthander *et al.* [Luthander et al., 2015] present a case study of 21 Swedish households with a focus on comparing individually-owned batteries to a centralised storage solution. In order to reach a certain level of self-consumption the centralised storage capacity is considerably smaller than the aggregated capacity of individually-owned batteries. The study in [Li and Danzer, 2014] is concerned with optimising the usage of a given photovoltaic-battery system. It investigates a number of different optimisation objectives and shows how these affect the eventual charging patterns of a household for two exemplary days. In contrast to their approach, Reference [Pilz and Al-Fagih, 2019a] makes use of a game-theoretic approach in which households schedule their individually-owned batteries with the goal to minimise their respective electricity bills. They perform simulations over the period of an entire year to allow for statistical analysis of the results.

One interesting question is: *What is the optimal capacity of a battery?* [Huang et al., 2018, Khalilpour and Vassallo, 2016, Talent and Du, 2018]. Reference [Talent and Du, 2018] focuses on the influence of different tariff schemes on the optimal battery size, whereas [Khalilpour and Vassallo, 2016] develops a decision-making tool which supports users that are investing in photovoltaic and battery systems. Recently, Huang et al. [Huang et al., 2018] developed an algorithm to determine the optimal size of a battery with respect to the achievable self-consumption. This research builds on their approach and develops a deeper understanding of the relation between demand and generation patterns, and the optimal battery capacity. In particular, we study two different demand-side management schemes. Within the first one, "Game-Theoretic Scheduling" (GTS), the households have the single goal of minimising their individual electricity bills (cf. [Pilz and Al-Fagih, 2019a]). The second scheme considers an additional preference of increasing the respective self-consumption of the household and is called "Game-Theoretic Scheduling With Constraint" (GTSWC) throughout.

The main contributions of this chapter are as follows:

(1) Based on seasonal and yearly simulations of households with real consumption and generation data, this research provides an in-depth insight on how optimal sizing of batteries depends not only on aggregated statistics but also on the specific temporal patterns that characterise individual households.

(2) Two different battery scheduling algorithms, i.e. GTS and GTSWC, are compared in terms of three metrics: (i) Self-consumption of solar energy, (ii) Peak-to-average ratio of the aggregated load as an indicator for grid stability, and (iii) Potential cost reductions due to the introduction of electricity storage systems.

(3) This research compares the optimal sizing for a centralised storage facility with individually-owned batteries and analyses their effect on the same metrics as mentioned above.

The chapter[1] is structured as follows. In Section 9.1, we first briefly introduce the two scheduling models that we are going to compare. Secondly, we describe the process of finding the optimal battery sizes. Based on these, the approaches are then compared according to self-consumption, effective peak-to-average (PAR) reduction, and potential cost savings. The results are discussed in Section 9.2 and we analyse

[1]A paper with the content of this chapter has been submitted for peer-review and was eventually published at [Pilz et al., 2019b].

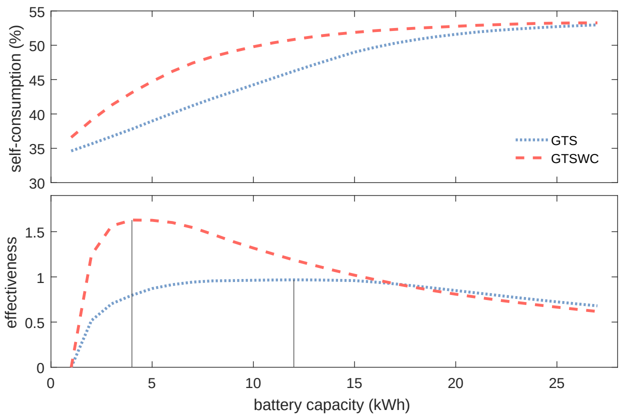

Figure 9.1. *Optimal sizing considerations.*
The self-consumption and the resulting effectiveness of an exemplary household are plotted over the battery size. The two vertical lines indicate the maximum of the effectiveness for the GTS and GTSWC approach and therefore the optimal size of the energy storage installation, respectively.

how the demand and generation patterns lead to the respective optimal battery sizes.

9.1 Optimal Battery Sizing Results

The batteries of the households are scheduled based on a dynamic game which is played between the individual households. The objective of the players/households is to minimise their individual electricity bill (4.15). The players act rationally and in a selfish manner. In the following section, two approaches are differentiated. The first approach is identical to the one proposed by [Pilz and Al-Fagih, 2019a], introduced as GTS. The game is played for an upcoming day based on forecasts for demand and generation.

The second approach, i.e. GTSWC, introduces an additional constraint to the GTS. Whenever the renewable photovoltaic (PV) generated energy is expected to be higher than the demand for an upcoming interval, charging the battery from the grid is prohibited. The idea behind this is to maximise the self-consumption rate of the PV system. In order to determine the optimal battery size, the process described in [Huang et al., 2018] has been followed. To do so, simulations are performed with different battery sizes for each household (per season and yearly) using both scheduling approaches. Battery capacities are in the range[2] between 1.0 kWh and 27.0 kWh. The upper limit would equal an installation of two Tesla Powerwall2 batteries [Tesla, 2017]. For each set of parameters, the 'effectiveness'

[2]We consider steps of 1.0 kWh, i.e. battery capacities in $s_{\max} = [1.0\text{ kWh}, 2.0\text{ kWh}, \ldots, 27.0\text{ kWh}]$.

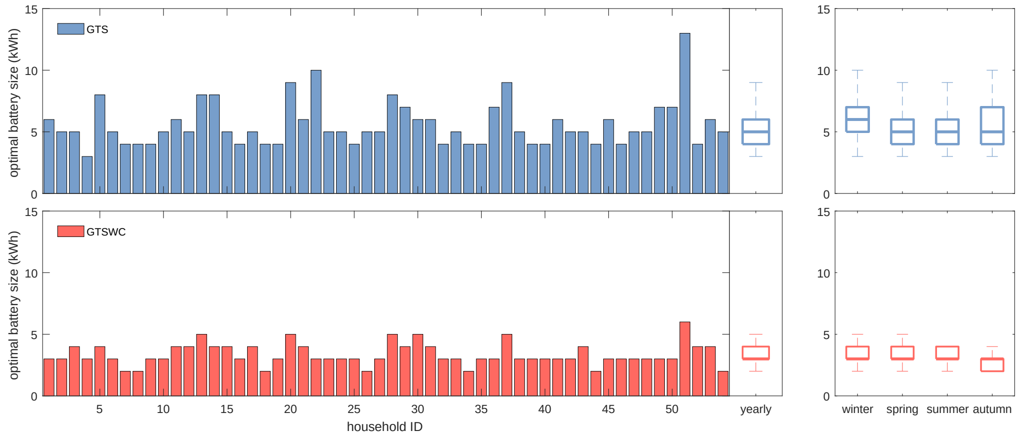

Figure 9.2. *Optimal battery sizes.*
The results are obtained through a process as described in [Huang et al., 2018].Battery capacities between 1 and 27 kWh were analysed. The optimal battery sizes for the individual households from simulation runs over the period of an entire year are reported. Furthermore, statistical results for these simulations as well as independent seasonal simulations are shown.

of the electricity storage is computed. The effectiveness is defined by the notion of how much the self-consumption of a household is increased per kWh of installed capacity:

$$\text{effectiveness} = \frac{sc_n - sc_1}{n}, \tag{9.1}$$

where sc_n is the self-consumption achieved by utilising storage of size n kWh. The maximum of this effectiveness is the sought after optimal battery size. An example for these steps is shown in Figure 9.1 for a randomly selected house and season.

The optimal battery size for each player over the course of an entire year for the two approaches (game-theoretic scheduling with and without self-consumption constraint) is shown in Figure 9.2. Furthermore, Figure 9.2 also reports the average results per season over all the 54 investigated households.

Overall, the optimal size for the GTSWC scenario does not exceed the GTS optimal battery size for any player and season. Houshold 4 shows the smallest difference between the two scenarios. All the capacities are the same except for summer where they differ by 1 kWh. The largest difference between the optimal battery size as determined for the two approaches of a particular season is found in household 14 (summer). Here the difference is 8 kWh (cf. Figure 9.1). The largest difference between the optimal battery size for two seasons and the same approach is seen in household 52 (winter: 11 kWh, summer: 3 kWh). In Section 9.2, these households are investigated in particular to understand how their battery usage patterns lead to the respective results.

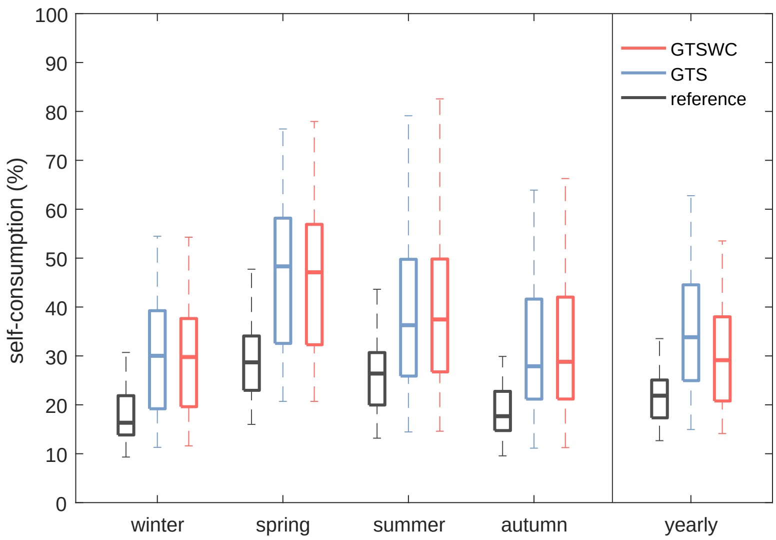

Figure 9.3. *Self-consumption analysis.*
Statistical results for the self-consumption rates are shown for all seasons and an entire year. For each period, the reference case in which no storage is available is compared with a configuration that includes the optimally sized batteries for each individual household for both the GTS and the GTSWC approach.

Table 9.1. *Self-consumption improvements.*
The median improvement (over all households) of the self-consumption due to the introduction of optimally sized batteries is shown. The simulations for each column were performed independently.

	winter	spring	summer	autumn	yearly
GTS	11.4%	17.8%	10.0%	11.3%	11.6%
GTSWC	12.1%	17.0%	10.7%	12.2%	12.5%

9.1.1 Self-Consumption

The solar PV self-consumption rate of a household is defined as the ratio between the solar energy being used and its demand. This includes a direct part which is consumed immediately and an indirect part used to charge the battery when the PV system generation exceeds the local demand. In the following, the increase in self-consumption due to the introduction of an optimally sized battery for both the GTS and GTSWC scenario is analysed. The seasonal results for the self-consumption can be found in Figure 9.3. Explicit improvements[3] are reported in Tab. 9.1.

It becomes clear that even with different optimal battery sizes for the GTS and GTSWC approach the median improvement in self-consumption is similar. The result was to be expected as the additional constraint in GTSWC is particularly

[3]Note that these improvements cannot be inferred from Figure 9.3 as there the median of the absolute self-consumption values are depicted. The median of differences is not equal to the difference of medians [Dr. Deng, 2015].

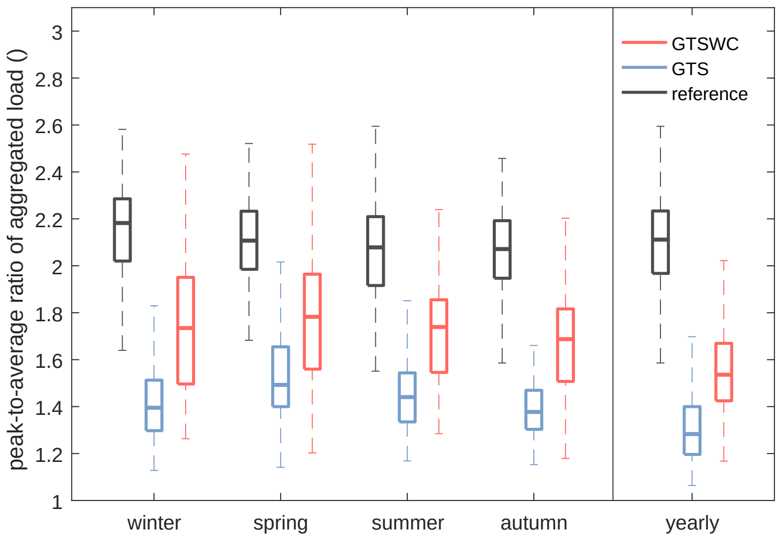

Figure 9.4. *Peak-to-average ratio (PAR) of the aggregated load.*
A statistical analysis of the achieved daily PAR values over the respective seasons is shown. For each period, the reference case in which no storage is available is compared with a configuration that includes the optimally sized batteries for each individual household for both the GTS and the GTSWC approach.

designed to place further emphasis on the increase of self-consumption. The spread around the median self-consumption approximately doubles when comparing the results with the reference case in which no batteries are present. This is due to the fact that some households benefit more than others from the introduction of a battery. There are many factors that play a role for this such as the aggregated solar production, the aggregated demand, and also the temporal patterns of production and demand. For example: Household 14 improves its self-consumption by 12.2% during the summer, while household 26 (with similar aggregated consumption and PV peak production) improves its self-consumption by 1.5%. Household 13, which has less aggregated demand than the two houses mentioned before and higher aggregated solar production, improves its self-consumption by 37.9%. A more detailed analysis of these households and how these differences are related to their demand patterns will be analysed in Section 9.2. In general, households that gain considerably at GTS also do so at GTSWC and vice versa. The average absolute difference of the self-consumption improvements between GTS and GTSWC for each household individually is < 1.4%.

9.1.2 PAR values

The PAR of the aggregated load (4.18) is an indicator for the stability of the grid [Bayram et al., 2014]. A value close to 1.0, i.e. a flat load profile, is preferred

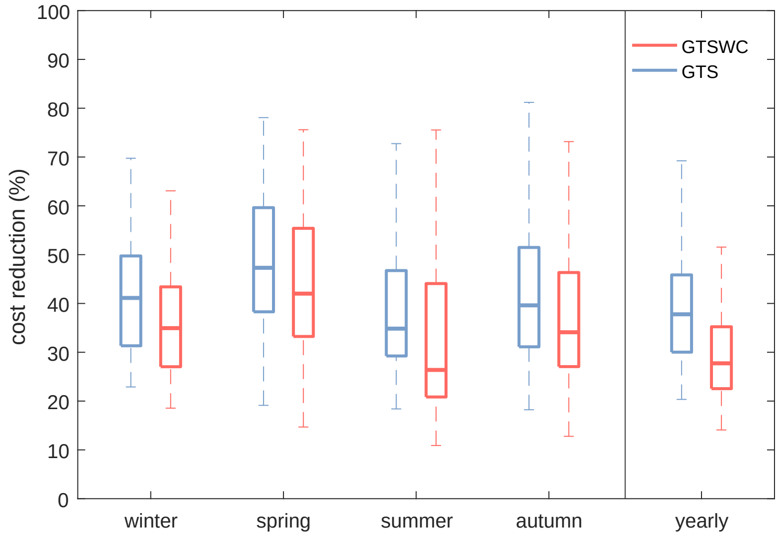

Figure 9.5. *Cost reductions*.
Statistical analysis of the amount of savings from the electricity bill over various billing periods is presented for the GTS and the GTSWC approach. The calculation of the unit energy price depends on the aggregated load as introduced in (4.15).

by a utility company as this allows them to save investment costs for fast-ramping energy production installations. PAR values are calculated for a period of one day. A statistical analysis for the 90 days that comprise each season is shown in Figure 9.4.

Overall, considerable improvements of the PAR value are achieved. The GTS approach leads to better PAR reductions than the GTSWC approach in both the median values and also the smaller spread around these.

9.1.3 Cost Reduction

As seen in Section 4.3, the cost function (4.14) depends on the aggregated load. Thus the price per unit of electricity changes for each half hour interval. When calculating the overall bill for each household with and without battery, it can be observed that it is decreasing in both approaches. The relative cost reduction of the electricity bill due to the introduction of an optimally sized battery is shown in Figure 9.5.

Overall, the introduction of energy storage leads to a considerable amount of savings from the electricity bill in both cases (GTS and GTSWC). The increase of self-consumption can directly be translated in a decrease of energy requested from the grid which in turn decreases the bill. As seen in the previous section (cf. Section 9.1.1), the achieved improvements in self-consumption are similar for the two approaches. This means this fact alone cannot explain the higher savings from GTS compared to GTSWC. The second factor that plays a role is the more effective PAR reduction observed for the GTS approach (cf. Section 9.1.2). Due to the

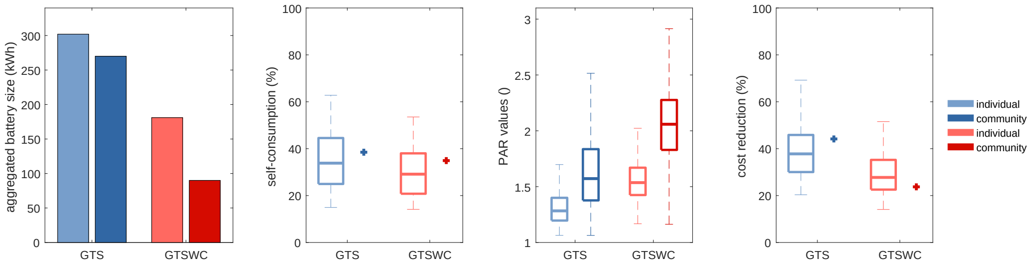

Figure 9.6. *Comparison between centralised and decentralised approach.*
The aggregated optimal battery sizes for the GTS and GTSWC approach in case of a single centralised battery and individually-owned decentralised batteries are shown. Furthermore the three metrics: self-consumption, peak-to-average ratio (PAR) of the aggregated load, and cost reduction are investigated for simulations based on these optimally sized storage installations. All simulations are performed over the period of an entire year, i.e. winter 2010 to autumn 2011.

quadratic relation between the aggregated load and the price per unit of electricity, consumption during peak times is billed highly. The spread around the median values for both approaches is similar.

9.1.4 Centralised vs. Decentralised Storage Systems

In all the previous simulations, each household was in possession of an individual battery of different size. Within this section, a scenario that has a single battery to serve the community is investigated. For a reasonable comparison, the efficiency of the battery and the DC/AC power electronics converter equal the values used before. Furthermore, the maximal charging and discharging rates were scaled up by the number of households. Firstly, full-year simulations with battery sizes varying between 10 kWh and 370 kWh were performed. Following the optimal sizing procedure by [Huang et al., 2018], the optimal battery capacity for both the GTS and GTSWC approach were calculated to be 270 kWh and 90 kWh, respectively. For these optimal sizes, the self-consumption, the peak-to-average ratio (PAR) of the aggregated load of all households, and the cost reduction according to the pricing function (4.15) are analysed. The results are shown together with the respective results from yearly simulations of individually-owned batteries in Figure 9.6.

The centralised optimal battery sizes are approximately 10% and 50% smaller than the aggregated capacities of the decentralised batteries for the GTS and GTSWC approach, respectively. This is in agreement with a previous study reported by Luthander *et al*. [Luthander et al., 2015]. In Section 9.2, we discuss that in case of asynchronous demand and generation profiles, a large battery is most beneficial, while in the opposite case a small battery is sufficient. When looking at the centralised battery, note that it is scheduled according to the aggregated demand and generation of all the households. An averaging effect for the demand profiles occurs, which makes the asynchronous case less likely and eventually leads to a smaller optimal storage capacity. The PV self-consumption reaches a comparable level to the decentralised simulations. Compared to the median self-consumption of all the households, a scenario with a centralised battery improves the self-consumption by approximately 5% for both the GTS and GTSWC approach. When analysing the daily PAR values, it becomes clear that due the considerably smaller size the community batteries perform worse both in terms of the achieved median values and also the spread around it. From the utility companies' perspective this is a unfavourable result. Their most desirable objective is to reduce the PAR value as it guarantees grid stability and financial benefits in the long run.

The right-most panel in Figure 9.6 shows the results for the cost reduction for both approaches comparing the centralised and decentralised neighbourhoods. For the GTS approach the centralised community achieves an approximately 5% higher cost reduction, while for the GTSWC approach the cost reduction is reduced by approximately 5% compared to the median cost reduction of all the households with individually-owned batteries. Both results for the centralised battery are within the interquartile range of the respective analysis for the decentralised system.

9.2 Discussion

While the aggregated demand of a household and the size of their installed solar panel can give a rough estimate for the optimal battery size, it remains important to look at the actual demand and generation patterns. In Section 9.1.1 it was visible that two households with similar aggregated demand and potential peak PV output benefited differently from their storage installation. In order to understand this difference, Figure 9.7 shows the demand and generation profile for a randomly chosen day together with the detailed battery usage for these two households. The demand of household 14 is low during the time when solar is available and peaks shortly afterwards, whereas the demand of household 26 is rather evenly distributed throughout the day. Household 26 is a prime example of a user that has a high percentage of non-curtailed solar energy even without a battery installation and cannot gain much through the utilisation of storage. Consequently, the optimal battery sizing algorithm determines a below-average optimal storage capacity for this household. In contrast to this, the battery of household 14 is optimally sized at an above-average capacity. Without storage a lot of the solar energy is curtailed due to the lack of demand at the particular time of generation. Since there is a peak in

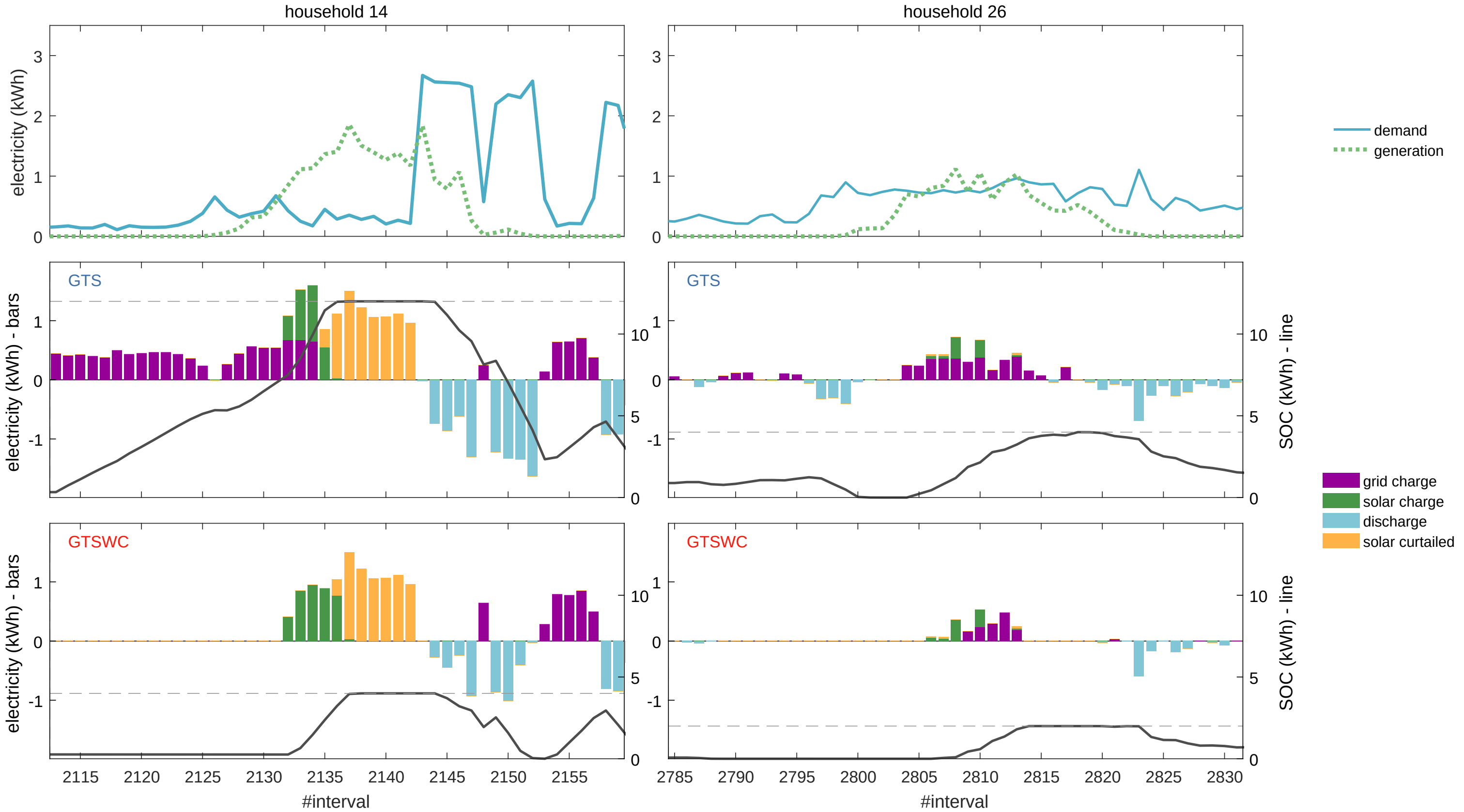

Figure 9.7. *Demand, generation, battery usage.*

The demand and generation profiles of household 14 (left) and household 26 (right) for representative days are shown. Furthermore, the specific battery usage based on the GTS and GTSWC approach are presented. For these four plots, the left hand axes represent the electricity values for the bars, while the right hand axes indicate the state of charge (SOC) of the respective battery. The dotted line indicates the optimal battery size for the respective household.

For this particular day household 14 improves their self-consumption by 6.0% / 10.4% through the GTS / GTSWC approach, respectively. Household 26 improves their self-consumption by 2.7% for both approaches.

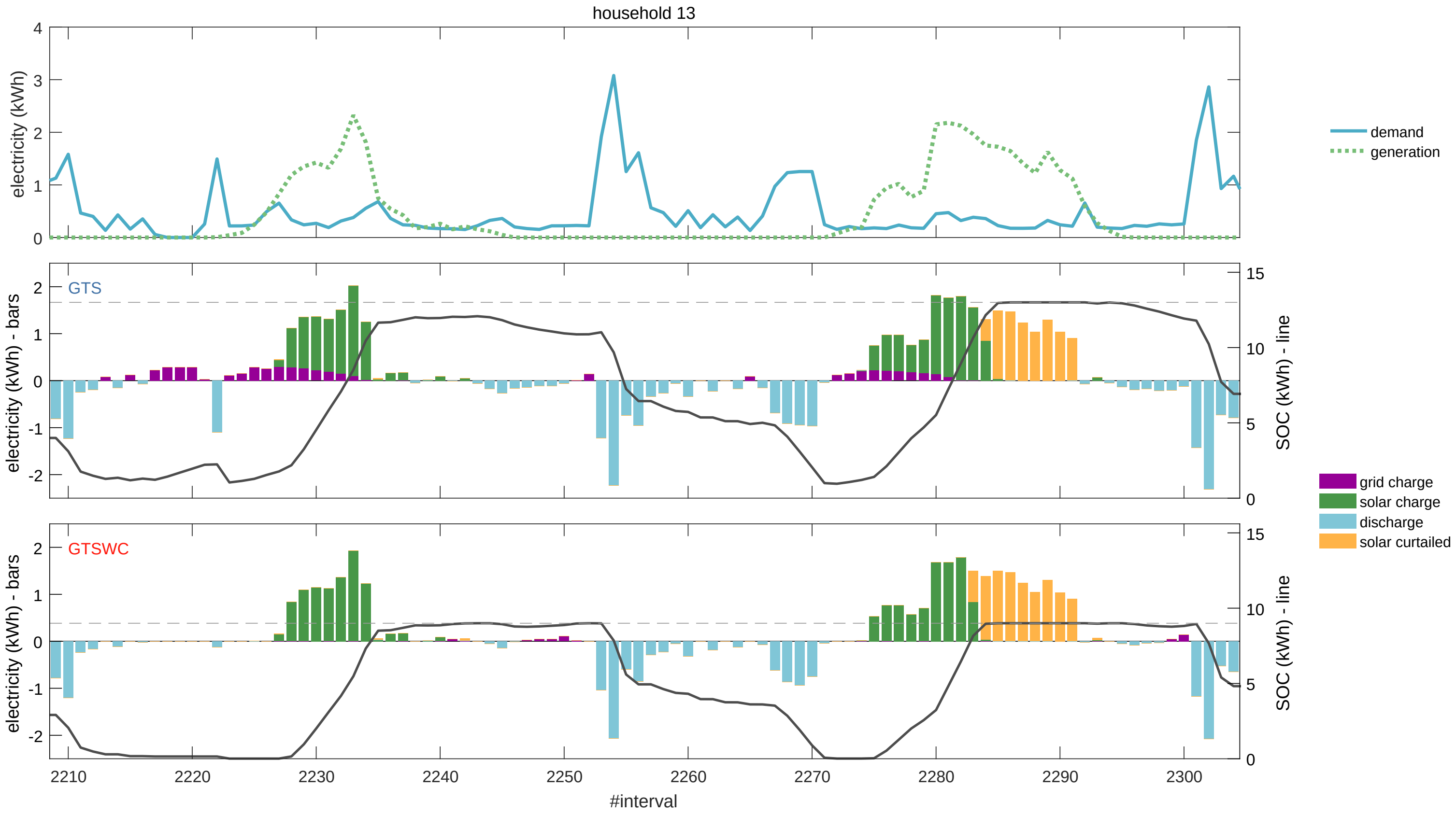

Figure 9.8. *Demand, generation, battery usage.*
The demand and generation profiles of household 13 for two representative days are shown. Furthermore, the specific battery usage based on the GTS and GTSWC approach are presented. For the lower two plots, the left hand axes represent the electricity values for the bars, while the right hand axes indicate the state of charge (SOC) of the respective battery.

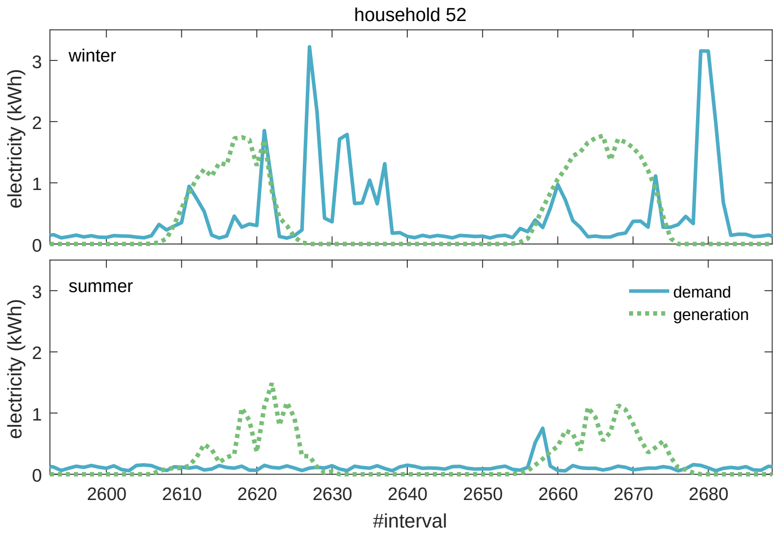

Figure 9.9. *Demand and generation for two seasons.*
The demand and PV generation of household 52 for two consecutive representative days of winter 2010 and summer 2010 are shown.

demand in the later hours, the self-consumption can be increased due to the storage capability.

The left-hand plots in Figure 9.7 also give insight into the differences between the GTS and GTSWC approach. During the fist half of the day, the GTS algorithm charges the battery from the grid, whereas the GTSWC anticipates the solar generation and thus restricts charging from the grid. The first two peaks in demand (cf. between interval 2144 and 2152) can then be met by previously saved electricity. In anticipation of another peak in demand at the end of the day, both algorithms charge the battery and are able to flatten the load curve considerably. It becomes clear that because no more solar production is to be expected during this time there are no constraints on charging the battery from the grid and both algorithms behave similarly.

Fig. 9.8 shows the demand and generation pattern together with the battery usage for two consecutive days of household 13. This household was chosen as it has the highest benefit during this particular season from installing an optimal battery size. A similar profile for the demand and generation as seen for household 14 in Figure 9.7 can be observed. The even higher improvement in self-consumption for this case stem from the more pronounced asynchronisation between solar generation and actual demand. Also, this household is equipped with a bigger solar panel.

This section is concluded by analysing the demand and generation profile (Figure 9.9) for the household that showed the biggest difference in optimal battery size between two seasons, i.e. household 52. For winter 2010 the optimal capacity is determined to be 11 kWh while in summer 2011 it is 3 kWh.

9.3 Conclusions

In this chapter, a community of households that take part in a demand-side management scheme is analysed. The focus was to gain deeper understanding of optimal battery sizing. Both the characteristics that lead to the optimal battery size determination as well as the effect this optimal size has on solar PV self-consumption ratio, grid stability/security, and cost reductions for the users have been investigated. A key insight is that the temporal patterns of consumption and generation impact the battery sizing critically. This means battery sizing which is solely based on aggregated data might lead to unfavourable results. Households which benefit most from installing a energy storage system are those where the peak-production and peak-consumption is asynchronous, i.e. during different intervals of the day.

Furthermore, two different approaches for the demand-side management scheme were compared. GTS is based on the ideas presented in [Pilz and Al-Fagih, 2019a]. Here the main objective of the individual households is to minimise their electricity bills. The second approach introduced an additional constraint to the GTS which puts PV self-consumption before the minimisation of the costs. As a result it lead to considerably smaller optimal battery sizes. The drawback of the more constrained approach are the larger peak-to-average ratio of the aggregated load, i.e. higher costs for the utility company to guarantee stability of the grid. In terms of costs a trade-off is achieved: On the one hand, the initial investments are smaller for GTSWC due to the smaller battery sizes. On the other hand, the cost reduction off the electricity bill are less beneficial.

Eventually, we compared individually-owned batteries with a scenario that includes a utility sized centralised storage system. The optimal battery size determined for the centralised system is smaller due to less pronounced asynchrony of the aggregated demand to the solar PV production.

This almost blank page is intentional.

Part III

Conclusions & Future Work

This almost blank page is intentional.

CHAPTER 10

CONCLUSIONS

This thesis investigated a demand-side management (DSM) scheme for prosumer energy storage systems. Within it, households maintain high levels of comfort as they do not have to change their actual demand patterns. This stands in contrast to demand-response approaches that rely on behavioural changes of the users. We assumed rational customers that are all served by the same utility company (UC). The UC implements a quadratic pricing function in which the price per unit of energy depends on the aggregated load of all the households in the neighbourhood. This is why even though every participant is only interested in reducing their own electricity bill, they all together achieve a collective goal of flattening the load profile.

10.1 Main Findings and Contributions to Knowledge

Over the course of the PhD, the game-theoretic scheduling approach was progressively refined to eventually achieve peak-to-average ratios (PAR) of the aggregated load that are close to 1.0 even under worst case conditions. Furthermore, due to the analytic solution that was derived for the best response problem in the dynamic game, run-times of the approach are such that the game can be applied in real-life.

As the system relies on the exchange of data between the participating households, an investigation on its cyber security was carried out. We developed a novel type of false data injection attacks and analysed the impact such attacks would have. Moreover, we extended an established game-theoretic concept for cyber security in order to study the decision-making process of the utility company, i.e. the defender within our model. The take away message is that attacks that cannot be detected only cause minor inconveniences to the end-user and the UC.

Thus there is a negligible risk in the data exchange. Nevertheless, it is important to understand the benefits that can be achieved by doing so. Our studies have shown that it is worth playing the game when compared to scheduling the batteries independently, especially in terms of PAR reduction and robustness against inevitable forecasting errors.

In a final study we gained in-depth insight on how the demand and generation patterns of the households affect their optimal battery size. It became clear that households with pronounced asynchrony between peak-demand and peak-production can achieve higher benefits from installing an energy storage system.

10.2 Limitations of the Work

The main limitation of the work is its fully theoretical nature. It has yet to be seen how the approach can be established in a real-world implementation. Usually, there are a number of issues that will only be detected once one reaches the pilot stage of the project. Some, but not exclusively, could be related to the technical realisation of the connections between the households and the connection between the households and the utility company. What happens for example if one of the users is not able to exchange their information at the beginning of the DSM protocol?

Another shortcoming of this thesis is the fact that there is only one utility company modeled as the initiator of this DSM scheme. In a realistic scenario, households are accustomed to the possibility of changing their energy supplier. Thus the model should be extended to cover the free-market competition between multiple utility companies. This extension and further areas of research in which this project could be extended in the future are described in the following chapter, i.e. Chapter 11.

CHAPTER 11

Future Work

This chapter explores different avenues for potential extensions to the PhD thesis. It is split into two sections. In Section 11.1, an energy sharing concept for prosumer communities[1] is proposed in detail. It is based on the assumption that the households have the ability to exchange electricity with one another. Section 11.2 gives a more general overview of further directions for future work.

11.1 An Energy Sharing Concept

Research combining storage technology and trading of renewable energies began to take shape in 2018 (e.g. [Zepter et al., 2019, Ghosh et al., 2018, Mediwaththe et al., 2018, Liu et al., 2018a]). The interest shifted from a one-off trade between households (or microgrids [Lee et al., 2015]), to a planning-oriented approach. Given forecasts for demand and generation (usually for the upcoming day), battery usage and trading activities are scheduled.

For instance, references [Zepter et al., 2019] and [Ghosh et al., 2018] describe a scenario in which a central operator/platform determines the optimal battery and trading decisions of a community such that the consumption from the external grid is minimised. This does not take into account the preferences of the utility company (UC). While the batteries in these examples are owned by individual

[1] The content of this section has been published at the IEEE International Conference on Communications, Control, and Computing Technology for Smart Grids 2019.

households, [Mediwaththe et al., 2018] and [Liu et al., 2018a] each employ a single centralised energy storage.

We expect that the most efficient system will have to combine energy exchange between households as well as the utilisation of energy storage. A fully decentralised smart grid might be advertised as the pinnacle of power systems, but it is not the most probable future scenario. We have to acknowledge the role of the UC within the system as they are already investing in large scale renewable energy resources, e.g. [EWE, 2019, EDF, 2019, Shell, 2019].

Furthermore, the energy trading scenarios proposed in the literature assume the willingness of people to initiate monetary transactions every time they exchange energy with one another. We believe that this is overwhelming for the customer. A modern billing scheme needs to be simple and still remain familiar to the existing system to find large scale adoption.

This section proposes a novel demand-side management (DSM) concept, which has the following advantages:

1. The scheme directly features the generation of energy from the UC and incentivises the community to follow this production.

2. Each household is treated as an individual and rational entity that wants to minimise their electricity bill. They can do so by scheduling their energy storage system as well as sharing energy with the community.

3. There are no monetary transactions connected to sharing energy. Nevertheless, it is beneficial for users to offer their excess renewable energy generation.

11.1.1 Decision Variables

Here, we introduce the decisions that can be taken by the households. It will become clear how the battery and renewable energy resource model (cf. Section 4.2) limit these choices.

In general, there are two types of decisions to make for each household $n \in \mathcal{N}$ during each interval $t \in \mathcal{T}$ of the upcoming day:

- how to use the battery (denoted by a_n^t)
- how to share energy (denoted by e_n^t)

For simplicity we combine these into a single decision vector $\mathbf{x}_n^t = [a_n^t, e_n^t]$. A collection of these decisions over the entire time period $\mathbf{x}_n = [\mathbf{x}_n^1, \mathbf{x}_n^2, \dots, \mathbf{x}_n^T]$ is called a schedule.

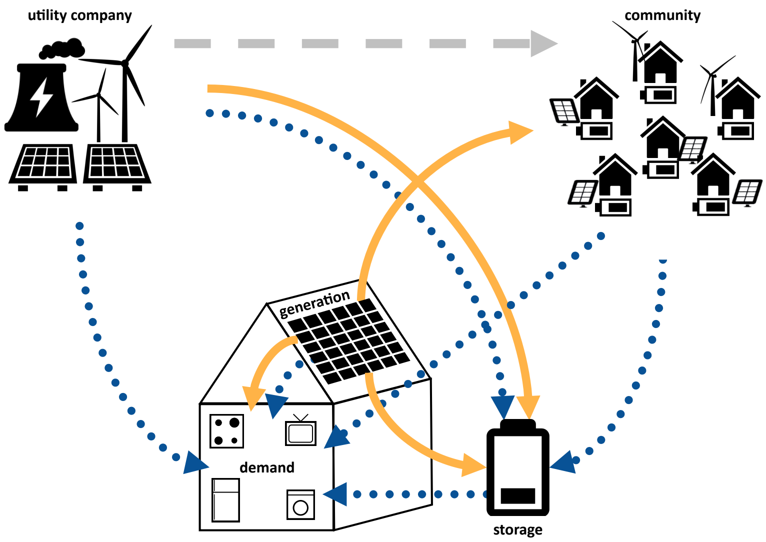

Figure 11.1. *Electricity flows.*
The potential electricity flows for an individual household of the prosumer community is shown. Dotted lines refer to flows of a 'taking' household, while solid lines reference a 'giving' household. These flows are also valid for all the other households in the community and summarised in the dashed line between the utility company and the community. (©2019 IEEE)

For each time interval, households are categorised as *giver* or *taker* of energy based on their net-demand (4.10). The classification in giver and taker introduces different boundaries to the decisions $\mathbf{x}_n^t$.

Definitions of giver and taker: If $d_n^t > 0$ it means that the demand of the household cannot be satisfied from their own renewable energy production. Thus they require further electricity from either the grid or other households. We call such a household *taker*.

If $d_n^t \leq 0$ it means that there is an excess of renewable energy which can be used to charge their own battery or be shared with the other households. During such an interval the household is categorised as a *giver*.

The load l_n^t of a user is defined as the amount of energy drawn from the grid, i.e. from the utility company. In the following section (Section 11.1.2), the explicit billing mechanism highlights how the electricity costs depend on the aggregated load of all households as well as their individual load. Here, we explain how the decisions taken by a household affect the load.

Decision space for 'taking' households: The load of a taking household $n \in \mathcal{N}$ at time $t \in \mathcal{T}$ is

$$l_n^t = d_n^t + a_n^t + e_n^t \,. \tag{11.1}$$

The battery decision a_n^t and sharing decision e_n^t have to fulfil the following constraints:

$$s_n^t - s_{\min} < \phi^-\left(s_n^t\right) \le a_n^t \le \phi^+\left(s_n^t\right) < s_{\max} - s_n^t \tag{11.2a}$$

$$-d_n^t - a_n^t \le e_n^t \le 0 \tag{11.2b}$$

$$\left|e_n^t\right| \le E^t \; . \tag{11.2c}$$

Equation (11.2a) describes the discharging and charging restrictions from left to right, respectively. Discharging cannot be done below the minimum state-of-charge (SOC) $s_{\min}$ and also the charging rate and efficiency are respected. The right hand side makes a similar statement for the charging process (cf. Section 4.2.1). Note that discharging refers to using energy from the battery to fulfil demand, while charging the battery explicitly refers to charging the battery from the grid.

Equation (11.2b) guarantees $l_n^t \ge 0$, meaning that the households can neither sell energy from their battery nor the energy they receive from their neighbours to the grid. Furthermore, the amount of energy they can obtain from the neighbours is restricted to the aggregated excess production E^t of them at time interval t (cf. (11.2c)). Note that charging the battery can effectively be done from shared energy.

The interaction with the battery directly influences the SOC. To reflect the correct state s_n^{t+1} of the upcoming interval we calculate

$$s_n^{t+1} = \begin{cases} s_n^t + \eta_{\text{inv}}\,\eta^+ a_n^t & ,\text{if } a_n^t > 0 \\ s_n^t + a_n^t/(\eta_{\text{inv}}\,\eta^-) & ,\text{if } a_n^t < 0 \\ s_n^t \cdot \left(1+\bar{\rho}\right)^{\Delta t} & ,\text{if } a_n^t = 0 \end{cases} .$$

Decision space for 'giving' households: The load of a giving household $n \in \mathcal{N}$ at time $t \in \mathcal{T}$ is

$$l_n^t = a_n^t \; . \tag{11.3}$$

All the demand $\bar{d}_n^t$ is already fulfilled from their renewable energy resource. Nevertheless, there is also a sharing decision to make: The household can offer (part of) their excess production d_n^t to the community, i.e.

$$E^t \leftarrow E^t + \bar{\eta} \cdot e_n^t \; , \;\; \text{with} \;\; 0 \le e_n^t \le -d_n^t \; ,$$

where $0 < \bar{\eta} \le 1$ denotes the line losses of the network. The remaining part, i.e. $-d_n^t - e_n^t$, is automatically used to charge the battery. This gives a further restriction to the amount to be charged from the grid as follows:

$$0 \le a_n^t - d_n^t - e_n^t \le \phi^+(s_n^t) < s_n^{\max} - s_n^t \; .$$

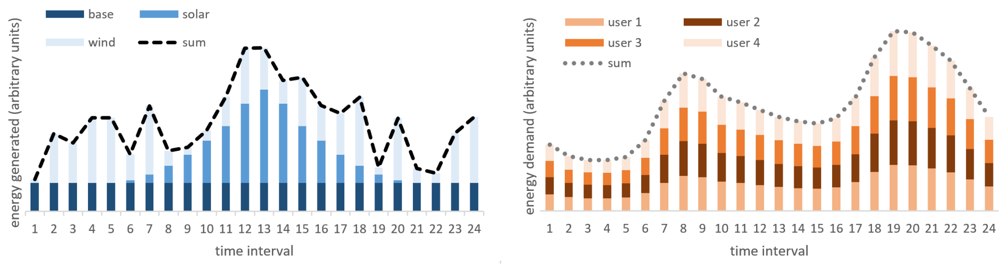

Figure 11.2. *Generation and demand.*
The exemplary energy generation of the utility company and demand of four households is shown on the left and right, respectively. Furthermore, the sum of the individual components are shown as lines.
g^t refers to the dashed line in the left-hand plot. The dotted line in the right-hand plot can be seen as the aggregated load L^t in a scenario where batteries are not used and energy is not shared. (©2019 IEEE)

In the case that the effective charging amount is exactly 0, the self-discharging process of the battery $s_n^{t+1} = s_n^t \cdot \left(1+\bar{\rho}\right)^{\Delta t}$ is considered. Otherwise the SOC for the upcoming interval is calculated to be

$$s_n^{t+1} = s_n^t + \eta_{\text{inv}}\, \eta^+ a_n^t + \eta^+ \cdot (-d_n^t - e_n^t)\,.$$

When charging the battery directly from locally produced renewable energy resources, only the battery efficiency η^+ has to be considered, whereas charging from the grid also requires conversion from AC to DC with the respective conversion efficiency η_{inv}.

The aggregated load: The aggregated load L^t at time interval t is the total amount of electricity requested by the community. With respect to the non-cooperative game (cf. Section 11.1.3) the following definition is used:

$$L^t = l_n^t + l_{-n}^t\,, \tag{11.4}$$

where l_n^t is the load of a specific household $n \in \mathcal{N}$ and l_{-n}^t is the load of all households except for n.

In the previous subsections it was shown how each household is able to directly influence their own load, i.e. Equations (11.1) and (11.3). Furthermore, it became clear that by means of the sharing ability they can also (indirectly) affect the load of other households in the community.

11.1.2 The Utility Function

In this section, the novel utility function, i.e. the electricity bill, for each participant of the game is presented.

Households are incentivised to follow the forecasted production pattern g^t of the utility company (cf. Fig. 11.2) by implementing the following price per energy unit for a given interval $t \in \mathcal{T}$ of the upcoming day:

$$p^t = \left(L^t - g^t\right)^2 + p_0 \ ,$$

where $p_0 > 0$ is constant and L^t is the aggregated load of all users as defined in (11.4). The closer the aggregated load L^t is to the generated electricity g^t, the smaller the price per energy unit for this particular interval $t \in \mathcal{T}$. The electricity bill for a particular household $n \in \mathcal{N}$ for one day is then calculated to be:

$$u_n = \sum_{t=1}^{T} l_n^t \cdot p^t \ . \tag{11.5}$$

In the non-cooperative game between the households, each user strives to minimise their individual electricity bill (11.5). In the interest of showing how the electricity bill for household $n \in \mathcal{N}$ depends on their own sharing/charging decisions x_n and the decisions x_{-n} of all the other households let us rewrite (11.5) explicitly with these dependencies:

$$\begin{aligned} u_n(\mathbf{x}_n, \mathbf{x}_{-n}) = \sum_{t=1}^{T} \Big\{ & l_n^t(\mathbf{x}_n) \cdot p_0 \\ & + l_n^t(\mathbf{x}_n) \cdot \left[l_n^t(\mathbf{x}_n) + l_{-n}^t(\mathbf{x}_{-n}) - g^t \right]^2 \Big\} \ . \end{aligned} \tag{11.6}$$

11.1.3 The Non-Cooperative Game

In this section, we define the non-cooperative game and explain the solution approach that leads to equilibrium schedules for the individual households[2].

The non-cooperative game is defined by $G = \{\mathcal{N}, \mathcal{X}, \mathbf{u}\}$ with

- $\mathcal{N}$ as the set of participants of the game.
- $\mathcal{X} = \mathcal{X}_1 \times \cdots \times \mathcal{X}_N$, where $\mathcal{X}_n$ is the set of all actions $\mathbf{x}_n$ that fulfil the restrictions detailed in Section 11.1.1.
- $\mathbf{u} = [u_1, \ldots, u_N]$, with the utility function (11.6) $u_n : \mathcal{X} \to \mathrm{I\!R}$ for player n.

An iterative best-response algorithm [Shoham and Leyton-Brown, 2009] is used to solve the game. The solution is a vector of battery/sharing-schedules $\hat{\mathbf{x}} = [\hat{\mathbf{x}}_n, \hat{\mathbf{x}}_{-n}]$, i.e. one for each participant[3].

[2] The structure of the utility function (11.5) and the constraints (e.g. (11.2)) indicates the existence of a Nash equilibrium. Nevertheless, a formal prove is beyond the scope of this section and remains future work.

[3] Equivalently, we can write the solution as $\hat{\mathbf{x}} = \left[\hat{\mathbf{x}}_1, \ldots, \hat{\mathbf{x}}_N\right]$ to emphasis the contribution of all households.

During each step of the iteration, the households determine their best strategy by solving the minimisation problem:

$$\hat{x}_n = \underset{\mathbf{x}_n \in \mathcal{X}_n}{\operatorname{argmin}}\, u_n(\mathbf{x}_n, \mathbf{x}_{-n}) \ . \tag{11.7}$$

A summary of the algorithm can be found in Algorithm 5. When this iteration

Algorithm 5: Best-response algorithm for finding a pure NE based on [Shoham and Leyton-Brown, 2009]

Input: g^t, $\mathbf{w}^t$, $\bar{\mathbf{d}}^t$

initialise random vector of schedules $\mathbf{x} = (\mathbf{x}_n, \mathbf{x}_{-n})$
while *there exists a player n for whom $\mathbf{x}_n$ is not a best response to $\mathbf{x}_{-n}$* **do**
  for each $n \in \mathcal{N}$ **do**
    $\hat{\mathbf{x}}_n \leftarrow$ best response to $\mathbf{x}_{-n}$ based on (11.7)
    $\mathbf{x} \leftarrow (\hat{\mathbf{x}}_n, \mathbf{x}_{-n})$
  end
end

Output: $\hat{\mathbf{x}} = \mathbf{x}$

procedure terminates, each household has determined a schedule $\mathbf{x}_n$ which is in equilibrium with all the other households. This means that there is no incentive to deviate from this strategy. Any unilateral deviation can only ever result in a worse outcome, i.e. a more expensive electricity bill.

Fig. 11.3 illustrates the potential effect of the scheme if it were to be applied on the data shown in Fig. 11.2[4]. By scheduling their batteries and sharing energy among each other, they are able to adapt to the forecasted generation of the UC.

11.1.4 Conclusions

The adoption of renewable energy resources helps to limit greenhouse gas emissions. This section proposed a DSM scheme which allows the integration of renewable energy resources on both the utility company's level (*large scale)* and the customer's level (*small scale)*. Within the scheme, households are financially incentivised to adjust their load to the forecasted electricity production of the utility company. They can accomplish this by scheduling their locally installed energy storage systems and by sharing energy with the community. The underlying process to organise the scheduling and sharing is based on a non-cooperative game in which every participant is only interested in achieving the best for themselves. We thus established a

[4]Note that this is for demonstration purposes only. Future work will implement the scheme, perform simulations, and report quantitative results.

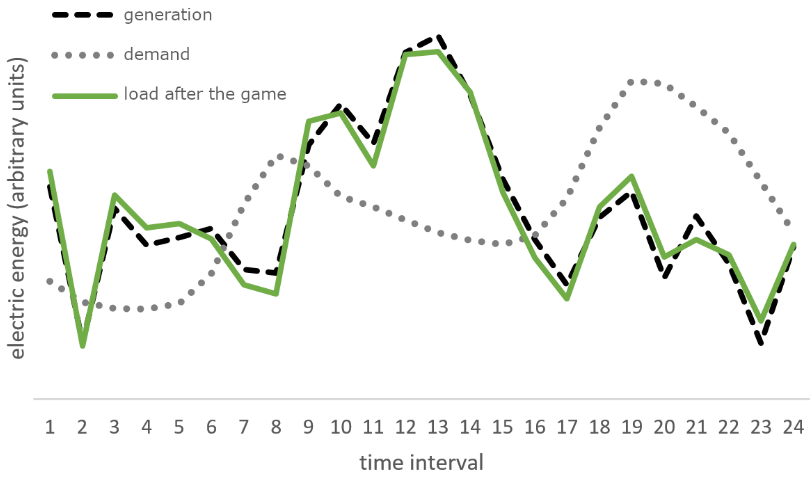

Figure 11.3. *Outcome of the game*.
The dashed and dotted lines are directly taken from Fig. 11.2 and refer to the generation of the utility and the demand of the community, respectively. The utility function (11.5) is designed such that it is most beneficial for the households to make use of the energy storage systems and share energy in a way that the aggregated load matches the forecasted supply. The solid line indicates the potential aggregated load of the households after playing the game. (©2019 IEEE)

mechanism for *selfish energy sharing* which does not require direct monetary transactions between the prosumers. In our opinion, this makes it more approachable for the user, fostering wide-spread adoption.

Future research will quantify the gains of our approach in terms of renewable energy self-consumption, how closely the utility's production curve can be followed, and financial rewards for the prosumers. Furthermore, a detailed comparison to energy trading schemes will be necessary to demonstrate the competitiveness of our proposition. Especially the robustness with respect to inevitable forecasting errors will be a key aspect of future studies. It is worth noting that since the optimal size of storage and generation for each household is derived using the billing scheme and energy trading model, their optimality has to be revisited for all of these DSM concepts.

11.2 Other Directions

Other than the introduction of true peer-to-peer energy sharing scheme between households in a community, there are various other ideas that propose viable directions of research. One of the most important issues in a day-ahead energy management scheme is the concern of forecasting errors. These errors will never be fully eliminated, we can only implement mechanisms that mitigate their negative effects. Currently there are two main streams of ideas for this particular problem.

Firstly, the treatment of uncertainties can be directly incorporated into the formulation of the game or optimisation scenario. For instance, a conditional value at risk approach (cf. [Li et al., 2017, Bahrami and Amini, 2018, Liu et al., 2018a]) for which a finite number of scenarios is considered at given probabilities. So far, this direction has not been considered in combination with a game-theoretic scheduling approach but only in centralised optimisation concepts. Most likely, it has to be integrated into a Bayesian game which can model the different scenarios as types of players (cf. Section 2.3).

Secondly, there are approaches that include a second stage into their scheduling approach. Similar to what was presented in this thesis, the first stage is usually completed before the actual scheduling period commences and plans the operations. In contrast to this, the second stage (cf. [Tushar et al., 2018a, Liu et al., 2018a]) is (repeatedly) run during the scheduling period and delivers real-time updates that treat the mismatch between planned loads and what can be realised. An advantages of this approach is that it can be developed completely independent of the first stage. Furthermore, if it can be proved to work without failure and fits into the business case of the scheme, efforts into developing the first stage mechanism can be reduced.

Another direction that will be important for future residential scenarios is the integration of electric vehicles (EVs). This affects two aspects of the system; The overall electricity demand will increase considerably, and EVs can provide substantial increase in flexibility when seen in combination with vehicle-to-grid technology. In the literature review (cf. Chapter 3), it became clear that the potential to charge the EV at one location and use this electricity at another place has yet to be investigated.

An additional branch of research that has not been covered within this thesis is the competitive nature of a free market including more than one utility company. This would add another dynamic dimension to the scheme and give better insights into the applicability of the approach in a real-world framework. The most suitable approach to study this concept would be the utilisation of a Stackelberg game. It can model the hierarchical structure of multiple utilities companies and multiple households with various appliances and energy storage facilities.

With a view on the bigger picture, i.e. the actual integration of such a demand-side management system into households, the aspect of suitable regulations needs to be considered as well. Following Mengelkamp *et al.* [Mengelkamp et al., 2018b], we can see that the micromarket setup and the microgrid setup, as introduced for instance in Section 11.1, needs to be embedded into a suitable legal environment. There are two ways this can be realised. We can investigate whether the system fits into current or planned regulatory frameworks and perform necessary changes, or we have to initiate a connection between blue-sky research and political parties to foster the development of new regulations that allow to implement the proposed demand-side management schemes.

Part IV

Appendix

This almost blank page is intentional.

APPENDIX

A

BATTERY JUSTIFICATION

Various companies produce home energy storage systems, e.g. Mercedes, Tesla, BMW, Nissan and Powervault. Some of them are specialised in second life batteries taken from their electric cars, while others (such as Tesla) produce these batteries for their special purpose. As most manufacturers provide

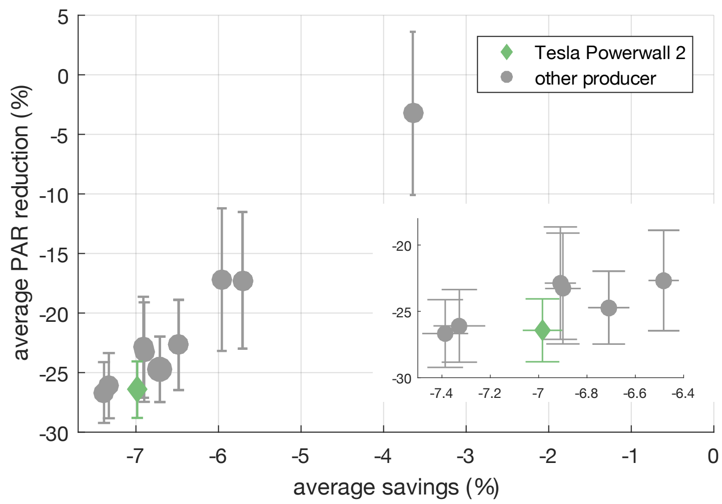

Figure A.1. *Battery justification.*
The mean PAR reduction of the aggregated load over 365 days is plotted over the mean savings for participants of the DSM scheme with different battery systems. For all runs we assumed $N/M = 76\%$, $\epsilon_d = 8\%$, $\epsilon_w = 10\%$, and the same pricing parameter as introduced in Section 6.2. A close-up of the bottom left-hand corner is shown in a subplot. We also provide the standard deviation in both variables.

technical data sheets, we were able to run our simulations for the DSM scheme assuming that households are equipped with different batteries.

The results in Figure A.1 stem from scenarios with 76% participation rate, forecasting errors as used in Section 6.2, and all participants with the exact same battery model. This is not supposed to compare different systems, but rather to show that this battery can be taken as a representative of state-of-the-art technology. It achieves a PAR reduction similar to the best in the field. Also the savings off the energy bill are close to the best competitors.

Appendix B

Literature Overview

[Mohsenian-Rad et al., 2010] present one of the very first approaches in which the interaction between households is leveraged to perform load-shaping. In their model, customers reschedule appliances for the upcoming day. The incentive mechanism is provided through a quadratic cost function which is implemented by the utility company serving the users. Since the pricing is based on the aggregated load of all participants it prevents synchronised reactions and thus the formation of new peaks. On average they achieve a PAR reduction of $\approx 20\%$.

[Mohsenian-Rad and Leon-Garcia, 2010] investigate a scenario in which households schedule their appliances based on real-time pricing forecasts. Note that there is no coordination/communication between the users. In order to avoid load synchronisation among them, they implement a method called inclining block rates. For instance, the two-level inclining block rate utilised by BC Hydro (cf. [British Columbia Utilities Commission, 2017]) means, that customers are charged at a higher rate if they consume beyond a predefined threshold. Eventually, PAR reductions of $\approx 22\%$ are reported.

A framework for trading electricity between interacting groups of electric vehicles is presented in [Saad et al., 2011]. A group consists of 500 to 1000 individual cars with a surplus of energy of more than half their total capacity. Each group acts as a single player of a non-cooperative game and decides on a strategy corresponding to the amount of energy that it is willing to trade. The utility function incorporates the trading and reservation prices, the amount of energy to sell, and a term that summarises costs for discharging the batteries. By means of a double auction, the players are incentivised to truthfully reveal their reservation price.

[Ramchurn et al., 2011] develop a demand-side management model that aims to reduce peak consumption of the upcoming day. By first studying a centralised control mechanism, they show its infeasibility and thus propose a decentralised approach. It achieves a $\approx 17\%$ decrease in peak demand.

A two-level hierarchical approach is shown in [Zhu et al., 2012]. While the lower level is concerned with optimal scheduling of household appliances, the upper level models the interaction of the households in a demand response scenario including uncertainties about the pricing. One of their main contributions is the formulation of a closed-form Nash equilibrium for the case of homogeneous users.

[Ilic et al., 2012] design an energy market place where future households can trade their surplus energy locally. In contrast to other approaches they do not investigate optimal decisions but rather focus on the design of the market, the clearing of the order book, and show that it reacts sensibly.

[Nguyen et al., 2012] propose a demand-side management technique that reduces the PAR value. In their model, they include both the scheduling of appliances as well as home energy storage systems. All batteries have perfect charging and discharging efficiencies and are neither limited in terms of charging nor discharging rates. The results of the non-cooperative game show reductions of the PAR value of about 25% which is shown to be comparable to what can be achieved through centralised optimisation.

[Atzeni et al., 2013] formulate two mechanisms for accommodating distributed energy production and storage: A non-cooperative scheduling approach and a centralised grid optimisation based on nonlinear programming. Similar to [Nguyen et al., 2012] their battery model does not include charging and discharging efficiency. While focussing on the convergence properties of the different methods, they also show a PAR reduction of 12.5%.

[Kim et al., 2013] design a non-cooperative scheduling game for the battery where the users decide between charging the battery, using stored energy for their appliances, or selling stored energy back to the grid. All this is set up in an environment of multiple customers that are connected to an aggregator, which is itself connected to the wider power grid. Participants will declare their expected demand for the following day to the aggregator, allowing it to organise the distribution. The fact that they deal with electric vehicles instead of stationary batteries is modelled within a constraint that denotes times of the day where it can be neither charged nor discharged. Since the aggregator is interested in making a profit on its own, a tiered billing function is implemented that charges a higher price for heavy users, i.e. users that demand more energy than average. This can also be seen as a measure of fairness, as otherwise these heavy users would drive up the price for all the other users. The need for such a pricing mechanism is justified, because the model is applied to a mixture of residential and industrial customers. Another consideration to safeguard the aggregator is the incorporation of uncertainty. Ensuing from the worst-case scenario eventually shows the robustness of their approach.

The optimal scheduling of household appliances, storage, and renewable generation of an individual household is the topic of [Kim and Giannakis, 2013]. They use a nonconvex optimisation method and show the robustness of the approach to price uncertainties and uncertainty of renewable resources.

The authors of [Maharjan et al., 2013] make use of a Stackelberg approach to coordinate multiple utility companies and multiple households. The households want to maximise their demand while minimising their costs, while the utility companies are interested in the maximum revenue. The paper also shows the potentially dangerous effects of an attacker tampering with the pricing data and how the utilities can protect themselves against those interventions by implementing energy reserves.

[Adika and Wang, 2014] present a demand-side management scheme in which an aggregator schedules appliances as well as energy storage installations at residential customers' homes. The battery model employed includes charging and discharging rates. They argue that it is more efficient and convenient to use dedicated storage systems compared to using EVs for this purpose. As their simulations are only based on two households, a reasonable statement about the PAR reduction cannot be made.

[Chai et al., 2014] introduce a two-level game approach in which multiple utility companies first decide about the price of electricity and then the households can decide from which company to buy their electricity from. The structure can be assumed to be a Stackelberg game in which the leaders play a non-cooperative game while the decisions of the followers are modelled by an evolutionary game. An evolutionary game extends the idea of a non-cooperative game by the notion of population. Players are able to observe the strategies of others in the same population and replicate them. Overall, the authors expect the system to reduce the PAR value, but as this work does not include multiple time intervals it remains an open assumption.

A novel utility function is proposed in [Fadlullah et al., 2014] in which the value of energy and the cost of energy are considered. Based on an iterative approach, households schedule their appliances which eventually leads to a reduction of the PAR value. It is difficult to quote an actual value for the potential PAR reduction as several contradicting results are presented. Nevertheless, it is shown that similar improvements can be achieved when comparing the novel utility function with the quadratic cost function while reducing the computational run time.

[Lee et al., 2014] make use of a coalitional game approach to determine fair pricing in a local energy trading scenario. Households with solar and wind generation aim to sell their surplus production to households in need. Revenue streams are analysed to show which distribution of the different renewable energy resources is most beneficial. Interestingly, when the number of producers is small, solar based renewables generate more revenue. When the numbers are large enough, both sides prefer wind based generation. In the area where the number of producers is similar to the number of consumers, the consumers prefer solar generation while the producers favour wind.

[Liu et al., 2014] investigate a multi-objective optimisation approach to household appliance scheduling which tries to find the balance between maximising the usage preferences of the consumer while simultaneously minimising the incurred costs. The incentives are formulated such that this eventually results in PAR reductions. They achieve results of $\approx 23\%$. Note that the absolute PAR value that is achieved is still comparatively high (2.1) to what is presented in other studies (cf. [Mohsenian-Rad et al., 2010, Mohsenian-Rad and Leon-Garcia, 2010, Deng et al., 2015]).

With the utility company as the leader and a group of households as the followers, [Soliman and Leon-Garcia, 2014] investigate a Stackelberg game approach that schedules appliances and energy storage systems in order to reduce the PAR value. While a simple non-cooperative scheduling approach only delivers small PAR reductions, the Stackelberg game shows near optimal performance. This was to be expected as the authors formally prove the equivalence between the cost reduction in the Stackelberg game and a minimisation of the PAR value. Another key insight is the fact that whenever selling stored energy is enabled, users prefer to do so instead of reducing their peak consumption.

[Tushar et al., 2014a] implement a Stackelberg game between prosumers and consumers to investigate the trading of electricity between them. The prosumers set the price, while the consumers have to decide how much they want to consume. In their manuscript they prove the existence and uniqueness of the Stackelberg equilibrium as well as the fact that the algorithm to compute it is strategy proof. Furthermore, they study a simplified battery management system in which charging and discharging is triggered based on whether the current price is lower or higher than a pre-defined threshold.

[Tushar et al., 2014b] look at a situation in which a central power station cannot cope with the high demand at a certain point in time and thus buys the needed energy from what they call energy consumers. These energy consumers are represented by electric vehicles, renewable energy farms, and smart homes, i.e. different grid participants that possess energy storage devices and a communication link to the central power station. Instead of optimizing each individuals' utility, the authors describe a non-cooperative Stackelberg game that opts to achieve a social optimal solution. With this they assure that each player can benefit from participating in the energy trading, implementing a pricing model where the unit energy price might differ for different energy consumers. The model rewards a higher unit energy price to consumers that can only provide small amounts of surplus energy compared to participants with large surpluses. The authors use an iterative algorithm to minimise the costs for the central power station and simultaneously maximise the sum of the utility functions of the energy consumers. The results show that after 1000 independent simulation runs, the algorithm converges quickly and reliably. Comparisons to a standard feed-in tariff scheme show improvement on average utility per consumer and reduced costs for the power station.

[Deng et al., 2015] describe the interaction between multiple utility companies and multiple users by means of a convex optimisation problem. The scheme operates on two time scales: First a day-ahead scheme estimates supply and demand parameters. Then those values are updated in real-time, i.e. once per denoted time slot. The results show PAR reductions of $\approx 35\%$.

[Lee et al., 2015] study the trading of energy among microgrids, where the microgrids do not directly trade with each other but rather try to sell surplus energy to the market or buy required energy from it. It is assumed that sellers might want to keep parts of their superfluous energy for later time periods, while buyers may buy even more energy than needed, possibly for later trading even though the scheme does not explicitly model time. In the multileader-multifollower Stackelberg game proposed, the sellers act as leaders and the buyers act as followers. The specific utility functions for both groups are set up in a way that achieves a certain level of fairness. The equilibrium solution for the non-cooperative game among the buyers is given in closed-form and only depends on the selling price and the number of players. A neat and reasonable result for the sum of the utility functions of both the leaders and followers, respectively, is shown. Due to the increasing competition between the buyers, the value monotonically decreases when the number of buyers increases. At the same time, the sum of the utility values for the sellers increases, because more costumers allow them to sell more.

[Nguyen et al., 2015] is a direct extension to their previously published conference paper [Nguyen et al., 2012] offering additional theoretical contributions. In this paper, they provide deeper insight into the existence and uniqueness of the proposed

Nash equilibrium solution. Furthermore, they go into more detail regarding the algorithms that are employed to solve the scheduling game. An analysis of the dependency between battery capacity and potential peak-to-average ratio of the aggregated load show that they are directly inverse to each other.

[Rahbar et al., 2015] optimise the operations of a single microgrid with renewable energy generation, storage system, and load by means of a sliding window dynamic programming approach. The solution consists of two steps. Initially an analytic solution is presented for the case without any forecasting errors. In the second step this solution is updated by taking the errors into account. They show that a large window size is desirable when storage capacity is large and forecasting errors of the renewable resource is small, and vice-versa.

The demand-side management goal of [Wang et al., 2015a] is to increase the overall efficiency of their system consisting of distributed generation and residential consumers. They use a coalitional game-theoretic approach to fairly distribute losses that inevitably occur and by doing so reduce the overall system losses.

In [Wang et al., 2015b], the authors study a demand-side management system which does not assume fully rational customers but rather employs prospect theory to model the impact realistic users have on the system. Prospect theory models a distortion between an actual probability and the subjective probability as felt by each individual. It usually means that one is risk-averse when thinking about gains, while one tends to be risk-seeking in face of losses. Their simulation results show that the mechanism can lead to unexpected results and that this critically depends on the subjective perception of each user.

[Yaagoubi and Mouftah, 2015b] study a demand-side management system in which the residential customers weight between two objectives: They want to minimise their bills and at the same time maximise their comfort. Users that are fully focussed on their electricity costs can achieve PAR reductions of up to $\approx 38\%$, while those who balance between the two goals obtain considerably worse results.

The first P2P trading framework that includes line losses between the selling and buying households is introduced in [Yaagoubi and Mouftah, 2015a]. In their approach the sellers denote their respective prices at which they want to exchange electricity. The buyers then play a non-cooperative game in which they determine the amounts they want to buy from each seller. To point out the local character of this trading, the utility function favours transactions with sellers that are close, i.e. with fewer power line hops between buyer and seller. For testing the game results, the authors also describe a centralised optimisation model which minimises the total system bill. The comparison between the methods shows that even though the buyers in the game try to minimise their individual energy bill, none of them achieves a lower bill than in the centralised optimisation.

[Bahrami and Sheikhi, 2016] propose a demand response system in which the dependency on the end-users is reduced. This is achieved through smart energy hubs which optimise their conversion of natural gas to either heating power or electricity depending on the customers' needs and pricing signals. As a result, peaks in electricity demand can be reduced considerably, i.e. they simulate two consecutive days and observe peak reductions of 27% and 46%.

A centralised optimisation approach is used by [Haider et al., 2016a] to reduce the electricity costs for consumers. In their day-ahead scheme, the upcoming day is split into 5 minute slots, which is finer than comparable studies in the literature. Eventually they achieve peak reductions of up to 35%.

[Haider et al., 2016b] describe a demand response scheme in which households schedule their individual appliances according to a given price signal. The pricing is designed such that most of the users will be able to reduce their bill. Their results show that this is achieved on the back of the high consuming households for which the costs of electricity is increased.

[He and Yan, 2016] implement a trading scenario between microgrids and analyse it based on a Bayesian-Stackelberg game approach. In their model, the microgrids can exchange information on secure channels with selected others which results in an incomplete information structure. This poses the question of whether to trust the other participants. They show that partial trust and careful probability estimation can marginally improve the outcome.

[Mediwaththe et al., 2016] study a system in which households schedule their usage of a community-owned battery storage system by means of a non-cooperative game. This can be understood as indirect trading between the participants. Their results show the importance of high participation rates in such schemes. When 50% of the customers take part in the scheme, they can achieve a PAR reduction of $\approx 25\%$.

A novel framework for bidding and scheduling of large scale storage in an energy market is proposed in [Mohsenian-Rad, 2016]. Various parameters of the batteries are considered such as location, seasonality, efficiency, life-time, and others. The system describes a two-stage approach with a first settlement in the day-ahead market and then the real-time market. They also discuss the topic of second-life batteries. Even after loosing half of their capacity, they can still achieve considerable annual profits when employed in such a scheme.

[Park et al., 2016] design a system for energy trading among microgrids based on a non-pricing mechanism. By offering energy, microgrids earn contribution points. These points are important for the time when they request energy from the aggregator. The buyers play a non-cooperative game that deals with the question of how much energy to request. Directly proportional to this amount and inversely proportional to their individual contribution value, each consumer will be assigned a number in a queue, i.e. they have to find a strategy in which they are served early enough while minimising the amount of energy necessary to require from the main grid. A nice property of the Nash equilibrium for this case is that even if participants deviate from it, the others will not be influenced negatively.

Similar to [Wang et al., 2015b], the authors of [Rahi et al., 2016a] make use of prospect theory to model non-rational users in an energy trading scenario. In this study, the users are prosumers equipped with energy storage and individual wind energy production. They play a non-cooperative game in which they decide on how much of the produced wind energy they want to sell. Prospect theory is able to cover the individual's perception of risk associated with the uncertain nature of the resource. Thus, [Rahi et al., 2016a] argue that their simulation results deliver better insights for utility companies.

Similar to the research in [Lee et al., 2015], the architecture shown in [Wang et al., 2016] comprises a number of microgrids that are connected with an aggregator through which they are enabled to trade excess energy. For security reasons, all communications are organised through the central independent operating unit. Viewed from the perspective of any of the microgrids, this leads to an incomplete information game, as nobody knows about the strategies and payoffs of the others. More specifically, the authors divide the microgrids into sellers and buyers, and design a two-stage Stackelberg game in which each of these groups tries to find their best actions by means of a reinforcement learning algorithm. Even without explicit knowledge of the strategies of the other participants, it is shown that the learning algorithm converges to a best reply which is equivalent to the solution of the corresponding optimisation problem for the sellers and buyers, respectively. The tradeoff for the increased privacy is the slower convergence of the iterative scheme.

[Zhang et al., 2016] present a multi-layer architecture comprised of power grid, communication, control, and business layer. The idea is to develop a eBay-style peer-to-peer trading system for future prosumers in the smart grid. Their preliminary results for a small scale benchmark microgrid show that the overall energy consumption could be reduced but they also observe higher peak loads than without the trading approach due to unfavourable synchronisation. Thus the PAR value increased.

[Zhumabekuly Aitzhan and Svetinovic, 2016] make use of blockchain technology to implement a proof-of-concept model for peer-to-peer energy trading. Their focus is on transaction security and on anonymously negotiating the trading parameters.

Thus they do not specify the decision-making process of how much or when to trade.

A cooperative approach for owners of renewable energy resources who want to sell their surplus electricity on the wholesale market is shown in [Bae et al., 2017]. The authors show that forming a grand coalition makes best use of the risk pooling effect that occurs when multiple (independent) uncertain energy resources are aggregated. Furthermore, they show the advantages of high quality forecasting compared to a probabilistic approach.

The notion of fairness in a consumer community is the central aspect of [Bistarelli et al., 2017]. Given a renewable production profile of the local energy provider, they answer the question of how the community should be billed to incentivise them to guarantee the balance between supply and demand. Furthermore, a fair billing scheme for the individual households, i.e. how to split the community bill among its users, is derived from a coalitional game model.

[Celik et al., 2017] investigate a system which comprises of multiple households with storage and renewable energy resource, and an aggregator. The aggregator facilitates a non-cooperative game between the prosumers who schedule their batteries for the upcoming day such that they minimise their individual electricity bill. In this study, the time-slots for which the decisions have to be taken are remarkably short with only 1 minute per interval. Eventually they are able to reduce the peak load by $\approx 27\%$.

[Croce et al., 2017] focus on a communication scheme for demand response purposes. Given a physical grid of interconnected households, they propose "Overgrid" which is unstructured P2P communication network. In this network the nodes do not know about the topology and specific connections to their neighbouring nodes. In order to initiate a specific load control, messages are disseminated following a gossip protocol. This procedure is intrinsically fault tolerant and provides suitable scalability for large scale networks. The approach is simulated for up to 10,000 nodes showing that even at high rates of packet loss, the average convergence time is $\approx 90\,s$.

[Hahn et al., 2017] implement a proof-of-concept for an auction mechanism applied to peer-to-peer energy trading. More specifically, they design a suitable smart contract which enables prosumers to trade electricity on the Ethereum platform [Buterin et al., 2015]. The underlying auction mechanism is a Vickrey auction, i.e. a second price auction, which can be shown to incentivise bidders to submit their true value (cf. [Shoham and Leyton-Brown, 2009]). The actual strategy or decision making process is not analysed.

[Kang et al., 2017] establish a consortium blockchain that enables electric vehicles to trade electricity in a peer-to-peer manner. A consortium blockchain is a semi-decentralised type of blockchain in which a group of *nodes* is in control. In the example of the paper, these authorised nodes are established by local aggregators who audit and record all the transactions. Given a set of discharging and charging vehicles, the trading price is established by means of an iterative double auction mechanism. What is lacking in their analysis is the connection to the actual power grid, i.e. vehicles are willing to discharge their batteries for a financial benefit but there is no incentive with regard to reducing peak consumption or the like.

An energy trading scenario between prosumers in a localised community is investigated in [Liu et al., 2017a]. Their focus lies on the formulation of a pricing model for the traded renewable resources as well as a utility function which incorporates the inconvenience caused by shifting appliances to enable the trading. Note that trading is performed through an aggregator which facilitates the process in return for a fee. Interestingly, the approach is shown to work in a day-ahead manner as well as a hour-ahead fashion; both achieving better results than a feed-in tariff which is used here as a reference.

[Liu et al., 2017b] present a system for energy trading between prosumers with a focus on the microgrid operator, i.e. an aggregator responsible for setting the selling and buying prices as well as the connection to the powergrid. Within their model, the aggregator is the leader in a Stackelberg game, while the prosumers are the followers who decide on how much energy to sell / buy. Eventually the situation is beneficial for all the participants: The aggregator sets the prices such that a profit is generated. The prosumers are better off than with a feed-in-tariff scheme. There are less line losses due to the preferential consumption inside the microgrid.

The authors of [Liu et al., 2017c] argue that uncontrolled charging of electric vehicles (at a large scale) will have a considerable negative impact on the peak-to-average ratio of the total load on the system. This is why they propose a day-ahead scheduling mechanism based on a non-cooperative game that can help to alleviate the pressure of the grid. In their simulations they make use of real driving data to model the usage and availability of the mobile batteries. As a result they are able to achieve a PAR reduction of 15%.

[Long et al., 2017] claim to assess the feasibility of peer-to-peer trading in multi-microgrid power networks but actually they answer the question of how much distributed generation capacity is needed to minimise the difference between supply and demand. In their approach they use a clustering method to obtain a deeper insight into the consumption patterns of the users.

[Longe et al., 2017] describe a battery and appliance scheduling scenario in which every individual household optimises their energy loads. The convex optimisation is performed on the smart meter and has the objective to minimise the costs while also minimising the dissatisfaction from shifting appliances. Since the pricing function assumes a fixed tariff for different periods of the upcoming day, it is surprising to see that no synchronisation is observed between the households, i.e. the mechanism does not create new peaks during times of low prices. Eventually a PAR reduction of $\approx 42\%$ is achieved for simulations with 100 flats.

[Ma et al., 2017a] develop a demand-side energy management solution for households based on non-convex optimisation. The model includes both the costs for generation as well as the 'discomfort' costs. They go into great detail of the algorithm that solves the specific optimisation problem. Then they apply their method to the management of heating, ventilation, and air conditioning systems. Simulations show that a tradeoff factor of 0.6 results in the lowest total costs for the customer.

In [Ma et al., 2017b], the authors develop a model for a microgrid in which the microgrid operator has a renewable energy resource (wind) and determines the unit price of electricity for all the households. They formulate a Stackelberg game with the operator as the leader and the households as the followers who can adjust their consumption given the pricing signal. This game is thoroughly solved by means of backwards induction including the uncertainty of the wind energy availability. The title of [Ma et al., 2017b] suggest a energy trading scenario but this is not the case.

[Opadokin et al., 2017] investigate an energy trading scenario between households in a microgrid. There are three types of households: those with solar photovoltaic units, those with solar and battery storage, and those which have neither of the two. This is being used to determine whether it will be classified as a seller or as a buyer but neither the renewable energy generation nor the battery are explicitly modelled. A Stackelberg game is employed with the sellers as leaders and the buyers as followers. The main contribution of the paper is the development of a prioritisation concept that declares in which order the households are being served.

[Park et al., 2017b] develop a scheme that can be seen as an extension to the model proposed in [Mohsenian-Rad and Leon-Garcia, 2010] as it additionally includes the users' satisfaction. Nevertheless, here again, the optimisation is performed only for one individual household. The question regarding load synchronisation, assuming the scheme would be applied to several customers, is not addressed. They rather show how the results behave when changing the weighing factor that puts emphasis on either costs or comfort. The ideas in this paper are further extended in the authors' next publication [Park et al., 2017a] where they develop two appliance scheduling approaches for residential demand-side management: a semi-automated and a fully-automated one. Furthermore, they introduce three types of appliances to make the model more expressive. The potential synchronisation problem remains.

An event-driven scheme is proposed in [Park et al., 2017c]. This means, instead of dividing the upcoming day into fixed time intervals, the scheme is triggered whenever one of the consumers in the system is in need of electricity. The procedure is modelled with a Stackelberg game that is facilitated by the aggregator / operator of the system. The leader, i.e. the requesting consumer, offers a reward for the amount of energy that they seek. The followers then have to decide how much electricity they choose to provide and are rewarded accordingly. A closed-form solution of the Stackelberg equilibrium is derived and rigorous simulations verify the stability of the system.

[Wang et al., 2017a] combine blockchain technology with a double auction mechanism to study direct electricity transactions between households in a microgrid. The process is divided in three parts: verification of identity, opening of the market, and closing of the market. For the first step a trusted third party, e.g. the government, is needed. Once the market is open, participants can submit their bids and quotes and according to the double auction, sellers and buyers are matched. During the settlement, the seller transfers a digital certificate to the consumer, who in turn transfers their payment. All of this can be done through the blockchain.

[Wang et al., 2017b] investigate a scheduling approach based on multi-objective optimisation which can deal with uncertainties in renewable energy generation and demand. It is scheduling both load shifting as well as the energy generation by minimising the operational costs and minimising the CO_2 emissions. In their simulations they achieve a emission reduction of $\approx 15\%$.

[Apostolopoulos et al., 2018] model a system with multiple utility companies and multiple consumers. Similar to many other studies they make use of a two-stage game approach, i.e. a Stackelberg game. What is special about their approach is the fact that the roles seem to be reversed. The customers are the leaders who first decide on their optimal electricity consumption by declaring how much they want to consume from each provider. In the second stage, the utility companies determine the optimal pricing.

In [Bahrami and Amini, 2018], the authors investigate a scheduling scenario in which an independent system operator sends control signals that give incentives to load aggregators and generators in the grid. Based on this the generators will schedule their power output for the upcoming day and make a choice about how to split it between conventional and renewable generation. One of their aims is to minimise the risk that is associated with the uncertainty of the renewable generation. The load aggregators determine their power profiles based on the control signal such that they minimise the total costs including the cost for discomfort. Various IEEE bus systems are used during testing to show quick convergence of the algorithm and benefits for all the participants.

[Celik et al., 2018] study an energy management system for a microgrid which includes prosumer households and a microgrid operator. All the communication is performed solely with the operator to avoid privacy concerns. In the system, the households schedule their appliances and local storage facilities based on a pricing signal from the aggregator. Throughout the manuscript the authors talk about group-based and turn-based coordinated optimisation models when describing the solution algorithm. One could argue that they actually designed a non-cooperative game and employ a best-response-type algorithm to solve it. Eventually they achieve average peak reduction over the course of a full-year simulation of $\approx 12\%$.

An energy trading scheme is presented in [Cui et al., 2018]. Similar to [Liu et al., 2017b], the architecture comprises of multiple prosumers and a microgrid operator. For the time of decision, the prosumers are split into buyers and sellers who have to determine the amount of electricity they want to procure and give away, respectively. They act as the followers in a two-stage Stackelberg game. Thus their decision depends on the pricing decision of the Stackelberg leader, i.e. the microgrid operator. As seen in [Celik et al., 2018], all the communication between the trading participants is done through the operator.

[Gaba and Chanana, 2018] develop a demand-side management approach that relies on interacting households to schedule their appliances according to a real-time pricing system. The costs per electricity unit are determined by the aggregated consumption of all participants. This results in a system that tries to flatten the load curve. In their simulation runs with 10 residential users, they achieve a PAR reduction of $\approx 61\%$. This seems to be much better than any of the previous approaches. A closer look reveals that the higher reduction stems from a higher reference PAR value of almost 3.0. The absolute PAR value after the scheduling is 1.15 which is comparable to what is for instance shown in [Soliman and Leon-Garcia, 2014, Longe et al., 2017].

[Horta et al., 2018] introduce an approach that aims to increase the amount of distributed renewable energy resources by locally balancing them with flexible consumption. Their system involves an auction mechanism that is implemented on a blockchain-based platform. In order to show its viability, they assess the impact of exchanging electricity between households on the power quality.

[Liu et al., 2018a] study an energy sharing scenario with multiple prosumers and a shared battery which is operated by a central operator, i.e. the organiser of the scheme. There are two modes of sharing: Direct sharing and buffered sharing. The scheme consists of two parts. Firstly, a day-ahead optimisation of the battery schedule based on uncertain data for load, generation and prices of the market is performed. Secondly, a real-time optimisation based on a Stackelberg game in which the leader (organiser) sets prices and the followers (prosumers) decide about their consumption. Results are shown for a small number of industrial prosumers with large scale PV installations. It becomes clear that the outcome highly depends on the operator.

[Liu and Hsu, 2018] present two optimisation approaches for scheduling household appliances of prosumers under uncertainty from their individually owned renewable energy resource. One of the approaches strictly delivers the optimal schedules, while the other is a heuristic approach. They show that the latter one can generate comparable results in terms of cost and PAR reduction and is much more scalable. In fact, with respect to the absolute PAR values in scenarios without uncertainty, they achieve the best results of any study today. For instance, for 30 participating customers, the reported PAR value are <1.0001 and <1.0090 for the strict and heuristic approach, respectively.

In [Liu et al., 2018b], an energy management system for connected and cooperative microgrids is presented. The system is overseen by a local operator which establishes an energy exchange platform and tries to centrally optimise the operations of the participants. In their model, microgrids are equipped with renewable energy resources and energy storage facilities. The objective is to minimise the overall losses in the system by sharing electricity locally, thus improving the energy efficiency. A non-convex optimisation method is employed to schedule the power flows in the day-ahead market. Simulations with various different network architectures show the importance of the position inside the network structure and suggest that it has an effect on different roles of the participants, e.g. a microgrid closer to the root of the distribution network tends to act as a energy provider.

[Liu et al., 2018d] implement a non-cooperative and a cooperative approach for scheduling battery energy storage in a multi-microgrid scenario. The overall system is similar to earlier studies on battery management for connected households (cf. [Celik et al., 2017]) with the difference of a larger scale for battery capacities, loads, and renewable energy generation. In their non-cooperative approach the microgrids act selfishly as players of a non-cooperative game (minimising their individual costs), whereas in the cooperative approach they are directed by a control center performing a convex optimisation (minimising the sum of all individual costs). Eventually it is shown that both approaches achieve similar results.

[Liu et al., 2018c] introduce a Bayesian game approach to schedule energy consumption in multiple interconnected communities with electric vehicles. In contrast to a non-cooperative as used by many other studies, in a Bayesian game not all information about utility functions and actions is required to be known to all players (cf. Section 2.2). Here, the authors describe a system in which each community has different service charges connected to selling back energy to the grid. This information is unknown to the other communities, thus when they schedule their trading activities for the upcoming day they have incomplete information. Eventually they report PAR reductions of ≈ 44% with only slight differences between simulations for different type combinations. Interestingly, the participation of EVs as storage only account for ≈ 5% of the observed PAR reduction.

A energy trading scenario for prosumers in a community is developed in [Long et al., 2018b]. It is organised by an energy sharing coordinator who optimises the operations within the microgrid such that the costs for each participant are minimised. To do so, a two-stage approach is implemented. It is based on a sliding window framework which calculates the optimal behaviour for the next 24 hours. These calculations are performed every 30 minutes. Their results show that local trading increases the self-consumption when compared to a scenario in which only selling back to the grid is possible.

[Long et al., 2018a] consider a network of prosumers and consumers who own individual batteries. The batteries are used to share energy among all of the households and are controlled by an aggregator. The paper does not include a section detailing how the system operator optimises the operations. It seems as if all variables such as solar generation, battery storage and demand are treated in an aggregated way resulting in rule-based charging and discharging instructions. Simulation results with one minute resolution show that the introduction of energy storage increases the self-consumption by up to ≈ 37%.

[Lüth et al., 2018] are the first who focus on the effects of battery storage in a true peer-to-peer energy trading scenario. They investigate two scenarios: One in which the batteries are owned by individual prosumers of the community, and one which incorporates a single community battery to be used by all the participants. Nevertheless, both approaches are solved by a centralised optimisation with the objective to minimise the consumption from external resources. Simulations with four households show that the highest savings on the electricity bill can be achieved with P2P trading and individually owned batteries. When looking at the individual contributions to this cost reduction it can be observed that both storage and trading account for approximately half of it.

[Mediwaththe et al., 2018] consider three energy trading systems among prosumers based on community energy storage. The first one is modelled as a fully competitive Stackelberg game in which the operator of the community battery is the leader and the prosumers are the followers. The second approach is similar to the first one with the addition of regulations the leader has to abide to that are favourable for the prosumers. The third approach discusses a centralised approach which optimises the overall costs for the system. As expected, when the households give away the control of how to interact in the system, i.e. the centralised optimisation, overall PAR reductions are better. The first approach and third approach achieve $\approx 33\%$ and $\approx 40\%$, respectively.

In [Nguyen et al., 2018a], the authors develop an optimisation model for electricity trading in communities where households are equipped with rooftop solar generation and battery storage systems. In their analysis they differentiate between individual days of the week. On a week day, savings with trading reach up to 17% for households with solar panels and without battery. In contrast to this, the highest savings on a weekend only reach 1.8% (for households with battery and without solar). Furthermore, they perform sensitivity analyses to obtain insight into how solar panel size and battery size influence the outcome. Based on their exemplary data they find that households who have only a battery are overall worse off than those which do not investing in neither solar nor storage.

[Prudhviraj et al., 2018] present the optimisation of a microgrid for the day-ahead when equipped with battery energy storage, controllable loads, solar photovoltaics, and diesel generators. They are the only reference that includes a fossil fuel based generator in their model. Other than this, the conference paper does not provide a considerable contribution but rather confirms what was shown beforehand, i.e. energy storage can lead to cost reductions.

[Rahbar et al., 2018] model two microgrids that cooperate with one another. This means they are willing to share energy and to have their operations being controlled by an external operator. One of their key findings is that the ability to share energy decreases the need for energy storage to obtain the same cost savings. Lastly, they present an option for how their methodology can be extended for more than two microgrids: split the overall population into groups of two and perform the respective optimisations.

[Tushar et al., 2018a] study the operations of a microgrid that comprises of prosumer households equipped with solar photovoltaic panels, individual battery storage, and electric vehicles. The scheme has two stages. In the first stage, the households play a non-cooperative game in which they decide on their charging and discharging schedules for the upcoming day based on predictions for renewable generation and their demand with the goal to flatten the load curve. The microgrid operator procures electricity according to the resulting Nash equilibrium for the upcoming day. During the day is the second stage. Deviations between predicted consumption and the actual values is treated with penalties from the microgrid operator. Thus the households repeatedly play another game in which they aim to minimise this difference.

There is no interaction between the participants of the scheme presented in [Sharma et al., 2018]. They have a renewable energy resource and a battery storage system installed. Furthermore they have the ability to sell energy back to the grid from their storage devices. In order to minimise the costs for the user, they implemented a optimisation routine that finds the best charging and discharging strategy for a given time slot based on all the future data and the current state of the battery. This optimisation is repeated for each interval of the upcoming day, while keeping the horizon fixed, that is at the end of the day. Scenarios with different scales, i.e. household, medium commercial site, industrial consumer, are performed and show cost reductions. Load synchronisation effects are not discussed.

[Zhou et al., 2018a] develop a model that includes three stages. In the first stage, households play a non-cooperative game to decide how they want to charge and discharge their electric vehicle, which is purely used as a storage device, for a single time interval. The utility function is designed such that they gain satisfaction from charging an empty and from discharging a full battery. This is done in multiple microgrids separately. The Nash equilibria then inform the microgrid operators about the load within their respective networks. What follows is a multileader-multifollower Stackelberg game between those microgrids that have a surplus of electricity (leaders) and those that are in need (followers). Their simulations result in a decreased peak-to-average ratio of the aggregated load within a microgrid. The results are surprising as the model does not include a temporal component and it is unclear how this coordination can be established.

In order to evaluate different peer-to-peer energy trading models, [Zhou et al., 2018b] implement a multiagent-based simulation framework which includes prosumers and an energy sharing coordinator. They identify two types of evaluation criteria for a meaningful comparison between different trading schemes: those which are connected to economics and those that express the technical performance. Since load profiles in a trading scenario include both positive and negative values, they introduce a novel index called the power flatness index which extends the notion of the usually used PAR value.

[Alam et al., 2019] introduces a true peer-to-peer energy trading system. That means there is no aggregator but rather only prosumer households that directly exchange electricity with each other. Nevertheless, the approach is organised by a central entity which optimises the operations without allowing for individual choices of the users. In order to determine the trading strategies for the upcoming day, they employ a linear programming model which is solved by a heuristic algorithm. The model strives for a Pareto optimal solution which guarantees a notion of fairness.

Their simulation results show that even though the solution is only approximated, it gives the optimal outcome in 99% of the cases. Interestingly, they observe that in the most beneficial scenario there are 50% of the households equipped with solar panels and 100% have their individual electricity storage.

[Chouikhi et al., 2019] present a three-level architecture which has similarities with the one shown in [Zhou et al., 2018a]. In contrast to households that make up a microgrid, here they look at apartments in a larger building. The households play a non-cooperative game to schedule their appliances for the upcoming day. On the higher level, the building operators interact with several utility companies in a multileader-multifollower Stackelberg game. The leaders (UCs) decide about the electricity pricing, while the followers react by deciding about where to procure the electricity from. Eventually PAR reductions of $\approx 33\%$ are reported.

[Cui et al., 2019] present a energy trading system consisting of several stages. The scheme is designed to start with a centralised optimisation to minimise the overall costs of the system by scheduling appliances, energy storage, and trading activities. As the clearing costs cancel each other in this aggregated step, the second step consists of a non-cooperative game which takes care of the actual clearing process. Both of these stages consider the day ahead. During the day, the authors propose real-time optimisations (one per time slot) to account for the uncertainties in demand and renewable energy generation. Simulation runs with four and ten buildings display convergence of the approach.

[Fanti et al., 2019] investigate an appliance scheduling scenario. Given pricing information for the upcoming day and limits for maximal consumption during specific intervals, the usage of appliances is shifted by a linear optimisation algorithm. To show the feasibility of their approach, the authors simulate five buildings with up to two appliances for the upcoming day divided into five intervals. This is not sufficient to obtain a good understanding of the potential of the strategy. Even when considering a small scale scenario, the computational times seem to be long.

A robust optimisation algorithm is developed in [Hosseini et al., 2019]. They investigate a system in which a household reacts to a day-ahead pricing signal. The home energy management system has the objective to minimise the costs by scheduling appliances and home energy storage while also considering their own renewable energy resource. Within the optimisation problem, a parameter is included that takes values from zero (no uncertainty) to one (maximum uncertainty). Thus the operator has the ability to take different levels of risk-aversion into account. The simulation results for their data reveals maximum cost reduction for a value of 0.4.

[Mediwaththe et al., 2019] design a Stackelberg game in which the operator of a shared energy storage installation acts as the leader and an energy retailer who coordinates the transactions between the grid and both the households and the storage operator acts as the follower. The households do not have a active role in the game. Nevertheless, it is them to charge the battery with their renewable energy generation. In the first stage, the storage provider schedules electricity trading activities with the grid for the upcoming day. Based on this decision, the energy retailer declares how much energy the households are trading with the grid on their behalf. Numerical simulations show reduction of PAR values of up to ≈ 45%.

Initially, another Stackelberg approach is developed in [Sivanantham and Gopalakrishnan, 2019]. It is played between a utility company (as the leader) and multiple households as followers. While the energy provider decides about the pricing for the upcoming day, the households react to this signal by scheduling their appliances. As this would lead to the appearance of new peaks in the aggregated load profile, the authors eventually adapt a real-time pricing strategy, thus reverting to a common optimisation problem for the households. Similar to [Fanti et al., 2019], simulations are performed for only three customers. In this scenario, peak reductions of 33% are observed.

[Zepter et al., 2019] develop a two-stage stochastic system in which a central entity optimises the operations of a prosumer community. In the first stage, the usage of batteries, trading among households, and selling electric energy back to the grid is optimised for the day ahead given uncertainties in the renewable production. The second stage is performed during the day and depends on the deviations between scheduled and actual loads. Thus peer-to-peer trading, battery usage and buying from the grid is adapted. To do all this, they employ a stochastic optimisation approach. This means, for a given day, multiple predictions for the renewable generation are created with equal probability. The optimisation then minimises the weighted sum of these scenarios. Eventually they show that both trading and storage contribute equally to a 60% cost reduction.

This almost blank page is intentional.

Appendix C

Curriculum Vitae

Education

2016 – present **Doctor of Philosophy**, *Computer Science and Mathematics*.
Kingston University London
supported by a University Alliance studentship (Doctoral Training Alliance Energy)
project title: *Game–Theoretic Approaches for Smart Prosumer Communitites*

2012 – 2015 **Master of Science**, *Theoretical Physics*.
University of Jena, Umeå University, *(1.1 - sehr gut; equivalent to UK first-class honours)*
spent one year in Sweden, supported by an Erasmus scholarship
thesis title: *A New ADER-DG Scheme Based on a Local Continuous Runge-Kutta Method*
(`DOI:10.13140/RG.2.1.3861.3844`)

2009 – 2012 **Bachelor of Science**, *Physics*.
University of Jena, *(1.4 - sehr gut; equivalent to UK first-class honours)*
thesis title: *Numerische Behandlung der Navier-Stokes Gleichungen*

Selected Experience

03'2017 – present **Research Student Representative**, *Kingston University London*.
- representing the opinions and concerns of postgraduate research students from the 'School of Computer Science & Mathematics'
- discussing issues at *Faculty Research Degrees Committee* meetings

10'2018 – 03'2019 **Hourly Paid Lecturer**, *Kingston University London*.
- teaching first year engineering students Excel, Maple, Matlab, as well as applied Mathematics
- marking end-of-term coursework

10'2017 – 04'2018 **Conference Committee Member**, *Kingston University London*.
12'2016 – 04'2017
- organising the 'SEC Conference 2017' and 'SEC Conference 2018'
- special responsibility for the conference booklet, budget and poster session

04'2017 – 03'2018 **Athena SWAN Committee Member**, *Kingston University London*.
- analysing staff and student data for the SEC faculty to understand gender equality issues
- the Athena SWAN bronze award was bestowed upon the SEC faculty in 01'2019

Selected Communications

05'2019 Talk at the *Three Minute Thesis competition* in Kingston upon Thames, UK
"Game-Theoretic Approaches for Smart Prosumer Communities"
awarded with the first prize - [online] `https://bit.ly/31QonoY`

10'2018 Talk at the *IEEE ISGT Europe 2018* in Sarajevo, BIH
"A Practical Approach to Energy Scheduling: A Game Worth Playing?"
[online] `DOI:10.13140/RG.2.2.31082.16320`

03'2018 Poster presentation at *STEM for BRITAIN 2018* (final round) London, UK
"A Smart Game For Energy Management" - [online] `DOI:10.13140/RG.2.2.13418.82883`

07'2017 Talk at the *IRCSEEME 2017* in Newcastle upon Tyne, UK
"Game–Theoretic Analysis of an Advanced Battery Model for Energy Storage Scheduling"
awarded with best paper award - [online] `DOI:10.13140/RG.2.2.20159.82081`

07'2016 Talk at *DIRC Seminar* in Kingston upon Thames, UK
"Artificial Neural Networks - Basics and Applications in Energy Related Problems"

02'2016 Talk at *Winter School of Theoretical Physics 2016* in Lądek Zdrój, PL
"Introduction to Artificial Intelligence Techniques for Data Analysis"
awarded for best short speech - [online] `DOI:10.13140/RG.2.1.4137.9607`

02'2015 Poster presentation at *Winter School of Theoretical Physics 2015* in Lądek Zdrój, PL
"ADER-WENO Scheme for Hyperbolic Conservation Laws"
awarded for best poster - [online] `DOI:10.13140/RG.2.1.3400.2008`

Selected Extracurricular Activities

SPARK! contest ***runner up*** and ***spirit of SPARK!*** prize in the contest 2018-2019
developed a compelling business case for an EV charging platform

HackXLR8 participated at the TechXLR8 Hackathon in London (06'2019)
explored maintaining user's privacy while training ML models with federated learning

ProjectHack3.0 ***first prize*** at the ProjectHack3.0 in London (06'2019) - [online] `https://bit.ly/2G1IAin`
developed an image-classifier for construction site pictures based on a deep-learning approach

Kerbspace Hack ***second prize*** at the Ford Hack in London (11'2019) - [online] `https://bit.ly/2vBJ1xP`
developed a secure-parking prototype based on the Ford Kerbspace API

HackLBS ***TechLBS prize*** HackLBS in London (02'2020) - [online] `https://bit.ly/3a6Iseh`
developed an educational app which identifies animal species from camera input and provides information about them

MOOCs **Blockchain Solution Architecture**, course by the Blockchain Training Alliance
finished course with 90% - [online] `https://bit.ly/2xeW2L2`
Deep Learning, a five-course specialisation on Coursera
finished course with 100% - [online] `https://bit.ly/31W6jdk`
Blockchain Foundation for Developers, course by IBM
finished course with 100% - [online] `https://bit.ly/2KEMvFR`

CPE **Cambridge English Proficiency**, highest-level qualification from Cambridge Assessment

climbing enthusiastic hobby boulderer and lead-climber, current level: **V4**, **6b+**

rope skipping member of the 'Universe Skippers' jump rope club since 09'2013
>20 show performances all around Thuringia - [online] `https://bit.ly/2X3IvFi`

Bibliography

[Adika and Wang, 2014] Adika, C. O. and Wang, L. (2014). Smart Charging and Appliance Scheduling Approaches to Demand Side Management. *International Journal of Electrical Power and Energy Systems*, 57:232–240.

[Alam et al., 2017] Alam, M. R., St-Hilaire, M., and Kunz, T. (2017). An Optimal P2P Energy Trading Model for Smart Homes in the Smart Grid. *Energy Efficiency*, 10(6):1475–1493.

[Alam et al., 2019] Alam, M. R., St-Hilaire, M., and Kunz, T. (2019). Peer-to-Peer Energy Trading Among Smart Homes. *Applied Energy*, 238.

[Alpcan and Basar, 2010] Alpcan, T. and Basar, T. (2010). *Network Security: A Decision and Game-Theoretic Approach*. Cambridge University Press, 1 edition.

[Apostolopoulos et al., 2018] Apostolopoulos, P. A., Tsiropoulou, E. E., and Papavassiliou, S. (2018). Demand Response Management in Smart Grid Networks: a Two-Stage Game-Theoretic Learning-Based Approach. *Mobile Networks and Applications*.

[Atzeni et al., 2013] Atzeni, I., Ordóñez, L. G., Scutari, G., Palomar, D. P., and Fonollosa, J. R. (2013). Noncooperative and Cooperative Optimization of Distributed Energy Generation and Storage in the Demand-Side of the Smart Grid. *IEEE Transactions on Signal Processing*, 61(10):2454–2472.

[Aumann, 1985] Aumann, R. (1985). What is Game Theory Trying to Accomplish. In Arrow, K. and Honkapohja, S., editors, *Frontiers of Economics*, pages 909–924.

[Aumann and Brandenburger, 1995] Aumann, R. and Brandenburger, A. (1995). Epistemic Conditions for Nash Equilibrium. *Econometrica*, 63(5):1161–1180.

[Ausgrid, 2019] Ausgrid (2019). Solar Home Electricity Data 2010-2013. https://bit.ly/2qg0Qe1. accessed: 2019-03-14.

[Avis et al., 2009] Avis, D., Rosenberg, G. D., Savani, R., and von Stengel, B. (2009). Enumeration of Nash Equilibria for Two-Player Games. *Economic Theory*, 42(1):9–37.

[Bae et al., 2017] Bae, S., Ryu, S., and Kim, H. (2017). Coalition–Based Bidding Strategies for Integrating Renewable Energy Sources in Electricity Market. *IEEE Power and Energy Society General Meeting*.

[Bahn et al., 2009] Bahn, O., Haurie, A., and Malhamé, R. P. (2009). A Stochastic Control/Game Approach to the Optimal Timing of Climate Policies. In *Uncertainty and Environmental Decision Making*, chapter 7, pages 211–237.

[Bahrami and Amini, 2018] Bahrami, S. and Amini, M. H. (2018). A Decentralized Trading Algorithm for an Electricity Market with Generation Uncertainty. *Applied Energy*, 218:520–532.

[Bahrami and Sheikhi, 2016] Bahrami, S. and Sheikhi, A. (2016). From Demand Response in Smart Grid Toward Integrated Demand Response in Smart Energy Hub. *IEEE Transactions on Smart Grid*, 7(2):650–658.

[Bao et al., 2017] Bao, T., Shoshitaishvili, Y., Wang, R., Kruegel, C., Vigna, G., and Brumley, D. (2017). How Shall We Play a Game?: A Game-Theoretical Model for Cyber-Warfare Games. *IEEE Computer Security Foundations Symposium*, pages 7–21.

[Batalla et al., 2017] Batalla, J. M., Vasilakos, A. V., and Gajewski, M. (2017). Secure Smart Homes: Opportunities and Challenges. *ACM Computing Surveys*, 50.

[Bayram et al., 2014] Bayram, I. S., Shakir, M. Z., Abdallah, M., and Qaraqe, K. (2014). A Survey on Energy Trading in Smart Grid. *IEEE Global Conference on Signal and Information Processing*, pages 258–262.

[Bichpuriya et al., 2016] Bichpuriya, Y. K., Soman, S. A., and Subramanyam, A. (2016). Combining Forecasts in Short Term Load Forecasting: Empirical Analysis and Identification of Robust Forecaster. *Sadhana*, 41(10):1123–1133.

[Bistarelli et al., 2017] Bistarelli, S., Mugnai, D., and Giuliodori, P. (2017). A Fair Payment Scheme for Virtuous Community Energy Usage. *International Symposium on Artificial Intelligence and Mathematics*.

[Boomsma et al., 2018] Boomsma, C., Hafner, R., Pahl, S., Jones, R. V., and Fuertes, A. (2018). Should We Play Games Where Energy Is Concerned? Perceptions of

Serious Gaming as a Technology to Motivate Energy Behaviour Change among Social Housing Residents. *MDPI sustainability*, 10.

[Boudko and Abie, 2018] Boudko, S. and Abie, H. (2018). An Evolutionary Game for Integrity Attacks and Defences for Advanced Metering Infrastructure. *ACM International Conference Proceeding Series*.

[British Columbia Utilities Commission, 2017] British Columbia Utilities Commission (2017). Report to the Government of British Columbia on the Impact of BC Hydro and FortisBC's Residential Inclining Block Rates. Technical report.

[Brousmiche et al., 2018] Brousmiche, K.-L., Anoaica, A., Dib, O., Abdellatif, T., and Deleuze, G. (2018). Blockchain Energy Market Place Evaluation: An Agent-Based Approach. *IEEE Annual Information Technology, Electronics and Mobile Communication Conference*.

[Buterin et al., 2015] Buterin, V., Wood, G., and Lubin, J. (2015). Ethereum. `https://bit.ly/1sG87iJ`. accessed: 2019-09-17.

[Celik et al., 2018] Celik, B., Roche, R., Bouquain, D., and Miraoui, A. (2018). Decentralized Neighborhood Energy Management With Coordinated Smart Home Energy Sharing. *IEEE Transactions on Smart Grid*, 9(6):6387–6397.

[Celik et al., 2017] Celik, B., Roche, R., Bouquain, D., Miraoui, A., and System, A. P. (2017). Coordinated Neighborhood Energy Sharing Using Game Theory and Multi-Agent Systems. *PowerTech*.

[Chai et al., 2014] Chai, B., Chen, J., Yang, Z., and Zhang, Y. (2014). Demand Response Management with Multiple Utility Companies: A Two-Level Game Approach. *IEEE Transactions on Smart Grid*, 5(2):722–731.

[Chen et al., 2017] Chen, H., Ngan, H., and Zhang, Y. (2017). *Power System Optimization: Large-Scale Complex System Approaches*.

[Chouikhi et al., 2019] Chouikhi, S., Merghem-Boulahia, L., Esseghir, M., and Snoussi, H. (2019). A Game-Theoretic Multi-Level Energy Demand Management for Smart Buildings. *IEEE Transactions on Smart Grid*.

[Clarivate, 2019] Clarivate (2019). Web of Science. `https://bit.ly/2kT2moU`. accessed: 2019-09-19.

[Cournot, 1838] Cournot, A. (1838). *Researches Into the Mathematical Priciples of the Theory of Wealth*.

[Croce et al., 2017] Croce, D., Giuliano, F., Tinnirello, I., Galatioto, A., Bonomolo, M., Beccali, M., and Zizzo, G. (2017). Overgrid: A Fully Distributed Demand Response Architecture Based on Overlay Networks. *IEEE Transactions on Automation Science and Engineering*, 14(2):471–481.

[Cui et al., 2018] Cui, S., Wang, Y.-W., and Liu, N. (2018). Distributed Game-Based Pricing Strategy for Energy Sharing in Microgrid with PV Prosumers. *IET Renewable Power Generation*, 12(3):380–388.

[Cui et al., 2019] Cui, S., Wang, Y.-W., and Xiao, J.-W. (2019). Peer-to-Peer Energy Sharing Among Smart Energy Buildings by Distributed Transaction. *IEEE Transactions on Smart Grid*.

[Deng et al., 2015] Deng, R., Yang, Z., Hou, F., Chow, M.-Y., and Chen, J. (2015). Distributed Real-Time Demand Response in Multiseller–Multibuyer Smart Distribution Grid. *IEEE Transactions on Power Systems*, 30(5):2364–2374.

[Diestelmeier, 2019] Diestelmeier, L. (2019). Changing Power: Shifting the Role of Electricity Consumers with Blockchain Technology – Policy Implications for EU Electricity Law. *Energy Policy*, 128:189–196.

[Dolara et al., 2015] Dolara, A., Leva, S., and Manzolini, G. (2015). Comparison of Different Physical Models for PV Power Output Prediction. *Solar Energy*, 119:83–99.

[Dr. Deng, 2015] Dr. Deng (2015). On Biostatistics and Clinical Trials. https://bit.ly/2lTnz20. accessed: 2019-09-13.

[EDF, 2019] EDF (2019). About EDF Renewables. https://bit.ly/2mfYPkW. accessed: 2019-04-09.

[Elsevier, 2019] Elsevier (2019). Mendeley. https://bit.ly/2CEO15T. accessed: 2019-09-19.

[European Commission, 2016] European Commission (2016). Paris Agreement 2015. https://bit.ly/2mhoFQi. accessed: 2017-02-06.

[Eurostat, 2019] Eurostat (2019). Energy Consumption in Households. https://bit.ly/2lNLgJi. accessed: 2019-09-13.

[EWE, 2019] EWE (2019). Pioneering Sustainable Energy Production. https://bit.ly/2mb4ZTb. accessed: 2019-04-09.

[Fadlullah et al., 2011] Fadlullah, Z. M., Nozaki, Y., Takeuchi, A., Kate, N., and Kato, N. (2011). A Survey on Game Theoretic Approaches in Smart Grid. In *IEEE International Conference on Wireless Communications and Signal Processing*, page 1.

[Fadlullah et al., 2014] Fadlullah, Z. M., Quan, D. M., Kato, N., and Stojmenovic, I. (2014). GTES: An Optimized Game-Theoretic Demand-Side Management Scheme for Smart Grid. *IEEE Systems Journal*, 8(2):588–597.

[Fanti et al., 2019] Fanti, M. P., Mangini, A. M., Pedroncelli, G., and Roccotelli, M. (2019). Cooperative Distributed Energy Scheduling of Smart Homes Appliances in a Smart District. *European Control Conference*, pages 3496–3501.

[Farraj et al., 2016] Farraj, A., Hammad, E., Daoud, A. A., and Kundur, D. (2016). A Game-Theoretic Analysis of Cyber Switching Attacks and Mitigation in Smart Grid Systems. *IEEE Transactions on Smart Grid*, 7(4):1846–1855.

[Gaba and Chanana, 2018] Gaba, M. and Chanana, S. (2018). Analysis of Distributed Energy Management Scheme for Residential Consumers Using Non-Cooperative Game. *Power India International Conference*, pages 1–6.

[Gallo et al., 2016] Gallo, A. B., Simões-Moreira, J. R., Costa, H. K. M., Santos, M. M., and Moutinho dos Santos, E. (2016). Energy Storage in the Energy Transition Context: A Technology Review. *Renewable and Sustainable Energy Reviews*, 65:800–822.

[Ghosh et al., 2018] Ghosh, A., Aggarwal, V., and Wan, H. (2018). Exchange of Renewable Energy among Prosumers using Blockchain with Dynamic Pricing. *arxiv preprint*.

[Goldberg, 1987] Goldberg, S. (1987). Some Very Deep Mathematical Problems That Anyone Can Understand. *Journal of Recreational Mathematics*, 19(2):119–125.

[Google, 2019] Google (2019). Google Scholar. https://bit.ly/1DmcnaO. accessed: 2019-09-19.

[Goulden et al., 2014] Goulden, M., Bedwell, B., Rennick-Egglestone, S., Rodden, T., and Spence, A. (2014). Smart Grids, Smart Users? The Role of the User in Demand Side Management. *Energy Research and Social Science*, 2:21–29.

[Gupta and Yadav, 2017] Gupta, A. and Yadav, A. (2017). Challenges in Demand Side Management in Smart Power Grid: A Review. *International Journal of Engineering, Science and Mathematics*, 6(8):120–125.

[Hahn et al., 2017] Hahn, A., Singh, R., Liu, C. C., and Chen, S. (2017). Smart Contract-Based Campus Demonstration of Decentralized Transactive Energy Auctions. *IEEE Power and Energy Society Innovative Smart Grid Technologies Conference*.

[Haider et al., 2016a] Haider, H. T., See, O. H., and Elmenreich, W. (2016a). Dynamic Residential Load Scheduling Based on Adaptive Consumption Level Pricing Scheme. *Electric Power Systems Research*, 133:27–35.

[Haider et al., 2016b] Haider, H. T., See, O. H., and Elmenreich, W. (2016b). Residential Demand Response Scheme Based on Adaptive Consumption Level Pricing. *Energy*, 113:301–308.

[Hammerstein, 1998] Hammerstein, P. (1998). What is Evolutionary Game Theory? In Dugatkin, L. A. and Reeve, H. K., editors, *Game Theory & Animal Behavior*, chapter 1. Oxford University Press.

[Harsanyi, 1967] Harsanyi, J. C. (1967). Games with Incomplete Information Played by "Bayesian" Players, I-III Part I. The Basic Model. *Management Science*.

[Harsanyi, 1968a] Harsanyi, J. C. (1968a). Games with Incomplete Information Played by " Bayesian " Players , I-III . Part II. Bayesian Equilibrium Points. *Management Science*.

[Harsanyi, 1968b] Harsanyi, J. C. (1968b). Games with Incomplete Information Played by " Bayesian " Players , I-III . Part III. The Basic Probability Distribution of the Game. *Management Science*.

[He and Yan, 2016] He, H. and Yan, J. (2016). Cyber-Physical Attacks and Defences in the Smart Grid: A Survey. *IET Cyber-Physical Systems: Theory & Applications*, 1(1):13–27.

[He and Wei, 2016] He, Y. and Wei, J. (2016). A Game-Theoretic Model for Energy Trading of Privacy-Preserving Microgrid Social Networks. *International Conference on Smart Grid Communications*.

[Horta et al., 2018] Horta, J., Kofman, D., Menga, D., and Silva, A. (2018). Novel Market Approach for Locally Balancing Renewable Energy Production and Flexible Demand. *IEEE International Conference on Smart Grid Communications*, (October):533–539.

[Hosseini et al., 2019] Hosseini, S. M., Carli, R., and Dotoli, M. (2019). Robust Day-Ahead Energy Scheduling of a Smart Residential User under Uncertainty. *European Control Conference*, pages 935–940.

[Huang et al., 2013] Huang, D., Thottan, M., and Feather, F. (2013). Designing Customized Energy Services Based on Disaggregation of Heating Usage. *IEEE PES Innovative Smart Grid Technologies Conference*.

[Huang et al., 2018] Huang, J., Boland, J., Liu, W., Xu, C., and Zang, H. (2018). A Decision-Making Tool for Determination of Storage Capacity in Grid-Connected PV Systems. *Renewable Energy*, 128:299–304.

[Huang et al., 2006] Huang, M., Caines, P. E., and Malhamé, R. P. (2006). Large Population Stochastic Dynamic Games: Closed-Loop McKean-Vlasov Systems and the Nash Certainty Equivalence Principle. *Communications in Information and Systems*, 6(3):221–252.

[Hunziker et al., 2017] Hunziker, C., Schulz, N., and Wache, H. (2017). Shaping Aggregated Load Profiles Based on Optimized Local Scheduling of Home Appliances. *Computer Science - Research and Development*.

[Ilic et al., 2012] Ilic, D., Da Silva, P. G., Karnouskos, S., and Griesemer, M. (2012). An Energy Market for Trading Electricity in Smart Grid Neighbourhoods. *IEEE International Conference on Digital Ecosystems and Technologies*.

[Ipakchi and Albuyeh, 2009] Ipakchi, A. and Albuyeh, F. (2009). Grid of the Future. *IEEE Power and Energy Magazine*, 7(2):52–62.

[Jacquot et al., 2017] Jacquot, P., Beaude, O., Gaubert, S., and Oudjane, N. (2017). Demand Side Management in the Smart Grid: an Efficiency and Fairness Tradeoff. *IEEE Innovative Smart Grid Technologies Europe*.

[Jenkins et al., 2015] Jenkins, N., Long, C., and Wu, J. (2015). An Overview of the Smart Grid in Great Britain. *Engineering*, 1(4):413–421.

[Kang et al., 2017] Kang, J., Yu, R., Huang, X., Maharjan, S., Zhang, Y., and Hossain, E. (2017). Enabling Localized Peer-to-Peer Electricity Trading among Plug-in Hybrid Electric Vehicles Using Consortium Blockchains. *IEEE Transactions on Industrial Informatics*, 13(6):3154–3164.

[Khalilpour and Vassallo, 2016] Khalilpour, R. and Vassallo, A. (2016). Planning and Operation Scheduling of PV-Battery Systems: A Novel Methodology. *Renewable and Sustainable Energy Reviews*, 53:194–208.

[Khan et al., 2015] Khan, Z. A., Mahmood, A., Ahmed, S., Razzaq, S., and Nawaz, R. (2015). Optimization Based Individual and Cooperative DSM in Smart Grids: A Review. *Power Generation Systems and Renewable Energy Technologies*, pages 374–379.

[Kim et al., 2013] Kim, B. G., Ren, S., van der Schaar, M., and Lee, J. W. (2013). Bidirectional Energy Trading and Residential Load Scheduling with Electric Vehicles in the Smart Grid. *IEEE Journal on Selected Areas in Communications*, 31(7):1219–1234.

[Kim and Giannakis, 2013] Kim, S.-J. and Giannakis, G. B. (2013). Scalable and Robust Demand Response With Mixed-Integer Constraints. *IEEE Transactions on Smart Grid*, 4(4):2089–2099.

[Kurt et al., 2018] Kurt, M. N., Yilmaz, Y., and Wang, X. (2018). Real-Time Detection of Hybrid and Stealthy Cyber-Attacks in Smart Grid. *IEEE Transactions on Information Forensics and Security*, 14(2):498–513.

[Lampropoulos et al., 2013] Lampropoulos, I., Kling, W. L., Ribeiro, P. F., and Van Den Berg, J. (2013). History of Demand Side Management and Classification of Demand Response Control Schemes. *IEEE Power and Energy Society General Meeting*, pages 1–5.

[Lasry and Lions, 2007] Lasry, J.-M. and Lions, P.-L. (2007). Mean Field Games. *Japanese Journal of Mathematics*, 2:229–260.

[Law et al., 2015] Law, Y. W., Alpcan, T., and Palaniswami, M. (2015). Security Games for Risk Minimization in Automatic Generation Control. *IEEE Transactions on Power Systems*, 30(1):223–232.

[Lee et al., 2015] Lee, J., Guo, J., Choi, J. K., and Zukerman, M. (2015). Distributed Energy Trading in Microgrids: A Game Theoretic Model and Its Equilibrium Analysis. *IEEE Transactions on Industrial Electronics*, 62(6):3524–3533.

[Lee et al., 2014] Lee, W., Xiang, L., Schober, R., and Wong, V. W. (2014). Direct Electricity Trading in Smart Grid: A Coalitional Game Analysis. *IEEE Journal on Selected Areas in Communications*, 32(7):1398–1411.

[Li et al., 2017] Li, C., Xu, Y., Yu, X., Ryan, C., and Huang, T. (2017). Risk-Averse Energy Trading in Multi-Energy Microgrids: A Two-stage Stochastic Game Approach. http://ieeexplore.ieee.org/document/8010361/.

[Li and Danzer, 2014] Li, J. and Danzer, M. A. (2014). Optimal Charge Control Strategies for Stationary Photovoltaic Battery Systems. *Journal of Power Sources*, 258:365–373.

[Li and Dong, 2018] Li, T. Y. and Dong, M. (2018). Real-Time Residential-Side Joint Energy Storage Management and Load Scheduling With Renewable Integration. *IEEE Transactions on Smart Grid*, 9(1):283–298.

[Liang et al., 2017] Liang, G., Zhao, J., Luo, F., Weller, S. R., and Dong, Z. Y. (2017). A Review of False Data Injection Attacks Against Modern Power Systems. *IEEE Transactions on Smart Grid*, 8(4):1630–1638.

[Liu et al., 2018a] Liu, N., Cheng, M., Yu, X., Zhong, J., and Lei, J. (2018a). Energy Sharing Provider for PV Prosumer Clusters: A Hybrid Approach using Stochastic Programming and Stackelberg Game. *IEEE Transactions on Industrial Electronics*, 65(8):6740–6750.

[Liu et al., 2017a] Liu, N., Yu, X., Wang, C., Li, C., Ma, L., and Lei, J. (2017a). An Energy Sharing Model with Price-based Demand Response for Microgrids of Peer-to-Peer Prosumers. *IEEE Transactions on Power Systems*, 32(5):3569–3583.

[Liu et al., 2017b] Liu, N., Yu, X., Wang, C., and Wang, J. (2017b). Energy Sharing Management for Microgrids with PV Prosumers: A Stackelberg Game Approach. *IEEE Transactions on Industrial Informatics*, 13(3).

[Liu and Hsu, 2018] Liu, R. S. and Hsu, Y. F. (2018). A Scalable and Robust Approach to Demand Side Management for Smart Grids with Uncertain Renewable Power Generation and Bi-Directional Energy Trading. *International Journal of Electrical Power and Energy Systems*, 97(June 2017):396–407.

[Liu et al., 2018b] Liu, T., Tan, X., Sun, B., Wu, Y., and Tsang, D. H. (2018b). Energy Management of Cooperative Microgrids: A Distributed Optimization Approach. *International Journal of Electrical Power and Energy Systems*, 96(October 2017):335–346.

[Liu et al., 2018c] Liu, X., Gao, B., Wu, C., and Tang, Y. (2018c). Demand-Side Management With Household Plug-In Electric Vehicles: A Bayesian Game-Theoretic Approach. *IEEE Systems Journal*, 12(3):2894–2904.

[Liu et al., 2018d] Liu, X., Gao, B., Zhu, Z., and Tang, Y. (2018d). Non-Cooperative and Cooperative Optimisation of Battery Energy Storage System for Energy Management in Multi-Microgrid. *IET Generation, Transmission and Distribution*, 12(10):2369–2377.

[Liu et al., 2009] Liu, Y., Ning, P., and Reiter, M. K. (2009). False Data Injection Attacks Against State Estimation in Electric Power Grids. In *Proceedings of the 16th ACM Conference on Computer and Communications Security*, pages 21–32.

[Liu et al., 2019] Liu, Y., Wu, L., and Li, J. (2019). Peer-to-Peer (P2P) Electricity Trading in Distribution Systems of the Future. *The Electricity Journal*.

[Liu et al., 2014] Liu, Y., Yuen, C., Huang, S., Ul Hassan, N., Wang, X., and Xie, S. (2014). Peak-to-Average Ratio Constrained Demand-Side Management With Consumer's Preference in Residential Smart Grid. *IEEE Journal on Selected Topics in Signal Processing*, 8(6):1084–1097.

[Liu et al., 2017c] Liu, Z., Wu, Q., Huang, S., Wang, L., Shahidehpour, M., and Xue, Y. (2017c). Optimal Day-ahead Charging Scheduling of Electric Vehicles through an Aggregative Game Model. *IEEE Transactions on Smart Grid*, 3053:1–1.

[Long et al., 2017] Long, C., Wu, J., Zhang, C., Cheng, M., and Al-Wakeel, A. (2017). Feasibility of Peer-to-Peer Energy Trading in Low Voltage Electrical Distribution Networks. *Energy Procedia*, 105:2227–2232.

[Long et al., 2018a] Long, C., Wu, J., Zhou, Y., and Jenkins, N. (2018a). Aggregated Battery Control for Peer-to-Peer Energy Sharing in a Community Microgrid with PV Battery Systems. *Energy Procedia*, 145:522–527.

[Long et al., 2018b] Long, C., Wu, J., Zhou, Y., and Jenkins, N. (2018b). Peer-to-Peer Energy Sharing Through a Two-Stage Aggregated Battery Control in a Community Microgrid. *Applied Energy*, 226(March):261–276.

[Longe et al., 2017] Longe, O. M., Ouahada, K., Rimer, S., Harutyunyan, A. N., and Ferreira, H. C. (2017). Distributed Demand Side Management with Battery Storage for Smart Home Energy Scheduling. *Sustainability*, 9(120).

[Lun et al., 2016] Lun, Y. Z., D'Innocenzo, A., Malavolta, I., and Di Benedetto, M. D. (2016). Cyber-Physical Systems Security: A Systematic Mapping Study. *arxiv preprint*.

[Lüth et al., 2018] Lüth, A., Zepter, J. M., Crespo del Granado, P., and Egging, R. (2018). Local Electricity Market Designs for Peer-to-Peer Trading: The Role of Battery Flexibility. *Applied Energy*, 229(August):1233–1243.

[Luthander et al., 2015] Luthander, R., Lingfors, D., Munkhammar, J., and Widén, J. (2015). Self-Consumption Enhancement of Residential Photovoltaics With Battery Storage and Electric Vehicles in Communities. *Proc. of eceee summer study on energy efficiency*, pages 991–1002.

[Ma et al., 2017a] Ma, K., Bai, Y., Yang, J., Yu, Y., and Yang, Q. (2017a). Demand-Side Energy Management Based on Nonconvex Optimization in Smart Grid. *Energies*, 10(10):1538.

[Ma et al., 2017b] Ma, K., Hu, S., Yang, J., Dou, C., and Guerrero, J. (2017b). Energy Trading and Pricing in Microgrids with Uncertain Energy Supply: A Three-Stage Hierarchical Game Approach. *Energies*, 10(5):670.

[Maghrabi et al., 2017] Maghrabi, L., Pfluegel, E., Al-Fagih, L., Graf, R., Settanni, G., and Skopik, F. (2017). Improved Software Vulnerability Patching Techniques Using CVSS and Game Theory. *International Conference on Cyber Security And Protection Of Digital Services*.

[Maharjan et al., 2013] Maharjan, S., Zhu, Q., Zhang, Y., Gjessing, S., and Başar, T. (2013). Dependable Demand Response Management in the Smart Grid: A Stackelberg Game Approach. *IEEE Transactions on Smart Grid*, 4(1):120–132.

[Mediwaththe et al., 2016] Mediwaththe, C. P., Member, S., Stephens, E. R., and Smith, D. B. (2016). A Dynamic Game for Electricity Load Management in Neighborhood Area Networks. *IEEE Transactions on Smart Grid*, 7(3):1329–1336.

[Mediwaththe et al., 2019] Mediwaththe, C. P., Shaw, M., Halgamuge, S. K., Smith, D., and Scott, P. M. (2019). An Incentive-Compatible Energy Trading Framework for Neighborhood Area Networks with Shared Energy Storage. *IEEE Transactions on Sustainable Energy*, 3029(c):1–1.

[Mediwaththe et al., 2018] Mediwaththe, C. P., Stephens, E. R., Smith, D. B., and Mahanti, A. (2018). Competitive Energy Trading Framework for Demand-Side Management in Neighborhood Area Networks. *IEEE Transactions on Smart Grid*, 9(5):4313–4322.

[Mengelkamp et al., 2018a] Mengelkamp, E., Bose, S., Kremers, E., Eberbach, J., Hoffmann, B., and Weinhardt, C. (2018a). Increasing the Efficiency of Local Energy Markets Through Residential Demand Response. *Energy Informatics*.

[Mengelkamp et al., 2019] Mengelkamp, E., Diesing, J., and Weinhardt, C. (2019). Tracing Local Energy Markets: A Literature Review. *preprint*.

[Mengelkamp et al., 2018b] Mengelkamp, E., Gärttner, J., Rock, K., Kessler, S., Orsini, L., and Weinhardt, C. (2018b). Designing Microgrid Energy Markets: A Case Study: The Brooklyn Microgrid. *Applied Energy*, 210:870–880.

[Mo et al., 2012] Mo, Y., Kim, T. H. J., Brancik, K., Dickinson, D., Lee, H., Perrig, A., and Sinopli, B. (2012). Cyber-Physical Security of a Smart Grid Infrastructure. *Proceeding of the IEEE*, 100(1):195–209.

[Mohsenian-Rad, 2016] Mohsenian-Rad, H. (2016). Optimal Bidding, Scheduling, and Deployment of Battery Systems in California Day-Ahead Energy Market. *IEEE Transactions on Power Systems*, 31(1):442–453.

[Mohsenian-Rad and Leon-Garcia, 2010] Mohsenian-Rad, H. and Leon-Garcia, A. (2010). Optimal Residential Load Control With Price Prediction in Real-Time Electricity Pricing Environments. *IEEE Transactions on Smart Grid*, 1(2):120–133.

[Mohsenian-Rad et al., 2010] Mohsenian-Rad, H., Wong, V. W. S., Jatskevich, J., Schober, R., and Leon-Garcia, A. (2010). Autonomous Demand-Side Management Based on Game-Theoretic Energy Consumption Scheduling for the Future Smart Grid. *IEEE Transactions on Smart Grid*, 1(3):320–331.

[Morstyn et al., 2018] Morstyn, T., Teytelboym, A., and McCulloch, M. D. (2018). Bilateral Contract Networks for Peer-to-Peer Energy Trading. *IEEE Transactions on Smart Grid*, 3053.

[Myung and Lee, 2018] Myung, S. and Lee, J.-H. (2018). Ethereum Smart Contract-Based Automated Power Trading Algorithm in a Microgrid Environment. *The Journal of Supercomputing*.

[NASA, 2019a] NASA (2019a). Global Temperature. https://go.nasa.gov/2mjzvJu. accessed: 2019-09-13.

[NASA, 2019b] NASA (2019b). The Effects of Climate Change. https://go.nasa.gov/2nIipFo. accessed: 2019-09-13.

[Nguyen et al., 2012] Nguyen, H. K., Song, J. B., and Han, Z. (2012). Demand Side Management to Reduce Peak-to-Average Ratio using Game Theory in Smart Grid. *IEEE Workshop on Communications and Control for Sustainable Energy Systems: Green Networking and Smart Grids*, pages 91–96.

[Nguyen et al., 2015] Nguyen, H. K., Song, J. B., and Han, Z. (2015). Distributed Demand Side Management with Energy Storage in Smart Grid. *IEEE Transactions on Parallel and Distributed Systems*, 26(12):3346–3357.

[Nguyen et al., 2018a] Nguyen, S., Peng, W., Sokolowski, P., Alahakoon, D., and Yu, X. (2018a). Optimizing Rooftop Photovoltaic Distributed Generation with Battery Storage for Peer-to-Peer Energy Trading. *Applied Energy*, 228(September 2018):2567–2580.

[Nguyen et al., 2018b] Nguyen, V. H., Besanger, Y., Tran, Q. T., and Le, M. T. (2018b). On the Applicability of Distributed Ledger Architectures to Peer-to-Peer Energy Trading Framework. *IEEE International Conference on Environment and Electrical Engineering*, pages 1–5.

[Nie et al., 2006] Nie, P. Y., Chen, L. H., and Fukushima, M. (2006). Dynamic Programming Approach to Discrete Time Dynamic Feedback Stackelberg Games with Independent and Dependent Followers. *European Journal of Operational Research*, 169(1):310–328.

[NREL, 2008] NREL (2008). User Manual for TMY3 Data Sets. https://bit.ly/2kM8IGD. accessed: 2017-06-05.

[Olaszi and Ladanyi, 2017] Olaszi, B. D. and Ladanyi, J. (2017). Comparison of different discharge strategies of grid-connected residential PV systems with energy storage in perspective of optimal battery energy storage system sizing. *Renewable and Sustainable Energy Reviews*, 75(November 2015):710–718.

[Opadokin et al., 2017] Opadokin, F., Roy, T. K., Akter, M. N., and Mahmud, M. A. (2017). Prioritizing Customers for Neighorhood Energy Sharing in Residential Microgrids with a Transactive Energy Market. *IEEE Power and Energy Society General Meeting*.

[Panaousis et al., 2014] Panaousis, E., Fielder, A., Malacaria, P., Hankin, C., and Smeraldi, F. (2014). Cybersecurity Games and Investments: A Decision Support Approach. In *Decisions and Game Theory for Security*, pages 266–286.

[Park et al., 2017a] Park, L., Jang, Y., Bae, H., Lee, J., Park, C., and Cho, S. (2017a). Automated Energy Scheduling Algorithms for Residential Demand Response Systems. *Energies*, 10(9):1–17.

[Park et al., 2017b] Park, L., Jang, Y., Cho, S., and Kim, J. (2017b). Residential Demand Response for Renewable Energy Resources in Smart Grid Systems. *IEEE Transactions on Industrial Informatics*, PP(99):1–1.

[Park et al., 2016] Park, S., Lee, J., Bae, S., Hwang, G., and Choi, J. (2016). Contribution Based Energy Trading Mechanism in Micro-Grids for Future Smart Grid: A Game Theoretic Approach. *IEEE Transactions on Industrial Electronics*, 0046(c):4255–4265.

[Park et al., 2017c] Park, S., Lee, J., Hwang, G., and Choi, J. K. (2017c). Event-Driven Energy Trading System in Microgrids: Aperiodic Market Model Analysis with a Game Theoretic Approach. *IEEE Access*, 5:26291–26302.

[Pedrasa et al., 2010] Pedrasa, M. A. A., Spooner, T. D., and MacGill, I. F. (2010). Coordinated Scheduling of Residential Distributed Energy Resources to Optimize Smart Home Energy Services. *IEEE Transactions on Smart Grid*, 1(2):134–143.

[Pilz and Al-Fagih, 2019a] Pilz, M. and Al-Fagih, L. (2019a). A Dynamic Game Approach for Demand-Side Management: Scheduling Energy Storage With Forecasting Errors. *Dynamic Games and Applications: Dynamic Games for Smart Energy Systems*.

[Pilz and Al-Fagih, 2019b] Pilz, M. and Al-Fagih, L. (2019b). Recent Advances in Local Energy Trading in the Smart Grid Based on Game–Theoretic Approaches. *IEEE Transactions on Smart Grid*, 10(2):1363–1371. (©2019 IEEE)

[Pilz and Al-Fagih, 2019c] Pilz, M. and Al-Fagih, L. (2019c). Selfish Energy Sharing in Prosumer Communities: A Demand-Side Management Concept. In *IEEE International Conference on Communications, Control, and Computing Technologies for Smart Grids*. (©2019 IEEE)

[Pilz et al., 2017a] Pilz, M., Al-Fagih, L., and Pfluegel, E. (2017a). A Game–Theoretic Approach to Energy Storage Scheduling for Households in a Smart Grid. *International Research Conference on Sustainable Energy, Engineering, Materials and Environment*.

[Pilz et al., 2017b] Pilz, M., Al-Fagih, L., and Pfluegel, E. (2017b). Energy Storage Scheduling with an Advanced Battery Model: A Game–Theoretic Approach. *Inventions*, 2(4):1–11.

[Pilz et al., 2019a] Pilz, M., Baghaei Naeini, F., Grammont, K., Smagghe, C., Davis, M., Nebel, J.-C., Al-Fagih, L., and Pfluegel, E. (2019a). Security Attacks on Smart Grid Scheduling and Their Defences: A Game-Theoretic Approach. *International Journal of Information Security*.

[Pilz et al., 2019b] Pilz, M., Ellabban, O., and Al-Fagih, L. (2019b). On Optimal Battery Sizing for Households Participating in Demand-Side Management Schemes. *Energies*, 12(18):3419.

[Pilz et al., 2018] Pilz, M., Nebel, J.-C., and Al-Fagih, L. (2018). A Practical Approach to Energy Scheduling: A Game Worth Playing? *IEEE PES Innovative Smart Grid Technologies Conference Europe*. (©2018 IEEE)

[Power Networks, 2014] Power Networks, U. (2014). Validation of PV Connection Assessment Tool. https://bit.ly/2mfYNJQ. accessed: 2017-12-12.

[Power2Switch, 2012] Power2Switch (2012). How Electricity Grew Up? A Brief History of the Electrical Grid... https://bit.ly/2jX9HTS. accessed: 2019-09-13.

[Prudhviraj et al., 2018] Prudhviraj, D., Kiran, P. B. S., and Pindoriya, N. M. (2018). Day-ahead Energy Management of a Microgrid with Battery Energy Storage Integration. *IEEE Innovative Smart Grid Technologies Asia*.

[Rahbar et al., 2018] Rahbar, K., Chai, C. C., and Zhang, R. (2018). Energy Cooperation Optimization in Microgrids with Renewable Energy Integration. *IEEE Transactions on Smart Grid*, 9(2):1482–1493.

[Rahbar et al., 2015] Rahbar, K., Xu, J., and Zhang, R. (2015). Real-Time Energy Storage Management for Renewable Integration in Microgrid: An Off-line Optimization Approach. *IEEE Transactions on Smart Grid*, 6(1):124–134.

[Rahi et al., 2016a] Rahi, G. E., Saad, W., Glass, A., Mandayam, N. B., and Poor, H. V. (2016a). Prospect Theory for Prosumer-Centric Energy Trading in the Smart Grid. *IEEE Power and Energy Innovative Smart Grid Technologies Conference*.

[Rahi et al., 2016b] Rahi, G. E., Sanjab, A., Saad, W., Mandayam, N. B., and Poor, H. V. (2016b). Prospect Theory for Enhanced Smart Grid Resilience Using Distributed Energy Storage. *Annual Allerton Conference*, pages 248–255.

[Rahman et al., 2015] Rahman, M. A., Manshaei, M. H., Al-Shaer, E., and Shehab, M. (2015). Secure and Private Data Aggregation for Energy Consumption Scheduling in Smart Grids. *IEEE Transactions on Dependable and Secure Computing*, (99):221–234.

[Rahman and Mohsenian-Rad, 2012] Rahman, M. A. and Mohsenian-Rad, H. (2012). False Data Injection Attacks with Incomplete Information Against Smart Power Grids. *IEEE Global Telecommunications Conference*, pages 3153–3158.

[Ramchurn et al., 2011] Ramchurn, S. D., Vytelingum, P., Rogers, A., and Jennings, N. (2011). Agent-Based Control for Decentalised Demand Side Management in the Smart Grid. *International Conference on Autonomous Agents and Multiagent Systems*, 1:207–229.

[Rana et al., 2016] Rana, M., Koprinska, I., and Agelidis, V. G. (2016). Solar Power Forecasting Using Weather Type Clustering and Ensembles of Neural Networks. *International Joint Conference on Neural Networks*.

[Ratnam, 2016] Ratnam, E. L. (2016). *Balancing Distributor and Customer Benefits of Battery Storage Co-Located With Solar PV*. PhD thesis.

[Rawat and Bajracharya, 2015] Rawat, D. B. and Bajracharya, C. (2015). Cyber Security for Smart Grid Systems: Status, Challenges and Perspectives. In *SoutheastCon*.

[RESPOND, 2018] RESPOND (2018). Demand-Side Management vs. Demand Response. https://bit.ly/2m9EnSz. accessed: 2019-09-13.

[Reyhanian et al., 2017] Reyhanian, N., Maham, B., Shah-Mansouri, V., Tushar, W., and Yuen, C. (2017). Game-Theoretic Approaches for Energy Cooperation in Energy Harvesting Small Cell Networks. *IEEE Transactions on Vehicular Technology*, 9545(c):1–17.

[Richtek, 2014] Richtek (2014). Designing Applications with Li-ion Batteries. https://bit.ly/2lOklwS. accessed: 2017-03-27.

[Saad et al., 2016] Saad, W., Glass, A. L., Mandayam, N. B., and Poor, H. V. (2016). Toward a Consumer-Centric Grid: A Behavioral Perspective. *Proceedings of the IEEE*.

[Saad et al., 2011] Saad, W., Han, Z., Poor, H. V., and Başar, T. (2011). A Noncooperative Game for Double Auction-Based Energy Trading Between PHEVs and Distribution Grids. *IEEE International Conference on Smart Grid Communications*, pages 267–272.

[Saad et al., 2012] Saad, W., Han, Z., Poor, H. V., and Başar, T. (2012). Game-Theoretic Methods for the Smart Grid: An Overview of Microgrid Systems, Demand-Side Management, and Smart Grid Communications. *IEEE Signal Processing Magazine*, 29(5):86–105.

[Sanjab and Saad, 2016] Sanjab, A. and Saad, W. (2016). Data Injection Attacks on Smart Grids with Multiple Adversaries: A Game-Theoretic Perspective. *IEEE Transactions on Smart Grid*, 7(4):2038–2049.

[Schumacher et al., 2019] Schumacher, K., Krones, F., McKenna, R., and Schultmann, F. (2019). Public Acceptance of Renewable Energies and Energy Autonomy: A Comparative Study in the French, German and Swiss Upper Rhine Region. *Energy Policy*, 126(November 2018):315–332.

[Scimago Lab, 2019] Scimago Lab (2019). Scimago Institutions Ranking. https://bit.ly/2U9Fv1E. accessed: 2019-09-13.

[Shareef et al., 2018] Shareef, H., Ahmed, M. S., Mohamed, A., and Al Hassan, E. (2018). Review on Home Energy Management System Considering Demand Responses, Smart Technologies, and Intelligent Controllers. *IEEE Access*, 6:24498–24509.

[Sharma et al., 2018] Sharma, A., Rathore, A. K., and Kumar, R. (2018). A Dynamic Battery Charging Approach for Energy Trading in the Smart Grid. *International Power Electronics Conference*, pages 2456–2461.

[Shell, 2019] Shell (2019). Energy and Innovation. https://go.shell.com/2qMqDfC. accessed: 2019-04-09.

[Shoham and Leyton-Brown, 2009] Shoham, Y. and Leyton-Brown, K. (2009). *Multiagent Systems*. Cambridge University Press, 1st edition.

[Sivanantham and Gopalakrishnan, 2019] Sivanantham, G. and Gopalakrishnan, S. (2019). A Stackelberg Game Theoretical Approach for Demand Response in Smart Grid. *Personal and Ubiquitous Computing*.

[Soliman and Leon-Garcia, 2014] Soliman, H. M. and Leon-Garcia, A. (2014). Game-Theoretic Demand-Side Management With Storage Devices for the Future Smart Grid. *IEEE Transactions on Smart Grid*, 5(3):1475–1485.

[Talent and Du, 2018] Talent, O. and Du, H. (2018). Optimal Sizing and Energy Scheduling of Photovoltaic-Battery Systems Under Different Tariff Structures. *Renewable Energy*, 129:513–526.

[Tan et al., 2017] Tan, S., De, D., Song, W.-Z., Yang, J., and Das, S. K. (2017). Survey of Security Advances in Smart Grid: A Data Driven Approach. *IEEE Communications Surveys and Tutorials*, 19(1):397–422.

[Tesla, 2017] Tesla (2017). Tesla Powerwall 2. https://bit.ly/2sGqRaR. accessed: 2017-06-05.

[Thakur and Breslin, 2018] Thakur, S. and Breslin, J. G. (2018). Peer to Peer Energy Trade Among Microgrids Using Blockchain Based Distributed Coalition Formation Method. *Technology and Economics of Smart Grids and Sustainable Energy*, 3(5):17.

[Tushar et al., 2018a] Tushar, M. H. K., Zeineddine, A. W., and Assi, C. (2018a). Demand-Side Management by Regulating Charging and Discharging of the EV, ESS, and Utilizing Renewable Energy. *IEEE Transactions on Industrial Informatics*, 14(1):117–126.

[Tushar et al., 2014a] Tushar, W., Chai, B., Yuen, C., Smith, D. B., Wood, K. L., Yang, Z., and Poor, H. V. (2014a). Three-Party Energy Management With Distributed

Energy Resources in Smart Grid. *IEEE Transactions on Industrial Electronics*, 62(4):1–12.

[Tushar et al., 2018b] Tushar, W., Saha, T. K., Yuen, C., Liddell, P., Bean, R., and Poor, H. V. (2018b). Peer-to-Peer Energy Trading with Sustainable User Participation: A Game Theoretic Approach. *arXiv preprint*.

[Tushar et al., 2014b] Tushar, W., Zhang, J. A., Smith, D. B., Poor, H. V., and Thiébaux, S. (2014b). Prioritizing Consumers in Smart Grid: A Game Theoretic Approach. *IEEE Transactions on Smart Grid*, 5(3):1429–1438.

[UK Power Networks, 2015] UK Power Networks (2015). Validation of Photovoltaic (PV) Connection Assessment Tool. Technical report. https://bit.ly/2me2zDn.

[U.S. Dept. of Energy, 2010] U.S. Dept. of Energy (2010). Building America House Simulation Protocols. https://bit.ly/2mgShCB. accessed: 2017-06-05.

[U.S. Dept. of Energy, 2013] U.S. Dept. of Energy (2013). Commercial and Residential Hourly Load Profiles for all TMY3 Locations in the United States. https://bit.ly/2kJFmbS. accessed: 2017-06-05.

[U.S. Energy Information Administration, 2019] U.S. Energy Information Administration (2019). Residential Energy Consumption Survey (RECS). https://bit.ly/2VyMDbt. accessed: 2019-09-13.

[von Neumann, 1928] von Neumann, J. (1928). Zur Theorie der Gesellschaftsspiele. *Mathematische Annalen*, 100(1):295–320.

[von Neumann and Morgenstern, 1944] von Neumann, J. and Morgenstern, O. (1944). *Theory of Games and Economic Behavior*. Princeton University Press, Princeton, NJ.

[von Stackelberg, 2010] von Stackelberg, H. (2010). *Market Structure and Equilibrium*. Springer Science and Business Media.

[Wang et al., 2016] Wang, H., Huang, T., Liao, X., Abu-Rub, H., and Chen, G. (2016). Reinforcement Learning in Energy Trading Game among Smart Microgrids. *IEEE Transactions on Industrial Electronics*, 63(8):5109–5119.

[Wang et al., 2017a] Wang, J., Wang, Q., Zhou, N., and Chi, Y. (2017a). A Novel Electricity Transaction Mode of Microgrids Based on Blockchain and Continuous Double Auction. *Energies*, 10(12).

[Wang et al., 2015a] Wang, K., Ouyang, Z., Krishnan, R., Shu, L., and He, L. (2015a). A Game Theory-Based Energy Management System Using Price Elasticity for Smart Grids. *IEEE Transactions on Industrial Informatics*, 11(6):1607–1616.

[Wang et al., 2017b] Wang, L., Li, Q., Ding, R., Sun, M., and Wang, G. (2017b). Integrated Scheduling of Energy Supply and Demand in Microgrids Under Uncertainty: A Robust Multi-Objective Optimization Approach. *Energy*, 130:1–14.

[Wang and Lu, 2013] Wang, W. and Lu, Z. (2013). Cyber Security in the Smart Grid: Survey and Challenges. *Computer Networks*, 57(5):1344–1371.

[Wang et al., 2015b] Wang, Y., Saad, W., Mandayam, N. B., and Poor, H. V. (2015b). Load Shifting in the Smart Grid: To Participate or Not? *IEEE Transactions on Smart Grid*, 7(6):2604–2614.

[Wu and Wang, 2018] Wu, H. and Wang, W. (2018). A Game Theory Based Collaborative Security Detection Method for Internet of Things Systems. *IEEE Transactions on Information Forensics and Security*, 13(6):1432–1445.

[Xiang and Wang, 2017] Xiang, Y. and Wang, L. (2017). A Game-Theoretic Study of Load Redistribution Attack and Defense in Power Systems. *Electric Power Systems Research*, 151:12–25.

[Yaagoubi and Mouftah, 2015a] Yaagoubi, N. and Mouftah, H. T. (2015a). A Distributed Game Theoretic Approach to Energy Trading in the Smart Grid. *IEEE Electrical Power and Energy Conference*, pages 203–208.

[Yaagoubi and Mouftah, 2015b] Yaagoubi, N. and Mouftah, H. T. (2015b). User-Aware Game Theoretic Approach for Demand Management. *IEEE Transactions on Smart Grid*, 6(2):716–725.

[Yaagoubi and Mouftah, 2017] Yaagoubi, N. and Mouftah, H. T. (2017). Energy Trading in the Smart Grid: A Distributed Game-Theoretic Approach. *Canadian Journal of Electrical and Computer Engineering*, 40(2):57–65.

[Yan et al., 2012] Yan, Y., Qian, Y., Sharif, H., and Tipper, D. (2012). A Survey on Cyber Security for Smart Grid Communications. *IEEE Communications Surveys and Tutorials*, 14(4):998–1010.

[Yang et al., 2016] Yang, X., He, X., Lin, J., Yu, W., and Yang, Q. (2016). A Game-Theoretic Model on Coalitional Attacks in Smart Grid. *Proceedings - 15th IEEE*

International Conference on Trust, Security and Privacy in Computing and Communications, 10th IEEE International Conference on Big Data Science and Engineering and 14th IEEE International Symposium on Parallel and Distributed Proce, pages 435–442.

[Zafar et al., 2017] Zafar, R., Mahmood, A., Razzaq, S., Ali, W., Naeem, U., and Shehzad, K. (2017). Prosumer based energy management and sharing in smart grid. *Renewable and Sustainable Energy Reviews*, (July).

[Zepter et al., 2019] Zepter, J. M., Lüth, A., Crespo del Granado, P., and Egging, R. (2019). Prosumer Integration in Wholesale Electricity Markets: Synergies of Peer-to-Peer Trade and Residential Storage. *Energy & Buildings*, 184:163–176.

[Zhang et al., 2016] Zhang, C., Wu, J., Cheng, M., Zhou, Y., and Long, C. (2016). A Bidding System for Peer-to-Peer Energy Trading in a Grid-connected Microgrid. *Energy Procedia*, 103(April):147–152.

[Zhang and Grijalva, 2016] Zhang, X. and Grijalva, S. (2016). A Data-Driven Approach for Detection and Estimation of Residential PV Installations. *IEEE Transactions on Smart Grid*, 7(5):2477–2485.

[Zhou et al., 2018a] Zhou, W., Wu, J., Zhong, W., Zhang, H., Shu, L., and Yu, R. (2018a). Optimal and Elastic Energy Trading for Green Microgrids: A Two-Layer Game Approach. *Mobile Networks and Applications*.

[Zhou et al., 2018b] Zhou, Y., Wu, J., and Long, C. (2018b). Evaluation of Peer-to-Peer Energy Sharing Mechanisms Based on a Multiagent Simulation Framework. *Applied Energy*, 222(November 2017):993–1022.

[Zhou et al., 2017] Zhou, Z., Xiong, F., Xu, C., and Jiao, R. (2017). Energy Management in Microgrids: A Combination of Game Theory and Big Data-Based Wind Power Forecasting. In *Development and Integration of Microgrids*, chapter 9, pages 209–231.

[Zhu and Başar, 2011] Zhu, Q. and Başar, T. (2011). Robust and Resilient Control Design for Cyber-Physical Systems With an Application to Power Systems. *Proceedings of the IEEE Conference on Decision and Control*, pages 4066–4071.

[Zhu et al., 2012] Zhu, Q., Han, Z., and Başar, T. (2012). A Differential Game Approach to Distributed Demand Side Management in Smart Grid. *IEEE International Conference on Communications*, pages 3345–3350.

[Zhumabekuly Aitzhan and Svetinovic, 2016] Zhumabekuly Aitzhan, N. and Svetinovic, D. (2016). Security and Privacy in Decentralized Energy Trading Through Multi-Signatures, Blockchain and Anonymous Messaging Streams. *IEEE Transactions on Dependable and Secure Computing*, 5971(c).

[Zou et al., 2017] Zou, S., Ma, Z., and Liu, X. (2017). Resource Allocation Game under Double-sided Auction Mechanism: Efficiency and Convergence. *IEEE Transactions on Automatic Control*, 63(5):1273–1287.

[Zou et al., 2016] Zou, S., Ma, Z., Shao, Y., Ran, L., and Liu, X. (2016). Efficient and Dynamic Double Auctions for Resource Allocation. *IEEE Conference on Decision and Control*, pages 6062–6067.

This almost blank page is intentional.